Embryo Signals for Successful Implantation

Scarlett Salter

A thesis submitted to the University of Warwick for the degree of Doctor of Philosophy.

Division of Translational and Systems Medicine

Warwick Medical School

University of Warwick

April 2016

Table of Contents

Chapter 4: ENDOMETRIAL RECOGNITION OF EMBRYO-DERIVED PROTEASES

Chapter 5: GENERAL DISCUSSION

APPENDICES

List of Figures

Chapter 1: INTRODUCTION

Chapter 3: EMBRYO-DERIVED TRYPSIN-LIKE PROTEASES AT IMPLANTATION

Chapter 4: ENDOMETRIAL RECOGNITION OF EMBRYO-DERIVED PROTEASES

List of Tables

Chapter 1: INTRODUCTION

Chapter 3: EMBRYO-DERIVED TRYPSIN-LIKE PROTEASES AT IMPLANTATION

Acknowledgments

Firstly, I am extremely grateful to Professor Jan J. Brosens for his supervision of this project. He has provided me with unwavering support, patience and kindness throughout, for which I am sincerely grateful. I have not met another individual with such immense enthusiasm and exemplary dedication towards their work.

I would like to express my gratitude to the Biomedical Research Unit and the Warwick Collaborative Postgraduate Research Scholarship (WCPRS) which jointly provided the financial backing required in order for my completion of this project.

I have been lucky to be part of a truly supportive and friendly team during my time at Warwick University. I would like to thank them all for their helpfulness and guidance, in particular; Dr Emma Lucas, Dr Anatoly Shmygol, Dr Jo Muter, Dr Debbie Taylor, Sarah Drury, Dr Paul Brighton, Dr Seley Gharanei, Dr Flavio Barros, Ruban Durairaj and Dr Katherine Fishwick.

I would like to thank the couples who have kindly donated their embryos and endometrial biopsies to this project and the clinicians and healthcare professionals involved in their collection and consent procedures. I offer my sincere thanks to those at the Centre for Reproductive Medicine (Coventry), Leicester Fertility Centre and the Centre for Reproductive Medicine (Vrije Universiteit Brussel, Brussels).

Finally, I offer thanks to my unfalteringly supportive family and friends. To Jack, for his exceptional generosity and proof-reading skills. To my husband, Tom, who has offered consistent support, friendship and advice that will be invaluable in the next stage of our lives together. And finally, to those who have always imparted the importance of education and hard work upon me; my Mum, Nanny and Grandad.

Declaration

This thesis is submitted to the University of Warwick in support of my application for the degree of Doctor of Philosophy. It has been composed by myself and has not been submitted in any previous application for any degree.

The work presented (including data generated and data analysis) was carried out by the author except in the cases outlined below:

i) Collaboration with Dr Anatoly Shmygol regarding data collection and analysis of Ca^{2+} signalling in Ishikawa cells

ii) Collaboration with Dr Flavio Barros in the purification and imaging of human endometrial epithelial cells

iii) Collaboration with Katherine Fishwick for preparation and imaging of fixed endometrial sections

iv) Collaboration with Reuben Durairaj, Jo Muter and Paul Brighton regarding sample collection and analysis of whole endometrial biopsies

Parts of this thesis have been published by the author:

Brosens, J. J., Salker, M. S., Teklenburg, G., Nautiyal, J., **Salter, S**., Lucas, E. S., Steel, J. H., Christian, M., Chan, Y., Boomsma, C. M., Moore, J. D., Hartshorne, G. M., Šućurović, S., Mulac-Jericevic, B., Heijnen, C. J., Quenby, S., Groot Koerkamp, M. J., Holstege, F. C. P., Shmygol, A., Macklon, N. S. (2014) Uterine selection of human embryos at implantation. *Scientific Reports*, v. 4: 3894, 1-9.

Abstract

Human pre-implantation embryos display a high prevalence of aneuploidy and chromosomal mosaicism, unique from any other species. The decreasing incidence of aneuploidy observed between the cleavage and blastocyst stages of pre-implantation embryo development infers a degree of 'self-correction' following activation of the embryonic genome. However, contrary to the previous assumption that only euploid embryos should be considered 'normal', new evidence has confirmed that mosaic embryos can result in the birth of healthy babies. Thus, aneuploidy should be viewed as an intrinsic feature of human pre-implantation embryo development, which presents a novel challenge at implantation. The endometrium must implement both positive and negative selection, in order to limit maternal investment to only viable embryos. The ability of the endometrium to act as a 'biosensor' of embryo quality has been well documented yet there is little direct evidence for the key regulators of this process.

For the first time, we demonstrate a biological context for embryo biosensoring. Firstly, we discover novel embryo-secreted proteases that are enhanced at the blastocyst stage and relate to implantation outcome upon embryo transfer. Secondly, we identify corresponding protease-sensitive receptors in the endometrium, heightened during the window of implantation. By demonstrating the cleavage and de-activation of endometrial toll-like receptor 4 (TLR4) by embryo conditioned medium, we link successful implantation to a diminished inflammatory response. Furthermore, we demonstrate that TLR4 levels in the endometrium constitute a selectivity checkpoint, which is supressed in women suffering from recurrent miscarriage (RM).

List of Abbreviations

µg	Microgram
8-br-cAMP	8-Bromoadenosine-3', 5'-cyclic monophosphate
AEBSF	4-(2-aminoethyl)benzenesulfonyl flouride hydrochloride
AKT	Protein kinase B
AMBP	Alpha-1-microglobulin/bikunin precursor
ART	Assisted reproductive technologies
BMI	Body mass index
BSA	Bovine serum albumin
Ca^{2+}	Calcium ion
Camp	Cyclic adenosine monophosphate
CD14	Cluster of differentiation 14
cDNA	Complementary DNA
COX2	Cyclooxygenase 2
CPA	Cyclopiazonic acid
cPLA2	Cytosolic phopholipase A2
D	Decidual cells
DAB	Daminobenzidine
DCC	Dextran coated charcoal
DCE	Developmentally competent embryo
DESC	Decidualized endometrial stromal cell
DIE	Developmentally incompetent embryo
DMEM	Dulbecco's modified eagles medium
DMSO	Dimethyl sulphoxide
DTT	Dithiothreitol
E_2	Estradiol
ECM	Embryo conditioned medium
EDTA	Ethylenediaminetetraacetic acid
EGA	Embryonic genome activation
EGFR	Epidermal growth factor receptor
ELISA	Enzyme-linked immunosorbent assay
En	Embryonic endoderm
ENaC	Epithelial sodium channel
Epi	Epiblast
ER	Endoplasmic reticulum
ERG	ETS-related gene
FBS	Fetal bovine serum
FISH	Fluorescence in situ hybridization
FSH	Follicle stimulating hormone
GEO	Gene expression omnibus
Gp41	glycoprotein 41
Gp43	glycoprotein 43
GPCR	G-protein-coupled receptor
hCG	Human chorionic gonadotrophin
HEEC	Human endometrial epithelial cell
HESC	Human endometrial stromal cell

hPL	Human placental lactogen
ICC	Immunocytochemistry
ICSI	Intra-cytoplasmic sperm injection
IGFBP1	Insulin-like growth factor binding protein-1
IHC	Immunohistochemistry
IL	Interleukin
IP	Prostacyclin receptor
IVF	In vitro fertilisation
JNK	c-Jun N-terminal kinases
LE	Luminal epithelium
LH	Luteinizing hormone
LH+	Days post LH surge
LIF	Leukaemia inhibitory factor
LY96	Lymphocyte antigen 96
MAPK	Mitogen activated protein kinase
MD-2	Myeloid differentiation factor 2
Mg	Milligram
miRNA	Micro RNA
MMP	Matrix metalloproteinases
MPA	17a-medroxyprogesterone actetate
MSC	Mesenchymal stem cell
MT-SP1	Membrane type serine protease 1
MUC1	Mucin-1
NF-kB	Nuclear factor kappa-B
NP	Not pregnant
NPGB	nitrophenol-p-guanidino benzoate
NT	Non-targeting
P	Pregnant
P_4	Progesterone
PAGE	Polyacrylamide gel electrophoresis
PAR	Protease-activated receptor
PBS	Phosphate buffered saline
PCR	Polymerase chain reaction
PDGF	Platelet-derived growth factor
PE	Primitive endoderm
PFA	Paraformaldehyde
PG	Prostaglandin
Pg	Picogram
PGE_2	Prostaglandin E2
PGI_2	Prostcyclin
PGS	Pre-implantation genetic screening
PMSF	Phenyl-methyl sulfonyl-flouride
PN-1	Protein Nexin 1
PR	Progesterone receptor
PRL	Prolactin
PRSS28	Protease, serine 28
PRSS8	Protease, serine 8
PTGS2	Prostaglandin-endoperoxide synthase 2

qRT-PCR	Quantitative real time PCR
RIF	Recurrent implantation failure
RIPA	Radioimmunoprecipitation assay
RM	Recurrent miscarriage
RNA	Ribonucleic acid
ROI	Region of interest
ROS	Reactive oxygen species
RT	Room temperature
S	Stroma
SDS	Sodium dodecyl sulphate
SET	Single embryo transfer
SGK1	Serum and glucocorticoid-inducible kinase-1
siRNA	Small interfering RNA
SOCE	Store operated calcium entry
SR	Sarcoplasmic reticulum
T	Trophoblast
TBS	Tris-buffered saline
TBS-T	Tris-buffered saline and Tween-20
TE	Trophectoderm
TGFβ	Transforming growth factor beta
TLCK	Na-Tosyl L-lysine chloromethyl ketone hydrochloride
TLR4	Toll-like receptor 4
TMPRSS15	Transmembrane protease, serine 15
TMPRSS2	Transmembrane protease, serine 2
TNFα	Tumour necrosis factor alpha
TTP	Time to pregnancy
TTSP	Type 2 transmembrane serine proteases
UCM	Unconditioned medium
uNK	Uterine Natural Killer cells
WOI	Window of implantation
XESP	Xenopus embryonic serine protease
XMP-SP1	Xenopus homolog of MT-SP1
ZP	Zona pellucida

Chapter 1

Introduction

1.1 The Human Endometrium

The endometrium constitutes the inner, mucosal layer of uterus. It acts as a lining to maintain patency of the uterine lumen by preventing adhesions between the two opposing myometrial layers. The primary reproductive function of the endometrium is to provide a nutritive microenvironment which supports viable embryo implantation (Tabibzadeh, 1998). Beyond implantation, the endometrium provides structural and nutritional support to the foetus and aids the removal of waste products. Thus the endometrium is an exceptionally adaptable tissue. Continuous, regular cycles of proliferation, differentiation and degeneration occur under the influence of ovarian steroid hormones throughout female reproductive maturity. Shedding of the functional endometrial layer takes place in the absence of an implanting embryo yet astonishingly the tissue is completely restored within just 2 weeks (Knobil, 2013). Re-establishment of the functional endometrial layer and priming of the tissue by oestrogen and progesterone restores its receptive state once again. The means by which the endometrium is regenerated is highly intricate and the underlying processes have not yet been established. Yet this process is understood to involve proliferation, angiogenesis, differentiation, epithelialization and extracellular matrix remodelling (Groothuis et al., 2007). In recent years, the focus has shifted to the role of endometrial stem / progenitor cells in cyclic endometrial regeneration (Gargett et al., 2015).

1.2 Structure of the Endometrium

The endometrium can be subdivided into two key layers; the stratum functionalis and the stratum basalis (Figure 1.2.1). The stratum basalis remains comparatively constant from cycle to cycle, whilst the stratum functionalis is dynamic and transient. Responsivity to ovarian steroid hormone results in cyclic expansion and vascularisation of the stratum functionalis before it becomes sloughed off during menstruation. In the event that an embryo implants, the basalis and the stratum

functionalis are maintained and in conjunction with the myometrial junctional zone contribute to the maternal fraction of the placenta (Brosens et al., 2002). Adjacent to the uterine lumen a single layer of prismatic epithelial cells coats the apical edge of the stratum functionalis. Yet beneath the basal lamina, stromal cells comprise the large majority of this highly vascularised cellular compartment (Rogers, 1996). The myometrium forms an underlying smooth muscle layer, composed predominantly of uterine myocytes. It provides structural and vascular support to the endometrium although its primary function is to permit uterine contractions at parturition. Radial arteries situated within the myometrium provide vascular support to the overlying endometrium by dividing first into basal arteries which supply the stratum basalis and then into spiral arterioles which supply the stratum functionalis. The characteristically coiled spiral arteries are unique amongst the uterine blood vessels in that they exhibit selective sensitivity to the cyclic hormonal changes of the menstrual cycle. This was most elegantly observed via the transplantation of endometrial fragments into the eye chamber of rhesus monkeys (Markee, 1978). The fragments implanted and developed on the iris but soon regressed upon progesterone and estradiol withdrawal. Subsequent coiling of the spiral arterioles and venostasis were succeeded by alternating episodes of vasodilation, vasoconstriction and bleeding of perivascular cells (Markee, 1978). The perivascular cells surrounding spiral arterioles are also sensitive to progesterone changes and produce inflammatory factors including cytokines and prostaglandins (Henriet et al., 2012). Although the exact mechanism of tissue breakdown is not yet fully understood, spiral arterioles may play a role in menstruation by regulating their own vasoconstriction and leukocyte influx (Henriet et al., 2012).

The stratum functionalis also contains uterine glands, tubular invaginations, lined with columnar epithelial cells. The primary function of the uterine glands is to provide nutrition to a developing conceptus via histotroph secretion (Gray et al., 2001). Due

to their topology within the functional layer of the endometrium, the appearance and secretions of the uterine glands fluctuate throughout the menstrual cycle. During the secretory phase of the menstrual cycle the uterine glands become enlarged and secretory.

In developed countries women of reproductive age are thought to undergo, on average, 400 menstrual cycles in their lifetime. Progenitor cells required for the regeneration of the stratum functionalis at each menstrual cycle are thought to originate from the enduring stratum basalis. Only recently has evidence for the presence of endometrial progenitor (or stem-like) cells with a role in cyclic remodelling emerged (Chan et al., 2004, Gargett and Masuda, 2010, Masuda et al., 2010). Mesenchymal stem-like cells (MSCs) reside within the endometrium and a population of stromal cells have been isolated that display multipotency, clonogenicity, immunoprivilege and the ability to contribute to endometrium upon transfer into mice via xenograft (Gargett and Masuda, 2010, Miyazaki et al., 2012, Wolff et al., 2007). Various techniques have been adopted in order to isolate endometrial stromal cells enriched in MSCs. Current indications are that endometrial stem-like cells are derived from the stratum basalis but may also be found within the stratum functionalis due to their identification in menstrual blood (Patel et al., 2008).

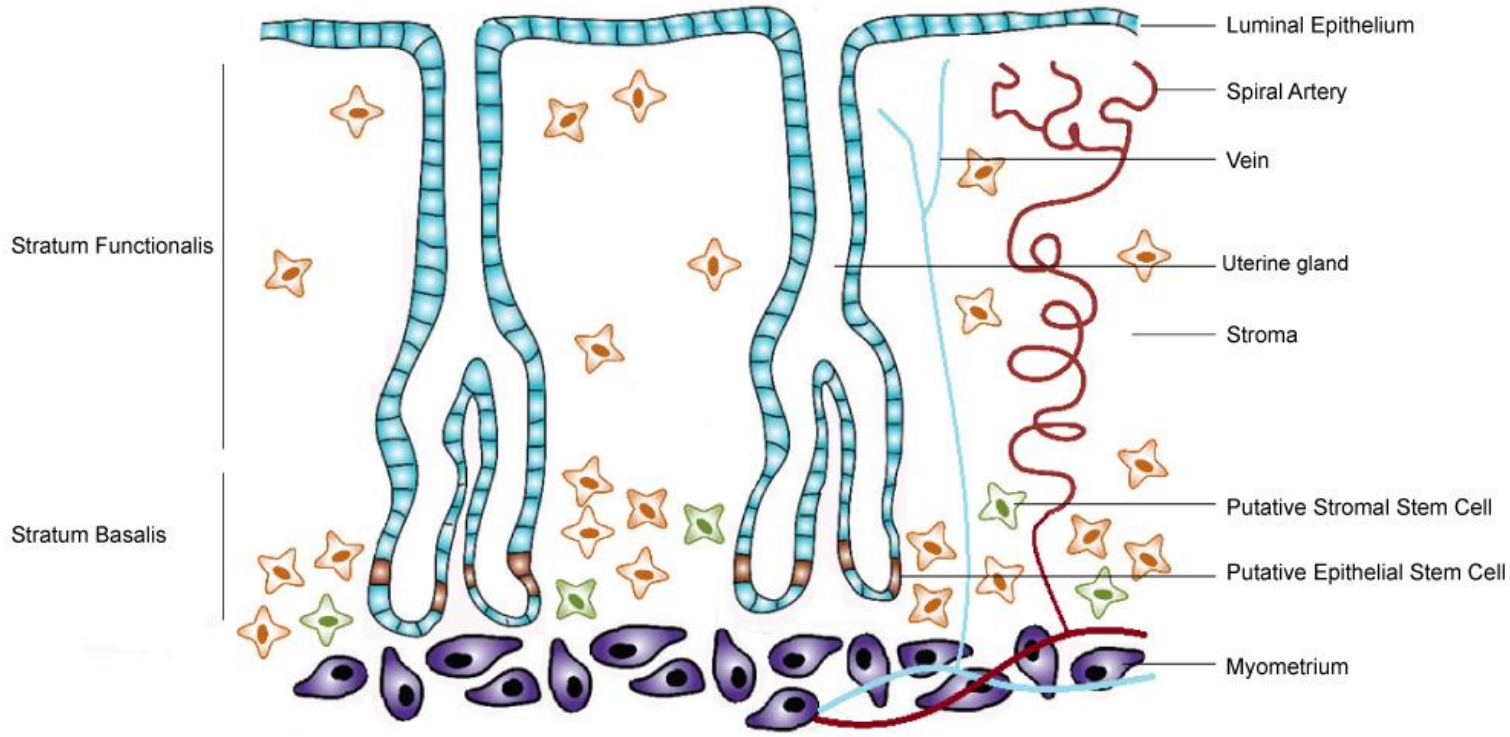

Figure 1.2.1: Diagram of the Human Endometrium

The human endometrium is formed of two components, the stratum functionalis and the stratum basalis. The stratum functionalis becomes remodelled each cycle whereas the stratum basalis remains constant. The apical surface of the endometrium is covered with a single layer of luminal epithelial cells and invaginations from the lumen form the uterine glands. Underlying stromal cells constitute the majority of the endometrium and stem-like cells from the stratum basalis permit the regeneration of the stratum functionalis each cycle. The endometrium is highly vascularised with the spiral arteries in the stratum functionalis originating from blood vessels in the underlying myometrium. Adapted from (Muter, 2015).

1.3 The Menstrual Cycle

Females achieve reproductive fitness due to cyclical modifications that occur in the endometrium as a result of fluctuating ovarian steroid hormone levels. These alterations result in distinct phases of proliferation, differentiation, inflammation, apoptosis and regeneration, which constitute the menstrual cycle (Figure 1.3.1). The proliferative phase encompasses days 5-13 of a 28 day cycle and results in thickening of the endometrial lining from 1-2 to 7-8 mm due to increasing oestrogen production by the granulosa cells residing within the ovarian follicle. The thickening results from mitotic proliferation of the endometrial stromal cell compartment, which occurs alongside lengthening of spiral arteries and the formation of narrow uterine glands by proliferation of endothelial and epithelial cells, respectively (Brosens et al., 2002, Gray et al., 2001). The secretory phase is initiated when heightened serum oestrogen levels induce a surge of luteinising hormone (LH), which in turn acts upon the corpus luteum to promote progesterone production. This post-ovulatory rise in progesterone halts the proliferative process and initiates a highly coordinated differentiation process. The secretory phase endows this newly thickened endometrial lining with a receptive phenotype capable of supporting embryo implantation and development through vast morphological and physiological changes. The spiral arteries become highly coiled, whilst uterine glands widen, coil and exude a glycogen-rich secretion. Areas of local oedema occur within the stromal layer, the extracellular matrix undergoes substantial remodelling and there is an influx of specialised innate immune cells termed uterine natural killer cells (uNK) (Gellersen and Brosens, 2003, Gellersen and Brosens, 2014, Hanna et al., 2006). Around day 23 of the cycle, coinciding with the closure of the putative window of implantation, stromal fibroblasts are transformed into specialized decidual cells (see section 1.4). In the presence of a viable, implanting embryo trophoblast-derived human chorionic gonadotrophin (hCG) maintains the corpus luteum and upholds progesterone

production permitting the continuation of this supportive environment. In the absence of a viable embryo the corpus luteum will degenerate, resulting in declining progesterone levels which initiates a chain of events culminating in proteolytic breakdown and menstruation.

Humans, fruit bats, elephant shrews and some old world primates are the only species who experience menstruation via monthly shedding of the endometrium (Emera et al., 2012) and display cyclic decidualization, which occurs spontaneously irrespective of the presence of an embryo. In these mammals menstruation and decidualization occur as a result of low and high serum progesterone levels, respectively. Menstruation emulates an inflammatory response highlighted by the high numbers of leukocytes within the endometrial compartment which, prior to menstruation, make up 40% of the entire cell population (Salamonsen et al., 2002). Leukocytes assist the release of pro-inflammatory cytokines, whilst matrix metalloproteases (MMP) induce degradation of the extracellular matrix. Local prostaglandins cause sudden constriction of the spiral arteries leading to ischaemia and shedding of the superficial endometrial decidual cells.

Menstruation is widely viewed as a process of re-initiating a cycle of endometrial preparations for implantation in the absence of a pregnancy. There have been various theories as to why menstruation would be evolutionarily advantageous. It may be that menstruation alleviates the metabolic pressures of supporting a continuously receptive endometrium (Strassmann, 1996) or prevents unnecessary maternal investment in a non-viable conceptus (Teklenburg et al., 2010a). The theory of uterine pre-conditioning suggests that exposure to repeated episodes of inflammation and oxidative stress associated with cyclic shedding and renewal of the endometrium and its vasculature serve to prepare the endometrium for deep placentation and protect against hyper-inflammation (Brosens et al., 2009).

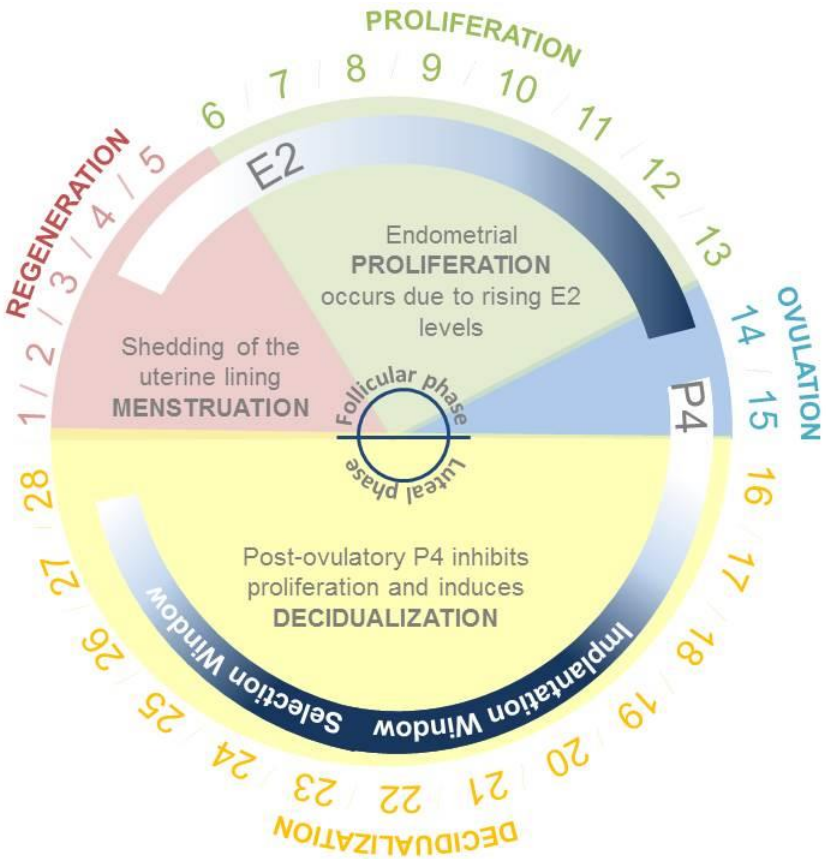

Figure 1.3.1: The Menstrual Cycle

The menstrual cycle occurs under the cyclical influence of the ovarian steroid hormones estradiol and progesterone. It can be divided into the follicular and luteal phases. In the follicular phase the endometrium is shed at menstruation and regenerated via the proliferation of endometrial stem cells under the influence of E_2. In the luteal phase, following ovulation, a rise in progesterone halts the proliferative phase and initiates a highly coordinated differentiation process that cumulates in the decidual transformation of the endometrium. Decidualization endows the endometrial stromal cells with migratory and selective capabilities required for embryo selection. Adapted from (Cha et al., 2012).

1.4 Decidualization of the Endometrium

Decidualization denotes the extensive remodeling process that the endometrium must undergo to support an implanting embryo. The decidual process is foremost characterised by the morphological transformation of elongated stromal fibroblasts into rounded, secretory decidual cells. This process is initiated during the mid-luteal phase of the cycle, coinciding with the endometrium transiently acquiring a receptive phenotype (Figure 1.4.1), although the characteristic decidual cell morphology in vivo becomes more prominent during the late-luteal phase. This 'window of implantation' starts approximately 6 days after the surge in luteinizing hormone (LH) and is thought to last no longer than 2-4 days.

Decidualization is induced by sensitization of the oestrogen-primed cells to a post-ovulatory rise in progesterone and rising intracellular cyclic adenosine monophosphate (cAMP) levels during the luteal phase. This remodeling process is first initiated at terminal spiral artery sites before extending throughout the endometrium and is accompanied by an influx of specific immune cells (Gellersen and Brosens, 2003).

A complex system of signaling pathways, transcription factors and cross-talk underlies this decidual reaction (Christian et al., 2002). The resulting morphological and biochemical changes are dramatic and involve the secretion of prolactin (PRL), insulin-like growth factor binding protein-1 (IGFBP-1) and numerous other factors, including; the NODAL-signaling pathway inhibitor LEFTY2, BMP2 (bone morphogenetic protein 2) and WNT4 (wingless-type MMTV integration site family, member 4) (Gellersen and Brosens, 2003, Gellersen et al., 2007, Gellersen and Brosens, 2014). Modifications at the cellular level include; extracellular matrix and cytoskeletal remodeling, expansion of cytoplasmic organelles and acquisition of a secretory phenotype, transcription factor modulation and altered expression of

numerous intracellular enzymes and signalling pathways (Gellersen and Brosens, 2014). Importantly, the decidual phenotype is not static. Instead, human endometrial stromal cells (HESCs) transit through distinct functional phenotypes, characterized initially by an acute pro-inflammatory response, which is followed by an anti-inflammatory response and acquisition of the characteristic rounded decidual cell morphology. The transient inflammatory stromal response induces the expression of receptivity genes, including leukemia inhibitory factor (LIF), interleukin-1 beta (IL-1β) and heparin-binding EGF-like growth factor (HB-EGF) (Salker et al., 2012); whereas acquisition of a mature decidual phenotype coincides with closure of the window. Failure to establish a receptive phenotype or premature closure of the receptivity window inevitably leads to implantation failure (Koot et al., 2016). Conversely, a disordered and prolonged pro-inflammatory decidual response promotes out-of-phase implantation and is associated with miscarriage (Muter et al., 2015, Salker et al., 2010, Salker et al., 2012).

The endometrium at implantation is characterized by an abundance of immune cells, predominantly uNK cells, macrophages and dendritic cells. These accumulate around the trophoblast cells at the implantation site (Mor et al., 2011). Yet, rather than inducing rejection of the embryo, as in the tissue allograft model, the influx of immune cells during decidualization promotes implantation and placentation. In fact, a depletion of immune cells in the decidua results in termination of pregnancy (Cha et al., 2012). The process of implantation may thus be described as secondary to the development of a pro-inflammatory phenotype (Cha et al., 2012). During implantation, uNK cells are crucial for trophoblast invasion, enabling the cells to permeate the stroma and reach the endometrial vascularity (Mor et al., 2011). Maternal immunologic tolerance of the embryo is achieved through entrapment of dendritic cells by decidual cells (Cha et al., 2012). This prevents a T cell-mediated immunological reaction by preventing contact of maternal T cells with fetal or

placental antigens. Epigenetic changes upon decidualization silence inflammatory chemokine genes, restricting chemokine expression within the decidua and preventing the recruitment of activated T cells to the sites of inflammation (Cha et al., 2012). Modifications during the transformation of HESCs into decidualized endometrial stromal cells (DESCs) also enable the maintenance of progesterone signalling and cellular homeostasis under the oxidative stress conditions imposed by pregnancy. Silencing of c-Jun N-terminal kinases (JNK) in DESCs averts hypersumoylation in response to reactive oxygen species (ROS) preventing transcriptional inhibition of the progesterone receptor (Leitao et al., 2010).

Errors during decidualization have been connected to adverse events later in pregnancy including placental defects, growth restriction and pre-term birth. Risk factors found to induce cellular senescence are also responsible for triggering pre-term birth. Furthermore, pre-term birth is more prevalent amongst women of advanced maternal age, suggesting a role for senescence in the induction of parturition. Mice with a uterine deletion of transformation-related protein 53 (Trp53) display normal implantation accompanied by increased rates of pre-term birth, fetal dystocia and death. Interestingly, these mice also exhibit defective decidualization and display higher levels of terminally differentiated, polyploid stromal cells. More recently, recurrent miscarriage (RM) has been associated with increased premature senescence of HESCs, resulting in aberrations of the decidual secretome that orchestrate early implantation events (Lucas et al., 2015).

Simultaneous to decidualization, histotrophic support is initiated, ensuring long-term growth and survival of the conceptus (Brosens et al., 2014, Burton et al., 2002). Due to the invasive nature of human implantation, perfusion of the developing conceptus was thought to provide nutritional support in the early stages of pregnancy. However, plugging of distal portions of the spiral arteries by

cytotrophoblast cells restrict significant blood flow to the placenta until 10-12 weeks of gestation (Hustin and Schaaps, 1987, Burton et al., 1999). Histotrophic support by uterine glands, HESC secretions and plasma filtrate from the endometrial vasculature is thus thought to support embryo and fetal development during the first trimester (Burton et al., 2002). An anaerobic, histotrophic environment is thought to be optimal for cellular differentiation during eutherian organogenesis as it minimises DNA damage and ROS (Burton et al., 2002). Uterine gland secretions enrich placental development during this phase, producing immunosuppressive cytokines that allow maternal tolerance of the placenta and assist remodelling of the utero-placental vessels (Burton et al., 2002).

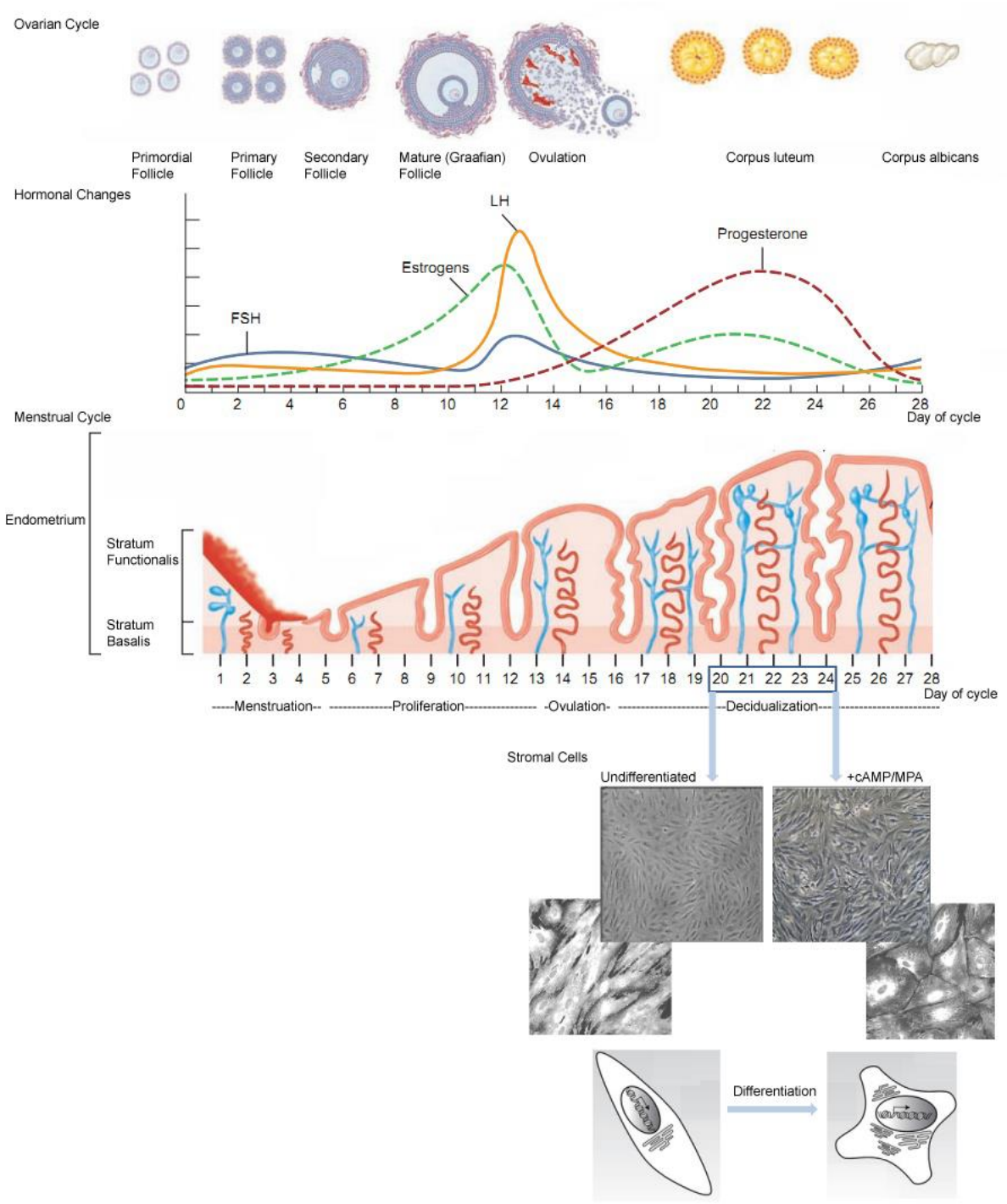

Figure 1.4.1*:* Decidual Transformation

Decidualization occurs in the mid-secretory phase of the menstrual cycle following a post-ovulatory rise in progesterone. Decidualization of HESCs can be achieved *in vitro* by treatment with a cell permeable cAMP analogue (8-br-cAMP) and a synthetic progestin MPA. Adapted from (Wiley, 2015, Brosens et al., 2014).

1.5 Implantation

Implantation has been historically described as a step-wise process involving (a) apposition of a polarised embryo to the maternal luminal epithelium (b) adhesion of the embryo to the epithelium at a specific site and (c) invasion resulting from migration of both stromal and trophoblastic cell types, until the embryo is fully encapsulated within the endometrium.

In the pre-existing step-wise model of implantation, the embryo was seen as the sole determinant of implantation outcome, actively invading a relatively passive endometrial matrix. This was supported by evidence of aggressive invasion of spiral arteries by endovascular extravillous trophoblast cells, in a manner likened to tumour metastasis (Ferretti et al., 2007). However, this view has since shifted in line with evidence for the endometrium in regulating the timing and extent of embryo invasion.

In humans, cyclical maternal preparations initiated by steroid hormone changes prime the endometrium for potential implantation and bestow spatiotemporal control over embryo implantation through the instruction of a 'window of implantation', as discussed previously (Koot et al., 2012, Gellersen and Brosens, 2003). This phase of receptivity occurs between day 20 and day 24 of the menstrual cycle (LH + 6 and LH + 10) and acts as a self-limiting time frame to ensure the synchronicity of endometrial and embryonic development. The restriction of endometrial receptivity in this way thus acts as a quality control mechanism which reduces the chance of maternal investment in non-viable embryos.

At the embryo-maternal interface during the time of implantation, overlying endometrial epithelial cells first make contact with the trophectoderm layer of the blastocyst. The endometrial epithelium has traditionally been viewed as a barrier to

implantation following evidence that mouse blastocysts could implant at any stage upon damage to this cellular compartment (Cowell, 1969) (Figure 1.5.1). Whether or not the luminal epithelium is a true barrier to implantation in humans has recently been challenged (Lucas et al., 2013). A barrier is essential in polytocous species, such as mice, where reproductive success is critically dependent on synchronized implantation of multiple blastocysts. Mouse embryos are capable of temporarily suspending development while awaiting the right maternal signals for implantation, a process termed embryonic 'diapause' (Lopes et al., 2004). This maternal signal is a surge in ovarian estradiol, which triggers synchronized implantation of chromosomally stable mouse embryos (Hamatani et al., 2004). However, human embryos do not normally exhibit diapause, are highly invasive and often chromosomally unstable (as discussed in section 1.9). In view of these characteristics, it has been argued that human embryos may rapidly breach the luminal epithelium unimpeded. Furthermore, recent co-culture studies have demonstrated the ability of DESCs to actively migrate towards and engulf hatched blastocysts (Grewal et al., 2008, Teklenburg et al., 2010b). In this model, implantation is critically determined by the initial embryo-decidual cell interactions.

Clues to the mediators of implantation require an understanding of the synchronised changes in both the endometrial milieu and the embryo at the time of implantation. *In vitro* cell cultures, animal models and clinical studies have enabled further understanding of the key factors involved at implantation (Table 1.5.1). Yet distinguishing between the maternal and embryonic contributions to successful implantation, as well as recognising the intra-species differences, provide ongoing challenges to this area of research.

Gene deletions, primarily in mouse models (Table 1.5.2), and expression profiling of human endometrial samples propose a preserved network of regulatory genes and

factors as critical in establishing a state of endometrial receptivity (Teklenburg et al., 2010a). The use of microarray technology has generated a wealth of gene expression data that requires further annotation and investigation in order to establish key regulators of the implantation process (Koot et al., 2012). Transcription factors, growth factors, cytokines and adhesion molecules have all been implicated in this pathway but not yet conclusively enough to be applied to the therapeutic setting of pregnancy failure.

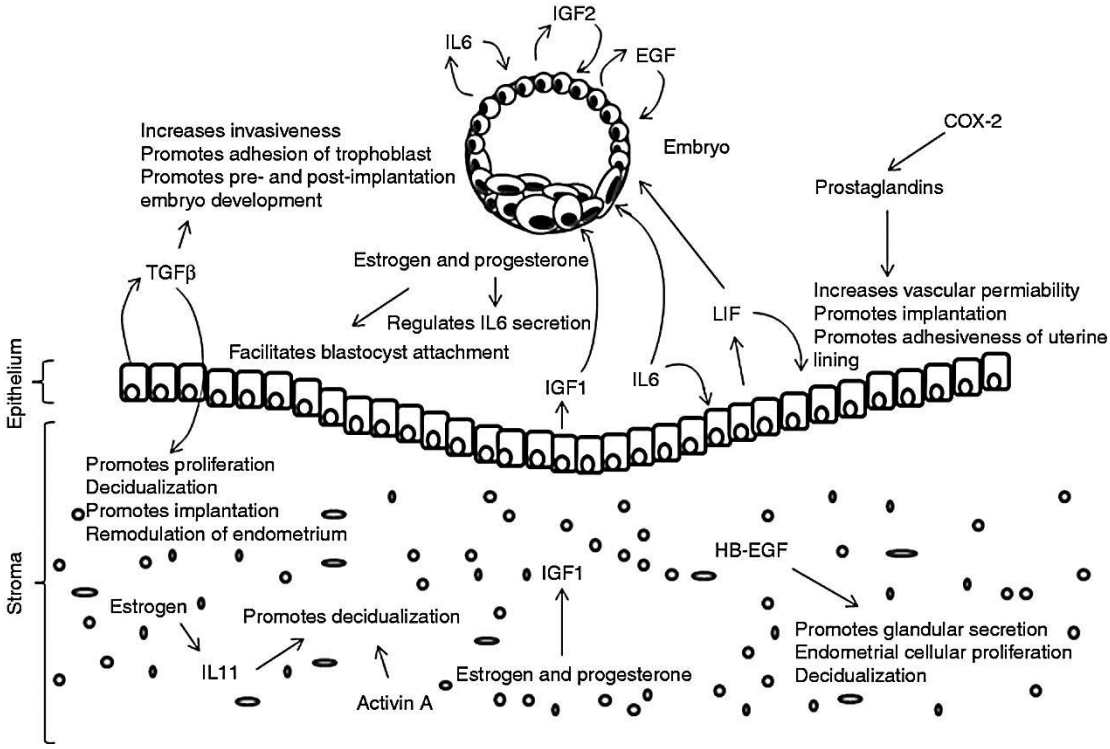

Figure 1.5.1 Cross-talk at Implantation

The expression of key growth factors, cytokines and hormones at the time of implantation highlights that the process involves cross-talk between the embryo, the endometrial epithelium and the underlying stromal compartment. From (Singh et al., 2011).

Table 1.5.1 Key Factors at Implantation

	Features	Role in Implantation	References
Cadherins	Required for calcium dependent cell-to-cell adhesions	P4 dependent expression of E-cadherin via calcitonin. E-cadherin downregulation is thought to be involved in embryo invasion.	Li et al., 2002; Achache and Revel, 2006
IL-1	Pro-inflammatory cytokine able to induce a range of responses in a variety of cell types Produced by macrophages, trophoblast and stromal cells. IL-1 agonists, IL-1α and IL-1β, are ubiquitously expressed in stromal, epithelial and endothelial cells. Yet IL-1α is expressed more strongly in human endometrium and upregulated in LE during the secretory phase Attributed to integrin regulation (increased integrin β3 expression seen in HEEC cultures supplemented with IL-1)	Thought to mediate embryonic-endometrial cross-talk at implantation IL-1 deficient mice are able to achieve pregnancy, yet implantation rates fall with injections of an IL-1 receptor antagonist IL-1 secretion by human embryos is quantifiable by ELISA in samples of embryo conditioned media, in contrast to IL-6 which was undetectable Levels in ECM are higher from successfully implanted embryos compared to those that failed to implant	Simon et al., 1994; Baranao et al., 1997; Simón et al., 1997; Tabibzadeh and Sun, 1992
IL-6	Induces an immune response upon secretion by T-cells and macrophages IL-6 receptors are detectable in both endometrium and blastocyst during implantation indicative of a paracrine/autocrine role	IL-6 deficient mice display reduced fertility due to implantation defects Abnormal IL-6 expression has been reported in RM patients Expression higher in HEECs than DESCs and induced by IL-1 in DESCs	Achache and Revel, 2006; Lim et al., 2000; Cork et al., 1999; Von Wolff et al., 2000; Laird et al., 2003; Laird et al., 1994

Integrins	Transmembrane glycoproteins involved in cell adhesion Identified as regulators of implantation in both the human and mouse $\alpha_v\beta_3$, $\alpha_3\beta_1$, $\alpha_6\beta_4$ and $\alpha_v\beta_5$ are expressed on the outer surface of blastocysts	Display steroid activation, up-regulation during the receptive phase (αVβ3 expression coincides with the WOI) Widely implicated in endometrial receptivity (Aberrant αVβ3 expression in unexplained infertility), embryo apposition and adhesion Proposed role in embryo spacing in mice Extent of their individual significance, mechanism of action and cross-talk in human pregnancy remains controversial	Aplin, 1997; Quenby et al., 2007; van Mourik et al., 2009; Klentzeris et al., 1993; Lessey et al., 1995
Leukaemia inhibitory factor (LIF)	A secreted glycoprotein that affects cell growth by regulating differentiation Promotes trophoblast differentiation toward an anchoring extravillous phenotype Co-culture of embryos with LIF expressing embryonic trophoblasts and recombinant LIF significantly enhanced blastocyst development, expansion and hatching Present in human endometrium and peaks in the secretory phase of the menstrual cycle LIF receptor mRNA has been identified on human blastocysts *in vitro* Enhanced embryo development in the presence of LIF at the late developmental stages (morula and beyond)	Increased in uterine flushings of fertile women between days LH+7 to LH+12. Levels were lower in women suffering from unexplained fertility (on day LH+10) Basal levels in HEECs differ according to biopsy timing, being highest at the late proliferative and early secretory phases High doses of estradiol and progesterone reduce LIF levels in HEECs *in vitro* Maternally controlled LIF expression in endometrial glands is highest at the time of implantation (in mice) Application of LIF receptor antagonist (PEGLA) to timed endometrial biopsies impaired blastocyst attachment Down-regulation of AKT and up-regulation of Caspase-3 activation, in the absence of LIF, indicate a role in regulating apoptosis at	Stewart et al., 1992; Dunglison et al., 1996; Jurisicova et al., 1999; Lalitkumar et al., 2013; Nachtigall et al., 1996; Kauma and Matt, 1995; Tsai et al., 1999; Arici et al., 1995; Charnock-Jones et al., 1994; Kojima et al., 1994; Bhatt et al., 1991; Laird et al., 1997

	Addition to media reported to increase blastocyst formation rates from 18.4% to 43.6%, but contradictory evidence exists Stromal secretion of LIF is enhanced by embryonic IL-1, TNFα, PDGF and TGFβ	implantation LIF-/- mice display impaired implantation (partially corrected by peritoneal infusion of LIF) yet LIF-/- blastocysts implant in wild-type pseudopregnant recipients RIF patients display reduced LIF induction from the proliferative to secretory phase However recombinant LIF administration to RIF patients failed to increase implantation rates	
Micro RNA (miRNA)	Involved in post-transcriptional regulation of gene expression though regulation of mRNA stability	13 miRNAs (that putatively regulate the expression of 3800 genes) were found to be differentially expressed in endometrial samples of RIF patients, compared to controls	Revel et al., 2011; Kuokkanen et al., 2010
Mucins	Highly glycosylated, large molecules found on apical LE cells Protect the mucosal surface from infection and the action of degradative enzymes Seen as a barrier to implantation as they cover the endometrium Loss of electronegative sulphated glycan from MUC-1 in the apical LE should encourage apposition of the blastocyst	MUC-1 is cycle dependent and acts as a barrier to implantation in mice Progesterone and estradiol priming induces up-regulation of MUC1 in receptive endometrium Human blastocysts express MUC1 in the TE and increase MUC1 expression in EEC but induces paracrine cleavage at the implantation site RIF patients display low MUC-1 levels	Aplin et al., 1996; Aplin, 1997; Meseguer et al., 2001
Pinopodes (endometrial apical plasma membrane protrusions)	Present on apical surface of LE during WOI Progesterone dependent expression Involved in endocytosis and pinocytosis Expressed throughout the luteal phase and early pregnancy	Originally thought to assist embryo apposition No direct role in embryo-endometrial interactions High level of inter-patient variation regarding their timing within the uterus Expression not restricted to the WOI	Bentin-Ley, 2000; Nikas et al., 1995; Nikas and Psychoyos, 1997; Quinn et al., 2007

Prostaglandins	Modulators involved in immune cell suppression, widely implicated in providing an integral maternal contribution to implantation Possess vasoactive factors which allow access to the maternal vascular system Synthesised by cytosolic phospholipase A2 (cPLA2), COX-1 and COX-2 enzymes, upregulated by P4 Studies of Ptsg2-/- mice highlighted the importance of PGI_2 and proposed a complementary role for prostaglandin-E2 (PGE-2) in implantation PGE_2 acts synergistically with estradiol and MPA to enhance differentiation of HESCs in a dose dependent manner PGI_2 acts via IP (PGI_2 receptor) activating extracellular signal regulated kinase (ERK1/2) and up-regulating pro-angiogenic genes via interaction with EGFR	Delayed implantation in cPLA2 knockout mice, rescued by exogenous PG administration Reduced cPLA2α and COX-2 expression in RIF patients Impaired implantation in estrogen stimulated mice treated with indomethacin (prostaglandin production inhibitor), restored upon PGE_2 treatment (10ug/6ul dose) PGE_2 is increased in endometrial fluid during the WOI in humans and in LE during the peri-implantation period in mice The exact role at implantation has been questioned as PGE-2 receptor (*EP2*) null mice displayed diminished ovulation rather than decidualization or implantation defects Iloprost, a stable PGI_2 analogue, enhances hatching of murine blastocysts and promotes implantation and live birth rates in cattle	Holmes et al., 1990; Holmes and Gordashko, 1980; Frank, 1994; Vilella et al., 2013; Lim and Dey, 1997; Matsumoto et al., 2001; Lim et al., 1999; Milling Smith, 2006; Huang et al., 2004; Song et al., 2009
Selectins	Single chain transmembrane glycoproteins involved in cell adhesion	Binding of L-selectin on the embryo surface to carbohydrate ligands on the maternal epithelium was found to generate a physiologically relevant interaction which enables orientation of the ICM towards the apical epithelium and promotes attachment in human implantation Impaired adhesion results from the application of L-selectin antibodies, but L-selectin deficient mice were found to be fertile	Dominguez et al., 2005; Genbacev et al., 2003

Table 1.5.2 Genes Critical to Implantation: Results of Mouse Knockout Models

Gene	Molecule encoded (Putative function)	Knockout phenotype in females	References
Bsg	Basigin (Immunoglobulin)	Defective fertilization; no implantation	Igakura et al., 1998; Kuno et al., 1998
Esr1	Estrogen receptor-α (NR,TF)	No uterine attachment, but uterine responsiveness to decidualization persists with P_4 priming	Lubahn et al., 1993; Paria et al., 1999
Fkbp52	FK506-binding protein-4 (Immunophilin co-chaperone for steroid hormone NRs)	Compromised P_4 function; no uterine receptivity (ME)	Tranguch et al., 2005
Gp130/Stat	GP130/Signal transducer and activator of transcription (Cytokine-receptor signalling)	No implantation (ME)	Ernst et al., 2001
Hmx3	H6 homeobox-3 (TF)	No implantation (ME)	Wang et al., 1998)
Hoxa10	Homeobox A10 (TF)	Defective decidualization; reduced fertility (ME)	Benson et al., 1996; Lim et al., 1999b; Satokata et al., 1995
Hoxa11	Homeobox A11 (TF)	Defective implantation and decidualization; infertility	Hsieh-Li et al., 1995
Il11ra1	Interleukin-11 receptor-1 (Cytokine signalling)	Impaired decidualization; infertility	Robb et al., 1998; Bilinski et al., 1998
Lif	Leukaemia inhibitory factor (Cytokine)	No implantation (ME)	Stewart et al., 1992
LpA3	Lysophosphatidic acid receptor-3 (LPA signalling)	Deferred, on-time implantation; aberrant embryo spacing; post-implantation defects; small litter size (ME)	Ye et al., 2005
Pgr	Progesterone receptor (NR,TF)	No implantation or decidualization (ME); Lack of decidual response even after P4 priming	Lydon et al., 1995
Pla2g4a	Phospholipase A2, group IVA [cytosolic Ca^{2+} dependent] (Arachidonic-acid-releasing enzyme)	Deferred on-time implantation; aberrant embryo spacing; post-implantation defects; small litter size (ME)	Song et al., 2002
Pparδ	Peroxisome proliferator-activated receptor-δ (NR,TF)	4–6 h delay in initiating embryo attachment; placental defects; subfertility	Lim et al., 1999a; Barak et al., 2002
Ptgs2	Prostaglandin-endoperoxide synthase-2 (Prostaglandin synthesis)	Multiple reproductive failures, including defective attachment reaction; genetic-background-dependent; Defective decidualization; reduced angiogenic response	Lim et al., 1997; Wang et al., 2004; Matsumoto et al., 2001

ME, maternal effect; NR, nuclear receptor; TF, transcription factor (Wang and Dey, 2006)

1.6 Pre-Implantation Embryo Development

Studies of mammalian, predominantly mouse, embryos have supplied fundamental insights into early embryo development (Wang and Dey, 2006). Yet species-specific differences mean that these findings are of limited relevance to our understanding of pre-implantation embryo development in humans. The emergence of ARTs (assisted reproductive technologies), particularly IVF (*in vitro* fertilization) to treat fertility problems, has since formed the key context of our understanding of human pre-implantation embryo development.

Fusion of oocyte and sperm at fertilization initiates the oocyte to embryo transition and is followed by pronuclei migration and fusion. Relative transcriptional silence characterises the first phase of pre-implantation embryo development, whereby genetic and epigenetic modifications and a series of cellular divisions occur entirely dependent on maternally inherited material. This phase incorporates the downregulation and degradation of over 1000 maternal transcripts in humans and terminates with a major wave of embryonic genome activation (EGA). In human embryos this initial phase lasts 3 days, from the 4 to 8 cell stage, and occurs entirely independently of cell number (Braude et al., 1988, Dobson et al., 2004). Timing of EGA activation varies markedly between species being undetectable prior to the 2-cell stage in mice, 4-cell stage in pigs and 8-cell stage in sheep (Braude et al., 1988, Braude et al., 1979, Crosby et al., 1988). Beyond the 8-cell stage human embryos undergo compaction, whereby the outer cells of the morula become tightly connected by desmosomes and gap junctions. This provides the first visible indication of interrupted radial symmetry and beyond this point morphological checkpoints become a function of embryo developmental timing as opposed to cell number. The development of a blastocyst occurs upon subsequent cell divisions and the initiation of a blastocoel cavity at the cavitation stage. A blastocyst may be

characterised by a distinct inner cell mass (ICM) and outer trophectoderm (TE) layer, which surrounds the fluid-filled blastocoele cavity. Prior to implantation the ICM separates into early epiblast, which will form the fetus, and primitive endoderm, which will give rise to extraembryonic endoderm cells which form the yolk sac. Human pre-implantation development largely occurs during passage of the embryo along the fallopian tube towards the uterine cavity. By the time the embryo reaches the blastocyst stage (day 5) it is thought to emerge from the fallopian tube and make contact with the endometrium. Periodic contractions and expansions between day 6 and 7 encourage the blastocyst to hatch from its protective, glycoprotein shell (zona pellucida). Successful convergence of the hatched blastocyst and endometrium at implantation is required for the subsequent survival and development of the human embryo and is thought to occur around day 8.

1.7 Species Differences Pre- and Post- Implantation

Human and mouse embryos similarly undergo cell divisions to form a blastocyst with apparent ICM and TE. Yet despite the morphological resemblance of human and mouse pre-implantation embryos, developmental timings have been found to differ notably between species with human embryo development lagging behind that of the mouse (Figure 1.7.1). A human blastocyst forms between day 5 and 6 of pre-implantation embryo development and typically contains around 256 cells. In contrast the cells of a mouse blastocyst, formed between day 3 and 4, are thought to undergo one less cell division and comprise around 164 cells (Niakan et al., 2012). This delayed embryo development includes a lag in the timing of EGA, compaction and blastocyst formation (Figure 1.7.1).

Species-specific differences extend into the post-implantation period and placentation whereby trophectoderm cell fates and invasive capacity are similarly divergent. In both species the ICM gives rise to the epiblast (Epi) and primitive endoderm (PE) layers, whilst the TE forms the trophoblast lineage of the placenta. The epiblast forms all tissues of the fetus whereas the PE forms the extraembryonic endoderm which creates the yolk sac. In humans the trophectoderm cells form placental cytotrophoblast cells which proliferate and differentiate into multinucleated syncytial cells and extravillous trophoblast which invade the decidualized endometrial cells (Figure 1.7.1) (Norwitz et al., 2001, Moffett and Loke, 2006). In mice, unlike the early invasion seen in humans, TE cells produce a proliferative stem cell pool of extraembryonic ectoderm cells that bud off polyploid trophoblast giant cells via a process of endoreduplication (Figure 1.7.1) (Simmons et al., 2007).

The developmental differences observed between human and mouse embryos may be explained by key molecular discrepancies, including; unique gene expression patterns (Dobson et al., 2004, Wang et al., 2004, Zeng and Schultz, 2005, Bell et al.,

2008), epigenetic modifications (Beaujean et al., 2004, Fulka et al., 2004), predisposition to genetic instability (Vanneste et al., 2009, Vanneste et al., 2011) and a protracted period of transcriptional silence in humans (Braude et al., 1988, Flach et al., 1982).

The process of implantation varies markedly between species. This is evident upon comparison of the physical interactions between the embryonic trophoblast, endometrial luminal epithelial and stromal cells at the 'invasion' stage in key animal models (Figure 1.7.2). In the mouse, the primary animal model used for human implantation, around 10 embryos will implant in a single implantation event. This requires a process of maternally controlled embryonic diapause whereby suspension of embryo development, via cell cycle arrest and reduced metabolism, delays implantation (Lopes et al., 2004). This permits the coordination of embryo development according to endometrial readiness for implantation. The implantation of multiple embryos requires unique mechanisms of embryo spacing throughout the uterine horn whilst uterine oedema and luminal closure appear to cause apposition of the maternal luminal epithelium to the spatially restricted murine embryos (Wang and Dey, 2006). In contrast, human implantation generally involves the acceptance of a single, highly invasive and often chromosomally abnormal embryo, with no known maternal control over its development. In humans the feature of uterine closure is entirely absent and the embryo has been described as a 'free-floating body' within the uterine cavity requiring an entirely distinct process of apposition (Genbacev et al., 2003). Interspecies variation in placentation and pregnancy (Table 1.7.2) highlights an evolutionary divergence in the degree of maternal investment in the conceptus. This presents a role for stringent embryo selection at the human maternal-embryo interface.

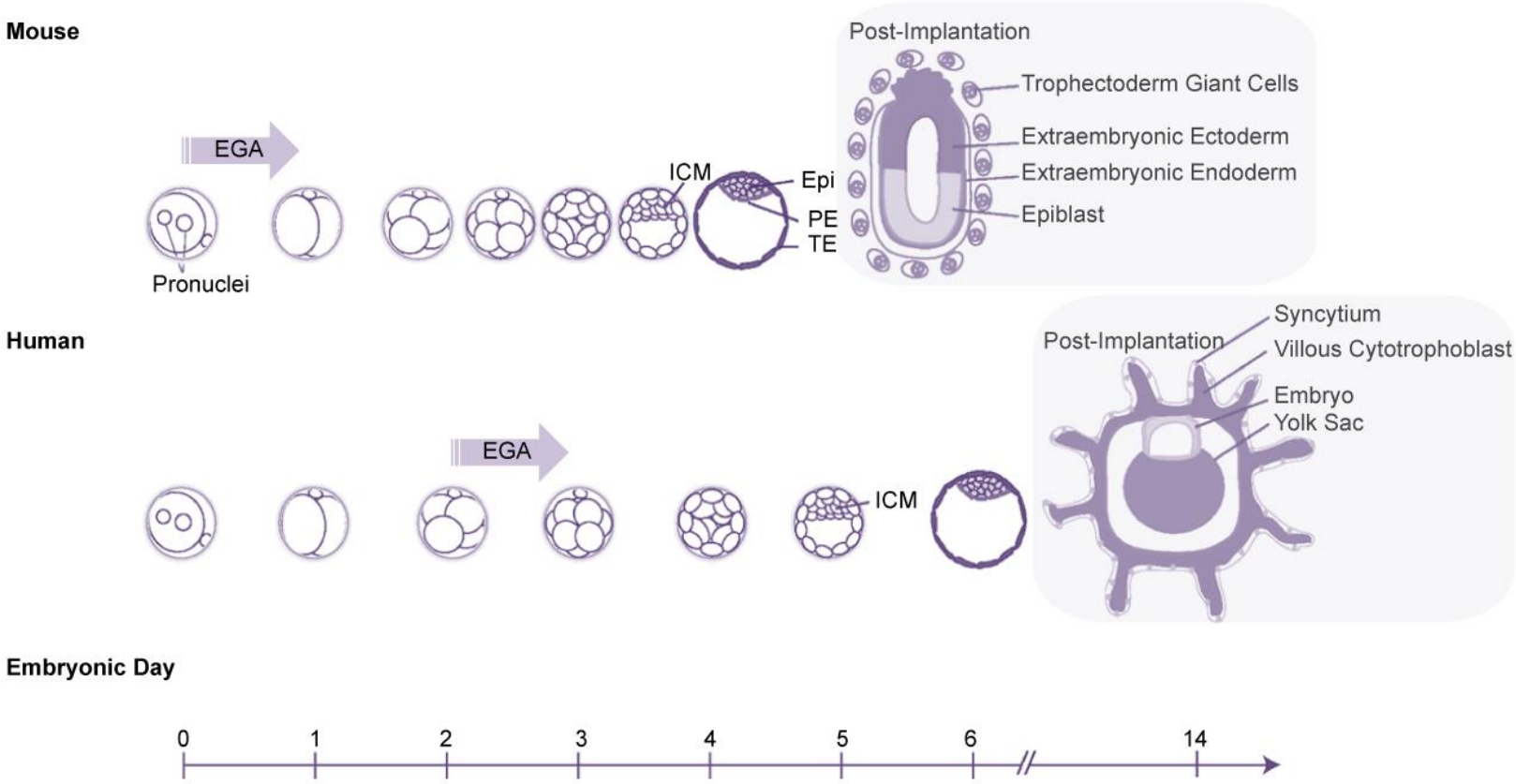

Figure 1.7.1 Developmental Timing and Cell Fate Decisions in Human and Mouse Pre-Implantation embryos.
Embryonic genome activation (EGA), inner cell mass (ICM), epiblast (Epi), primitive endoderm (PE), trophectoderm (TE). Adapted from (Niakan et al., 2012).

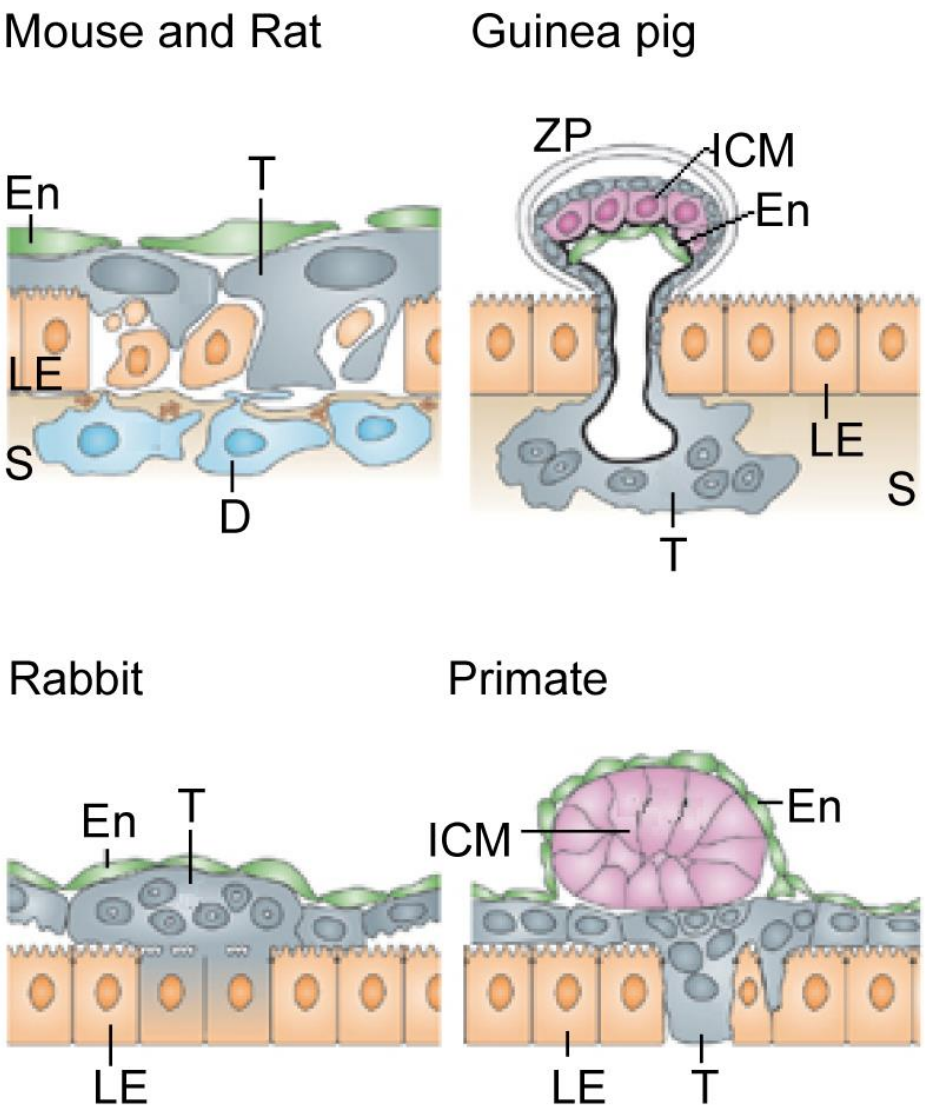

Figure 1.7.2 Distinct Modes of Implantation in Various Species

The key objective of implantation is anchorage of the trophoblast (T) into the stroma (S). In mice and rats the embryonic endoderm (En) attaches to the luminal epithelium (LE), inducing localised apoptosis of the LE and permitting T migration into the S. D = decidual cells. In guinea pigs focal protrusions of the zona pellucida (ZP) by the syncytial trophoblast is followed by embedding of trophectoderm into the S. In rabbits, clusters of trophoblast cells fuse with the LE to form symplasma. In mammals the trophectoderm derived T breaches the LE and migrates into the underlying S. Adapted from (Wang and Dey, 2006).

Table 1.7.1 Comparison of pregnancy and placentation in mice and humans

	Mouse	Human
Implantation	Secondarily interstitial	Primary interstitial
Yolk sac	Inverted yolk sac placenta functions to term	Yolk sac floats free in exocoelom during first trimester
Trophoblast invasion of uterine arteries	Shallow; limited to proximal decidua	Extensive; reaching myometrial vessels
Transformation of uterine arteries	Dependent on maternal factors (uNK cells)	Dependent on trophoblast
Area of placental exchange	Labyrinthine	Villous
Trophospongium	Three trophoblast layers; outer one cellular, inner two syncytial	Absent
Interhaemal barrier	Extensive	Single layer of syncytial trophoblast
Placental hormones	Placental Lactogens	hCG, hPL, Placental Growth Hormone; major source of Progesterone
Time of Gestation	Three weeks	Nine months

1.8 Challenges of Human Reproduction

The efficiency of human reproduction is low when compared to other mammalian species. Humans display a monthly fecundity rate (chance of achieving a pregnancy in a single menstrual cycle) of ~20-30%, compared to 80% in baboons and 90% in rabbits (Chard, 1991, Foote and Carney, 1988, Stevens, 1997). Despite medical assistance being available to address fertility problems in humans, embryo transfers following ARTs only result in pregnancy in around 50% of cases (Boomsma et al., 2009). Furthermore, over 50% of these conceptions are estimated to ultimately end in pregnancy failure due to the additional human challenges of embryo wastage and increased pregnancy loss (Macklon et al., 2002). The rate of pregnancy loss, in humans, has been estimated as occurring most commonly during early pregnancy, prior to 6 weeks gestation (Figure 1.8.1). Yet the clinical pregnancy loss at 12 weeks gestation is estimated to be 10-15 % (Chard, 1991, Macklon et al., 2002). RM, defined as 3 or more consecutive losses, affects 1-2% of fertile couples (Jauniaux et al., 2006, Rai and Regan, 2006). Pre-clinical pregnancy loss therefore presents an additional reproductive challenge in humans and is distinct from subfertility (Koot et al., 2010).

Pregnancy loss, whether sporadic or recurrent, is thought to originate from aberrations either of the embryo (chromosomal or developmental) or the uterine environment. Yet no specific anatomical, immunological, endocrine or genetic aetiologies have been predominantly linked with RM. Rather, an association between decreased time to pregnancy (TTP) and RM has been observed. The anecdotal notion of superfertility, determined by a TTP $\leq$3 months, is estimated to affect 3% of the population (Macklon et al., 2002). A retrospective analysis of 560 patients affected by RM revealed that 40% could be defined as ‘superfertile’ (Salker et al., 2010). In association with a decreased TTP, the superfertile population

experience fewer pre-clinical pregnancy losses, but greater post-clinical losses (Figure 1.8.1). These findings have led to the development of a 'receptivity versus selectivity' paradigm (Figure 1.8.1).

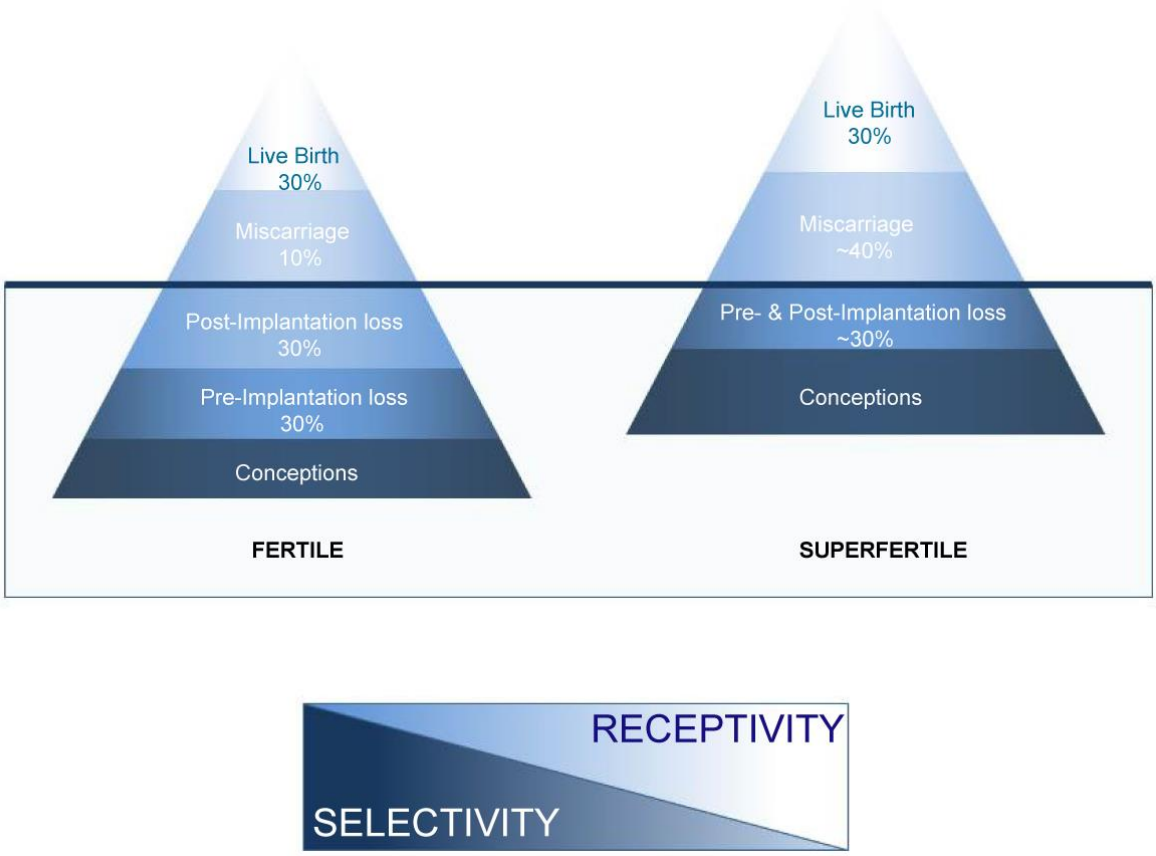

Figure 1.8.1 The Embryo Wastage Iceberg

The outcome of conceptions in fertile and superfertile populations, whereby the 'sea-level' distinguishes pregnancy losses before the missed menstrual period and clinically recognised pregnancies. Adapted from (Teklenburg et al., 2010a).

1.9 Embryo Selection or ‘Biosensoring’

The need for embryo receptivity to be coupled with selectivity in humans is in line with the characterisation of pre-implantation human embryos as highly invasive and frequently chromosomally abnormal. Human pre-implantation embryos were first characterised in the 1950s, where they were extracted from volunteers undergoing elective hysterectomy (Hertig et al., 1954, Hertig et al., 1956). Even during this early work, it was hypothesised that developmental abnormalities affect up to 50% of all human embryos, *in vivo*. Subsequent genetic studies have confirmed that human embryos exhibit chromosomal aberrations at a rate ten times that of other mammalian species (Macklon and Brosens, 2014, Vanneste et al., 2009, Wells and Delhanty, 2000, Voullaire et al., 2000). Cytogenetic analysis of oocytes and embryos, via array-based comparative genomic hybridization (aCGH), revealed a diverse array of chromosomal abnormalities, which have not been observed later in pregnancy (Fragouli et al., 2013). In this study, only 26% of 420 oocytes examined were found to be haploid after the completion of meiosis II, with errors being largely attributable to premature separation of sister chromatids. A transient increase in aneuploidy rate, reaching 83%, was observed amongst 754 embryos at the cleavage stage with 20-25% of these embryos displaying complex chromosomal abnormalities (Fragouli et al., 2013). Yet 58% of 1046 blastocysts were found to contain aneuploidies with 10% being highly abnormal (Fragouli et al., 2013). These findings suggest that chromosomal abnormalities are tolerated during the first embryo divisions, where a reliance on maternal transcripts and proteins persists. EGA around the 4-8 cell stage is then thought to cease further division or activate cell-regulatory mechanisms that enable clearance of abnormal cells. However, this method of ‘self-correction’ from cleavage to the blastocyst stage is by no means unanimous as the resulting majority of embryos exhibit mosaicism, despite appearing morphologically normal (Mertzanidou et al., 2013, Fragouli et al., 2013).

Although aneuploidy affects around 5% of clinical pregnancies, most of which result in miscarriage (Hassold and Hunt, 2001), the prevalence of abnormalities amongst embryos is far greater. This paradigm suggests a loss of abnormal embryos, via selection, around the time of implantation.

Recently, theories have emerged regarding the evolution of aneuploidies amongst human embryos and suggest that rather than being entirely detrimental, they may in fact confer an implantation advantage, comparable to cancer cells (Brosens et al., 2014). Nevertheless the sheer variation observed amongst human embryos calls for selectivity in order to restrict maternal investment to only viable embryos. Thus the high rates of implantation failure and pre-clinical pregnancy losses in humans may in fact reflect a stringent selection mechanism imposed by maternal tissues.

Evidence for a discerning endometrium originated from studies in cattle, whereby embryos of differing origins induced differential endometrial gene expression patterns upon pregnancy (Sandra and Renard, 2011). This work introduced the concept of the endometrium as a biosensor of embryo quality, which has since been extended to humans. Adequately decidualized HESCs not only sense embryo quality but also respond selectively in order to eliminate compromised embryos (Weimar et al., 2012a, Salker et al., 2010, Brosens et al., 2014). The observation that HESCs from women suffering from RM are unable to discriminate between human embryos according to embryo quality (Weimar et al., 2012b) indicates that biosensoring by the endometrium is a pre-requisite to successful pregnancy.

1.10 Embryo-Derived Signals

Human embryonic signals have been shown to differentially regulate maternal gene expression when separated into two groups representing good and poor quality embryos (Brosens et al., 2014). Signals from embryos deemed unsuitable for transfer (developmentally incompetent embryos (DIE)) were found to alter the expression of 447 human and 544 murine genes when cultured with HESCs or flushed through the uterus of a mouse, respectively. In stark contrast only 13 human genes and 90 murine genes were affected by the presence of signals from successfully implanted embryos (developmentally competent embryos (DCE)) (Figure 1.10.1). This work highlights the prescence of a conserved embryo-derived signal, able to convey develomental potential to the maternal cells in order to actively promote or prevent implantation. In addition, this signal appears to be preserved within human embryo culture supernatants.

A recent study investigated how embryo-derived signals might control chemical signals within the endometrium in order to influence decidualization of the stromal cell compartment, despite the lack of direct cell-cell contact (Ruan et al., 2012). Although it has long been considered a barrier to implantation in humans, the endometrial epithelium is a crucial pre-requisite for decidualization in the mouse (Lejeune et al., 1981). In mice, in the presence of an intact endometrial epithelium, decidualization may be induced purely by mechanical stimuli, such as oil or air intraluminal injection (Finn, 1966) or endometrial scratching (Lejeune et al., 1982).

Serum and glucocorticoid-inducible kinase (SGK1), known to regulate epithelial ion transport and cell survival, was found to be upregulated particularly in the luminal epithelium of mid-secretory endometrial biopsies from women with unexplained infertility (Salker et al., 2011). Furthermore, SGK1 was downregulated in biopsies from women with RM and DESCs from these patients were sensitized to oxidative

cell death (Salker et al., 2011). *Sgk1*$^{-/-}$ mice showed unaffected implantation rates but exhibited pregnancy complications including bleeding at the decidual-placental boundary, fetal growth retardation and compromised induction of pregnancy-specific genes involved in oxidative stress defences (Salker et al., 2011). These findings suggest that SGK1 in the luminal epithelium plays a protective role against oxidative damage at the feto-maternal interface required for successful implantation and the prevention of pregnancy complications.

Epithelial Na^+ channel (ENaC) channels, located in the apical epithelium, have been shown to be up-regulated at the peri-implantation period in mice (Kellenberger and Schild, 2002). They play a role in water and electrolyte resorption, with potential to influence uterine closure seen at implantation in mice, and are known to be activated by mechanical stimuli and serine proteases (Kleyman et al., 2009, Vallet et al., 1997, Fronius and Clauss, 2008). Serine proteases, such as trypsin, are known to be abundant at the embryo-endometrial interface, released by murine embryos and essential for implantation, although there are as yet no reports implicating embryo-derived trypsin proteases in human implantation (Salamonsen and Nie, 2002, Sawada et al., 1990).

Ruan et al. (2012) found that the treatment of murine endometrial cell cultures with trypsin (20ug ml^{-1}) induced morphological changes that mimicked decidualization (Ruan et al., 2012). The group illustrated that trypsin acted via ENaC in epithelial cells, to produce a sustained $[Ca^{2+}]_i$ rise which facilitated a cyclooxygenase-2 (COX-2) dependent increase in prostaglandin E_2 (PGE_2) release (Figure 1.10.2). These findings are significant as the activities of voltage sensitive calcium channels, which can be activated by membrane depolarization, have been implicated as a pre-requisite for decidualization in the mouse (Sakoff and Murdoch, 1996). Furthermore, PGE_2, formed from the enzymatic conversion of Phospholipase A_2

(PLA_2)-derived arachidonic acid by cyclooxygenases at the endometrial stromal-epithelial interface, is known to be essential for decidualization (Ruan et al., 2011) and Ca^{2+} mobilisation has been shown to enable COX2-dependent PGE_2 production (Ruan et al., 2008).

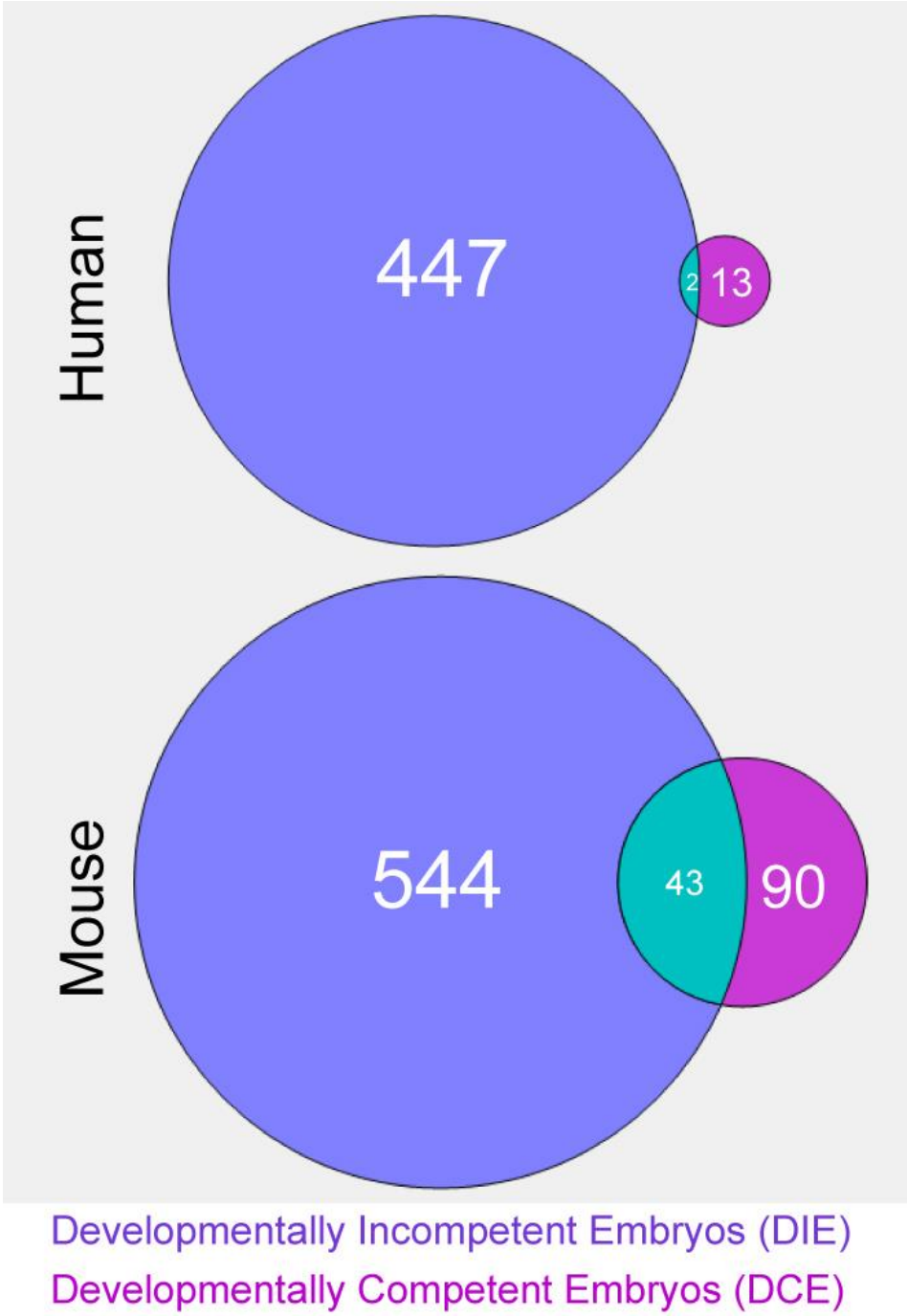

Figure 1.10.1 Human embryo signals elicit a conserved gene response in human DESCs and whole mouse uterus. Quantitative Venn Diagram to show the number of transcripts significantly (*P* <0.01) regulated in DESC (Human) and whole mouse uterus (Mouse) by exposure to signals from succesfully implanted embryos (DCE) versus poor quality embryos (DIE). (Brosens et al., 2014)

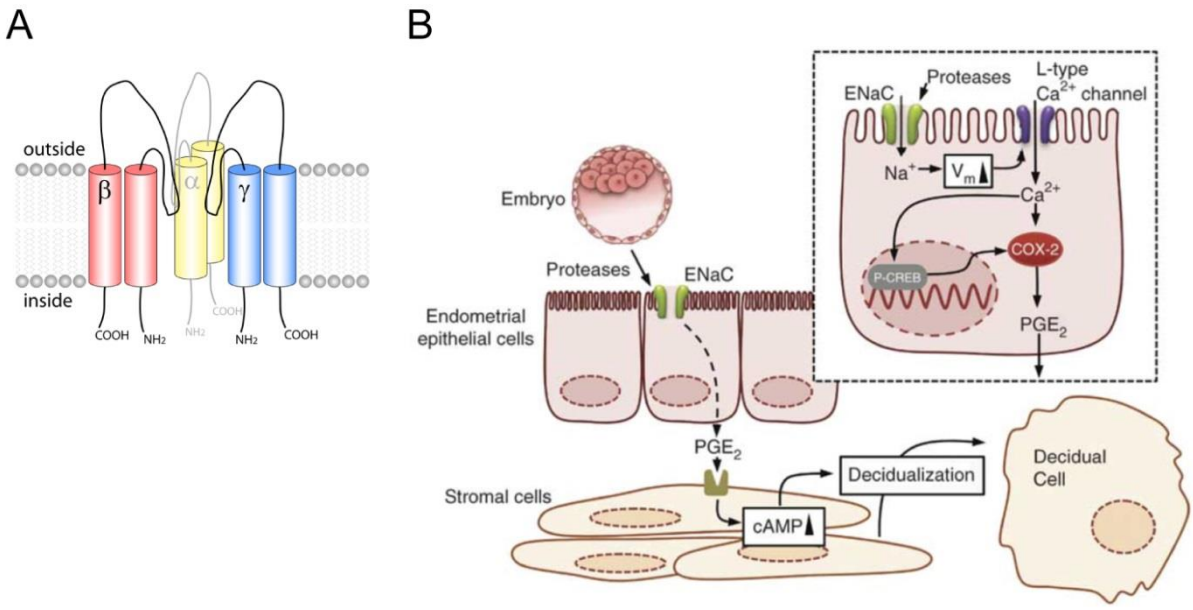

Figure 1.10.2 Embryo derived proteases are capable of mounting an implantation response in the endometrial stromal cells via activation of the epithelial sodium channel (ENaC). a) ENaC channels are transmembrane ion channels which contain 3 structurally related subunits α, β and γ. The α and γ subunits, in particular, are targets of proteolytic processing with cleavage by proteases, such as trypsin, facilitating transepithelial Na^+ transport causing epithelial cell membrane depolarization. b) Epithelial cell membrane depolarization resulting from cleavage and activation of ENaC activates L-type Ca^{2+} channels resulting in Ca^{2+} influx and up-regulation of COX-2 expression in endometrial epithelial cells. The resulting release of PGE_2 activates cAMP-related pathways contributing to decidualization in stromal cells. Adapted from (Ruan et al., 2012) and (Wikimedia, 2015)

1.11 ARTs

A prolonged time-to-pregnancy coupled with a far higher rate of pregnancy losses in humans compared to alternate species has led to the development of many ARTs in order to address the fertility-related challenges (Wilcox et al., 1989). As of 2012, it was reported that the use of ARTs has now given rise to over 5 million offspring (European Society of Human Reproduction and Embryology, 2012).

ARTs were first introduced in order to increase the chances of conception in cases of severe subfertility and studies first began in animal models. Artificial insemination was first performed, in dogs, as early as 1785 (Spallanzani, 1785). Between 1950 and 1970 animal oocyte and sperm retrieval were routine and, in some species, optimised embryo culture conditions had even been established (Reviewed by; Jones, 2003, Clarke, 2006). The breakthrough in human ARTs came in 1969 when IVF was first described using human oocytes (Edwards et al., 1969). Human embryo culture, at the cleavage stages, was subsequently reported in 1970 and by 1978 the first IVF conceived baby, Louise Brown, was born (Edwards et al., 1970, Steptoe and Edwards, 1978, Edwards et al., 1980).

Increasing patient demand, rather than enhanced understanding, led to the emergence of ARTs as a newly recognised medical practice. The increasing popularity of subfertility treatments has resulted in numerous technological advances in the field namely; improved culture conditions of pre-implantation embryos, intra-cytoplasmic sperm injection (ICSI) and enhanced gamete and embryo cryopreservation techniques (e.g. vitrification). However, it has been calculated that only 5% of oocytes collected in a fresh IVF cycle and only 36.5% of top quality embryos transferred will actually result in a live birth (Patrizio and Sakkas, 2009, De Neubourg et al., 2004).

It is not yet fully understood whether this high rate of gamete and embryo wastage reflects the *in vivo* human condition or the limitations of our *in vitro* laboratory techniques. Animal work would suggest that *in vitro* culture detriments embryo gene expression, morphology, metabolic activity and developmental kinetics but the effect in humans is undetermined (Knijn et al., 2006, Corcoran et al., 2006, Lonergan and Fair, 2008, McHughes et al., 2009, Holm et al., 2002, Lopes et al., 2007).

Our incomplete understanding of human pre-implantation embryo development, and reliance on divergent animal models, thus continues to limit IVF success rates. The development of *ex vivo* human models of early- and post-implantation events would undoubtedly promote ART success yet these remain restricted by ethical limitations and a scarcity of research embryos.

An apparent need remains for increased understanding of implantation in humans, which involves both embryo and endometrial counterparts. Assessing *in vitro* embryos, which are known to differ from their *in vivo* derived equivalents, independently from the implantation environment fails to contextualise the challenge of human reproduction. As a result the treatment of reproductive difficulties via IVF, despite continual technological advances, commonly leads to a failed pregnancy.

1.12 Hypothesis and Aims

Despite decades of intense investigation, the search for clinically useful markers of embryonic competence and endometrial receptivity continues to be the Holy Grail of Reproductive Medicine. This journey, which promises to eliminate IVF failure and early pregnancy loss once and for all, has so far been disappointing. At the heart of the current malaise lies the prevailing belief that reproductive success depends on binary drivers, such as ‘good and bad’ embryos and ‘receptive and non-receptive’ endometria.

I hypothesize that human implantation is much more dynamic and adapted to deal with a highly invasive and genetically diverse blastocyst. Furthermore, I speculate that effective strategies to prevent implantation failure and early pregnancy loss must be based on an in-depth understanding of the mechanisms that control embryo selection at implantation.

The specific goals of my study were:

- Identification of embryonic signals that enable uterine biosensoring at implantation.

- Characterisation of endometrial receptors involved in embryo selection and rejection.

Chapter 2

Materials and Methods

2.1 Materials

2.1.1 Cell Culture Media and Materials

Media

Reagent	*Manufacturer*	*Catalogue No.*
Antibiotic-Antimycotic Penicillin (10,000 µg/ml)-Streptomycin (10,000µg/ml)	GIBCO®, Invitrogen	15240
L-Glutamine (200mM) 100x	GIBCO®, Invitrogen	25030
B-Estradiol>95%	Sigma-Aldrich	E8875
Charcoal	Sigma-Aldrich	O5105
Collagenase	Sigma-Aldrich	C9891
Deoxyribonuclease I (DNase 1)	Roche	11284932001
Dextran	Fisher Scientific	
Dulbecco's Modified Eagle Medium (DMEM)/F12 (1:1) with L-glutamine, no phenol red	GIBCO®, Invitrogen	11039
Dulbecco's Modified Eagle Medium (DMEM)/F12 (1:1) with L-glutamine, with phenol red	GIBCO®, Invitrogen	31330
Fetal Bovine Serum (FBS) heat inactivated	GIBCO®, Invitrogen	10500
Insulin (Recombinant, Human)	Sigma-Aldrich	91077C
L-Glutamine	Gibco	25030-081
Primocin (500mg)	Source Bioscience UK Limited	ant-pm-1

Materials

Reagent	*Manufacturer*	*Catalogue No.*
6-well plates	Corning® Costar®,	T-3506-6
Cell culture flask (25cm^2)	CellStar®	690160
Cell culture flask (75cm^2)	CellStar®	658170
Cell scraper, small, Corning	APPLETON WOODS	BC323
Glass bottomed petri dishes (35mm)	MatTek Corporation	P35GCol-1.5-14.C
Immuno 96-well plate	NUNC	442404
Luer lok™ Syringe (50ml)	BD Plastipak™	300865
Sterile Filter Tips (0.1-10µl)	Alpha Laboratories	ZP1010S
Sterile Filter Tips (1-40µl)	Alpha Laboratories	ZP1204S
Sterile Filter Tips (1-100µl)	Alpha Laboratories	ZP1200S
Sterile Filter Tips (1-300µl)	Alpha Laboratories	ZP3300S
Sterile Filter Tips (100-1000µl)	Alpha Laboratories	ZP1250S
Syringe (10ml)	BD Plastipak™	302188
Syringe Filter (0.2µm)	Minisart®	16534

Cell Lines

Ishikawa Cell Line human, endometrial adenocarcinoma, Sigma-Aldrich, 99040201-1VL

2.1.2 Cell Culture Treatments

Hormone	*Concentration*	*Manufacturer*
8-br-cAMP (cAMP)	0.5mM	Sigma-Aldrich
Medroxyprogesterone acetate (MPA)	1µM	Sigma-Aldrich

Reagent	*Concentration*	*Manufacturer*	*Catalogue No.*
Trypsin (0.22µ filtered)	10nm to 1uM	Worthington	LS003734
Lipopolysaccharides (LPS) from *Escherichia Coli* 0111:B4	1ug/ml	Sigma-Aldrich	L4391
TLR4 inhibitor Peptide set	50uM	Novus Biologicals	NBP2-26244
Soybean trypsin inhibitor	1mg/ml	Worthington	LS003570

2.1.3 siRNA

SiRNA	*Manufacturer*	*Catalogue No.*
siGENOME Non-Targeting siRNA Control Pool	GE HEALTHCARE UK LTD	D-001206-13-05
PRSS8 Silencer® Select Pre-designed siRNA, 5 nmol	Fisher Scientific	10782097

2.1.4 Antibodies

Primary

Antibody	*Manufacturer*	*Catalogue No.*	*Raised in*		*Dilution*
AMBP	Novus Biologicals	H00000259-M01	Mouse	mAb	1:100
β-actin	Abcam	AB8277	Rabbit	pAb	1:100,000
COX2	Cell Signalling	4842	Rabbit	pAb	1:1000
Cytokeratin 18	Abcam	AB668	Mouse	mAb	1:100
PAR2	Abcam	AB180953	Rabbit	mAb	1:250
PRSS8	Antibodies Online	ABIN761891	Rabbit	pAb	1:100~ 1:250*
SCNN1A	Sigma-Aldrich	HPA012939-100UL	Rabbit	pAb	1:100~ 1:250*
SCNN1G	Proteintech	13943-1-AP	Rabbit	pAb	1:100~ 1:250*
SPINT1	Sigma-Aldrich	SAB1409704-50UG	Mouse	pAb	1:100
TLR4	Cell Signalling Technology	NB100-56566	Mouse	mAb	1:250* 1:100~
TMPRSS2	Antibodies Online	ABIN716876	Rabbit	pAb	1:100
TMPRSS15	Novus Biologicals	NBP1-55616	Rabbit	pAb	1:100
Vimentin	Dako	M7020	Mouse	mAb	1:100~
Vimentin	Cell Signalling	SG3F10	Mouse	mAb	1:1000*

*Western blotting, ~Immunocytochemistry

Secondary

Antibody	*Manufacturer*	*Catalogue No.*		*Dilution*
Goat IgG-Alexa Fluor 488	Molecular Probes	A21222	Rabbit	1:2000* 1:100~
Mouse IgG-Alexa Fluor 555	Molecular Probes	A21424	Goat	1:6000* 1:100~

*Western blotting, ~Immunocytochemistry

Antibody Blocking Peptides

Blocking Peptide	*Manufacturer*	*Catalogue No.*
AMBP Blocking Peptide	Fitzgerald	33R-9450-FIT
SCNN1G Fusion Protein	Proteintech	ag5286

2.1.5 Chemical Reagents

Reagent	*Manufacturer*	*Catalogue No.*
30% Acrylamide/Bis Solution, 37.5:1 500ml	BIO-RAD LABORATORIES LTD	161-0158
Ammonium persulfate (APS)	Sigma-Aldrich	A3678-25G
Chloroform	Fisher Scientific	C298-4
Ethanol	Fisher Scientific	BP2818-4
Ethylenediaminetetraacetic acid (EDTA)	Roche	11 836 170 001
Glycerol	Sigma-Aldrich	G5516-100ML
Glycine	Fisher Scientific	G/P460/53F
Isopropanol	Fisher Scientific	BP2618-4
Methanol	Fisher Scientific	M/4000/17F
Mineral Oil	Sigma-Aldrich	M-8410
N,N,N,N'-tetramethyl-ethane-1,2-diamine (TEMED)	Sigma-Aldrich	T9281-25ML
Non-fat dried milk powder	VWR International Ltd.	A0830.1000
PageRuler Plus Pre-stained Protein Ladder	ThermoScientific	26619
Paraformaldehyde (PFA)	Sigma-Aldrich	P-6148
Pierce® ECL Plus Western Blotting Substrate	ThermoScientific	32132 32134
Power SYBR® Green PCR Mastermix	Fisher Scientific	VY4368702
Protein Assay Dye Reagent	BioRad	#500-0006
RIPA Lysis Buffer 10x	Upstate [Millipore]	20-188
RNA STAT-60	Amsbio	CS110
siRNA Universal Buffer 5x	Fisher Scientific	11821924
Sodium chloride (NaCl)	Fisher Scientific	S/3160/60F
Sodium dodecyl sulfate	Sigma-Aldrich	L4390-25G
Triton X-100	Sigma-Aldrich	T-8787
Trizma®Base	Sigma-Aldrich	T1503-1KG
Trypan Blue	ThermoScientific	15250-061
Tween®20	Fisher Scientific	BP337-500F
Vectashield Mounting Medium with DAPI	Vector Laboratories	H-1200

2.1.6 Miscellaneous Reagents

Reagent	*Manufacturer*	*Catalogue No.*
10kDA Spin Column	Abcam PLC	ab93349
5X siRNA Universal Buffer 100mL	Fisher Scientific	11821924
7500 Real Time PCR system	Applied Biosystems	
Amersham Hybond™ PVDF membrane	GE HEALTHCARE	RPN 303F
Amersham Hyperfilm™MP	GE HEALTHCARE	28906844
Gel Casting Cassettes	NOVEX® by Life Technologies	NC2015
MicroAmp® Optical 96-well Reaction Plate	Life Technologies	N8010560
Mineral Oil	Sigma	M-8410
Multiskan Ascent	ThermoScientific	51118300
PageRuler Plus Pre-stained Protein Ladder	ThermoScientific	26619
Pierce® ECL Plus Western Blotting Substrate	ThermoScientific	32132 32134
Power SYBR® Green PCR Mastermix	Fisher Scientific	VY4368702
Protein Assay Dye Reagent	BioRad	#500-0006
RNA STAT-60	Amsbio	CS110
RNAse Zap	Invitrogen	AM9780
ThermalSeal RT2RR 50-µm-thick Sealing Films	Applied Biosystems	TS-RT2RR-100
Vectashield Mounting Medium with DAPI	Vector Laboratories	H-1200
WellWash	ThermoScientific	4 MK2 220/240V
XCell SureLock® Mini-Cell and XCell II™ Blot Module	Invitrogen	EI0002

2.1.7 Kits

Kit	*Manufacturer*	*Catalogue No.*
ECL Prime Western Blotting Detection Kit	Scientific Laboratory Supplies Ltd.	RPN2232
EnzChek Protease Assay Kit (Green fluorescence)	Life Technologies	E6638
Factor D ELISA Kit	ABCAM	ab99969
Human HAI-1 ELISA Kit	Raybio®	ELH-HAI1
Human Prostasin ELISA Kit	Raybio®	ELH-Prostasin
Human TMPRSS2 ELISA Kit	ELABSCIENCE BIOTECH CO.	E-EL-H1418
JetPRIME®	Polyplus transfection	114-07
Proteome Profiler™ Human Phosph-MAPK Array	R&D Systems®	ARY002B
QIAquick® Gel Extraction Kit	Qiagen	28704
Quantitect Reverse Transcription Kit	QIAGEN	205311
Trypsin Activity Assay Kit (Colorimetric)	Abcam	AB102531

2.1.8 Buffers and Solutions

2.1.8.1 General

Phosphate Buffered Saline (PBS)
140 mM NaCl
2.5 mM KCl
1.5 mM KH_2PO_4, pH 7.2
1.5 mM Na_2HPO_4, pH 7.2

Tris Buffered Saline (TBS)
130mM NaCl
20mM Tris
pH 7.6

TBS-Tween 20 (TBS-T)
0.2% Tween 20 in TBS (1x)

RIPA Buffer
50mM Tris HCl pH 7.4
1% NP40
0.5% deoxycholate
0.1% SDS
150mM NaCl
2mM EDTA
50mM NaF

DNA Loading Buffer
0.2% (w/v) Bromophenol blue
40% (v/v) glycerol 0.25M EDTA pH8.0

Laemmli Buffer
50mM Tris-HCl, pH 6.8
1% (w/v) SDS
10% (v/v) glycerol
2% (v/v) β-mercaptoethanol
0.002% (w/v) Bromophenol blue

2.1.8.2 Immunohistochemistry

4% PFA Solution
4% PFA (W/v) in PBS
pH 9.2 with NaOH

Cell Permeabilisation Solution
0.1% Triton-x (w/v) in PBS

Blocking Solution and Antibody Incubation Solution
1% (w/v) BSA in PBS

2.1.8.3 Western Blotting

SDS Tris-Glycine Running Buffer 10X
250mM Tris Base
1.9M Glycine
pH 8.3
1% (w/v) SDS

SDS Tris-Glycine Transfer Buffer 10X
0.05M Tris-HCl (pH 6.8)
0.4M Glycine
20% (v/v) Methanol
1% SDS

Stripping Buffer
15g Glycine
1g SDS
10ml Tween®20
Adjust pH to 2.2
Bring volume to 1.0 L

Western Blocking Buffer and Antibody Incubation Solution
5% (w/v) non-fat milk in TBS-T

2.1.8.4 SDS Polyacrylamide Gels

Resolving Gel
375mM Tris (pH 8.8)
0.1% (w/v) SDS
0.1% (w/v) APS
10% Acrylamide Bis Solution (37.5:1)
TEMED added at 1 in 1000

Stacking Gel
80mM Tris (pH6.8)
0.1% (w/v) SDS
0.1% (w/v) APS
5.8% Acrylamide Bis Solution (37.5:1)
TEMED added at 1 in 1000

2.1.8.5 Calcium Profiling

Krebs'-Heinselet Buffer

133mM NaCl
4.7mM KCl
11.1mM Glucose
1.2mM MgSO4
1.2 KH2PO4
2.5mM CaCl
10mM TES pH 7.4

2.2. Methods

2.2.1 Human Endometrial Biopsies

Endometrial biopsies were acquired from patients attending the research-led Implantation Clinic at University Hospital Coventry and Warwickshire. Informed written consent was obtained from all patients and the study was approved by the NHS National Research Ethics Committee of Hammersmith and Queen Charlotte's Hospital NHS Trust. Biopsies were taken in the mid-secretory phase, 5 to 11 days after the post-ovulatory LH surge, and all patients were withdrawn from any hormonal treatment at least 3 months prior to the biopsy appointment. Each biopsy, where appropriate, was processed in three stages. Biopsy addition to 7ml DMEM-F12 supplemented with 10% dextran-coated charcoal treated foetal bovine serum (DCC-FBS) (v/v) allowed direct isolation of endometrial stromal cells. Snap freezing of biopsies in liquid nitrogen provided a sample for protein analysis, which was subsequently stored at -80°C. Immersion of biopsy tissue fragments in RNA later followed by storage at -80°C provided material for RNA studies.

2.2.1.2 Ishikawa Cells

Ishikawa cells were purchased from Sigma (99040201-1VL) and thawed according to manufacturer's protocol. The cells were routinely cultured and passaged (as in section 2.2.2.5) in a continuous cell culture laboratory. Cells were closely monitored and regularly tested for mycoplasma contamination. Mycoplasma-free cells were stored according to section 2.2.2.7.

2.2.2 Cell Culture

2.2.2.1 Dextran-Charcoal Stripping of FBS

FBS contains endogenous steroids hormones which may mask the effect of exogenously applied ligands. Therefore DCC treatment was used to strip serum of small molecules. FBS was defrosted for 24 hours at 4°C. 1.25 g charcoal, 125 mg Dextran and 500 ml FBS were thoroughly mixed and incubated at 57°C for 2 hours, inverting every 30 minutes. Following centrifugation at 400 x g for 30 minutes the supernatant was filter sterilised using a 0.2µm filter and stored in aliquots at -20 °C. The DCC-FBS aliquots were defrosted either at 4°C overnight or at room temperature (RT) on the day required.

2.2.2.2 Cell Growth Medium

DMEM:F12 supplemented with 10% DCC-FBS (v/v)

500 ml DMEM:F12 (with phenol red and L-Glutamine)

50 ml DCC-FBS

5 ml L-Glutamine

5 ml Antibiotic-Antimycotic (100x)

100 µl Insulin (10mg/ml stock)

5 µl Estradiol (10^{-4} stock)

DMEM:F12 supplemented with 2% DCC-FBS (v/v)

500 ml DMEM:F12 (without phenol red)

10 ml DCC-FBS

5 ml L-Glutamine

5 ml Antibiotic-Antimycotic (100x)

The thawed DCC was supplemented with L-Glutamine, AB/AM solution, Insulin and Estradiol (as above) and added to DMEM:F12 by sterile filtration. The media was stored at 4 °C for up to 4 weeks, filter sterilised and warmed to 37°C prior to use.

2.2.2.3 Preparation of Isolated Endometrial Stromal Cells

Endometrial biopsies were collected in DMEM:F12 supplemented with 10% DCC-FBS (v/v). Biopsies were decanted into a petri dish, isolated by removal of media/mucus and mechanically minced for 5 minutes with sterile scalpels. Enzymatic digestion was achieved using 10ml of additive free DMEM:F12 supplemented with 0.5mg/ml Collagenase and 0.1mg/ml DNase 1 for 1 h at 37°C with vigorous shaking every 20 minutes. The collagenase acts to digest the ECM and the DNase removes viscous DNA produced after apoptosis of some of the cells during digestion. 10ml of DMEM:F12 supplemented with 10% DCC-FBS (v/v) was applied to deactivate the enzyme action and the sample was centrifuged at 400 x *g* for 5 min. Following aspiration of the supernatant the pellet was resuspended in 12ml DMEM:F12 supplemented with 10% DCC-FBS (v/v) , transferred to a 75cm^2 culture flask and incubated at 37°C with 5% (v/v) CO_2 overnight to allow attachment. Aspiration of the media the following day removed blood, epithelial and unattached cells whilst replenishment using 12ml of DMEM:F12 supplemented with 10% DCC-FBS (v/v) every 2 days maintained the proliferating HESC culture. Upon confluency, HESCs were passaged (as previously described) and cultured at an appropriate dilution. Experiments were performed in DMEM:F12 supplemented with 2% DCC-FBS (v/v) and decidualization was induced by supplementation with 0.5mM Bromo-cAMP and 1mM MPA. All experiments were performed prior to the fourth passage.

2.2.2.4 Isolation of Endometrial Epithelial/Stromal Cells

Biopsies were collected from consenting patients and processed immediately as above but; Following culture in 10ml of additive free DMEM:F12 supplemented with 0.5mg/ml Collagenase and 0.1mg/ml DNase 1 for 1 h at 37°C the sample was passed through a 40nm filter, fitted above a 50ml tube (Falcon) to isolate the stromal cells. The filter was then moved to a fresh tube and backwashed with 20ml DMEM:F12 supplemented with 10% DCC-FBS (v/v) to extract the epithelial cells. The cells were spun by centrifugation for 5 minutes at 1000 x RPM, supernatant aspirated and pellet re-suspended in DMEM:F12 supplemented with 10% DCC-FBS (v/v) with progesterone (P_4)10^{-4} and placed into culture.

2.2.2.5 Routine Mammalian Cell Culture

Mammalian cells were routinely grown in monolayers using 75cm^2 culture flasks maintained at 37°C in a humid atmosphere containing 5% (v/v) carbon dioxide (CO_2) using a Heracell incubator. Cells were maintained in DMEM:F12 supplemented with 10% (v/v) DCC-FBS which was changed every other day and passaged when near confluent (1-2 times per week depending on growth rate).

In brief, the media was aspirated using a vacuum, cells washed using 5 ml PBS and 1ml pre-warmed Trypsin-EDTA added. Following incubation for 5 minutes at 37 ºC the cells were loosened by tapping (confirmed by inspection under the microscope). 9ml of DMEM:F12 supplemented with 10% DCC-FBS (v/v) were added to neutralize the Trypsin and cells transferred to a 14ml Falcon tube. The cell suspension was centrifuged at 400 x *g* for 5 minutes, supernatant aspirated and the pellet re-suspended in DMEM:F12 supplemented with 10% DCC-FBS (v/v) at a suitable dilution (Usually 1:3).

Culture media in all cases was pre-warmed to 37°C in a water bath and syringe filtered using a 0.2µm filter and all work was carried out in a Class I safety cabinet.

2.2.2.6 Preparation of Whole Tissue Samples for RNA Extraction

Endometrial biopsies were stored in RNA later. Around 1 mm of tissue was chopped using sterile scalpels and transferred into STAT 60 (1 ml) within a 2 ml RNase-free tube. The sample was homogenised using a Kinematica POLYTRON® PT 1200 E homogenizer, thoroughly cleaned using the following wash steps; 1 x RNAse zap, 3 x nuclease free water, 1 x 70% (v/v) ethanol, 1 x STAT 60. The homogenised sample was left at RT for 5 minutes and 200 µl chloroform added before placing it onto dry ice and storing overnight at -80 ˚C. RNA extraction was subsequently performed according to protocol.

2.2.2.7 Storage of Cell Stocks

A cryoprotectant solution (2x) was prepared by adding 20% DMSO to DCC-FBS and filter sterilised. Cells were harvested and pelleted as described above and then re-suspended in DCC-FBS (1ml per vial). The cryoprotectant was added drop-wise with gentle tapping (1ml/vial) to give a final concentration of 10% DMSO. The cell suspension was then aliquotted into labelled cryovials (1.8ml/vial) transferred to an isopropanol filled freezing container and placed at -80 °C overnight, before transferring into a liquid nitrogen tank for long-term storage. Cells recovered from liquid nitrogen were thawed rapidly at 37°C, pelleted as before and re-suspended in a 75cm^2 culture flask containing 12ml pre-warmed DMEM:F12 supplemented with 10% DCC-FBS (v/v).

2.2.2.8 Hormonal treatment

Confluent monolayers of cells were cultured in DMEM:F12 (without phenol red) supplemented with 2% DCC-FBS (v/v) overnight and hormonal treatments were applied the following day. For routine decidualization treatment, HESCs were treated in DMEM:F12 (without phenol red) supplemented with 2% DCC-FBS (v/v), 0.5mM 8-bromo-cAMP (cAMP) and 1µM medroxyprogesterone acetate (MPA). All cell treatments were carried out before the fourth passage.

2.2.2.9 Cell Treatment Protocol

Endometrial cells were cultured in DMEM:F-12 supplemented with 10% DCC-FBS (v/v) (2ml/well). Cells were monitored and passaged (1:4) when at 80-90% confluence into 6-well plates (2ml cell suspension/well) in DMEM:F-12 supplemented with 10% DCC-FBS. Plates were monitored for cell growth and media replenished daily until 80-90% confluence. Cells were then down-regulated overnight in DMEM (with no phenol red, supplemented with 2% DCC-FBS (v/v)). At time of treatment the prepared aliquots were thawed, vortexed and diluted to a working stock in serum free, additive free DMEM.

ECM was diluted 1:100, Soybean trypsin inhibitor with diluted to 1mg/ml, Trypsin was diluted from 1mM stock, LPS was diluted to 1ug/ml, TLR4 inhibitor (VIPER) and the accompanying control peptide were diluted to 50µM. All media was aspirated from the cells prior to treatment, cells were washed with PBS (1ml/well) and treatments were applied in triplicate (0.5ml/well). Serum free DMEM was used as the control. Cells were incubated at 37°c with 5% CO_2 for the course of treatment. After the exposure time the treatment was aspirated, cells washed with PBS (1ml/well) and either harvested or cultured further at 37°c with 5% CO_2 in DMEM:F12 supplemented with 2% DCC-FBS 2ml/well.

2.2.3 Transient Transfections

Transfections of primary HESCs were performed at 80% confluence in DMEM:F12 supplemented with 10% DCC-FBS (v/v) in 6-well plates. Transfections were achieved using the Lipofectamine®RNAiMAX Transfection Reagent, a cationic, lipid formulation. 50nM of siRNA was diluted in opti-MEM® Medium and incubated with Lipofectamine®RNAiMAX Reagent at an appropriate volume for 5 minutes. The transfection solution was added dropwise to cells to give a final volume of 250µl/well. Cells were incubated at 37 °C and harvested 24 hours post-transfection. siGENOME Non-Targeting siRNA Pool 1 was used as a control.

2.2.4 Protein Analysis

2.2.4.1 Protein Extraction

HESCs were harvested from 6-well plates using RIPA buffer supplemented with protease inhibitors (60µl/well) following a PBS wash (1ml/well). Cell Scrapers were used to collect the lysates which were then pipetted into 0.6 µl eppendorfs and centrifuged at 13,200 RPM for 10 min at 4°C. The supernatant was transferred to a fresh eppendorf and stored at -80°C. Protein concentration was determined and between 10 and 20µg was combined with loading buffer, boiled at 95°C for 10 minutes (in order to denature the proteins allowing the antibody to access the epitope) and loaded into SDS-polyacrylamide gels.

2.2.4.2 Determination of Protein Concentration

The Bradford Assay was used to quantify the concentration of protein in the cell lysates preceding Western blot analysis. This method employs a Coomassie Blue dye which binds to the protein and enables quantification by comparison with a

standard curve generated by known concentrations of a standard (BSA).

A series of BSA dilutions from 0 to 20 µg of protein were prepared in a final volume of 800 µl. All lysates were diluted for analysis (2µl in 798µl dH_2O) and vortexed. 200µl of Protein Assay Dye Reagent was added to all standards and samples, which were vortexed and incubated at RT for 15 minutes. Standards and samples were loaded in duplicate into a flat-bottomed optically clear 96-well plate (200µl/well) and absorbance measured at 595 nm (Multiskan Ascent).

2.2.4.3 Sodium Dodecyl Sulfate Polyacrylamide Gel Electrophoresis (SDS-PAGE)

Proteins were resolved on discontinuous polyacrylamide gels using the Invitrogen XCell SureLock® Mini-Cell apparatus. Gels were prepared by adding two solutions to a Novex Gel Casting Cassette, one to form a resolving gel and the other to form a stacking gel. The resolving gel typically contained 8% acrylamide, 1% SDS and 375 mM Tris-HCL pH 8.8. The stacking gel consisted of 5% acrylamide, 1% SDS and 125mM Tris-HCl pH 6.8. TEMED and APS were used to induce polymerization of the gels. First the resolving gel was added to the cassette reaching 1.5cm from the top and isopropanol was overlaid to prevent evaporation during polymerization. Once polymerization was achieved the isopropanol was rinsed away, the resolving gel was overlaid with the stacking gel and a comb was inserted. Once set, the comb and tape were removed from the cassette and it was clamped into place within the electrophoresis tank, overlaid with Running Buffer. Equal volumes of the prepared protein samples were then added to the wells, typically 20 µl/well, alongside 10 µl of Pre-stained Protein Ladder. Gels were run at 125 V for up to 2 hours until the dye front had migrated to the base of the gel, at which time the cassettes were opened and the gels used for Western blot.

2.2.4.4 Western Blotting

The protein samples were resolved using SDS-PAGE and transferred onto a PVDF membrane, activated in methanol, using a wet blotting method. The PVDF membrane, filter paper and pads were pre-equilibrated in Transfer Buffer (1x) and used to assemble a 'sandwich' within the cathode shell. This consisted of layering pads, filter paper, SDS-PAGE gel, PVDF membrane, filter paper and pads to give good contact between the electrodes. The electrode assembly was then fitted into the tank with the membrane towards the anode and the gel towards the cathode. Transfer Buffer was poured onto the blot module until full and into the tank until half full and the transfer was performed at 230 mA for 2 hours. The membrane was then transferred onto filter paper and left to dry. The membrane was reactivated in methanol, rinsed in 1 x TBS and incubated in Blocking solution (5% Milk in TBS-T for 1 hour at RT) to prevent non-specific binding. The membrane was then washed once in TBS-T for 15 minutes and three times in TBST for 5 minutes before incubation with the primary antibody, diluted in Western Antibody Incubation Solution at 4 °C overnight (unless specified otherwise on the datasheet). The dilutions used were as follows: SCNN1A, SCNN1G, TLR4, PRSS8, PAR2 at 1: 250; β-actin at 1: 100 000. The TBS-T wash step was repeated before incubation with the HRP-conjugated antibody, raised against the primary antibody, diluted in Western Antibody Incubation Solution for 1 hour at RT. The TBS-T wash step was repeated, before a 5 minute wash in TBS following which protein bands were visualised using enhanced chemiluminescence with ECL Western blot detection system according to the manufacturer's instructions.

2.2.4.5 Stripping Membranes for Western Blotting

To re-probe membranes with alternative primary antibodies, membranes were incubated in Stripping Buffer for 10 minutes, twice before washing in TBS-T (as

above). Alternatively membranes were incubated in boiling water for 3 minutes and then placed into cold TBS-T.

2.2.5 Assessment of proteases in embryo conditioned medium (ECM)

Embryo conditioned medium was obtained from two IVF units;

The Centre for Reproductive Medicine (CRM) Coventry & Warwickshire NHS Trust with approval from the Ethics committee and the couples' written, informed consent. Embryos were cultured in individual 20µl drops of ISM1™ (Origio) and BlastAssist™ (Origio). During this study the CRM changed their culture method to include the ORIGIO® Sequential Series™ (Fert™, Cleav™, Blast™).

The Brussels Centre for Reproductive Medicine (Vrije Universiteit Brussel, Brussels) with the approval of the Institutional Committee of the University Hospital Brussels. Embryos were cultured individually in 25µl drops of Q1 (Quinn's Protein Plus Cleavage Medium) and Q2 (Quinn's Advantage™ Protein Plus Blastocyst Medium) (Sage In Vitro Fertilization). During this study the unit changed their culture method to include the ORIGIO® Sequential Series™ (Fert™, Cleav™, Blast™).

If the embryos were suitable for culture to the blastocyst stage embryo drops were collected on Day 6 following embryo transfer on Day 5. If embryos were transferred on Day 2 the embryo drops were collected at the time of transfer. All drops were stored at -80°C and thawed on day of use. Empty drops, incubated alongside the drops used for embryo culture, were used as a control.

2.2.5.1 Protease activity assay

Protease activity was measured using the EnzChek Protease Assay Kit for green

fluorescence (E6638, Life Technologies) according to manufacturer's protocol. This kit contains a casein derivative that has been extensively labelled with the pH-insensitive, green-fluorescent BODIPY® FL dye, which results in a quenching of the fluorescent dye. Protease-catalysed hydrolysis releases the highly-fluorescent BODIPY® FL dye-labelled peptides, allowing for quantitative detection of protease activity in solution. The green-fluorescent BODIPY® FL dye has excitation and emission spectra similar to those of fluorescein. Samples were thawed, warmed to room temperature and diluted as follows; 7.5µl ECM + 92.5µl 1x Digestion Buffer per well. Samples and standards were applied in duplicate and incubated for 24 hours at room temperature, protected from light. Fluorescence was measured at 505/513 nm and concentrations determined by comparison to the standard curve.

2.2.5.2 Trypsin Activity Assay

The Trypsin Activity Assay Kit (Colorimetric) (ab10253, ABCAM) was used according to the manufacturer's instructions to accurately measure trypsin activity in ECM. The cleavage of a given substrate, by trypsin, generates p-nitroaniline (p-NA) which is detected at λ=405nm and the resulting colour intensity is thus proportional to p-NA content.

Reagents were added to 0.6ml nuclease-free tubes prior to plating as follows; Positive Control: 90µl Trypsin Assay Buffer and 10µl Positive Control Solution. pNA Standards: 0, 4, 8, 12, 16, 20µl p-NA Standard (2 mM) with corresponding volumes of Trypsin Assay Buffer to give a final volume of 100µl per tube (to generate 0, 4, 8, 12, 16, and 20 nmol/well of the *p*-NA standard). All reagent tubes were inverted to mix and samples applied to an Immuno 96-well plate (442404, NUNC) in duplicate. Undiluted ECM/control media was added directly to the plate. A mastermix of 48µl Trypsin Assay Buffer and 2µl Trypsin Substrate (in DMSO) per well was prepared, vortexed and 50µl applied to each well. 1µl of 10mM Chymotrypsin Inhibitor Solution

(N-tosyl-L-phenylalanylchloromethyl ketone or TPCK) was added to each well and incubated at room temperature for 10 minutes. 1µl of 20 mM Trypsin Inhibitor Control (Tosyllysine Chloromethyl Ketone hydrochloride or TLCK) was added to TLCK control wells only and incubated for 5 minutes at room temperature. Absorbance was measured at 405nm using a Multiskan Ascent (51118300, ThermoSceintific) at 0, 1, 2, 3 and 4 hour time points. The plate was incubated at 25°c and protected from light for the duration.

The results were calculated as follows: For the colour generated at each time point: A405nm = (A2 – A2C) – (A1 – A1C), where A1 = absorbance at zero hours, A1C = trypsin inhibitor control at zero hours, A2 = absorbance at subsequent time point, A2C = trypsin inhibitor control at subsequent time point. The zero p-NA standard was subtracted from all readings and standard curves generated from the p-NA values at each time point. A405nm was applied to the standard curve to give the nmol of *p*-NA generated in the reaction wells. Trypsin activity was determined by applying the values to the following equation: Trypsin Activity = B/((T1-T2)xV) x Sample Dilution Factor = nmol/min/ml = mU/ml. Where B is the *p*-NA calculated from the Standard Curve (in nmol), T1 and T2 are the times of the first and second readings (in minutes) and V is the sample volume added into the reaction well (in ml).

2.2.5.3 PRSS8 (Prostasin) ELISA

The total abundance of prostasin in ECM samples was measured using RayBio® Human Prostasin ELISA Kit (ELH-Prostasin, RayBiotech, Inc.) according to the manufacturer's protocol. Samples were thawed, warmed to room temperature and diluted as follows; 7.5µl ECM + 92.5µl Assay Diluent D per well. Samples and standards were applied to the 96-well plate (mounted with immobilised antibody) in duplicate and incubated overnight at 4°c, with gentle shaking. Following incubation

with HRP-conjugated streptavidin and the addition of a TMB substrate solution, the kit provides a colour change from blue to yellow according to the quantity of prostasin present in the sample. The absorbance was read at 450nm and the sample concentrations were determined by comparison to the standard curve.

2.2.5.4 TMPRSS2 ELISA

The total level of Tmprss2 in the samples was determined using the Human TMPRSS2 ELISA Kit (E-EL-H1418, Elabscience) according to the manufacturer's protocol. Samples were thawed, warmed to room temperature and diluted as follows; 7.5µl ECM + 92.5µl Reference Standard & Sample Diluent per well. The samples and standards were loaded, in duplicate, into the 96 well plate, pre-coated with an antibody specific to TMPRSS2. Next, Avidin conjugated to Horseradish Peroxidase (HRP) was added to each well and incubated. After the addition of TMB substrate solution only those wells that contain TMPRSS2, biotin-conjugated antibody and enzyme-conjugated Avidin will exhibit a colour change. The enzyme-substrate reaction was terminated by the addition of sulphuric acid solution and the colour change was measured at 450nm. The concentration of TMPRSS2 in the samples was then determined by comparing their optical density (OD) to the standard curve.

2.2.6 Gene Expression Analysis by qRT-PCR

2.2.6.1 Quantitative Real-time Polymerase Chain reaction (qRT-PCT)

Gene expression was determined by qRT-PCR. qRT-PCR involves the detection of a fluorescent signal which is generated relative to the amount of PCR product generated each cycle, i.e. in real time in contrast to endpoint detection.

The SYBR Green detection system was used. The SYBR® Green dye, fluorescently

undetectable in its unbound form, binds to all dsDNA molecules resulting in the emission of a fluorescent signal proportional to amplicon quantity. The fluorescence can then be read by a sequence detector in real time, in this instance a 7500 Real Time PCR system (Applied Biosystems). Amplification of the fluorescent signal, at each cycle, indicates the increasing accumulation of dsDNA resulting from the annealing and subsequent polymerisation of the cDNA. The change in fluorescence intensity (∆Rn) resulting from amplification is calculated as follows; $\Delta Rn = Rn^{+} - Rn^{-}$, where Rn^{+} is the fluorescence emission of the product at each time point and Rn^{-} is the fluorescence emission at the baseline. The baseline represents background fluorescence where there is no detectable increase resulting from amplification of PCR products. The 7500 Real Time PCR software generates amplification plots of ∆Rn *vs* cycle number. During the initial cycles the ∆Rn does not exceed the baseline but as the reaction progresses the fluorescence intensity reaches a threshold defined as a statistically significant point above the baseline. Based on the variability within the baseline an arbitrary threshold is selected at a point in the linear phase of exponential amplification, usually defined as 10 times the standard deviation of the baseline, within cycles 3 to 15. The cycle threshold (Ct) is subsequently calculated by determining the point at which the fluorescence crosses the chosen threshold limit relative to the initial amount of target. Thus Ct values decrease linearly with increasing target quantity. The number of PCR cycles undertaken in order for the level of fluorescent signal to cross the given threshold is used to allocate a Ct value which enables the determination of dsDNA quantity.

2.2.6.2 RNA Extraction

RNase ZAP, RNase-free plasticware and DEPC-treated water were routinely used to minimize degradation of RNA. Total RNA was extracted from cells cultured in 6-well plates by direct lysis using STAT-60 (200 µl/well), following a PBS wash (1ml/well).

Cell Scrapers were used to harvest the RNA into pre-cooled eppendorfs which were placed on ice. 0.2 volumes of chloroform was added to samples which were shaken vigorously for 15 seconds then centrifuged at 12,000 x *g* for 15 minutes at 4˚C. This separates the sample into an aqueous, organic and interphase. The RNA resides exclusively in the upper, colourless aqueous phase which is then transferred to a fresh Eppendorf. To encourage precipitation 0.5 volumes of cold isopropanol are added to the RNA before vortexing and storing at -80 ˚C for at least 30 minutes. The tubes were then centrifuged at 12,000 x *g* for 10 minutes at 4˚C. The supernatant was discarded and pellet washed with 1 volume of 75% (v/v) ethanol by repeat re-suspension and centrifugation at 7500 x *g* for 5 minutes at 4˚C. The purified RNA was air-dried for 2 minutes in a clean, undisturbed environment before adding a suitable volume of nuclease free water and storing at – 80 ˚C. RNA concentration was determined using a spectrophotometer (Nanodrop 1000). Pure RNA has an A_{260}/ A_{280} ration of 1.9-2.1 and lower ratios indicate contamination. Samples were diluted to 1µg/µl with nuclease free water and stored at -80 °C.

2.2.6.3 cDNA Synthesis

Quantitect Reverse Transcription Kit (QIAGEN) was used to produce complementary deoxyribonucleic acid (cDNA) from the RNA, according to the manufacturer's instructions.

Reagents were placed on ice to thaw and the work area was cleaned with IMS and RNase Zap. The heating block was set to warm to 42˚c whilst nuclease free tubes (0.6ml) were prepared and labelled (two per RNA sample, one labelled '-RT'). Once thawed all reagent tubes were vortexed to prevent concentration gradients, spun and placed back on ice.

Two nuclease free tubes for each RNA sample were prepared as follows;

2µl (7x) gDNA Wipeout Buffer, 1µg Template RNA and RNAse-free water to give a final volume of 14µl. Tubes were gently spun to mix and then heated at 42°c for 2 minutes before placing on ice. This step removes any traces of contaminating genomic DNA.

Two separate mastermixes were then prepared with a final volume 10% greater than required.

(1) Reverse Transcription Reaction;

1µl Quantiscript RT, 4µl Quantiscript RT Buffer (5x), 1µl Primer Mix

(2) Reverse Transcriptase Negative Control;

1µl nuclease free water, 4µl Quantiscript RT Buffer (5x), 1µl Primer Mix

These were vortexed and 6µl of (1) was added to one of the duplicate tubes containing 14µl of RNA whilst 6µl of (2) was added to the remaining 14µl of RNA, labelled '-RT'. Tubes were spun to mix and heated at 42˚c for 30 minutes before heating at 95˚c for 3 minutes to inactivate the Reverse Transcriptase reaction. The resulting cDNA was diluted in nuclease free water and stored at -20˚c.

2.2.6.4 Primer Design

The NCBI database was used to access gene sequences in order to design primers by hand. The Roche probe library's qRT-PCR Assay Design feature was utilised as a starting point.

The melting temperature (Tm) was calculated with the formula Tm = 69.3+(41(GC/L))- (650/L) where GC is the number of G and C bases in the primer and L is the length of the primer.

Primers were amended by length and G/C content to fulfil the following requirements;

- Sequences should be exon spanning to distinguish between cDNA and gDNA
- Primer length between 18-24 base pairs
- Tm between 58.0°c -59.9°c
- Amplicon length between 75-110 bases
- Tms of forward and reverse primer within 1°c of one another
- At the 3' end of the primer two of the last five bases should be G/C
- No more than four of the same base in succession
- Amplicon Tm = 64.9+(0.41x(((C+G)/L)x100)-(500/L)
- Sequences entered into the Nucleotide BLAST program (NCBI) should show 100% accuracy and specificity with no other genes with over 85% match for that transcript, where possible

All primer sequences are provided in Appendix 1.

2.2.6.5 Primer Preparation

Primers were supplied lyophilised and re-suspended according to the manufacturer's instructions. To avoid any risk of contamination primers were prepared in the PCR hood and primer tubes were first centrifuged to ensure collection at the bottom of the tube. The lyophilised primers were diluted in nuclease-free water to give a final concentration of 100µM. Tubes were vortexed and centrifuged to ensure thorough mixing. Working stocks (to prevent repeat freeze-thawing of primers) were prepared for each primer by adding 20µl of diluted primer with 180µl of nuclease free water, in nuclease free tubes, to give a final working concentration of 10µM. Primers were stored at -20°c until required.

2.2.6.6 Primer Optimization

All reagents and samples were thawed on ice and thoroughly vortexed and centrifuged at each step of the procedure to ensure thorough mixing.

Working in the PCR hood to prevent contamination, a mastermix was prepared for each primer pair to be tested (with a final volume 10% greater than that required to allow for pipetting error). Forward and reverse primers were used at 300nM in a total volume of 19µl in a SYBR Green master mix per well. The mastermix was added to a MicroAmp® Optical 96-well Reaction Plate (19µl/well) followed by 1µl/well of pooled cDNA (or nuclease free water for controls), in triplicate, according to a pre-prepared template. The plates were sealed (using ThermaSeal RT2 film) and centrifuged for 3 minutes at 3000 RPM before placing in the 7500 Real Time PCR system (Applied Biosystems) covered with a mask.

RT-qPCR was performed for 40 cycles (95 °C for 15 seconds, 60 °C for 1 min), after an initial incubation at 95 °C for 10 minutes. L19, a non-regulated ribosomal housekeeping gene, was employed as an internal control. Upon cycle completion the contents of the wells were aliquotted into 0.6ml RNA free tubes (combining triplicates) and stored at -20˚c.

2.2.6.7 Agarose Gel Electrophoresis

1g of powdered Agarose and 100ml of (1x) TBE solution combined and heated by microwaving until totally dissolved. 2µl of Ethidium Bromide (an intercalating dye that binds non-specifically to DNA/RNA and fluoresces in UV light) was added to the gel solution upon cooling and solution swirled to mix. The gel solution was poured into a prepared gel tray, fitted with comb, and left to set. The gel was then positioned within the gel electrophoresis machine (comb removed) and covered with 1xTBE up to the fill line. The PCR samples were combined with loading dye, mixed and

pipetted carefully into the wells, in duplicate. 2µl of an appropriate ladder (e.g. Hyperladder™ V (BIO-33031, Bioline)) was added to wells either side of samples in order to determine size of the product. Gels were run at 10V per 1cm of gel.

2.2.6.8 Agarose Gel Extraction

A pre-weighed sample pot was prepared for each sample. DNA bands were visualised under UV light, cut from the gel using sterile scalpels and placed into the sample pots. Samples were weighed to determine volumes of reagents required for each sample (100mg ~ 100µl). Three volumes of Buffer QG were added per volume of gel and samples incubated at 50°c for 10 minutes. Once dissolved one volume of isopropanol (to precipitate DNA) was added, samples pipetted onto the provided QIAquick columns and centrifuged for 16,000G for 1 minute (at room temperature). The flow through was discarded (as the DNA remains bound to the membrane of the QIAquick columns) and this process repeated until the entire sample has been used.500µl of Buffer QG was applied to each column, centrifuged (as before) and flow through discarded. 750µl Buffer PE (to wash the sample) was added, column centrifuged (as before) and flow through discarded.

The columns were moved into 1.5ml nuclease free tubes, 30µl Buffer EB/nuclease free water added and samples left to incubate for 3 minutes before centrifuging (as before) to elute the DNA.

Samples were stored at 2°c until assessed using a Nanodrop to determine DNA concentration. DNA then diluted to 1ng/µl in nuclease free water.

2.2.6.9 Standard Curve Analysis

8 serial 1/10 dilutions were created in labelled nuclease free tubes per primer pair as

follows; 10µl cDNA + 90µl nuclease free water. These were vortexed, centrifuged and the process repeated for each dilution to give final concentrations ranging from 100pg/µl to 10ag/µl. qRT-PCR was performed using 300nM of the designed primers in a SYBR green mastermix (as before) and serial dilutions applied in triplicate. Ct Values were measured and primer efficiencies were calculated from the resulting data.

The log of the cDNA concentration was plotted against the mean Ct values and the primer efficiency calculated as follows: Primer Efficiency = -1/(10^gradient of the line).

2.2.7 Intracellular Calcium Profiling

Cells were grown to ~90% confluence in 35mm glass-bottomed petri dishes (MatTek, US). Cells were incubated with physiological saline solution (PSS) containing 5µM Fura-2/Flou-4 AM for 40 minutes at room temperature. Pluronic F127 (0.025%, w/v) non-ionic detergent was added to assist with dye loading. Cells were then washed with PSS and the dish was positioned on the stage of a confocal microscope (LSM 510 META, Carl Zeiss, UK) and temperatures were maintained at 37^{o}C with a peltier unit. Krebs'-Heinselet, warmed to 35°C, was superfused for 20-30 minutes to ensure de-esterification of Fura-2/Flou-4 AM was complete. Perfusion was stopped and the volume of solution in the dish altered to 200µl in order for image acquisition. On the stage of a Zeiss Axiovert 200M inverted microscope and visualized with a 40x objective lens, Fura-2/Flou-4 AM fluorescence was excited using a krypton/argon laser at 488nm and emitted light was collected above 510nm (LSM 510 META, Carl Zeiss, UK). Images were captured at 1 frame per second via the C-Apochromat 63×/1.20 W objective lens.

For the ECM experiments, two time sequences were assimilated for each dish. The

first time sequence recorded baseline activity for 2 minutes, 10ul of embryo conditioned medium was applied (to give a 1/20 dilution) and images were recorded for the following 5 minutes. After a 10 minute interval the second recording was initiated using the same viewing field in order to detect longer term $[Ca^{2+}]i$ signals. 10 µl of unconditioned ECM was added as a control and experiments with trypsin and trypsin inhibitor were conducted in a similar manner. A cooled charge-couple device camera at a rate of approximately one frame per second was used to capture the fluorescence which was used to indicate $[Ca^{2+}]i$ fluxes. Within each field of view regions of interest (ROI) were drawn around a selected cell. The Multi Measure function in the ImageJ ROI Manager was used to mine intensity profiles for each ROI over time. Origin 8.5 (OriginLab Corporation, USA) was used for further processing, graphing and statistical analysis of the imported intensity profiles. Traces were normalised to their corresponding baseline to give a self-ratio trace (F/F_0). $[Ca^{2+}]i$ signaling was quantified for the first and last five minute time periods by area under the curve (AUC) calculated above the baseline ($\Delta F/F_0$). Data was analysed and plotted to show oscillatory frequency, peak response and area under the curve.

2.2.8 Microscopy

2.2.8.1 Immunohistochemistry

Paraffin-embedded, formalin fixed endometrial specimens were immunostained using the Novolink polymer detection system. A microtome was used to create 5µm sections which were dewaxed in histoclear, rehydrated in descending ethanol solutions before rinsing with water. Sections were exposed to 30% (v/v) hydrogen peroxide for 5 minutes and then rinsed with TBS. Slides were then placed in a humidified chamber for 5 minutes at room temperature with immunohistochemistry blocking solution, which contained serum matched to the species in which the

secondary antibody was raised. Immunostaining with primary antibodies was carried out in a humidified chamber overnight at 4 °C. The primary antibody was omitted and replaced by the corresponding immunoglobulin isotype in the case of negative controls. Slides were washed twice in TBS and incubated with a post primary solution for 30 minutes. Slides were washed in TBS and incubated with Novolink Polymer for 30 minutes, to achieve visualisation of mouse/rabbit immunoglobulin primary antibodies. Slides were washed in TBS and peroxidase activity was developed using a diaminobenzidine (DAB) solution which produces a visible brown precipitate at the antigen site. Sections were counterstained with Hematoxylin and overlaid with coverslips.

2.2.8.2 Immunofluorescence

Human and mouse embryos were collected at various stages of development and stored in 4% Para-formaldehyde/PBS at 2-8 °C. HESCs were cultured in 35mm glass-bottomed petri dishes. They were fixed in 4% Para-formaldehyde/PBS for 1 hour at room temperature, following removal of media and a PBS wash, then stored at 2-8 °C. Samples were first washed in PBS and permeabilised (where appropriate) for 1 hour in 0.01% (v/v) Triton X-100 in PBS at room temperature. Following a PBS wash incubation in 1% w/v BSA in PBS for 1 hour at 4 °C, with rocking, was performed to prevent non-specific antibody binding. Samples were then incubated in the primary antibodies (diluted as stated in 'Materials 2.1.4') overnight at 4 °C, with rocking. 1% w/v BSA in PBS without primary antibody was used for the negative control. The following day samples were washed in 1% w/v BSA in PBS for 10 minutes at 4 °C and then incubated in the secondary antibodies (diluted as stated in 'Materials 2.1.4') for 2 hours at 4 °C, with rocking. For visualisation embryos were washed in 1% w/v BSA in PBS and mounted onto 35mm glass-bottomed petri dishes in 10µl Vectashield® with DAPI for nuclear counterstain and overlaid with a glass coverslip. Visualisation was

achieved using a Zeiss LSM 510 confocal imaging system.

2.2.9 Data Mining

In silico analysis was performed on the following publicly available datasets from the Gene Expression Omnibus (Edgar et al., 2002):

Pre-implantation embryonic development (Homo sapiens): GDS3959

Pre-implantation embryonic development (Mus musculus): GDS813

Endometrium through the menstrual cycle (Homo sapiens): GDS2052

Data were exported to Microsoft Excel for analysis and graphs were generated using GraphPad Prism® Software. Statistical analysis was performed using SPSS Software, IBM and GraphPad Prism® Software.

2.2.10 Statistical Analysis

Differences amongst three or more group means were determined using the one-way analysis of variance (ANOVA) followed by the Games-Howell post-hoc test. Variables that did not fit a normal distribution were analysed using the Mann-Whitney U test. Correlative analysis was performed using the Spearman's rank test. Results were expressed as means ± standard error of the mean (SEM). Values of $P<0.05$ were considered statistically significant.

Chapter 3

Embryo-derived Trypsin-like Proteases in Implantation

3.1 Introduction

Human pre-implantation embryos are known to be distinctively invasive and unpredictable in terms of their developmental competence and chromosomal composition (Vanneste et al., 2009, Wells and Delhanty, 2000, Voullaire et al., 2000). Humans display correspondingly high rates of pregnancy loss, affecting up to 50% of conceptions. Although 50% of miscarriages result from aneuploidies, the specific and complex chromosomal rearrangements seen in blastocysts have not been detected in clinical miscarriage samples (Fragouli et al., 2013). The genetic diversity observed in human embryos may render implantation events adaptable to a changing environment and aneuploidy could in fact infer an implantation advantage, as in cancer cells (Macklon and Brosens, 2014, Vanneste et al., 2009). However this diversity also poses a requirement for a selective human endometrium that impedes implantation of developmentally incompetent embryos, in order to safeguard the mother against prolonged investment in a non-viable conceptus (Macklon and Brosens, 2014).

In order to develop a receptive yet selective phenotype the functional endometrial compartment undergoes vast morphological and biochemical remodeling, including decidualization, which occurs cyclically and spontaneously in humans. Insufficient decidual preparation of the endometrial stromal cell layer results in out of phase implantation and pregnancy loss (Teklenburg et al., 2010b). Although the embryo is thought to make initial contact with the upper endometrial epithelium, the role of this cellular compartment in implantation is still under debate and may differ between species (Lucas et al., 2013). The interaction between epithelial and stromal cells, however, is thought to orchestrate the implantation process, creating a dynamic micro-environment capable of reacting and adapting to local requirements. In this way the endometrium may be seen as a biosensor of embryo quality, a feature

illustrated by differential endometrial gene expression patterns upon exposure to embryos of altered origins or varying quality (Sandra and Renard, 2011, Brosens et al., 2014, Salker et al., 2010). In addition to supporting implantation of viable embryos, HESCs specifically target and eliminate compromised embryos (Brosens et al., 2014) and thus malfunction of the endometrial biosensor may lead to a prolonged maternal investment in non-viable embryos (Weimar et al., 2012b, Salker et al., 2010). This theory has been substantiated by the observation that HESCs from women suffering with RM fail to discriminate between viable and non-viable embryos (Teklenburg et al., 2010a).

In order for the endometrium to function as a biosensor, human embryos must produce mechanical or chemical signals that convey their developmental potential to the maternal cells. It is expected that such signals would be heightened at the blastocyst stage, when the embryo implants. Various factors have been studied and implicated in the process of implantation (Table 1.5.1), mainly using gene deletion studies in rodent models, but none have been shown to result in a defined human maternal response in line with the biosensoring theory. However a recent study, focusing on the mouse, has comprehensively implicated a role of embryo-derived serine proteases, notably trypsin, in regulating the decidual response through cleavage of the epithelial sodium channel (ENaC) (Ruan et al., 2012).

In this chapter I use a variety of methods, ranging from a comprehensive literature search, analysis of microarray databases, protein measurements and co-culture experiments, in order to identify candidate embryo-derived signals involved in maternal embryo recognition and biosensoring.

I demonstrate that tryptic proteases play an important role in the implantation process in the human. Both evolutionarily conserved and non-conserved pathways

contribute to the generation of a complex protease signal that act on specific receptors in human decidualising stromal cells. Furthermore, the embryo-derived protease signals fluctuate between human embryos according to their ability to implant *in vivo*.

3.2 Results

3.2.1 Trypsin literature search

As discussed in Chapter 1, a key role for embryo-derived trypsin-like proteases has been described in murine implantation (Ruan et al., 2012). I performed an electronic literature search using the PubMed database focusing on a role of trypsin and trypsin-like proteases in embryo development and/or implantation. The keywords 'trypsin' or 'protease' in conjunction with 'embryo', 'implantation' or 'reproduction' in the title or abstract, were used. I restricted the search to articles published in the English language between 1970 and December 2015. This literature search identified 1456 articles and implicates embryo-derived trypsin activity as an important mediator of implantation across, at least, ten different species (Table 3.2.1).

The results of the literature search reveal that trypsin-like proteases are involved in early/pre-implantation embryo development of the salmon louse, tiger mosquito, marine crab, Xenopus frog and mouse (Table 3.2.1). Furthermore, the search directly implicates trypsin-like proteases in regulating zona lysis and embryo hatching in rabbit, mouse, rat, sheep and hamster embryos (Table 3.2.1). The literature even details a role for protease activity beyond hatching, promoting embryo attachment and penetration of endometrial cells in mice and rats, and placental development in Rhesus monkeys (Table 3.2.1). Implantation-related trypsin activity in mice is reported to encompass a complex system of at least two types of proteolytic activity, either locally secreted or located at the cell surface. In this species, trypsin and protease inhibitors were found to reduce the number of implantation sites, promote fetal loss and reduce fetal birth weight *in vivo* (Table 3.2.1). No study to date has designated a role for trypsin in either human blastocyst development or implantation.

Table 3.2.1 The Role of Trypsin-like Proteases in Implantation: A Review of the Literature

Species	Experimental Details	Conclusions	Reference
Aedes Albopictus	- Analysis of trypsin-like serine peptidase profiles in eggs, larvae and pupae by zymography and SDS-page. - Differing proteolytic bands were observed at each stage, and could be inhibited by a serine protease inhibitor (phenyl-methyl sulfonyl-fluoride/PMSF) and trypsin-like serine protease inhibitor (Nα-Tosyl L-lysine chloromethyl ketone hydrochloride/TLCK), in larvae and pupae.	- Trypsin-like serine proteases are important in early mosquito development.	(Saboia-Vahia et al., 2013)
Hamster	- Measured the effect of various proteases on zona pellucida (ZP) dissolution. - Cysteine protease inhibitors completely inhibited ZP escape whereas trypsin inhibitors had a reduced effect.	- Cysteine proteases may mediate blastocyst hatching in hamsters. - This differs from previous evidence which demonstrated a role of trypsin-like proteases in this process.	(Mishra and Seshagiri, 2000)
L.Salmonis	- Trypsin-like *LsTryp10* mRNA was found to be evenly distributed in ovaries and oocytes and produced both maternally and by embryos. - Maternally deposited and embryonic *LsTryp10* appear to be translated from dissimilar pools of mRNA; one being maternally transcribed and the other being transcribed post- fertilization. - Maternally derived *LsTryp10* is thought to regulate the yolk degradome.	- A trypsin-like protease, of both maternal and embryonic sources, was detected in oocytes. - The protease was differentially regulated and had different functions according to its origin.	(Skern-Mauritzen et al., 2009)
Marine Crab	- Biochemical composition and digestive enzyme activity was analysed throughout embryonic development.	- Trypsin activity is detectable during early and late embryonic development.	(Xu et al., 2013)

	- Increased trypsin activity was detected in the early and late stages.		
Mouse	- Tested a range of enzymes and their effects on the ZP. - Lysis of ZP *in vitro* could only be achieved by trypsin or pronase.	- The lysin secreted by the embryo prior to implantation must be a proteolytic enzyme.	(Bowman and McLaren, 1970)
Mouse	- Embryos were cultured on monolayers of decidual cells and exposed to soybean trypsin inhibitor and nitrophenol-p-guanidino benzoate (NPGB). - NPGB alone had the greatest inhibitory effect on blastocyst development compared to alternative trypsin inhibitors alone. - However when inhibitors were combined the inhibitory effect was even greater.	- Suggests a complex system of at least two types of proteolytic activity is required for implantation and embryo attachment in mice.	(Kubo et al., 1981)
Mouse	- Applied a trypsin assay to homogenised embryo pellets and embryo culture supernatants. - Tested the effect of inhibitors on *in vitro* embryos. - The most significant results were found when using trypsin inhibitors which were too large to enter the blastocyst, suggesting a cell surface or secreted enzyme.	- Strypsin is a membrane associated trypsin-like protease involved in blastocyst hatching.	(Perona and Wassarman, 1986)
Mouse	- Enzymatic activity measured in embryo culture medium - Embryo protease activity increased during hatching and could be strongly inhibited following administration of trypsin inhibitors. - Only weak inhibition was observed with non-trypsin specific inhibitors.	- Protease activity of hatching blastocysts results from trypsin and/or trypsin-like serine proteases.	(Sawada et al., 1990)

Mouse	- Pregnant mice were injected, intraperitoneally, with Ascaris trypsin inhibitor on day 12 to 15 of pregnancy. - On day 19 implantation sites, early resorptions and living and dead foetuses were counted. - Ascaris trypsin inhibitor leads to maternal deaths, abortions, increased fetal deaths and decreased mean fetal weight of living fetuses	- Implicates a role for trypsin in both uterine and embryonic development.	(Blaszkowska, 2005)
Mouse	- Intrauterine injection of serine protease inhibitor 4-(2-aminoethyl)benzenesulfonyl fluoride hydrochloride (AEBSF) on day 3 of pregnancy. - Mice were sacrificed and uterine horns harvested on day 8 to count the number of implantation sites. - The number of implantation sites was reduced in response to increasing AEBSF concentration. - This effect was reversible and AEBSF has cytotoxic effect on the uterine epithelia.	- AEBSF impairs implantation, possibly due to interference in extracellular matrix remodelling.	(Sun et al., 2007)
Mouse	- Used liquid chromatography/mass spectrometry to analyse secreted proteins from recently activated oocytes. - Prss1 was the most abundant of all 18 proteins found in the ZP free group. Only 6 proteins were found in ZP intact group.	- Prss1, Trypsinogen 7, Trypsin 4 and Trypsin 10 are secreted from recently activated oocytes suggesting a direct role in regulation of fertilisation and embryonic development.	(Peng et al., 2012)
Rat	- Intrauterine injections of protease inhibitors (of chymotrypsin-like, thiol-, metallo- and trypsin-like proteases) on day 5 of pregnancy. - 5 to 6 hours later embryos were flushed from the uterine horns and examined.	- A number of proteases play specific roles in embryo development and hatching in rats; - Trypsin-like and metallo- proteases are implicated in zona lysis.	(Ichikawa et al., 1985)

		- Chymotrypsin-like proteases and thiol proteases are implicated in growth and development of the embryo.	
Rat	- Cervical dislocation of pregnant mice on day 3 of pregnancy. Uterine horns dissected and endometrial cells collected. Blastocysts collected prior to dissection via uterine flushing and co cultured with endometrial cells and AEBSF. - AEBSF containing wells showed abnormal aggregation of endometrial cells and inner mass shrinking of the blastocyst leading to blastocyst and cell death.	- Protease activity is required for blastocyst hatching and penetration of endometrial cells *in vitro.*	(Jiang et al., 2011)
Rabbit	- The effect of various proteases, including trypsin, were measured on the development and hatching of blastocysts. - Trypsin was one of the enzymes sufficient in low concentrations to result in blastocyst complete hatching.	- Rabbit blastocyst hatching *in vivo* may involve trypsin-like proteases.	(Kane, 1986)
Rhesus Monkey	- ISH (In situ hybridisation) experiment investigating mRNA localisation of and *PN-1* (protease nexin-1). - Intense localisation of mRNAs was observed in trophoblastic shell and column, glandular epithelium and placental villi on day 12-18. - *PN-1* mRNA levels increased significantly on day 26.	- *Prss8* is implicated in endometrial epithelial morphology establishment, tissue remodelling, and trophoblastic invasion during early pregnancy. - The cognate Serpin, *PN-1*, was not reciprocally expressed, generating a tissue environment supporting the proteolytic activities of *Prss8* throughout early pregnancy.	(Lin et al., 2006)
Sheep	- Enzymatic removal of the ZP *in vitro* of both fertilised and unfertilised eggs using various proteases.	- Pronase may have a greater effect than trypsin on the lysis of the ZP prior to implantation in sheep.	(Moor and Cragle, 1971)

	- Pronase was the major protease showing a lytic effect on fertilised egg ZP however trypsin and chymotrypsin had a significant effect after a prolonged period of time. - However greater sample numbers were used for pronase analysis.		
Xenopus Laevis	- A secreted trypsin-like oviducal protease, oviductin, renders Xenopus eggs fertilizable by the conversion of glycoproteins gp43 to gp41. - Isolated, unfertilised egg envelopes were incubated with trypsin, chymotrypsin, p-aminobenzamindine and leupeptin. - A sperm binding assay revealed that trypsin treatment dramatically increased sperm binding to egg envelopes.	- Trypsin activity renders Xenopus eggs penetrable by sperm and capable of fertilization by selectively cleaving gp43 on the egg envelope mimicking oviductin action.	(Lindsay and Hedrick, 1998)
Xenopus Laevis	- Cloning of cDNA from Xenopus embryos using RT-PCR and comparison against human membrane type serine protease 1 (MT-SP1) and trypsin. - Overexpression of Xenopus embryonic serine protease 2 (*XESP-2)* and the Xenopus homolog of MT-SP1 (*XMP-SP1*) had significant defects to embryo development. - Injecting XESP-2 inhibited progression through to blastophore closure. - *XESP-2* has a cysteine rich scavenger receptor, similar to the protease encoded by *TMPRSS2*.	- Isolated three embryo-derived TTSPs cDNAs with distinct patterns of regulation during embryogenesis. - *XESP-2* and *XMP-SP1* were found to play a role in regulating embryo development.	(Yamada et al., 2000)

3.2.2 Trypsin activity in human embryos

In order to determine a role for trypsin activity in human implantation, embryo culture media (ECM) drops, in which embryos were cultured for IVF treatment, were routinely collected and stored at -80°C. These culture drops were tested for the presence of protease and trypsin activity in order to identify whether such activity may be as important in human implantation as observed in other species. The ECM either contained a number of co-cultured embryos from a single patient ('pooled'), or embryos that were cultured individually for time-lapse imaging ('individual').

Protease activity was measured using the Enzchek® assay. This assay measures protease catalysed hydrolysis of a casein derivative, which causes release of the quenched fluorescently labelled peptides (BODIPY FL dye). The level of fluorescence measured is proportional to protease activity. Trypsin activity was measured using an assay that employs a trypsin-specific substrate, which upon cleavage by trypsin generates p-nitroaniline (p-NA) detectable at OD = 405. The colour change is thus proportional to p-NA content.

To determine if trypsin activity is generated by human embryos, ECM of 163 pooled embryos from 16 individuals were analysed using the trypsin assay (Figure 3.2.2.1a). As shown, trypsin activity was detectable, although the level of activity varied widely between culture droplets (median: 20.9 mU/ml; range: 0.7 to 45.4 mU/ml).

In order to obtain more precise measurements of protease and trypsin activity, ECM of 87 individually cultured embryos from 21 individuals were analysed using the Enchek® and trypsin assays (Figure 3.2.2.1b,c). Embryos were divided into two groups according to the day of pre-implantation embryo development at the time of ECM collection (day 2 or day 5). Data were normalised to activity in unconditioned medium (UCM) droplets, which were not used for embryo culture, and mean values

are displayed.

Protease activity was measured in 47 individual ECM droplets and was increased in the ECM of day 5 embryos (median: 247.7 % change from control; range: 0.0 to 806.6 % change from control) compared to day 2 embryos (median: 38.3 % change from control; range: 0.0 to 546.1 % change from control) (Figure 3.2.2.1b).

Trypsin activity was measured in 40 individual ECM droplets and similar to protease activity, was increased in the ECM of day 5 embryos (median: 34.7 % change from control; range: 2.1 to 76.7 % change from control) compared to day 2 embryos (median: 10.3 % change from control; range: 0.0 to 46.4 % change from control) (Figure 3.2.2.1c).

The recorded levels of protease and trypsin activity varied markedly between individual ECM droplets (range: 0 to 806.6 % change from control; range: 0 to 76.7 % change from control, respectively) (Figure 3.2.2.1b,c). This variation is partly, but not entirely, explained by increased activity from embryos at day 5.

A high rate of attrition is observed during *in vitro* culture of human embryos with a majority of embryos arresting before the blastocyst stage. Therefore separation of ECM according to the day of development does not accurately reflect the developmental stage of the embryo. In our unit embryo transfers are conducted according to developmental day rather than embryo developmental stage. To determine whether trypsin activity reflected embryo developmental stage, 39 ECM droplets from day 5 transferred embryos were separated according to the developmental stage of the embryo (morula, cavitating, blastocyst) and subjected to the trypsin assay (Figure 3.2.2.2). Although the majority of embryos included in this analysis had reached the blastocyst stage (n = 24), this data shows a close trend towards increasing trypsin activity in line with developmental maturation.

Day 5 transferred blastocysts are routinely graded according to the Gardner grading system (Gardner et al., 2000), which assigns values to the level of blastocoel expansion in combination with the morphological quality of two polarised cell compartments that comprise the blastocyst. The outer shell-like TE that will give rise to the extraembryonic membranes and the inner cluster of cells that will give rise to the fetus, the ICM. These compartments are graded independently by an embryologist just prior to embryo transfer and the grades have been shown to reflect embryo implantation potential (Gardner et al., 2000).

Blastocoel expansion is graded as follows:

1, the blastocoel is less than half of the volume of the embryo;

2, the blastocoel is half of or greater than half of the volume of the embryo;

3, the blastocoel completely fills the embryo;

4, the blastocoel volume is larger than that of the early embryo, with a thinning zona;

5, the trophectoderm is starting to herniate though the zona;

6, the blastocyst has completely escaped from the zona.

For fully formed blastocysts (with a blastocoele grading of 3-6) the inner cell mass is graded as follows:

A, tightly packed, with many cells;

B, loosely grouped, with several cells;

C, very few cells.

For fully formed blastocysts (with a blastocoele grading of 3-6) the trophectoderm is graded as follows:

A, many cells forming a cohesive epithelium;

B, few cells forming a loose epithelium;

C, very few large cells.

To determine if trypsin activity varies between high and low quality embryos, 21 individual ECM drops from blastocysts transferred on day 5 were measured using the trypsin assay, and separated according to their morphological grading via the Gardner scale (Figure 3.2.2.3). In brief, groups A and B denote good to average quality embryos whereas group C denotes poor quality embryos. Though numbers are limited, this analysis revealed that increased trypsin activity was detectable in ECM drops from embryos with poorer quality trophectoderm. This may be explained by a propensity of trypsin, produced by the embryo, to leak out between the cells within the trophectoderm layer in cases where the cells are more loosely packed. The result may be decreased trypsin levels within the blastocyst itself potentially impairing the ability of the blastocyst to adequately undergo the hatching process, a prerequisite for implantation.

This work provides novel evidence of trypsin activity being produced by human embryos, which complements the wealth of literature designating a role for trypsin during the implantation process (Table 3.2.1). Although the exact role of trypsin in human implantation requires further investigation I speculate that it may mirror that of other species and contribute to blastocyst hatching, embryo attachment, invasion and maternal recognition.

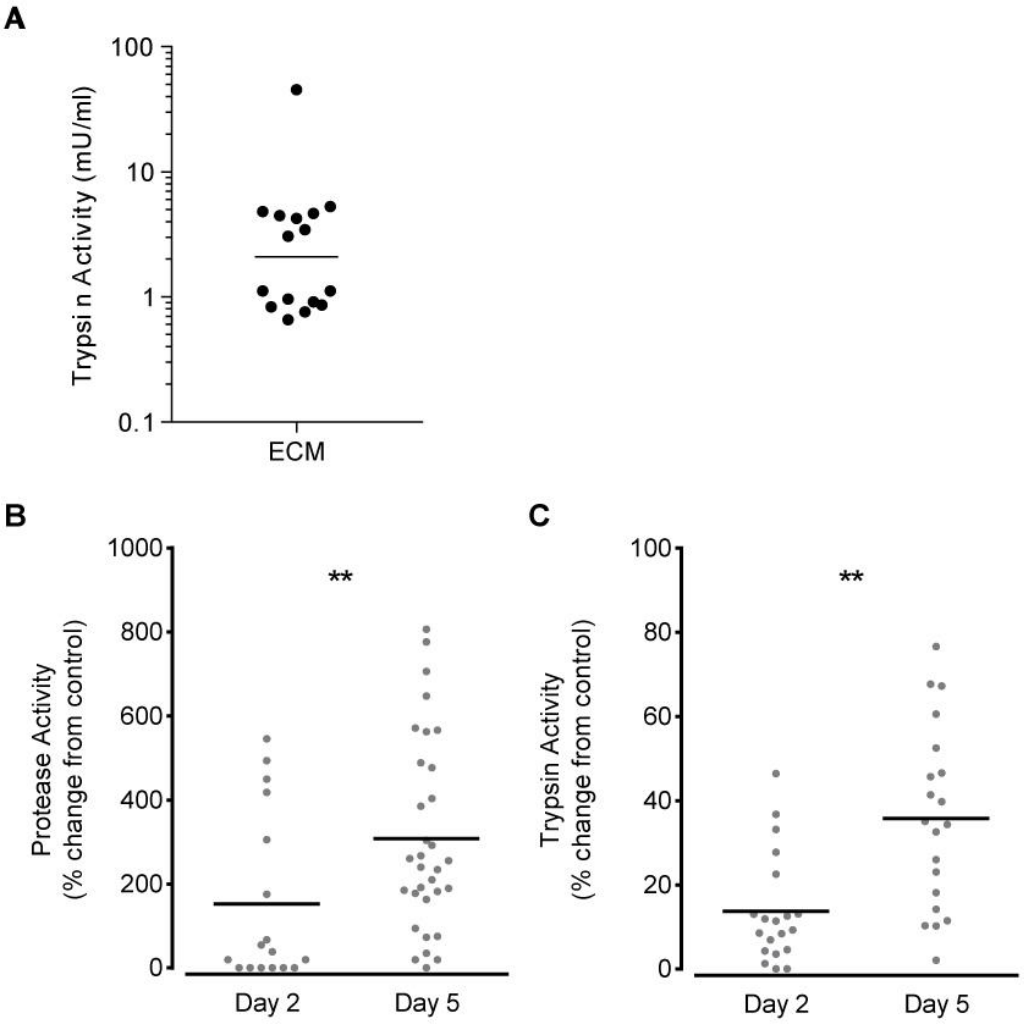

Figure 3.2.2.1 Protease and Trypsin activity in ECM a) Trypsin activity in day 5 pooled ECM (n = 16). b) Protease activity in individual ECM (*n* = 49, *P* = 0.006) using the Enzchek® assay. c) Trypsin activity in individual ECM (*n* = 38, *P* = 0.0015). All measurements were performed in duplicate, normalised to UCM and are displayed as mean values. Mann Whitney statistical analysis was applied. *P < 0.05; **P < 0.01; ***P < 0.001.

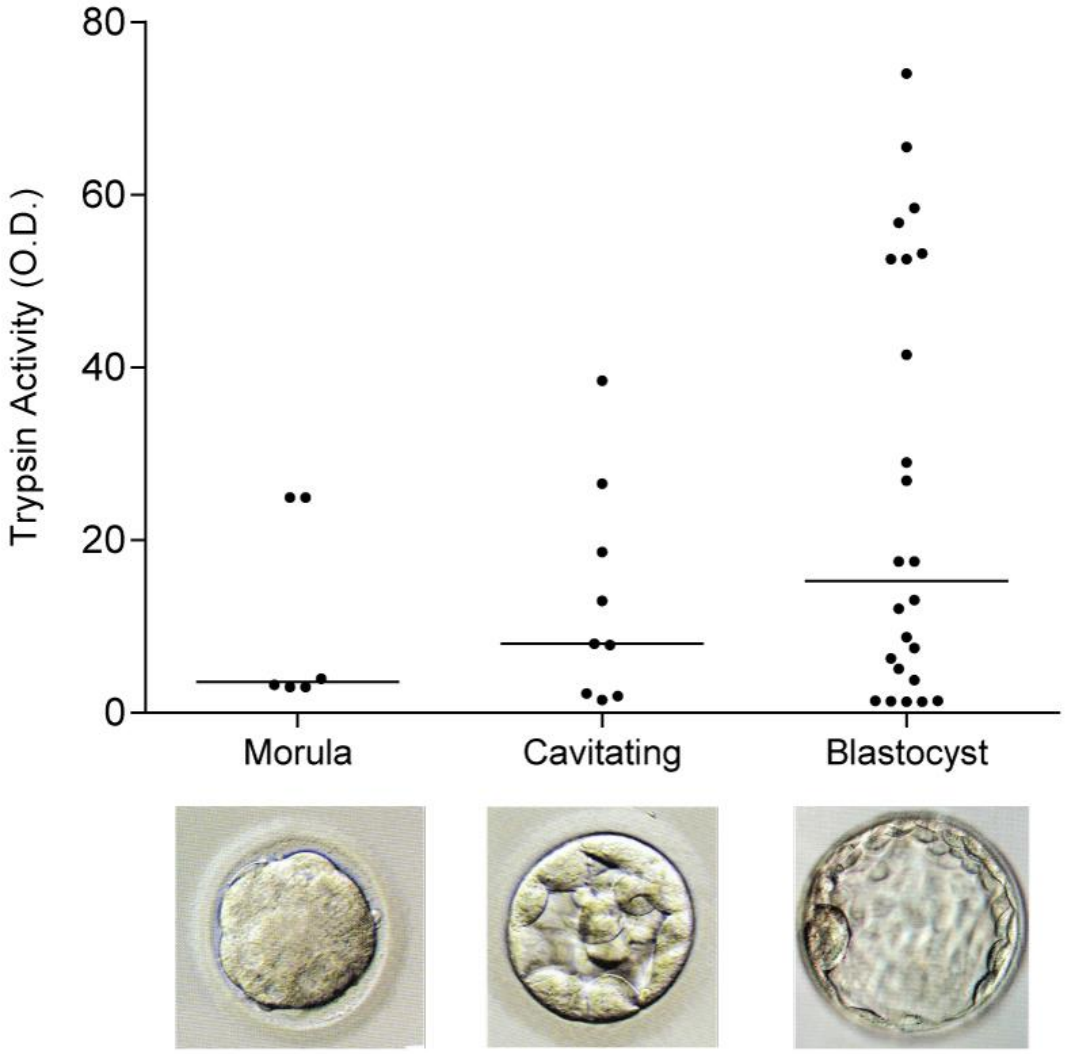

Figure 3.2.2.2 Trypsin activity and pre-implantation embryo development. Trypsin activity in individual ECM (*n* = 39). All measurements were performed in duplicate, normalised to UCM and are displayed as mean values. Median values are displayed for each group. ANOVA statistical analysis was applied (F = 1.569, *P* = 0.2133) with Brown-Forsythe test (P = 0.0757).

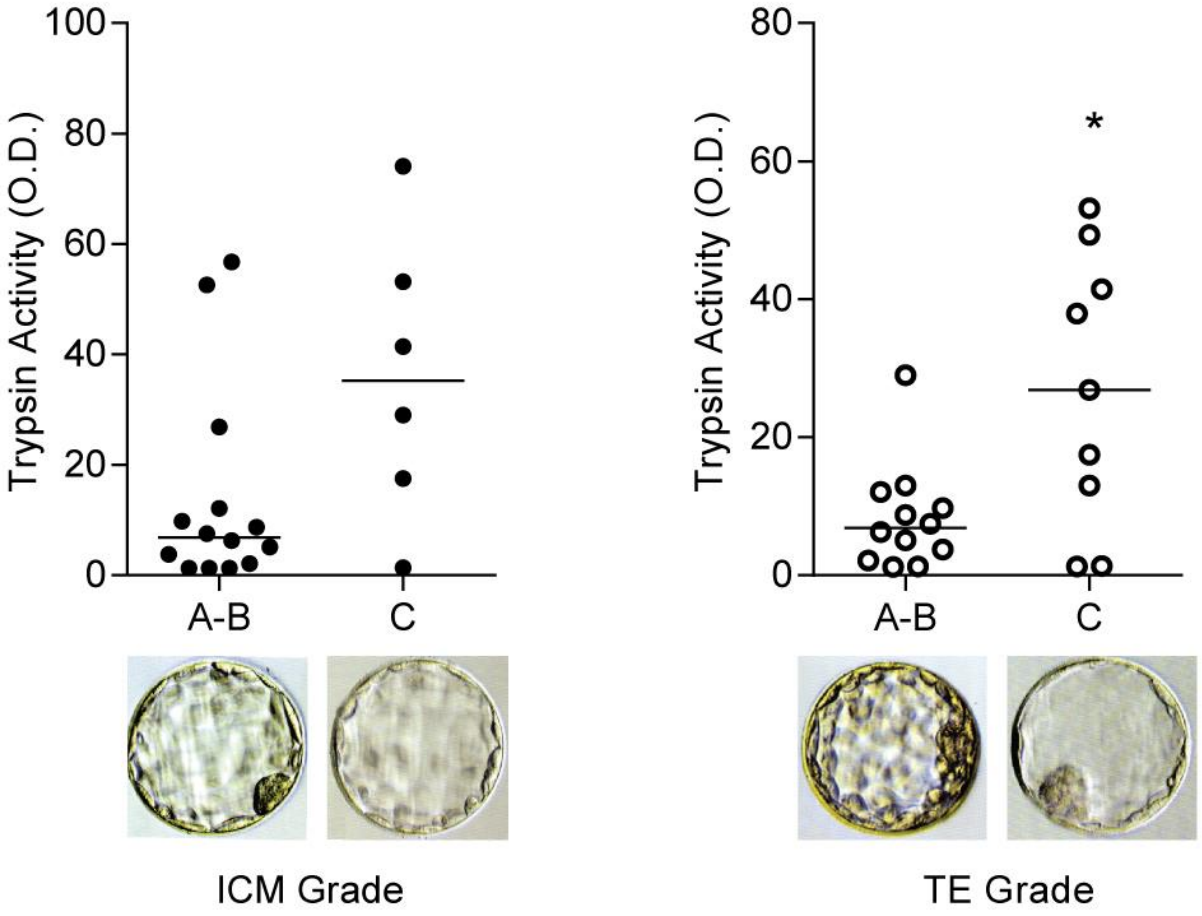

Figure 3.2.2.3 Trypsin activity and morphological grade. Trypsin activity in individual ECM from blastocysts transferred on day 5 (*n* = 21) and separated according to morphological grade (A = good, B = satisfactory, C = poor). All measurements were performed in duplicate, normalised to UCM and are displayed as mean values. Median values are displayed for each group. Mann Whitney statistical analysis was applied (ICM *P* = 0.0622, TE *P* = 0.0355).

3.2.3 Trypsin induces calcium Ca^{2+} oscillations in Ishikawa cells

A recent study illustrated that trypsin could induce morphological changes that mimicked decidualization in murine endometrial cell cultures via a sustained rise in intracellular calcium ions ($[Ca^{2+}]_i$) (Ruan et al., 2012). The authors speculated that embryo-derived trypsin activity may similarly regulate implantation in humans (Ruan et al., 2012).

Ca^{2+} coordinates various physiological and biochemical processes, acting as widespread secondary messengers in signal transduction pathways. To establish whether trypsin induces Ca^{2+} signaling in human endometrial cells, we monitored Ca^{2+} oscillations in individual Ishikawa cells, a well-studied human endometrial adenocarcinoma cell line, by confocal microscopy. Ishikawa cells were first pre-loaded with fura-2 (0.5 µg/ml), a sensitive, high affinity, ratiometric indicator dye that is widely used for accurate $[Ca^{2+}]_i$ measurements around basal concentrations. A shift in the excitation spectrum of fura-2 upon binding to Ca^{2+} permits ratio measurements, which overcome problems associated with uneven dye loading, leakage, photobleaching and unequal cell thickness. Upon treatment with trypsin (10 nM) $[Ca^{2+}]_i$ oscillations were observed and persisted for around 10 minutes (Figure 3.2.3.1a).

Ca^{2+} may enter the cytoplasm from external sources via calcium channels in the cell membrane, or from emptying of internal stores, i.e. mitochondria and endoplasmic reticulum. To determine the nature of the Ca^{2+} response to trypsin, the previous experiment was repeated in the absence of extracellular Ca^{2+}. This resulted in a single $[Ca^{2+}]_i$ transient, followed by a decline in $[Ca^{2+}]_i$ to below the baseline level (Figure 3.2.3.1b). Re-addition of Ca^{2+} to the extracellular solution resulted in resumption of oscillations (Figure 3.2.3.1b). The data indicate that a single initial increase in $[Ca^{2+}]_i$ upon trypsin application originates from the emptying of an

intracellular store, whilst store-operated Ca^{2+} entry channels (SOCE) are crucial to the sustained calcium signalling response to trypsin.

Sarco/Endoplasmic Reticulum Ca^{2+} ATPase (SERCA) resides in the sarcoplasmic reticulum (SR) where it transfers Ca^{2+} from the cell cytosol to the SR lumen via ATP-hydrolysis. The "Ca^{2+} re-addition" protocol (Bird et al., 2008) was used in order to determine the existence of SOCE in Ishikawa cells. SERCA was inhibited, in the absence of extracellular Ca^{2+}, using cyclopiazonic acid (CPA), which resulted in depletion of Ca^{2+} content from the ER due to passive Ca^{2+} leakage (Figure 3.2.3.1c). The amplitude and rate of rise of $[Ca^{2+}]_i$ upon re-addition of extracellular Ca^{2+} demonstrates SOCE activation in Ishikawa cells. Furthermore, an increased rate and amplitude of the $[Ca^{2+}]_i$ rise upon application of CPA in addition to trypsin (10 nM) suggests that trypsin potentiates SOCE (Figure 3.2.3.1d).

These findings clearly demonstrate that trypsin can induce sustained, SOCE-dependent Ca^{2+} oscillations in human endometrial (Ishikawa) cells.

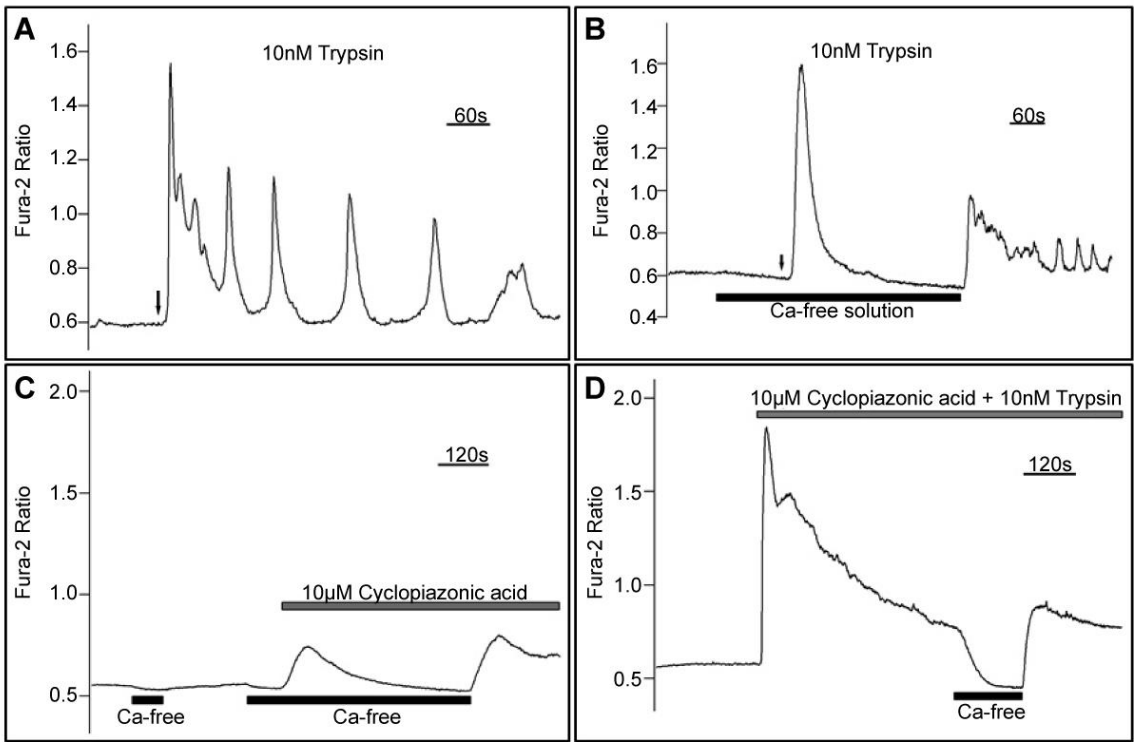

Figure 3.2.3.1 Trypsin-induced Ca^{2+} oscillations in Ishikawa cells. a) 10 nM trypsin application in the presence of extracellular Ca^{2+}. b) 10 nM trypsin application in the absence of extracellular Ca^{2+} followed by re-addition of extracellular Ca^{2+} after 5 minutes. c) Inhibition of the SERCA pump via CPA and activation of SOCE via the "Ca^{2+} re-addition protocol" (Bird et al., 2008). d) As (c) but in the presence of trypsin (10 nM). Fluorescence intensity for fura-2 (0.5 μg/ml) is shown as the 340/380 ratio, calculated from excitation at 340 nm (high calcium) and 380 nm (low calcium) with emission set at 510 nm (LSM 510 META, Carl Zeiss, UK). Work done in collaboration with Dr Anatoly Shmygol.

3.2.4 Trypsin-dependent gene expression in Ishikawa and HEECs

Ca^{2+} signaling, mediated by embryo-derived trypsin, has been shown to induce *Ptgs2* expression, which codes for COX-2, a key mediator of prostaglandin synthesis in mouse implantation (Ruan et al., 2012).

In order to assess whether trypsin impacts this prostaglandin synthesis pathway in humans, trypsin (10 nM) was applied to confluent cultures of Ishikawa cells and human endometrial epithelial cells (HEECs). Trypsin was withdrawn after 15 minutes and RNA was harvested for qRT-PCR 24 hours later. This brief exposure to trypsin was sufficient to induce *PTGS2* expression 5-fold in Ishikawa cells (Figure 3.2.4.1a,) and 1.8-fold in HEECs (Figure 3.2.4.1b).

To determine whether increased *PTGS2* expression upon trypsin exposure correlates with COX-2 levels, Ishikawa cells were exposed to increasing concentrations of trypsin (0 to 100 nM) for 15 minutes. Protein was harvested after 24 hours and COX-2 protein levels were measured via SDS-PAGE and Western blot (Figure 3.2.4.1c). The findings indicate that induction of *PTGS2* in response to a tryptic signal is paralleled by the induction of COX-2 at protein level.

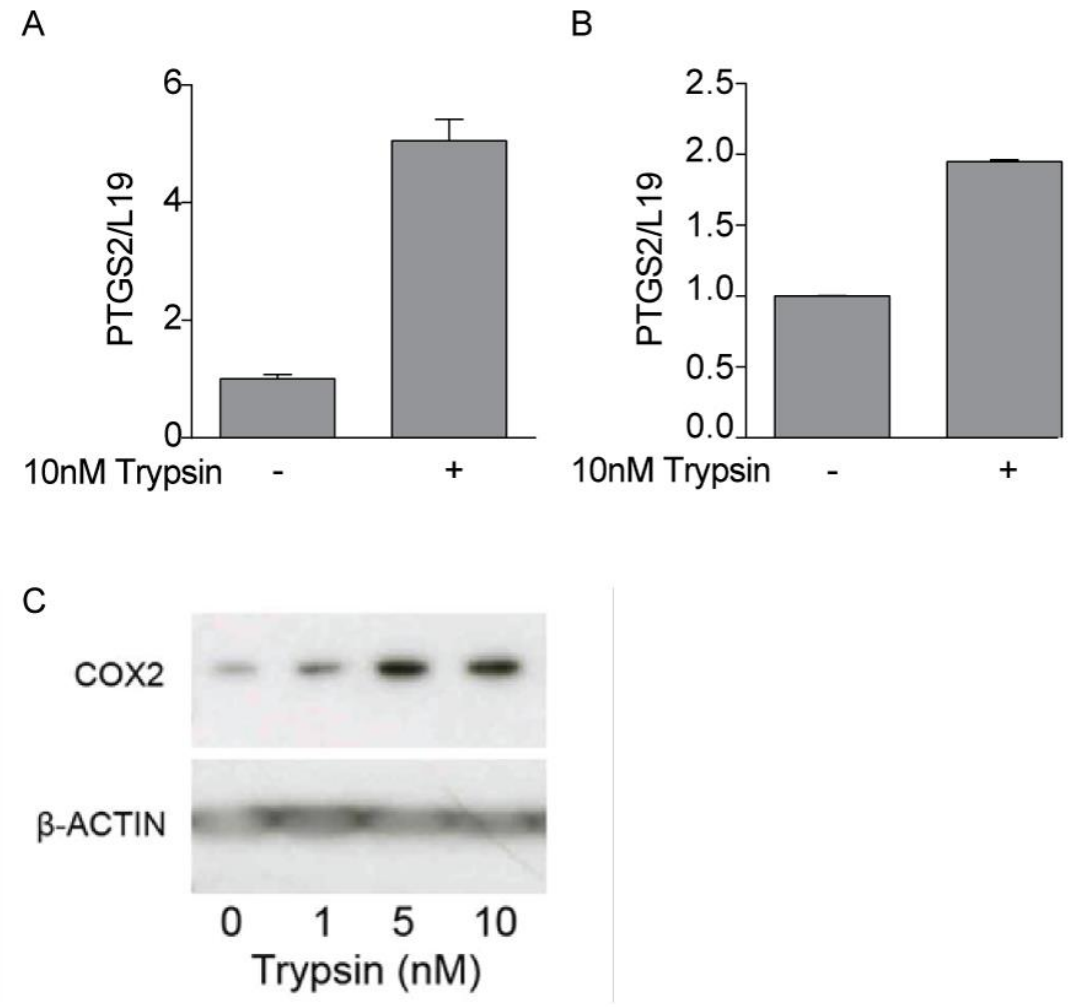

Figure 3.2.4.1 *PTGS2* and COX-2 expression upon trypsin exposure.

a) Ishikawa cells exposed to trypsin (10 nM, 15 minutes). b) Pooled HEECs exposed to trypsin (10 nM, 15 minutes). RNA was harvested at 24 hours and *PTGS2* transcript levels analysed, in triplicate, via qRT-PCR. Data are normalized to *L19* and shown as mean values (+SD). c) Ishikawa cells exposed to increasing trypsin concentrations (0 to 10 nM) for 5 minutes. Protein was extracted at 24 hours and COX-2 levels measured via western blot. B-actin was used as a loading control.

3.2.5 Embryo-derived trypsin induces Ca^{2+} signaling in Ishikawa cells

To determine whether embryo-derived trypsin activity could induce Ca^{2+} signaling in endometrial cells, Ishikawa cells were treated with ECM (diluted 1:20). In order to monitor Ca^{2+} concentrations, cells were pre-loaded with fluo-4 AM (5 μM), a non-fluorescent acetoxymethyl ester, which is cleaved intracellularly to give the single-wave, green-fluorescent calcium indicator fluo-4. Despite possessing lower affinity for Ca^{2+} than fura-2, fluo-4 permits measurements of greater rises in calcium levels, accurately detecting Ca^{2+} concentrations from 100 nM to 1 μM (Gee et al., 2000). Following application of ECM, the cells were subsequently monitored for 15 minutes (Figure 3.2.5.1a,b).

ECM induced Ca^{2+} oscillations in Ishikawa cells that varied markedly according to embryo quality (Figure 3.2.5.1a,b). ECM from competent embryos, i.e. successfully implanted, induced a sharp but transient rise in $[Ca^{2+}]_i$, lasting 3.5 minutes (Figure 3.2.5.1a). In contrast, ECM from embryos deemed unsuitable for transfer ('poor quality') induced a sharp initial rise in $[Ca^{2+}]_i$ followed by sustained, repetitive, Ca^{2+} oscillations, which persisted for the entire observation period (Figure 3.2.5.1b). This data suggest that embryo-derived signals can induce Ca^{2+} in the endometrium. Crucially 'good quality' and 'poor quality' embryos induce differential endometrial responses.

To determine whether the observed Ca^{2+} responses in Ishikawa cells resulted from trypsin activity in ECM, cells were pre-loaded with soybean trypsin inhibitor (1 mg/ml) before adding ECM (Figure 3.2.5.1c). This resulted in a dramatic reduction in the initial $[Ca^{2+}]_i$ rise in response to ECM addition (Figure 3.2.5.1a,b) and entirely abolished subsequent Ca^{2+} oscillations (Figure 3.2.5.1c). These findings indicate that embryo-derived trypsin activity is required for the Ca^{2+} signaling responses observed upon treatment of Ishikawa cells with ECM.

To further characterize the Ca^{2+} signaling responses observed upon application of ECM, Ishikawa cells were treated with trypsin (10 nM) (Figure 3.2.5.1d). Sustained, repetitive Ca^{2+} oscillations were detected following exposure to trypsin (Figure 3.2.5.1d), which mimicked the response to ECM from poor quality embryos (Figure 3.2.5.1b). As expected, the magnitude of the Ca^{2+} peaks were greater upon trypsin application, compared to ECM, but the pattern and duration of the Ca^{2+} oscillations were comparable (Figure 3.2.5.1b,d). Pre-treatment of the Ishikawa cells with soybean trypsin inhibitor (1 mg / ml) diminished the response to trypsin and curtailed the prolonged Ca^{2+} oscillations observed previously (Figure 3.2.5.1e).

These findings confirm a role for trypsin as a potential embryonic signal, detectable by endometrial cells and containing intrinsic information on embryo competency.

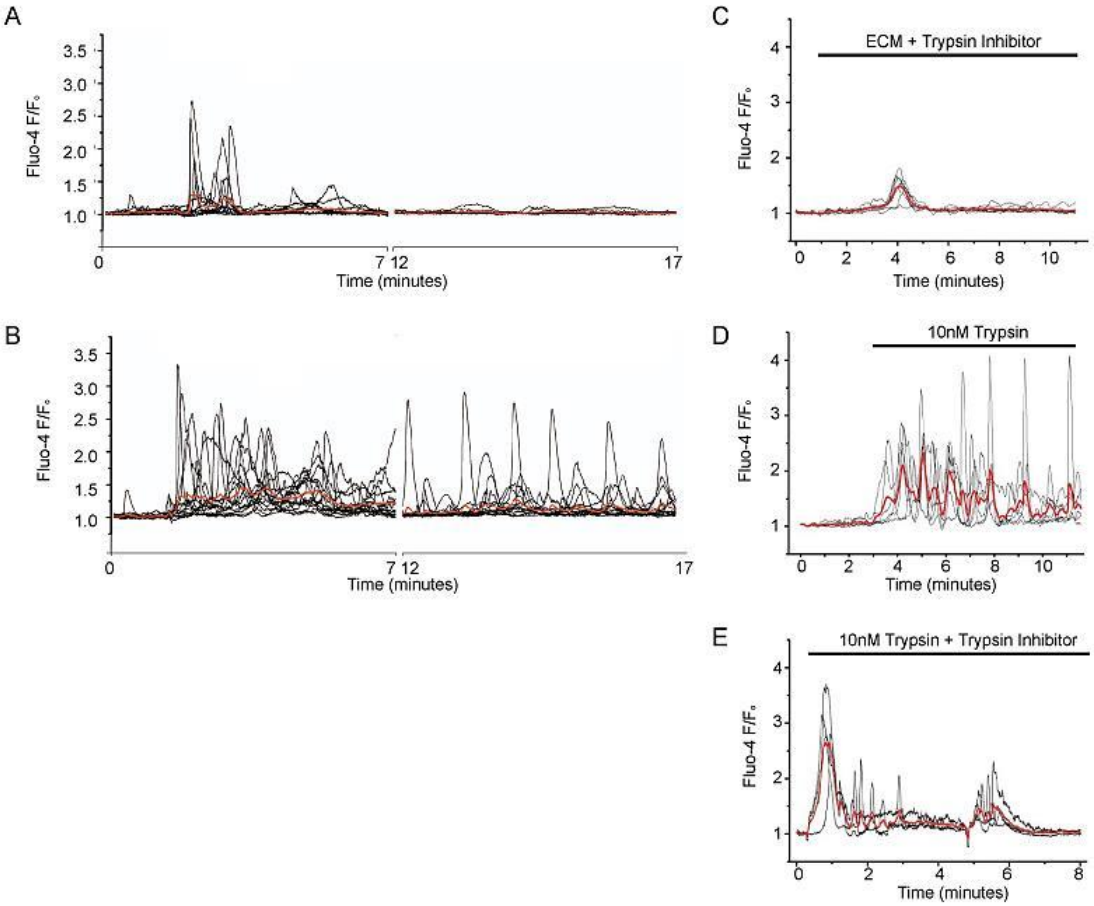

Figure 3.2.5.1 [Ca^{2+}]i oscillations in Ishikawa cells with ECM and trypsin. a) ECM (1:20 dilution) from successfully implanted embryos applied at 2 minutes. b) ECM (1:20 dilution) from poor quality embryos applied at 2 minutes. c) Cells pre-treated with soybean trypsin inhibitor (1 mg/ml), ECM (1:20 dilution) added at 2 minutes. d) 10 nM trypsin applied at 2 minutes e) Cells pre-treated with soybean trypsin inhibitor (1 mg/ml), 10 nM trypsin added at 0 minutes. Ishikawa cells were loaded with 5μM fluo-4-AM, excitation achieved at 488 nm and emitted light collected above 510 nm. Images were captured by confocal microscopy at 1 frame per second via the C-Apochromat 63 ×/ 1.20 W objective lens (LSM 510 META, Carl Zeiss, UK). Traces show fluorescence within individual cells expressed as a fold increase over fluorescence at time 0 (F/F_0). Data are representative of 4 replicates. Work done in collaboration with Dr Anatoly Shmygol.

3.2.6 Embryo-derived trypsin induces Ca^{2+} signaling in DESCs

The endometrial epithelium is largely regarded as a barrier to implantation in the mouse, which embryo(s) must breach in order to make contact with the underlying stromal cells and initiate decidualization. In humans, the stromal compartment undergoes cyclic decidualization, in the absence of an embryo, and co-operation between the stroma and overlying epithelial compartments is thought to orchestrate implantation. Consequently we speculated that, in humans, the maternal response induced by embryo-derived trypsin activity would extend beyond the epithelial layer and encompass the DESCs.

ECM was previously shown to induce differential calcium signalling responses in Ishikawa cells according to the quality of the cultured embryos ('poor quality' embryos compared to successfully implanted embryos). To more accurately assess whether embryo-derived trypsin activity determines implantation outcome, we compared ECM from day 5 transferred embryos according to the resulting pregnancy outcome (P = Pregnant, NP = Not Pregnant). In this way embryos were morphologically and developmentally alike and Ca^{2+} signaling responses could be directly attributed to implantation outcome.

To determine whether trypsin-dependent Ca^{2+} signalling extends to the stromal compartment, primary DESCs were pre-loaded with fura-2 and treated with ECM (diluted 1:50). The cells were subsequently monitored for 15 minutes.

ECM from transferred embryos was found to induce Ca^{2+} signalling responses in DESCs that varied strikingly according to their implantation competence (Figure 3.2.6.1a,b). ECM from successfully implanted embryos (P) induced a sharp initial rise in $[Ca^{2+}]_i$ followed by a suppression of subsequent Ca^{2+} oscillations (Figure 3.2.6.1a). In contrast, ECM from embryos which failed to implant (NP) induced

sustained Ca^{2+} oscillations (Figure 3.2.6.1b).

After 15 minutes of ECM treatment, trypsin (10 nM) was applied to the DESCs in order to identify whether ECM and trypsin induced Ca^{2+} signaling via a common pathway. Trypsin application following ECM treatment induced an initial rise in $[Ca^{2+}]_i$ (Figure 3.2.6.1a,b) but the Ca^{2+} oscillations were short lived and greatly reduced when compared to the control (Figure 3.2.6.1c). This data implicates trypsin as the embryo-derived signal inducing Ca^{2+} oscillations in DESCs.

These findings are very similar to those observed in epithelial cells (Figure 3.2.5.1a,b) suggesting that Ca^{2+} signalling in response to embryo-derived trypsin also encompasses the stromal compartment in the human endometrium. Overall the Ca^{2+} transients appear to be less prominent in DESCs compared to Ishikawa cells. However, this difference may be explained by the higher ECM dilution used (1:50 compared to 1:20) and the difference in Ca^{2+} sensitive probes (fura-2 compared to fluo-4).

The data further confirm a role for trypsin as an embryo-derived signal and indicate that biosensoring is not confined to the pre-implantation embryo but continues upon breaching of the luminal epithelium.

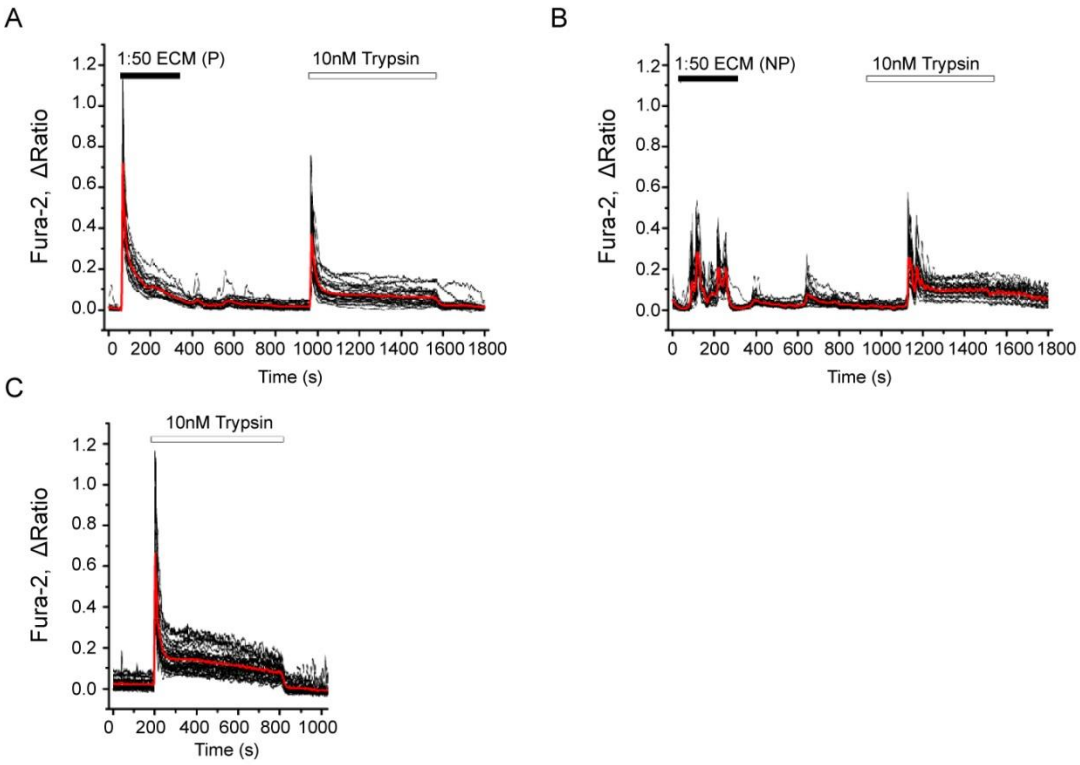

Figure 3.2.6.1 [Ca^{2+}]i oscillations in DESCs. a) ECM (1:50) from successfully implanted embryos (P, pregnant), then 10 nM Trypsin at 15 minutes. b) ECM (1:50) from embryos which failed to implant (NP, not pregnant), then 10 nM Trypsin at 15 minutes. c) 10 nM Trypsin. Cells were collected from mid-luteal endometrial biopsies, loaded with 5μM fura-2 and imaged by confocal microscopy. Fluorescence intensity for fura-2 (0.5 μg/ml) is shown as the 340/380 ratio, calculated from excitation at 340 nm (high calcium) and 380 nm (low calcium) with emission set at 510 nm (LSM 510 META, Carl Zeiss, UK). Traces show fluorescence within individual cells. Data are representative of 4 replicates. Work done in collaboration with Dr Anatoly Shmygol.

3.2.7 Trypsin biosynthesis pathway

Trypsin is formed by enzymatic degradation of trypsinogen and its activity may be modulated by the action of numerous trypsin and protease inhibitors. A simplified regulatory pathway of trypsin production has been described in the pancreas (Figure 3.2.7.1) (Ir et al., 1996, Itoh et al., 1996). Enteropeptidase (encoded by *TMPRSS15*) is deemed the 'master regulator' of trypsin activity due to its role in cleavage and activation of the trypsin zymogen, trypsinogen (Ir et al., 1996). This activation initiates a cascade of trypsin release, which is able to auto-activate trypsinogen, further increasing trypsin production. Alpha-1 microglobulin/bikunin precursor (*AMBP)*, on the other hand, encodes a complex plasma glycoprotein which, upon proteolytic processing, produces bikunin which is a urinary trypsin inhibitor (Itoh et al., 1996).

I analysed microarray data in both human and murine embryos at differing pre-implantation developmental stages in order to identify the expression patterns of genes implicated in the trypsin pathway.

The gene encoding trypsinogen itself, *PRSS1*, is not regulated during pre-implantation development (Figure 3.2.7.2). However, in line with a role for trypsin in implantation, *TMPRSS15* expression is markedly increased beyond the 8-cell stage in human embryos (Figure 3.2.7.2). This pattern was not reciprocal in the mouse where there is no change in *Tmprss15* expression with embryo development (Figure 3.2.7.3). Concurrently, *AMBP* expression is decreased beyond the 8-cell stage in human embryos whereas expression is unchanged in mouse embryos (Figures 3.2.7.2 and 3.2.7.3).

The Inter-alpha trypsin inhibitor (IαI) family contains serine protease inhibitors formed from three of the four IαI heavy chains (ITIHs). Transcriptional regulation of the *ITIH* genes during pre-implantation development could thus potentially influence embryo-

derived trypsin activity. Interestingly *ITIH* expression patterns are clearly distinct between mouse and human embryos. *Itih1* decreases from the 1-cell stage to the blastocyst stage in mice but conversely, *ITIH1* increases in human embryos beyond the 4-cell stage (Figures 3.2.7.2 and 3.2.7.3). Whilst *Itih4* expression peaks at the 2-cell stage and *Itih2* and *Itih3* expression levels appear analogous between developmental stages in mouse embryos (Figure 3.2.7.3) *ITIH2*, *ITIH3* and *ITIH4* all gradually decrease beyond the 2-cell stage in human pre-implantation embryos (Figure 3.2.7.2). These findings indicate decreasing trypsin inhibition at later stages of human pre-implantation embryo development, strengthening a role for trypsin as a vital embryonic signal at implantation.

Microarray analysis of these classical trypsin pathway genes in pre-implantation embryos highlights a human-specific mechanism of trypsin activity at the blastocyst stage, whereby increased expression of the trypsinogen activator, *TMPRSS15,* is coupled with decreased expression of the trypsin inhibitors, *AMBP* and *ITIH2-4*.

Immunocytochemistry was used to confirm the presence of the TMPRSS15 and AMBP proteins at four different pre-implantation embryonic stages in both human and mouse embryos (Figures 3.2.7.4 and 3.2.7.5). The presence of TMPRSS15 and absence of AMBP in the inner cell mass of the human blastocyst, suggest a net increase in trypsin activity at this stage (Figures 3.2.7.4 and 3.2.7.5). The staining for both proteins is less distinct in the mouse blastocyst, in line with lack of conserved TMPRSS15/AMBP regulation between species.

These findings demonstrate an intricate, and previously unidentified, regulation of trypsin production and activity by pre-implantation embryos. Importantly, the gene expression patterning responsible for regulating tryptic activity appears to vary notably between human and mouse embryos.

In summary, advancing stages of human pre-implantation embryos appear to display enhanced trypsin regulation through increased conversion of trypsinogen and reduced trypsin inhibition. This evidence presents an alternative method of trypsin biosynthesis in human embryos, which may have compensated for the loss of implantation-specific trypsin proteases, such as *Prss28*, in the mouse (O'Sullivan et al., 2001).

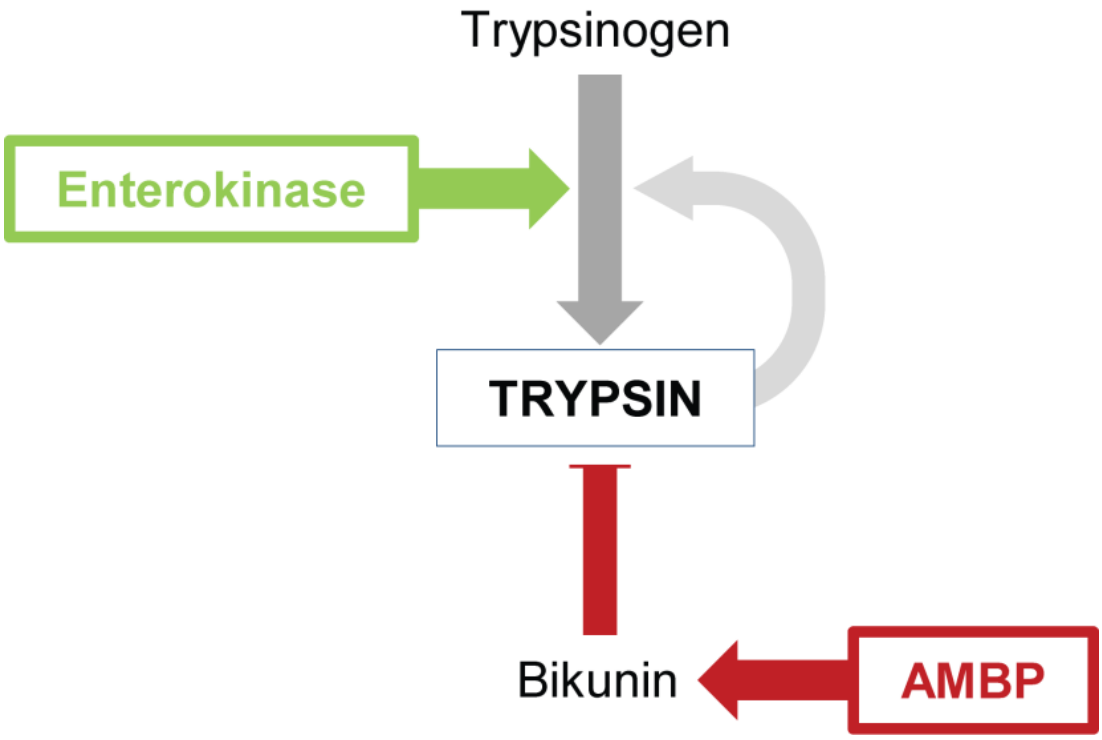

Figure 3.2.7.1 The Trypsin regulatory pathway. *TMPRSS15* encodes the enzyme Enterokinase which has been deemed the master regulator of trypsin activity. Enterokinase is required to convert the inactive trypsin precursor (trypsinogen) into its active state. Trypsin is then able to auto-activate trypsinogen causing a cascade of trypsin release (Kunitz, 1939). *AMBP* encodes a complex plasma glycoprotein which, upon proteolytic processing, produces bikunin, which is a urinary trypsin inhibitor.

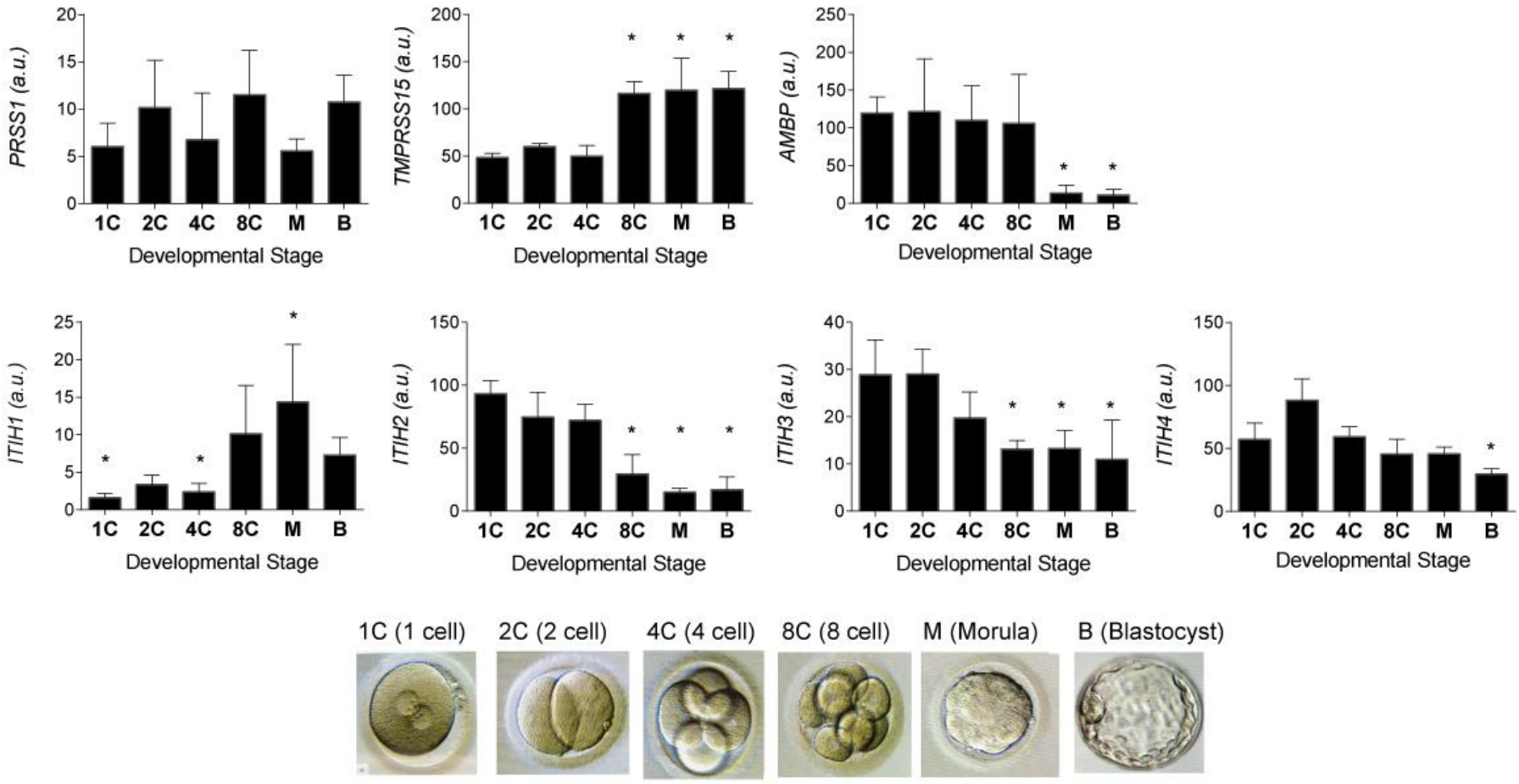

Figure 3.2.7.2 *In vivo* expression of trypsin regulatory genes during human pre-implantation embryo development. Analysis of microarray data from the Gene Expression Omnibus [accession numbers GSD3959 (Edgar et al., 2002)] shows the up-regulation of *TMPRSS15* and down-regulation of *AMBP, ITH2, ITH3* and *ITH4* with human pre-implantation embryo development. Transcripts were measured at the 1 cell, 2 cell, 4 cell, 8 cell, morula and blastocyst stages of embryonic development from 18 samples using Affymetrix Human Genome U133 Array. Data are presented as means ± S.D and One-way ANOVA statistical analysis was applied. *P <0.05; **P <0.01; ***P <0.001.

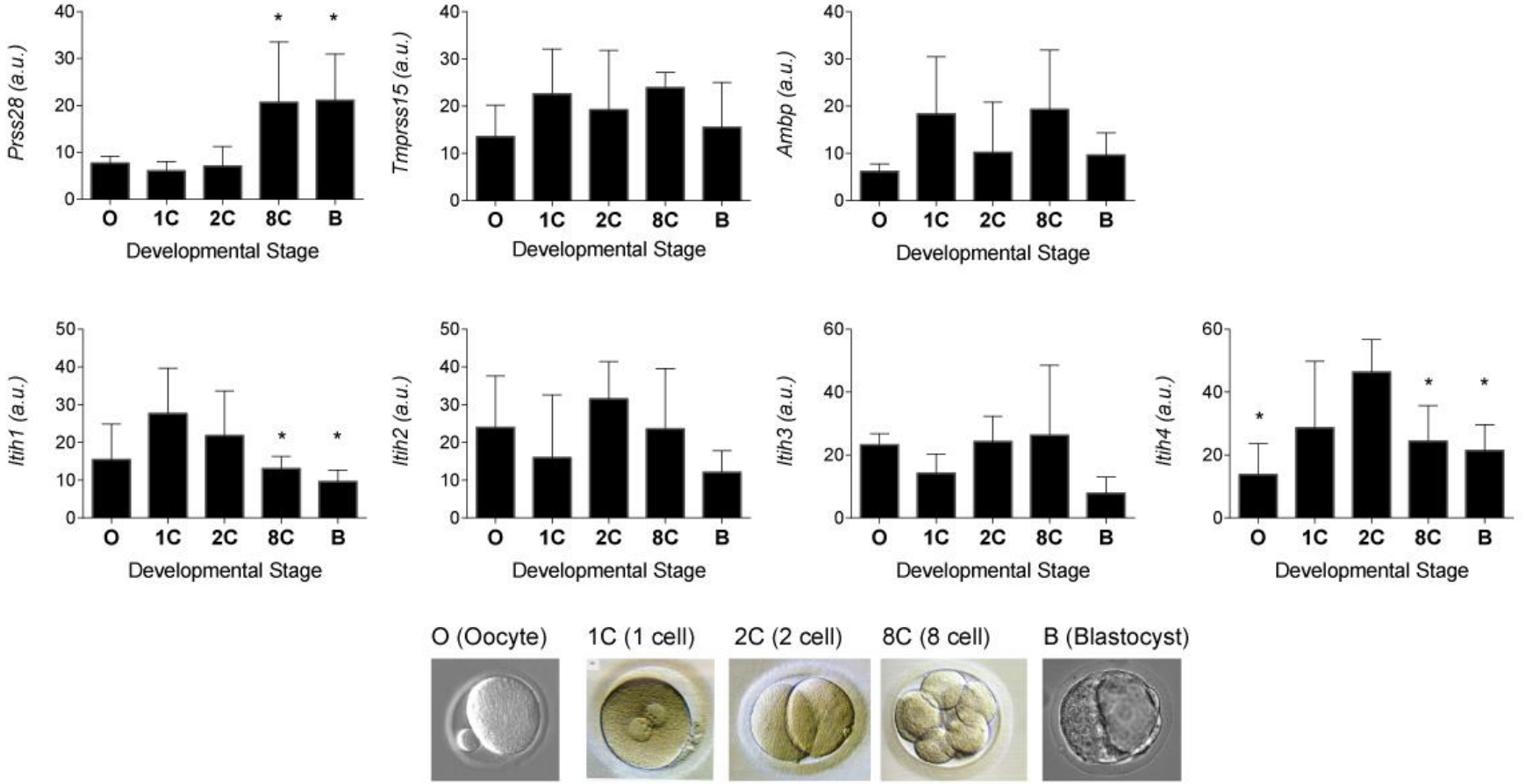

Figure 3.2.7.3 In vivo expression of trypsin regulatory genes during mouse pre-implantation embryo development. Analysis of microarray data from the Gene Expression Omnibus [accession number GDS813 (Edgar et al., 2002)] shows the up-regulation of *Prss28* with pre-implantation embryo development but a lack of regulation of *Tmprss15* and *Ambp, Itih2* and *Itih3*. Murine transcripts were measured at the oocyte, 1 cell, 2 cell, 8 cell and blastocyst stages of embryonic development from 20 samples using Affymetrix Human Genome U133 Array. Data are presented as means ± S.D and One-way ANOVA statistical analysis was applied. *P <0.05; **P <0.01; ***P <0.001.

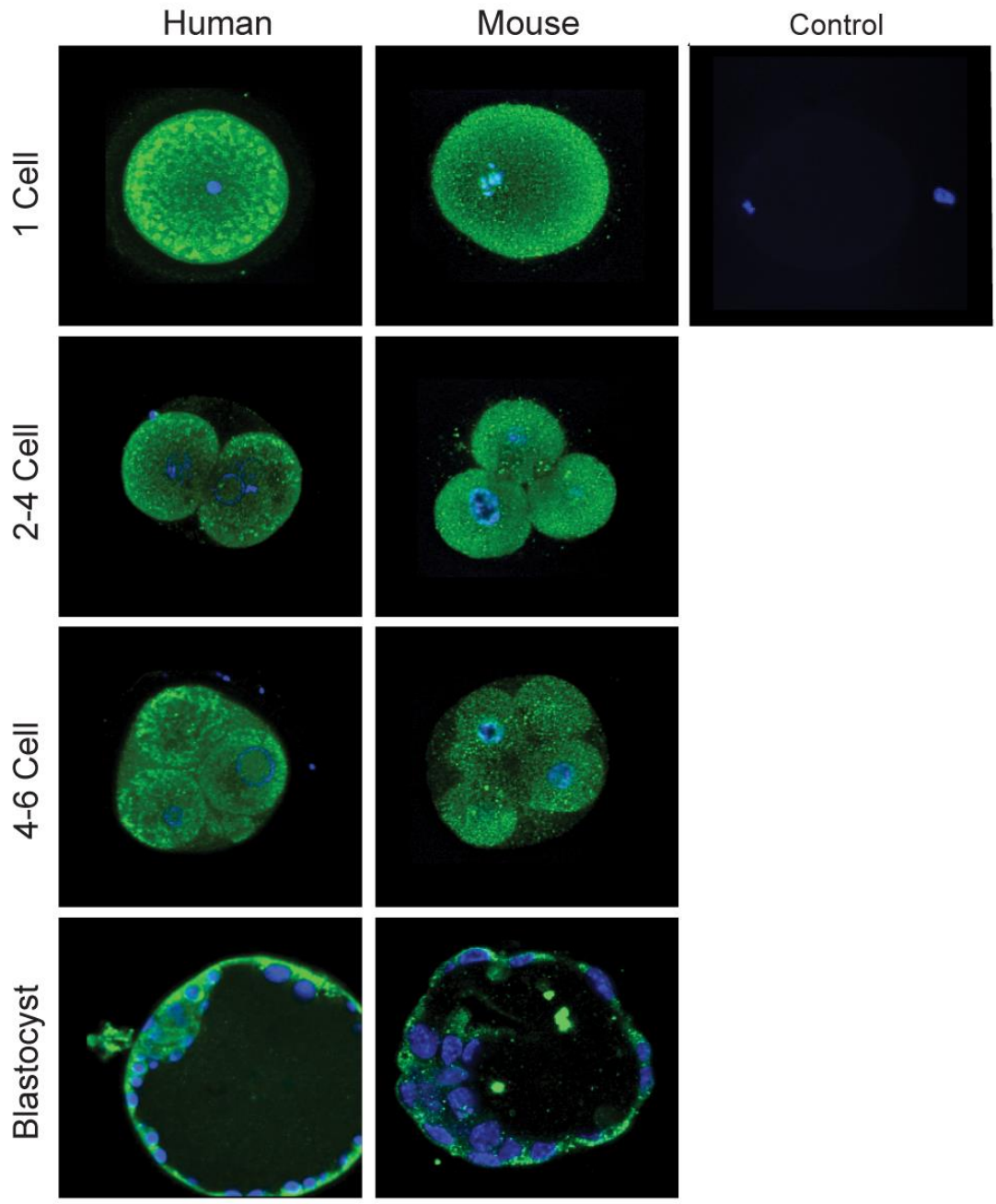

Figure 3.2.7.4 TMPRSS15 expression in human and murine pre-implantation embryos. Immunoflourescent labelling of human and murine embryos at different pre-implantation developmental stages (1 cell, 2-4 cell, 4-6 cell, blastocyst). Embryos were fixed in 4% w/v PFA/PBS at 2-8 °C. Polyclonal antibodies against TMPRSS15 were purchased from Novus Biologicals, NBP1-55616. 1% w/v BSA in PBS without primary antibody was used for the negative control. Embryos were mounted onto 35mm glass-bottomed petri dishes in 10ul Vectashield® with DAPI. Visualization was achieved using a Zeiss LSM 510 confocal imaging system.

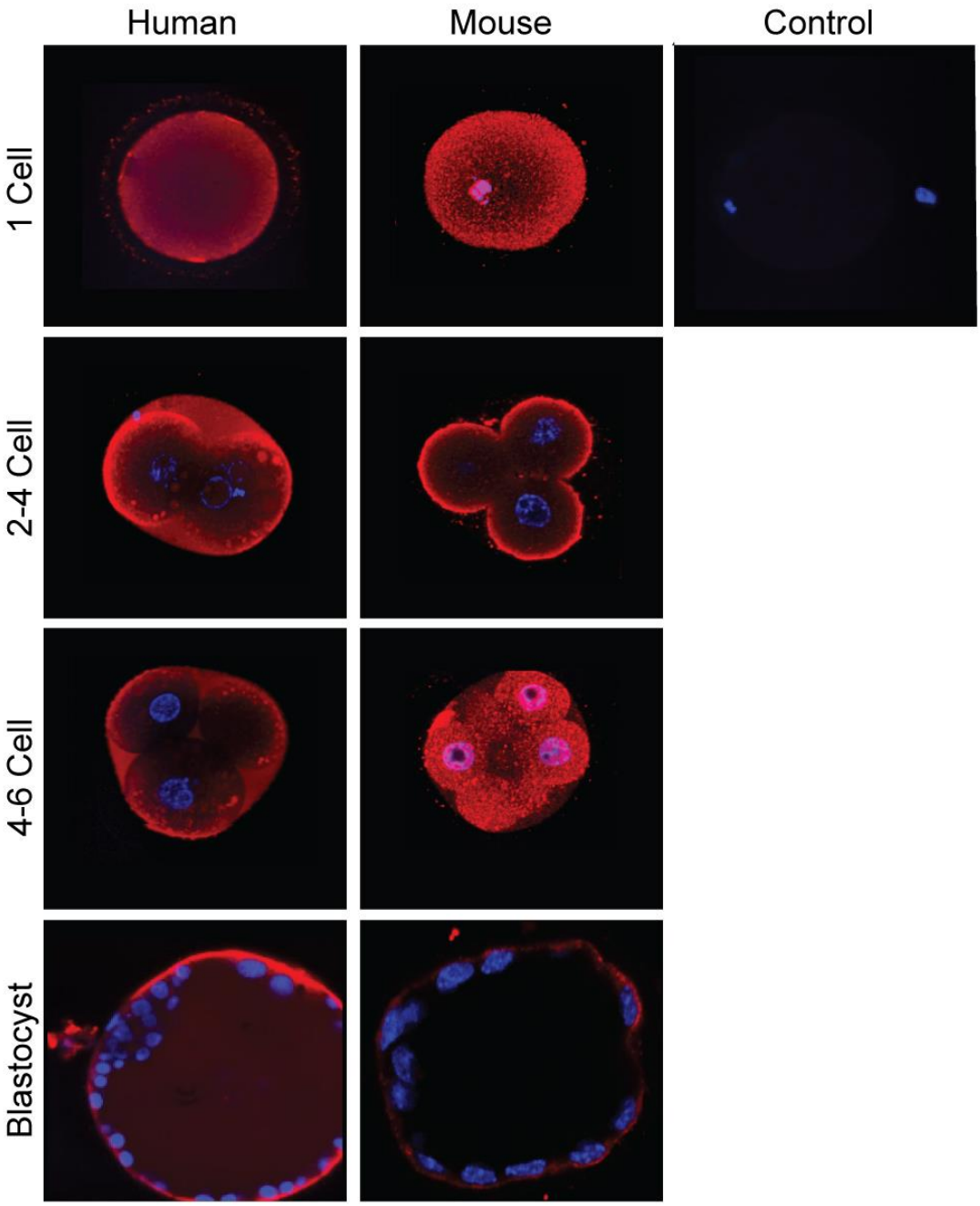

Figure 3.2.7.5 AMBP expression in human and murine pre-implantation embryos. Immunoflourescent labelling of human and murine embryos at different pre-implantation developmental stages (1 cell, 2-4 cell, 4-6 cell, blastocyst). Embryos were fixed in 4% w/v PFA/PBS at 2-8 °C. Monoclonal antibodies against AMBP were purchased from Novus Biologicals, H00000259-M01. 1% w/v BSA in PBS without primary antibody was used for the negative control. Embryos were mounted onto 35mm glass-bottomed petri dishes in 10ul Vectashield® with DAPI. Visualization was achieved using a Zeiss LSM 510 confocal imaging system.

3.2.8 Evolutionarily conserved proteases

Human embryonic signals were previously shown to regulate maternal gene expression in a manner conserved between human DESCs and whole mouse uterus (Brosens et al., 2014). In addition, ECM from DCE has been shown to induce the expression of numerous implantation genes when flushed through the mouse uterus. According to this concept, the origin of the embryo-secreted protease activity, which imparts embryo developmental potential to the endometrium, may be partly conserved between humans and mice (Brosens et al., 2014).

Gene Expression Omnibus (GEO) data mining was used to identify any protease encoding trancripts that displayed conserved up-regulation from the oocyte/1 cell stage to the blastocyst stage in both human and mouse pre-implantation embryos. In total 581 human and 588 mouse protease genes were identified (Puente et al., 2003), for which 505 and 434 had available microarray data, respectively. In each case, differences between the pre-implantation developmental stages were first identified using one-way ANOVA statistical analysis via SPSS software. The Games-Howell post-hoc test was applied on genes differentially expressed between 2 or more developmental stages (P <0.05, one-way ANOVA). As I aimed to identify specifically blastocyst regulated genes, I also calculated the fold change in transcript level from each developmental stage compared to that of the blastocyst stage. The results are listed in Appendix 2.

The most highly regulated serine protease genes in human and mouse embryos between the 8 cell stage and blastocyst stage were *Tmprss2* and *Prss8* (Figure 3.2.8.1). *TMPRSS2* and *PRSS8* transcripts were also significantly up-regulated at the blastocyst stage in human embryos (Figure 3.2.8.2).

Immunocytochemistry was used to confirm the presence of the PRSS8 and

TMPRSS2 proteins throughout pre-implantation development in both human and mouse embryos (Figures 3.2.8.3 and 3.2.8.4). Staining is strongest at the blastocyst stage and particularly high in the TE compartment, compared to the ICM (Figures 3.2.8.3 and 3.2.8.4).

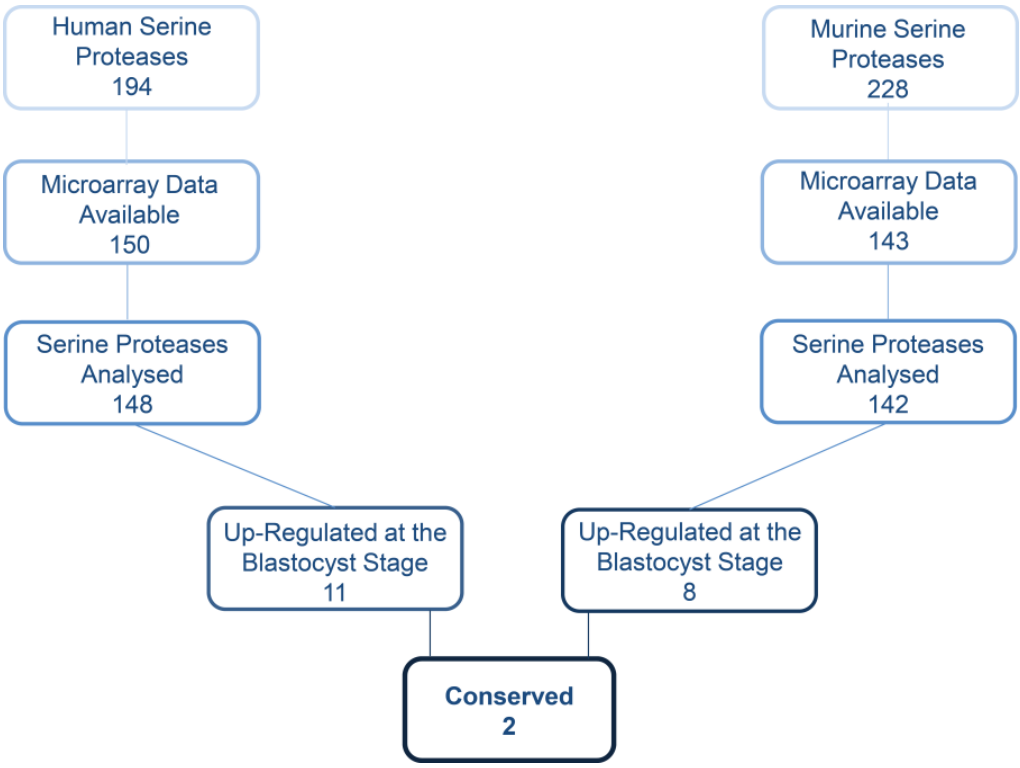

Figure 3.2.8.1 Microarray analysis of genes significantly up-regulated at the blastocyst stage in humans and mice. Out of 194 and 228 serine protease genes, respectively, just 2 were conserved, *PRSS8* and *TMPRSS2*. In silico analysis was performed on publicly available datasets from the Gene Expression Omnibus (Edgar et al., 2002), accession number GSD3959 (*homo sapiens*) and GDS813 (*mus musculus*). SPSS Software (IBM) was used for statistical analysis. One-way ANOVA was used for statistical analysis followed by the Games Howell post hoc test ($P < 0.05$).

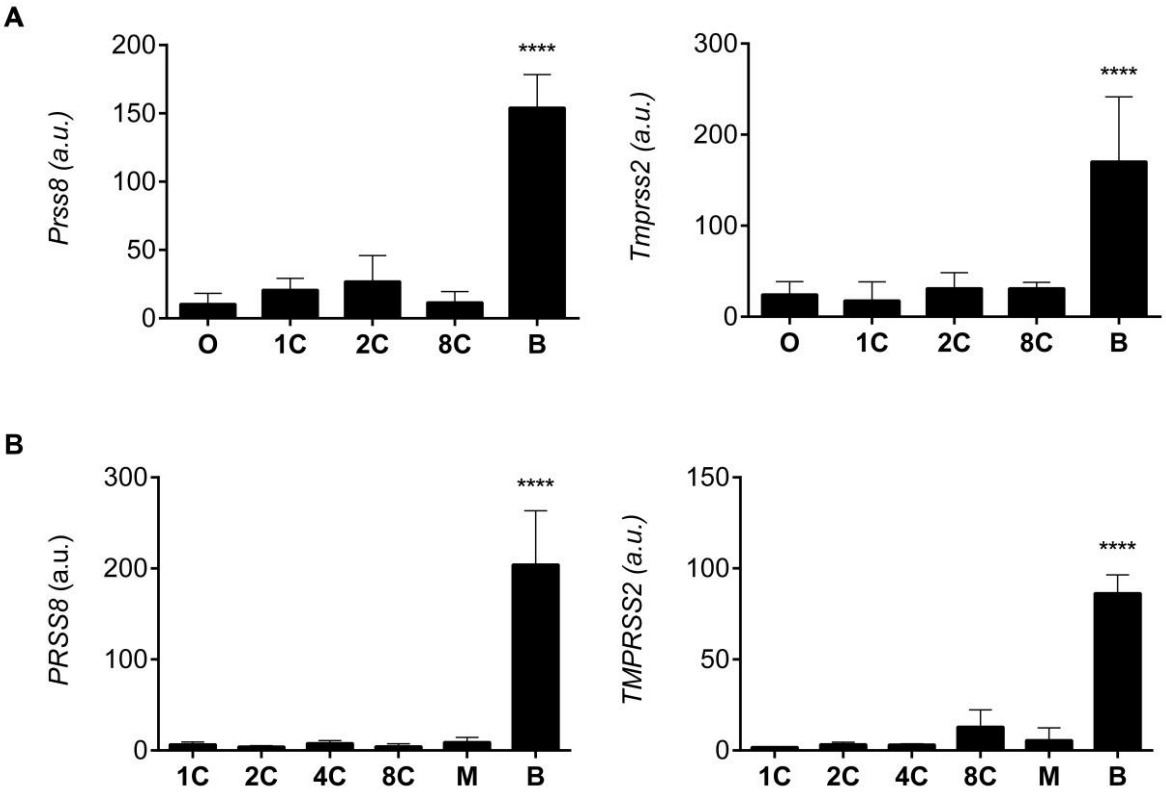

Figure 3.2.8.2 *PRSS8* and *TMPRSS2* transcript levels in human and mouse pre-implantation embryo development. Analysis of microarray data from the Gene Expression Omnibus [accession numbers GSD3959, GDS813 (Edgar et al., 2002)]. **a) Murine transcripts** measured at the oocyte, 1 cell, 2 cell, 8 cell and blastocyst stages of embryonic development from 20 samples using Affymetrix Human Genome U133 Array. *n* =20, *P* <0.0001 [Tmprss2]) *n* =20, *P* <0.0001 [Prss8]. **b) Human transcripts** measured at the 1 cell, 2 cell, 4 cell, 8 cell, morula and blastocyst stages of embryonic development from 18 samples using Affymetrix Human Genome U133 Array. *n* =18, *P* <0.0001 [TMPRSS2], *n* =18, *P* <0.0001 [PRSS8]. Data are presented as means ± S.E.M and One-way ANOVA followed by Games Howell post hoc analysis was applied.

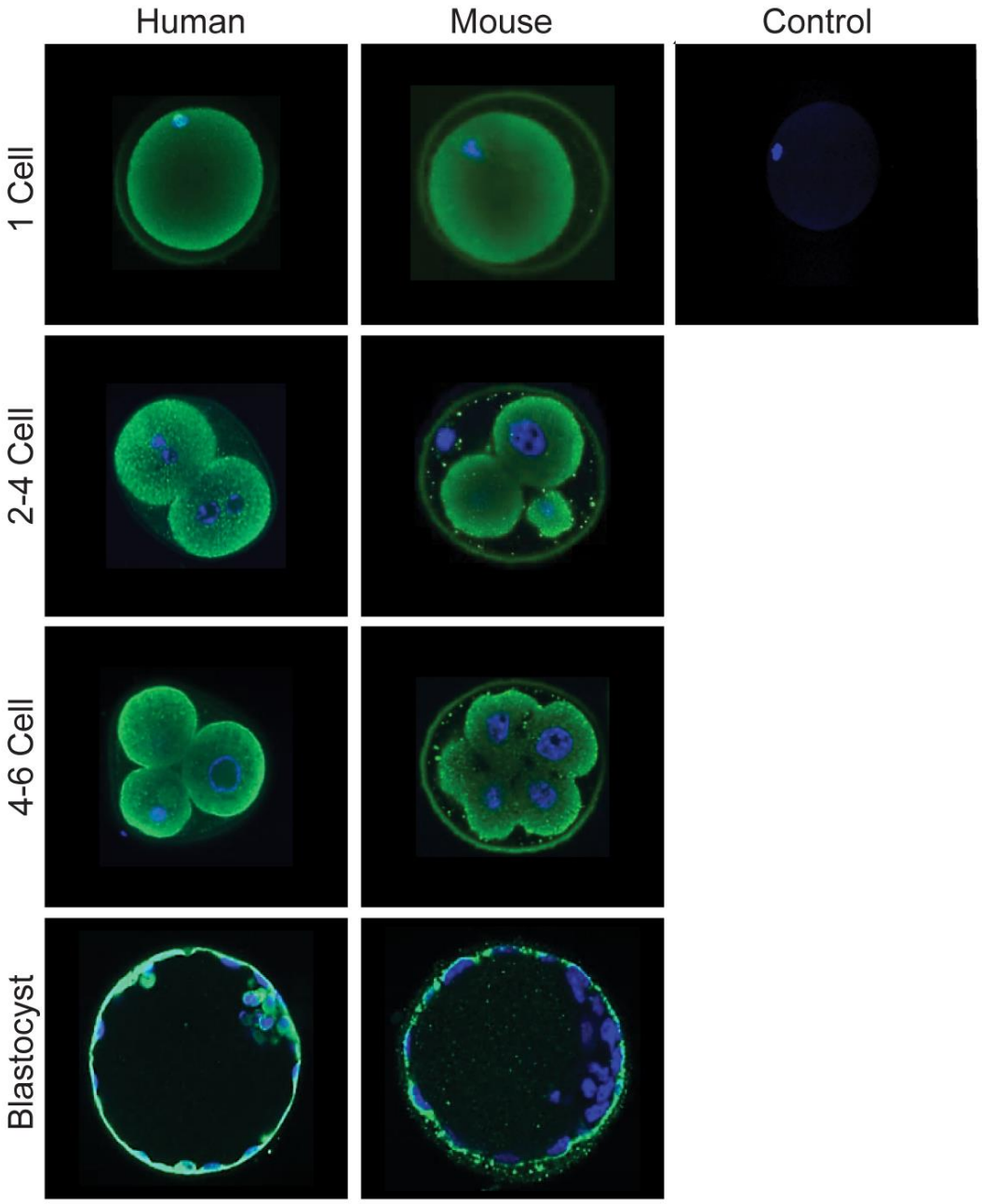

Figure 3.2.8.3 PRSS8 expression in human and mouse pre-implantation embryos. Immunoflourescent labelling of human and murine embryos at different stages of pre-implantation embyo development. Embryos were fixed in 4% w/v PFA/PBS at 2-8 °C. Polyclonal antibodies against PRSS8 were purchased from Antibodies Online, ABIN761891. 1% w/v BSA in PBS without primary antibody was used for the negative control. Embryos were mounted onto 35mm glass-bottomed petri dishes in 10ul Vectashield® with DAPI. Visualization was achieved using a Zeiss LSM 510 confocal imaging system.

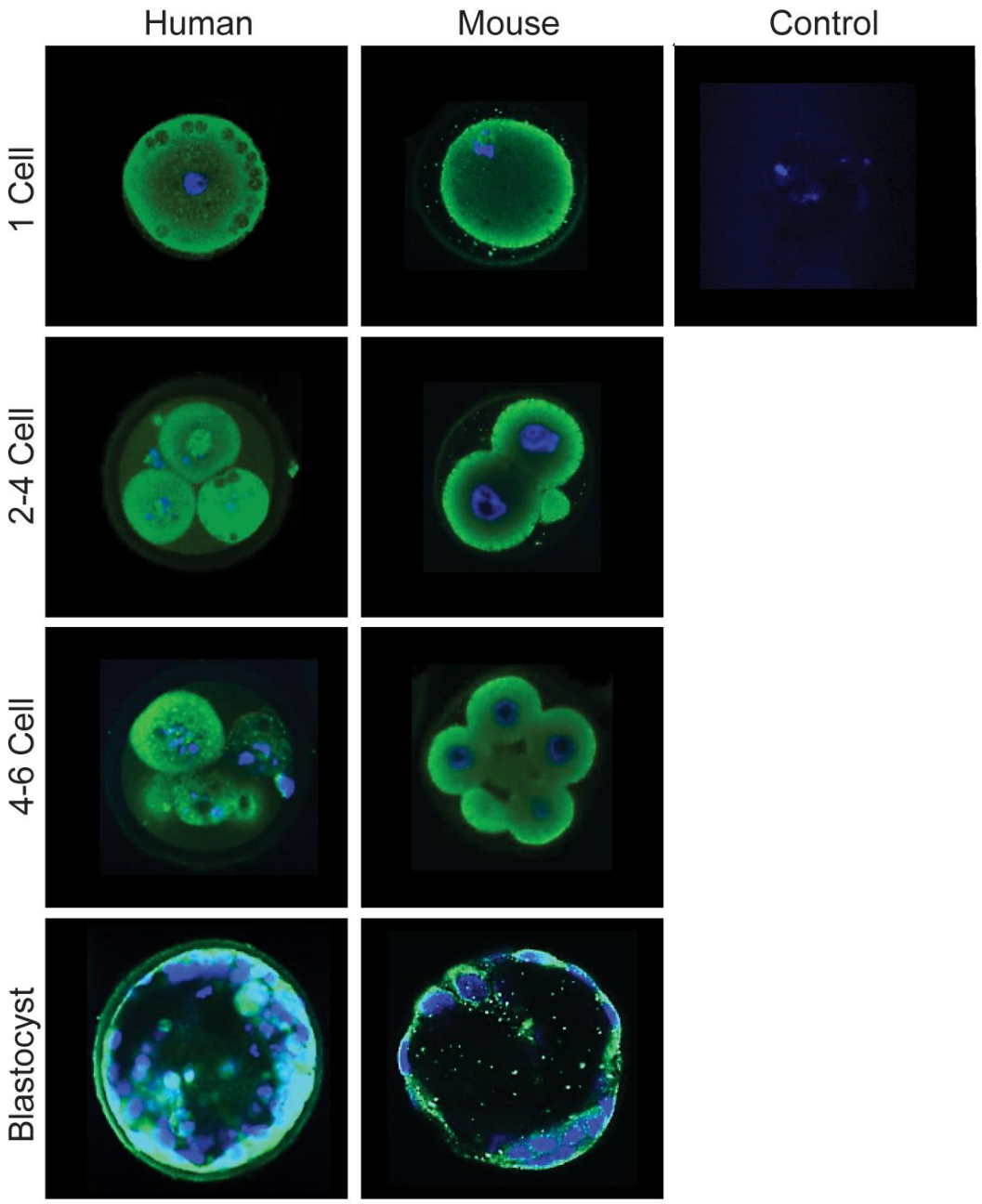

Figure 3.2.8.4 TMPRSS2 expression in human and mouse pre-implantation embryos. Immunoflourescent labelling of human and murine embryos at different stages of pre-implantation embyo development. Embryos were fixed in 4% w/v PFA/PBS at 2-8 °C. Polyclonal antibodies against TMPRSS2 were purchased from Antibodies Online, ABIN716876. 1% w/v BSA in PBS without primary antibody was used for the negative control. Embryos were mounted onto 35mm glass-bottomed petri dishes in 10ul Vectashield® with DAPI. Visualization was achieved using a Zeiss LSM 510 confocal imaging system

3.2.9 Embryo-derived proteases and implantation

A key aim of my study was to characterise the nature of embryo-derived soluble factors that enable maternal recognition and selection at implantation. Defining such signal(s) may improve the selection of IVF embryos, enhance pregnancy rates after transfer, provide new insights into the mechanisms responsible for implantation failure and early pregnancy loss, and – potentially – lead to new strategies to enhance or prevent implantation.

To evaluate whether the proteases identified over the course of this chapter may serve as indicators of embryo implantation potential, levels of trypsin activity, PRSS8 and TMPRSS2 were measured in ECM from individual day 5 single embryo transfer (SET) embryos. The criteria for SET in our unit are; maternal age < 37 years, at least one good quality blastocyst (ICM and TE grade BB or above), and no previous failed IVF cycles. Therefore selecting ECM from SETs controlled for patient age, embryo quality, embryo developmental stage and prognosis, meaning that the protease levels detected in ECM could be directly related to pregnancy outcome.

Trypsin activity was measured using the trypsin assay as described previously (Chapter 3.2.2). PRSS8 and TMPRSS2 levels were quantified using custom designed enzyme-linked immunosorbent assays (ELISAs), in a 96-well format. All assays were carefully optimised using ECM in order to establish optimal experimental conditions and dilution factors.

Due to the limited volume of individual ECM drops (20µl), loss resulting from embryo carry-over and the use of a paraffin oil overlay, 15µl was deemed the maximum usable volume of ECM. As ECM drops were applied to the assays in duplicate, for

accuracy, the final dilution of ECM was 1:13.3 and UCM (also diluted 1:13.3) was included as a control. In each case, values were normalised to the UCM and values falling below the UCM or outside the standard curve were excluded from the analysis. In total 328 ECM drops were applied across the three assays, 71 of which met the selection criteria (day 5 SET).

Interestingly, trypsin activity was found to be significantly higher in ECM from embryos that failed to implant following SET when compared to successfully implanted embryos (median: 49.5 % change from control (NP), 20.6 % change from control (P); range: 11.5 to 76.7 % change from control (NP), 2.1 to 39.8 % change from control (P)) (Figure 3.2.9.1). Total TMPRSS2 levels were similarly increased in ECM from embryos that failed to implant (median: 57.2 % change from control (NP), 0.0 % change from control (P); range: 0.0 to 154.6 % change from control (NP), 0.0 to 11.5 % change from control (P)) (Figure 3.2.9.1). Conversely, total PRSS8 levels were shown to be significantly higher in ECM from embryos that successfully implanted following SET (median: 0.0 % change from control (NP), 67.8 % change from control (P); range: 0.0 to 211.9 % change from control (NP), 0.0 to 338.7 % change from control (P)) (Figure 3.2.9.1).

These intriguing results suggest that protease levels in embryo culture supernatants may provide an indication of implantation potential prior to transfer. Further understanding and refinement of such analysis could potentially provide a novel supplementary means of embryo grading and selection for IVF treatment, in addition to morphology.

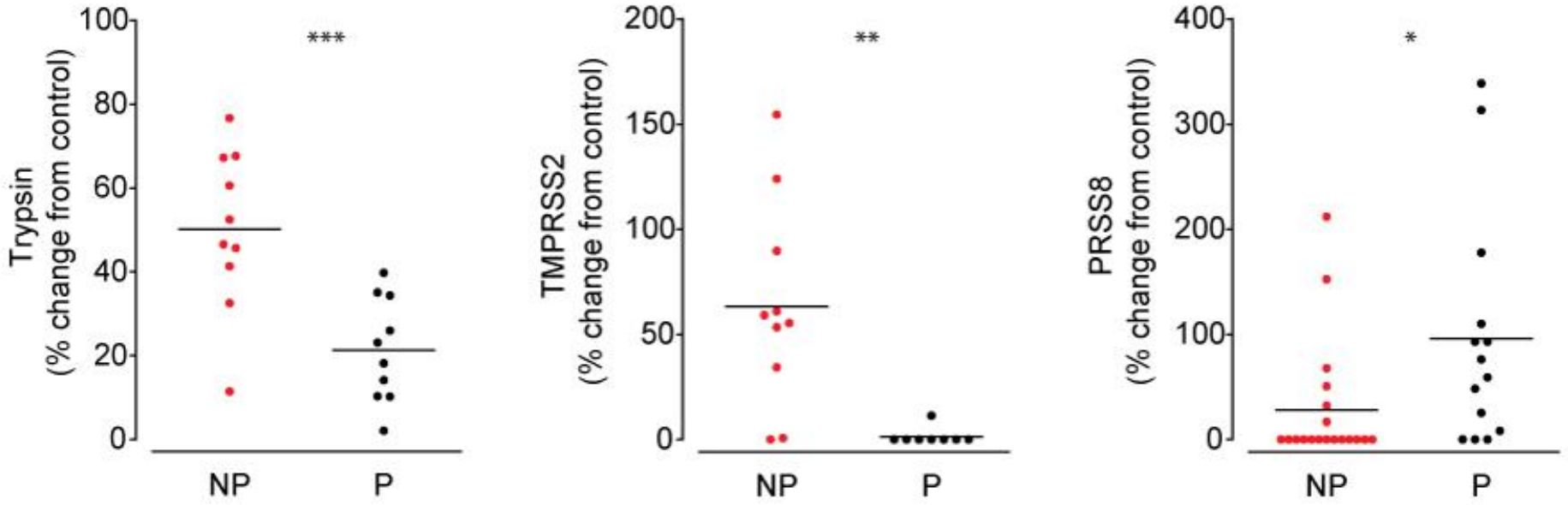

Figure 3.2.9.1 Proteases in ECM related to implantation outcome. Trypsin activity and total abundance of TMPRSS2 and PRSS8 were measured in day 5 ECM from SETs. Outcome was determined by hCG test result following embryo transfer (P = pregnant, NP = not pregnant). Trypsin: *n* = 20, *P* = 0.0015. TMPRSS2: *n* = 19, *P* = 0.0007. PRSS8: *n* = 32, *P* = 0.0071 [PRSS8]. Data are presented as mean values and the median of each group is shown. The Mann Whitney test was used for statistical comparison. *P <0.05; **P <0.01; ***P <0.001.

3.3 Discussion

Embryo derived trypsin-like proteases have been implicated as crucial at implantation in mice (Ruan et al., 2012). By performing a literature search I show that a wealth of evidence supports a role for trypsin and trypsin-like proteases at implantation in various species, but not humans.

By measuring protease, specifically trypsin, levels in embryo culture droplets from IVF patients, I demonstrate that trypsin activity is produced by human embryos and enhanced at the implantation stage of embryo development. Trypsin activity was detectable even in ECM from individually cultured human embryos and found to be related to the day and stage of embryo development. This novel finding establishes embryo-derived trypsin-like activity as a conserved feature of implantation and implicates trypsin-like activity as a marker of embryo implantation potential.

It was suspected that embryo-derived trypsin activity may regulate Ca^{2+} signalling and gene expression in a similar mechanism to that identified in mice (Ruan et al., 2012). We show that human ECM and trypsin induce $[Ca^{2+}]_i$ oscillations in Ishikawa cells via a mutual signal transduction pathway. Crucially the $[Ca^{2+}]_i$ oscillations observed in Ishikawa cells were highly divergent between embryo signals from successfully implanted embryos and poor quality embryos. This data shows that embryo signals convey embryo developmental potential to the endometrium and induce long-lasting cellular changes that actively determine implantation outcome. The abolition of $[Ca^{2+}]_i$ oscillations by pre-treatment of cells with soybean trypsin inhibitor prior to embryo conditioned medium validates a role for trypsin as crucial to this embryo-endometrial crosstalk. Importantly, trypsin and ECM were able to induce similar responses in DESCs. In addition, consistent with the hypothesis proposed by

Ruan et al., this data demonstrates that trypsin modulates PTGS2 transcript expression and COX-2 protein levels in Ishikawa and HEECs.

In order to identify a species-specific mechanism of trypsin production in human embryos, I analysed microarray data of key genes involved in trypsin regulation throughout pre-implantation embryo development. An up-regulation of the trypsinogen activator, *TMPRSS15*, and a down-regulation of a urinary trypsin inhibitor gene, *AMBP,* were observed and confirmed using immunocytochemistry of embryos at different pre-implantation stages. These findings show a human specific mechanism of trypsin regulation during pre-implantation embryo development which may explain the increased trypsin activity detected at the blastocyst stage.

Evidence from a previous study suggested that the embryonic signal at implantation may be partly conserved between humans and mice (Brosens et al., 2014). This data identifies two conserved trypsin-like serine proteases, TMPRSS2 and PRSS8, which are specifically up-regulated at the blastocyst stage during both human and mouse pre-implantation embryo development.

A main aim of this research was to identify key embryo secreted factors which may provide a non-invasive marker of implantation potential. This data confirms that trypsin, PRSS8 and TMPRSS2 levels in ECM, from individually transferred embryos on day 5, differ according to pregnancy outcome. Interestingly trypsin and TMPRSS2 levels were noticeably higher in embryos that failed to implant, whilst PRSS8 levels were higher in successfully implanted embryos.

Taken together, this novel data demonstrates that embryo-derived trypsin-like proteases are produced by human embryos and can regulate human implantation. This enhances our understanding of human implantation and presents candidate

proteases for a novel, non-invasive method of embryo selection that, with further advancement, may enhance pregnancy rates following IVF.

Chapter 4

Endometrial Recognition of Embryo-derived Proteases

4.1 Introduction

In the previous chapter, human embryos were shown to produce specific proteases at the blastocyst stage that can induce Ca^{2+} signalling and regulate the expression of key implantation genes and proteins in endometrial cells. These embryo-derived proteases may play a central role in maternal biosensoring, as the levels detectable in ECM were found to reflect implantation outcome upon single embryo transfer.

In this chapter, I describe the characterisation of endometrial receptors that may be responsive to embryo-derived proteases.

I demonstrate that several protease-sensitive receptors are present in the endometrium, more highly expressed in stromal cells, and that expression peaks during the window of implantation. Furthermore, I show that proteases in ECM rapidly cleave TLR4 expressed on decidualizing cells, which abolishes the induction of pro-inflammatory genes, such as *IL-8*, upon activation of the receptor. My data reveal that human embryos imbue maternal tolerance upon implantation by dampening innate immune responses in the decidua. Additionally, preliminary data show that suboptimal cleavage of TLR4 by ECM of individually cultured embryos is associated with subsequent implantation failure. Conversely, I also demonstrate that suboptimal expression of TLR4 in the endometrium, which arguably impairs active disposal of developmentally compromised embryos, is associated with recurrent miscarriage.

4.2 Results

4.2.1 Putative receptors responsive to embryo-derived TMPRSS2 and PRSS8

A systematic literature search of putative targets of TMPRSS2 and PRSS8 led me to focus on the following receptors and target proteins: ENaC, TLR4 and PAR2. These transmembrane receptors all possess extracellular domains which, upon proteolytic activation by extracellular proteins, regulate cell signalling.

ENaC facilitates the bulk movement of Na^{2+} across the epithelium, maintaining electrolyte and water homeostasis (Garty and Palmer, 1997). The channels contain three of the four structurally related subunits, α, β and γ or δ, β and γ, though the latter is less well-studied (Kleyman et al., 2009). Proteolytic cleavage sites within the extracellular finger domains of the α and γ subunits can be activated by various proteases to regulate ENaC function (Kleyman et al., 2009). Several studies have shown that ENaC can be activated by trypsin (Chraïbi et al., 1998, Caldwell et al., 2004, Kleyman et al., 2009). PRSS8 cleaves the γ subunit at a defined site and is capable of activating ENaC in mice and *Xenopus* oocytes (Bruns et al., 2007, Vallet et al., 1997). A study of human airway epithelium described opposing roles for PRSS8 and TMPRSS2 in ENaC regulation, increasing and decreasing ENaC currents, respectively (Donaldson et al., 2002).

The protease-activated receptor (PAR) family contains four G-protein-coupled receptors (GPCRs); PAR1, PAR2, PAR3 and PAR4. PARs are uniquely activated by serine proteases, with trypsin primarily activating PAR2 and to a lesser extent PAR4. Proteolytic activation of PARs occurs at the extracellular amino terminus (N terminus), where cleavage exposes tethered peptide ligands, which facilitate self-activation (Déry et al., 1998). PAR2 has been identified in the stromal and epithelial compartments of the endometrium and has been implicated in tissue remodeling,

inflammation and repair (Hirota et al., 2005). Activation of PAR2 by trypsin or TMPRSS2 induces elevated [Ca^{2+}]i, due to Ca^{2+} release from intracellular stores, making it a candidate endometrial receptor for embryo-derived protease activation (Nystedt et al., 1995, Wilson et al., 2005).

The family of toll-like receptors (TLRs) are highly conserved, pathogen-recognition receptors involved in activation of innate immunity (Liu et al., 2014, Lu et al., 2008). TLRs were first identified in Drosophila, where *drosophila* Toll receptor (the homologue of mammalian TLR4) was found to be essential for dorso-ventral pattern establishment in developing embryos. TLRs are present in HESCs and HEECs and have been shown to be regulated during the menstrual cycle (Hirata et al., 2007). The best studied TLR interaction is the activation of TLR4 by its endogenous ligand lipopolysaccharide (LPS), found on the outer cell wall of Gram-negative bacteria. TLR4-LPS binding occurs via accessory molecules, cluster of differentiation 14 (CD14) and myeloid differentiation factor 2 (MD-2), to mediate the production of pro- and anti- inflammatory cytokines, as demonstrated in uterine epithelial cells of oestrous mice (Robertson et al., 2011). Trypsin, TMPRSS2 and PRSS8 have been shown to regulate TLR4 activity. Isoforms of the TMPRSS2-ERG fusion gene differentially up-regulate Nuclear Factor Kappa-B (NF-κB) associated genes, including TLR4 (Wang et al., 2011). Trypsin downregulates TLR4 activity via degradation of the TLR4 accessory molecules CD14 and MD-2 in murine peritoneal macrophages (Komatsu et al., 2012). By contrast PRSS8, the only embryo-derived protease found to be increased in ECM from successfully implanting embryos, can directly cleave and de-activate TLR4 in the liver (Uchimura et al., 2014).

4.2.2 Endometrial expression of ENaC, PAR2 and TLR4

GEO data mining was used to analyse the expression of transcripts encoding these key protease-regulated receptors during different phases of the menstrual cycle (Figure 4.2.2.1). Well-characterised samples were collected by pipelle or curetting of the endometrium from normo-ovulatory women with regular cycles. Phases were assigned to the samples according to the criteria of (Noyes et al., 1950) via independent analysis by up to four pathologists (Talbi et al., 2006).

A three-fold increase in *SCNN1A* expression (encoding the ENaC α subunit) is observed during the early- and mid- secretory phases compared to the proliferative and late secretory phases (Figure 4.2.2.1). However, this pattern is not analogous to the corresponding ENaC γ subunit, *SCNN1G* (Figure 4.2.2.1). *F2RL1,* which encodes PAR2, is significantly up-regulated throughout the luteal phase of the cycle (Figure 4.2.2.1). Yet, of all 42,203 genes measured, *TLR4* was among the most highly up-regulated upon transition from the early- to the mid- secretory phase (Figure 4.2.2.1) (Talbi et al., 2006).

Immunofluorescence and Western blot analyses were used to compare the expression of the aforementioned candidate receptors in purified HESCs and HEECs. Cytokeratin 18 and vimentin were used to demonstrate enrichment of HEECs and HESCs, respectively. The expression levels of PAR2 were comparable between HEECs and HESCs (Figure 4.2.2.2a,b). Using immunofluorescence, TLR4 expression was seemingly equivalent between the two cell types (Figure 4.2.2.2a), yet Western blot analysis demonstrated higher levels of this receptor in primary HESC cultures (Figure 4.2.2.2). Despite ENaC being designated an epithelial channel, both methods show that the expression of α and γ ENaC subunits is constitutively higher in cultured HESCs when compared to purified HEECs (Figure 4.2.2.2a,b).

Following confirmation that these protease-regulated receptors are expressed in the stromal compartment, I measured their protein levels in HESCs undergoing decidualization *in vitro,* for 2, 4 or 8 days. Interestingly, all three protease-sensitive receptors demonstrated a biphasic expression pattern upon decidualization, characterized by rising expression that peaks on day 4 of the differentiation process, and declining levels at day 8 (Figure 4.2.2.3).

In summary, expression profiling, both *in vivo* and *in vitro*, points towards a potential role for ENaC, PAR2 and TLR4 in deciphering embryo-derived proteases at the time of implantation. Furthermore, the discovery that ENaC and TLR4 are more abundantly expressed in HESCs when compared to HEECs, at least in culture, suggests a role for these receptors in regulating implantation once the blastocyst has breached the luminal epithelium.

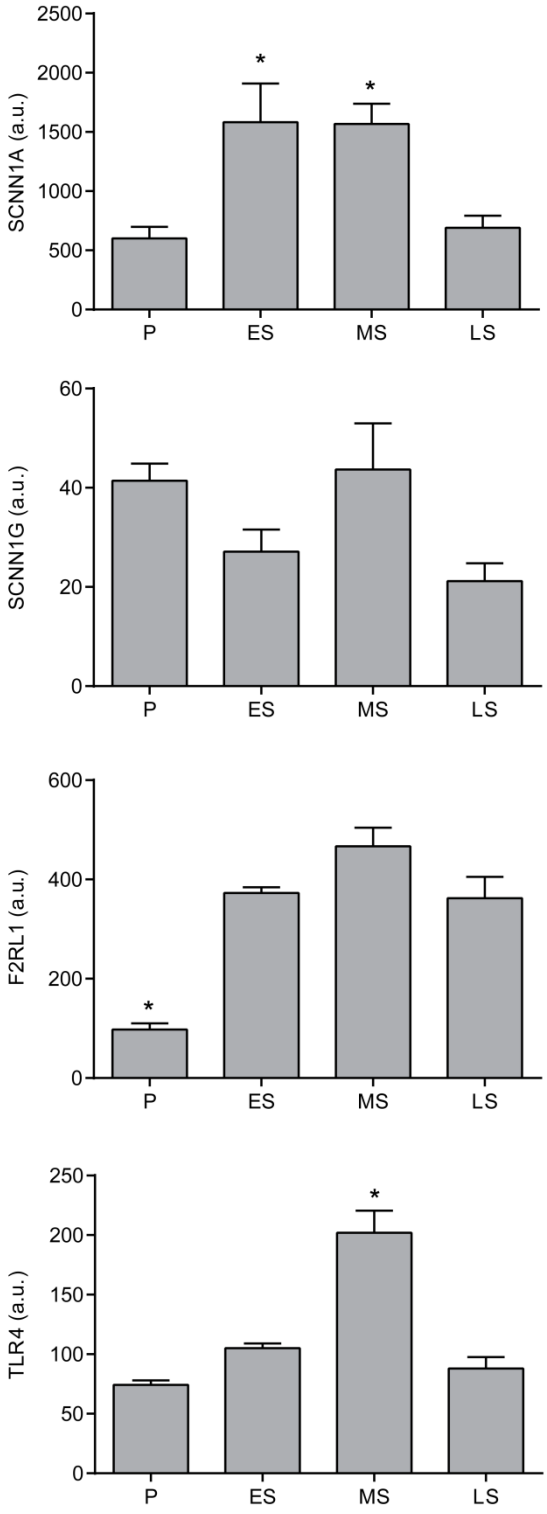

Figure 4.2.2.1 Expression of key protease-regulated receptor genes during the menstrual cycle. GEO profile microarray of protease activated receptors; *SCNN1A* (α ENAC), *SCNN1G* (γ ENAC), *TLR4* and *F2RL1* (PAR2) during the proliferative (P), early secretory (ES), mid-secretory (MS) and late secretory (LS) phases of the menstrual cycle, using Affymetrix Human Genome U113 array. Data are presented as means ± S.E.M of 22 samples. One-way ANOVA statistical analysis was applied, followed by Games-Howell post-hoc test. *P < 0.05.

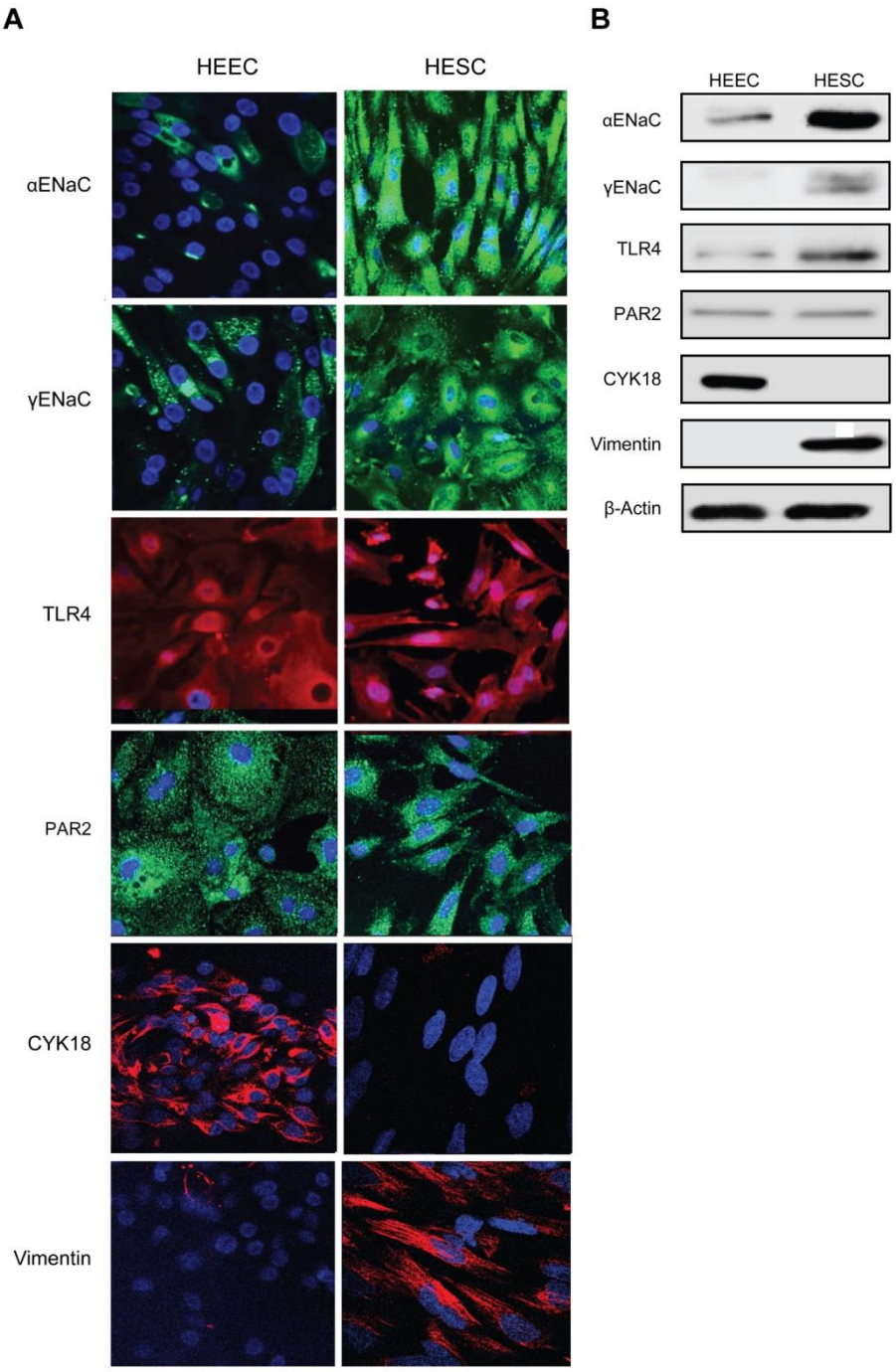

Figure 4.2.2.2 Candidate protease-regulated receptor expression in HESCs and HEECs purified from mid-luteal endometrial biopsies. a) Immunoflourescent labelling of purified HESC and HEEC cultures. Images are representative of 3 samples. b) Western blot analysis of purified HESC and HEEC lysates. β-actin was used as a loading control. Blot is representative of 3 replicates. Purity of the epithelial and stromal cells was assessed by cytokeratin (CYK18) and vimentin expression, respectively. Dr Flavio Barros assisted with the isolation and culturing of HEECs.

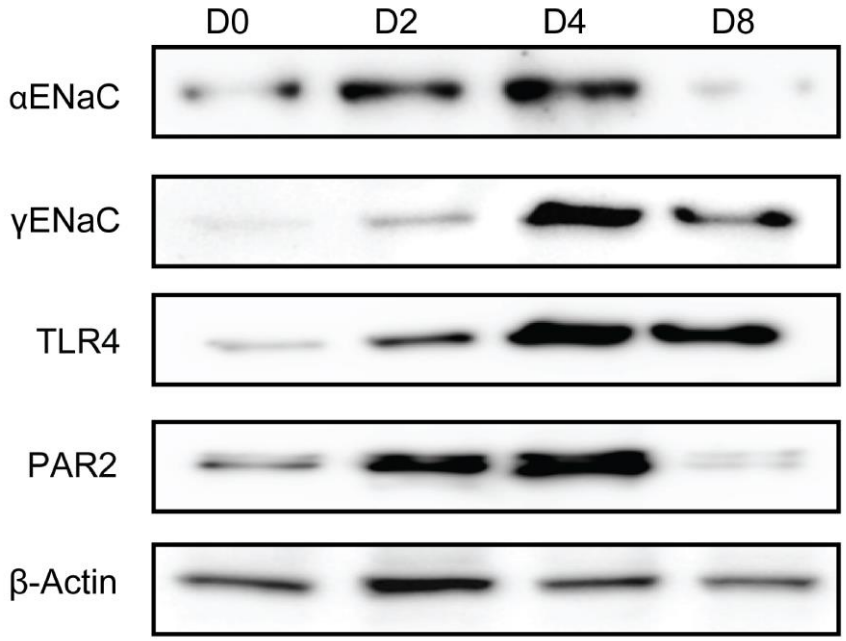

Figure 4.2.2.3 ***In vitro*** **expression of key protease-regulated receptors during the decidualization of HESCs.** Western blot analysis of total cell lysates of undifferentiated or decidualized HESCs (2-8 days). Protein was harvested after 0 (D0), 2 (D2), 4 (D4) or 8 (D8) days of cAMP/MPA treatment. β-actin was used as a loading control. Western blots are included in Appendix 8.

4.2.3 Embryo-derived proteases cleave and inactivate TLR4 in decidualizing stromal cells

Putative protease-responsive receptors are most highly expressed on day 4 of decidualization. To test if these receptors are cleaved by embryo-derived signals, decidualized cultures were exposed to either ECM or UCM, both diluted 1:100. The dilution factor was pragmatic as it enabled assessment of endometrial cell responses to ECM of individually cultured embryos. After 15 minutes, the cells were harvested and total protein lysates subjected to Western blot analysis. Unexpectedly, I found no evidence of either PAR2, α ENaC or γ ENaC cleavage. Lack of cleavage could reflect insufficient protease activity in diluted ECM samples or, alternatively, the secretion of specific protease inhibitors by decidualizing cells. By contrast, there was a conspicuous loss of TLR4 in decidual cells exposed to ECM (Figure 4.2.3.1a). The kinetics of this response, within 15 minutes, can only be accounted for by the sudden loss of the epitope, located in the extracellular domain of the receptor (amino acids 542 - 631) (Panter and Jerala, 2011).

In a preliminary experiment, ECM from 8 individually cultured and transferred embryos was separated according to implantation outcome, diluted 1:100 and applied to day 4 DESCs for 15 minutes. Embryo-derived proteases from successfully implanted embryos had a greater inhibitory effect on TLR4 than those from embryos which failed to implant (Figure 4.2.3.1b). This is a striking finding, which firmly implicates PRSS8 in TLR4 cleavage of decidual cells. However, these observations require further validation in a larger study.

To validate TLR4 cleavage in response to ECM, parallel cultures were fixed in 4% Para-formaldehyde, but not permeabilized with Triton X-100. Confocal microscopy

showed abundant TLR4 expression on the surface of decidualized HESCs exposed to UCM. However, pre-treatment of the cells with ECM for 15 min resulted in a marked decrease in TLR4 immunofluorescence (Figure 4.2.3.2a).

TLR4 is a toll-like receptor responsible for activating the innate immune system, commonly characterised by its ability to bind LPS. Yet, alternative ligands of TLR4 include numerous viral proteins, polysaccharide and several endogenous proteins such as low-density lipoprotein, beta-defensins, and heat shock proteins (Brubaker et al., 2015). TLR4 associates with MD-2 to form a heterodimer that identifies a common 'pattern' amongst structurally diverse LPS molecules (Shimazu et al., 1999). Mining of existing microarray data (Takano et al., 2007) revealed that MD-2 transcripts, coded by lymphocyte antigen 96 (*LY96)*, are abundantly present in undifferentiated and decidualizing HESCs, indicating that these cells should be responsive to LPS in a TLR4-dependent manner. To test this hypothesis, primary HESCs decidualized for 4 days were treated with LPS (0.5 µg/ml). Since IL-8 is a major cytokine induced by TLR4 in HESCs (Hirata et al., 2005), the induction of *IL-8* transcripts was measured by qRT-PCR 30, 60 and 120 minutes following LPS exposure. As shown in Figure 4.2.3.3a, *IL-8* transcript levels increased by approximately 10-fold, 120 minutes following exposure of decidualizing cells to LPS. To test if this induction is mediated by TLR4, decidualizing cells were pre-treated with a TLR4-specific inhibitor peptide, VIPER. VIPER completely repressed the induction of *IL-8* in response to LPS treatment (Figure 4.2.3.3c). In fact, VIPER reduced *IL-8* transcript levels below those observed in vehicle-treated control cells, suggesting that TLR4 may be endogenously activated in decidualizing cells. More importantly, pre-treatment with ECM but not UCM also blocked LPS-dependent induction of *IL-8* in decidualizing cells (Figure 4.2.3b).

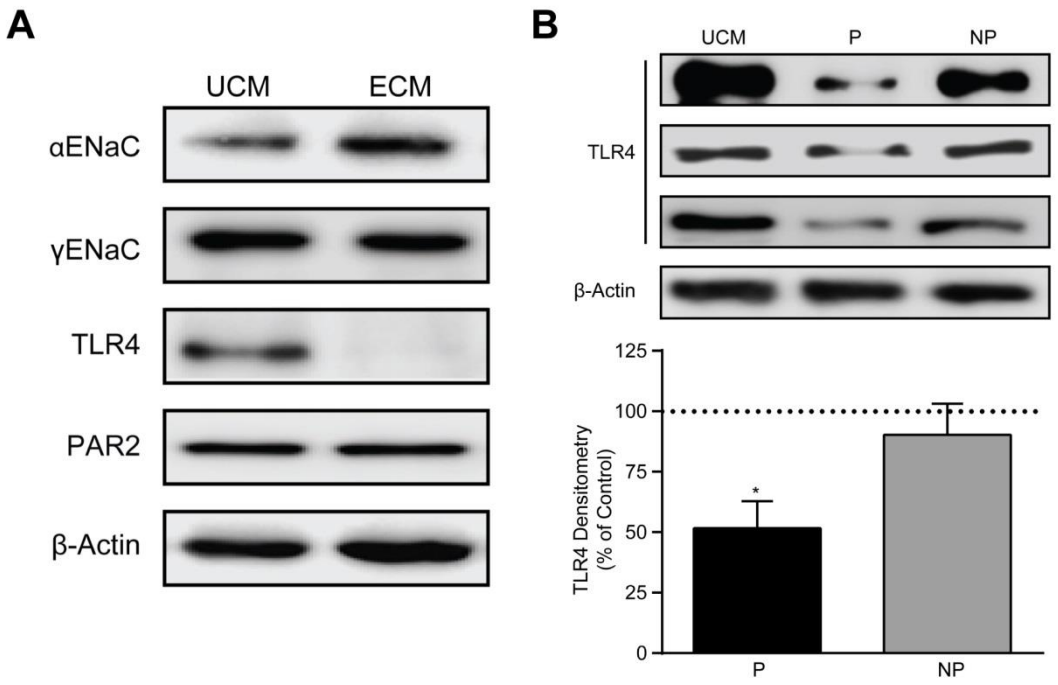

Figure 4.2.3.1 Embryo conditioned medium (ECM) applied to day 4 DESCs inhibits TLR4 expression. a) Confluent day 4 DESCs were exposed to UCM (1:100) or ECM (1:100), for 15 minutes. Protein was extracted and α ENAC, γ ENAC, PAR2 and TLR4 levels measured via Western blot. β-actin was used as a loading control. The complete blot is included in Appendix 9. b) Confluent day 4 DESCs were exposed to UCM (1:100) or ECM (1:100) from single embryo transfers (P = Pregnant, NP = Not pregnant), for 15 minutes. Protein was extracted and TLR4 levels measured via Western blot. β-actin was used as a loading control. Blot is representative of 4 independent experiments using 4 samples. Densitometry was performed using Syngene GeneTools analysis software and the results are shown as % change from UCM (n = 4, *P* = 0.0158). Data are presented as mean $\pm$ S.E.M and ANOVA was used for statistical analysis.

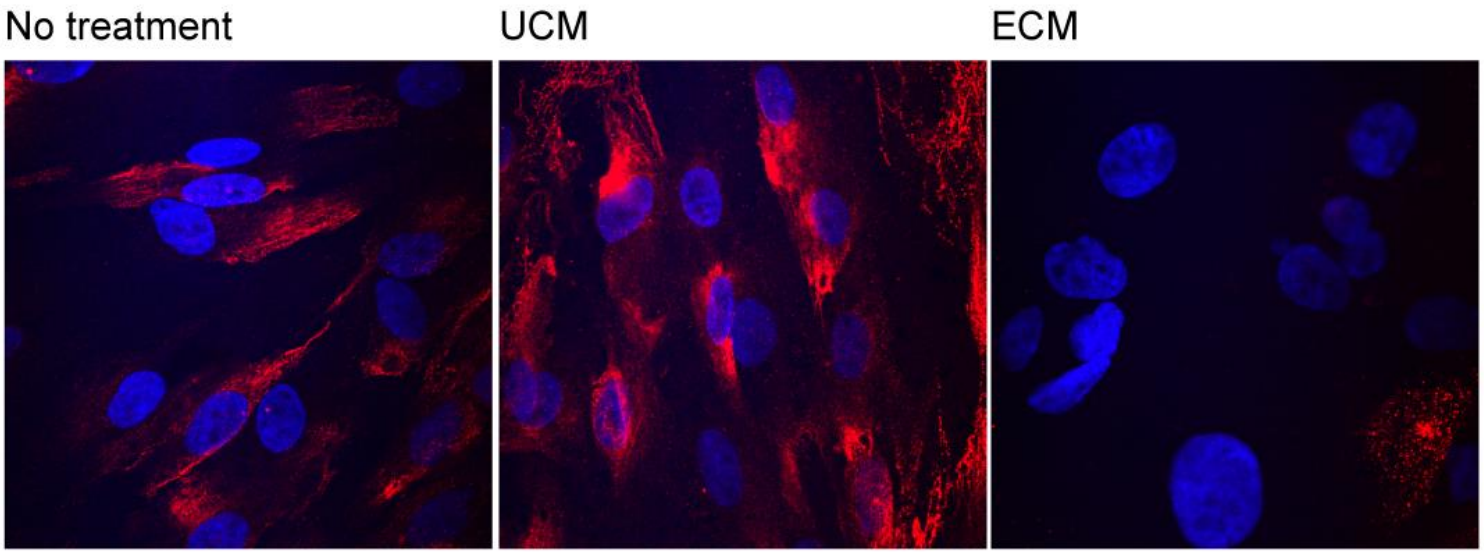

Figure 4.2.3.2 TLR4 expression in DESCs purified from mid-luteal endometrial biopsies. Immunoflourescent labelling of purified DESCs (day 4), with no treatment, exposure to UCM (1:100) or exposure to ECM (1:100) from successfully implanted SET embryos (P) for 15 minutes. Images are representative of 3 samples. Dr Seley Gharanei assisted with the treatment and imaging of the HESCs.

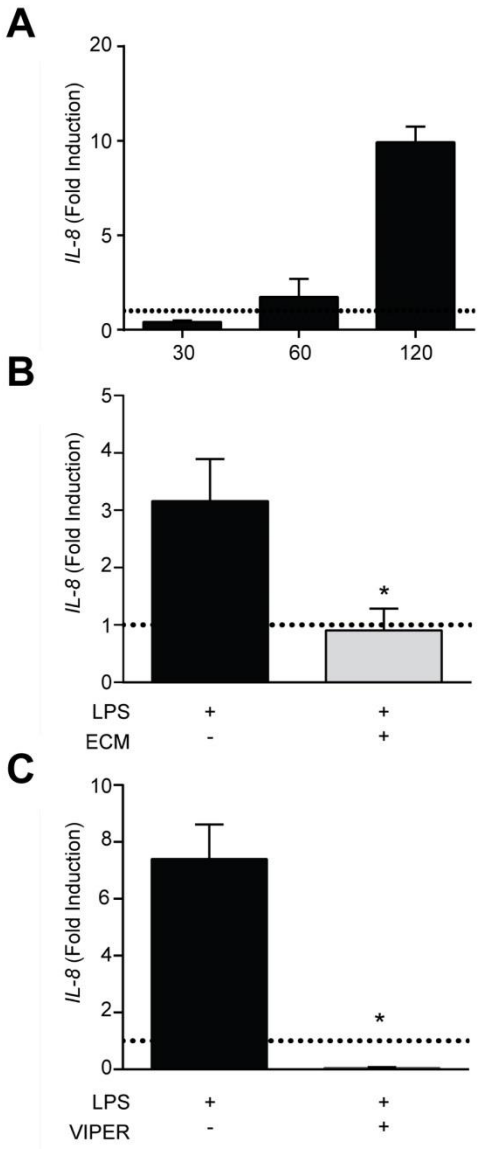

Figure 4.2.3.3 *IL-8* expression in day 4 DESCs upon exposure to LPS. a) Day 4 DESCs were treated with LPS (0.5 µg/ml) for 30, 60 and 120 minutes. b) Day 4 DESCs were treated with ECM from successfully implanted embryos (1:100) for 30 minutes, washed with PBS and then exposed to LPS (0.5 µg/ml) for 60 minutes (n = 3, *P* = 0.05). c) Day 4 DESCs were treated with VIPER (TLR4-specific inhibitor peptide; 500µM) for 30 minutes, washed with PBS and then exposed to LPS (0.5µg/ml) for 60 minutes (n = 3, *P* = 0.03). In all experiments RNA was harvested, cDNA synthesised and *IL-8* transcript levels measured using qRT-PCR. Transcript levels were normalised to *L19*. Data are presented as means ± S.E.M, representative of 3 replicates. The unpaired t-test was used for statistical analysis.

4.2.4 TLR4 expression in mid-luteal phase endometrium

To validate the expression of TLR4 in human endometrium, fixed endometrial sections from mid-luteal biopsies were analysed using immunohistochemistry (IHC). As shown in Figure 4.2.4.1, TLR4 expression within the stromal compartment was heterogeneous. While some stromal cells displayed little staining, others showed intense TLR4 immunoreactivity. Stromal cells displaying prominent staining appeared more abundant in areas of localised oedema (O). A whirling pattern of staining was observed in stromal cells adjacent to the spiral arteries (SA). TLR4 staining was predominantly cytoplasmic in stromal cells. Prominent TLR4 immunoreactivity was also apparent in the apical border of luminal epithelial cells (LE). By contrast, the glandular epithelium (GE) mostly exhibited weak staining. Luminal epithelial cells likely constitute a minor subpopulation of isolated endometrial epithelial cells propagated in culture; which in turn explains the differential expression of TLR4 expression between HEECs and HESCs. However, the finding that TLR4 is expressed on luminal epithelial cells does suggest a role for this receptor in pre-implantation endometrial responses.

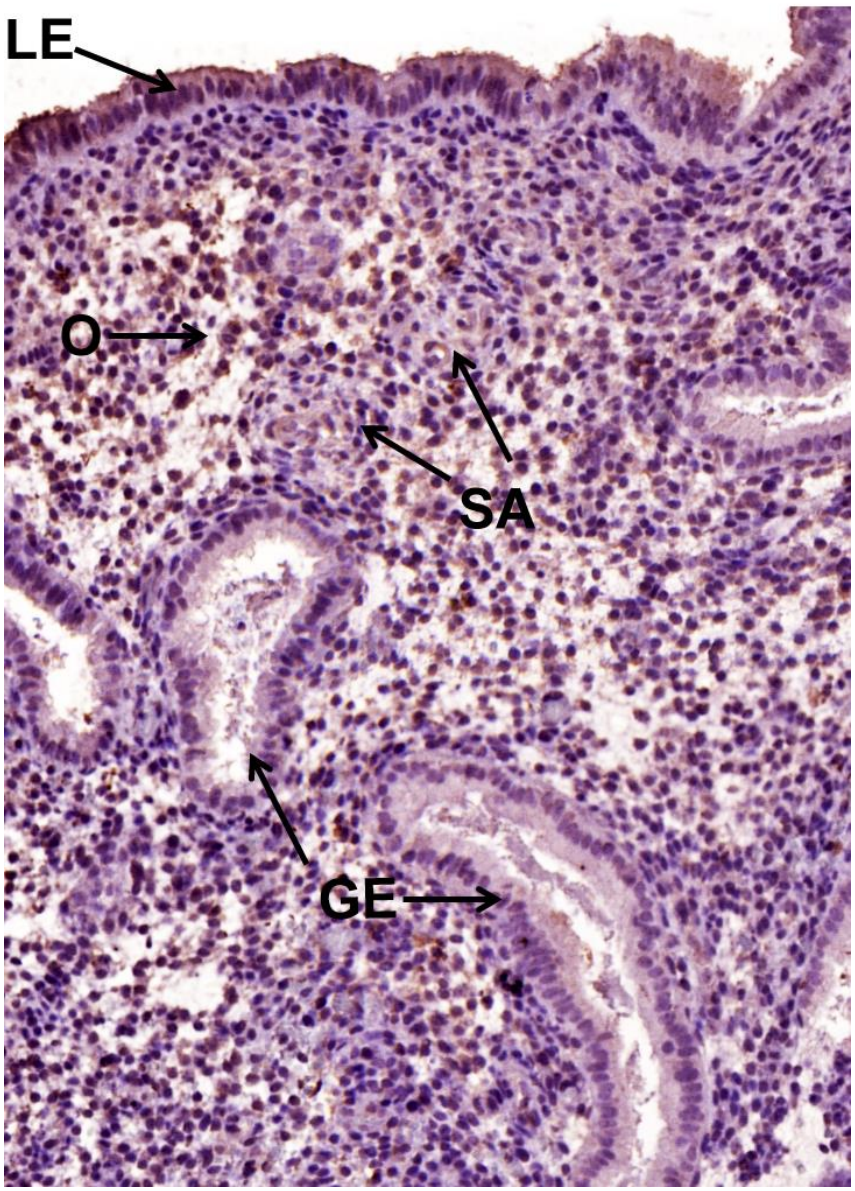

Figure 4.2.4.1 TLR4 in mid-luteal phase endometrial sections. Fixed sections from endometrial biopsies, collected via pipelle, were rehydrated and incubated with TLR4 antibody (1:5000). Novolink Polymer solution (Leica) enabled visualisation of primary antibody staining (brown) and haematoxylin was used to visualise nucleii (violet). Dr Katherine Fishwick assisted with the preparation and imaging of the slides. *Luminal epithelium (LE), oedema (O), glandular epithelium (GE), spiral arteries (SA).*

4.2.5 Endometrial Expression of TLR4 in Reproductive Failure

If TLR4 is an important determinant of endometrial responses to embryonic cues, deregulation of this TLR family member could contribute to reproductive failure. To test this hypothesis, I examined the expression of *TLR4* mRNA and protein in patients suffering either recurrent implantation failure (RIF) or recurrent miscarriage. For the purpose of this study, RIF was defined as implantation failure (i.e. negative pregnancy test) in 3 or more consecutive IVF treatment cycles; and RM as 3 or more consecutive miscarriages. Two RIF subjects and 3 RM patients suffered secondary infertility and secondary miscarriages, respectively. Both clinical groups were matched in age and body mass index (BMI). The median [range] day of biopsy was LH+9 [+7 - +12] and LH+9 [+7 - +11] in the RIF and RM groups, respectively. The demographic details are tabulated in Appendix 5.

Total RNA was extracted from whole tissue samples stored in RNA later solution, from 14 RIF subjects and 14 RM patients. The RNA was reverse transcribed and *TLR4*, *F2RL1* (coding for PAR2) and *SCNN1A* (coding for α ENaC) transcript levels determined by qRT-PCR. As shown in Figure 4.2.5.1, *SCNN1A* and *TLR4* transcript levels were significantly higher in the RM patients when compared to RIF subjects ($P = 0.0021$ and $P = 0.0395$, respectively). By contrast, *F2RL1* mRNA levels were comparable between both groups ($P > 0.05$). Notably, there was a positive correlation between *TLR4* and *F2RL1* transcript levels (Spearman's rank test, $r = 0.39$, $P = 0.03$), *TLR4* and *SCNN1A* mRNA levels ($r = 0.51$, $P = 0.004$), and *F2RL1* and *SCNN1A* mRNA levels ($r = 0.53$, $P = 0.002$) (Figure 4.2.5.2); suggesting coordinated transcriptional regulation of these protease-sensitive receptors in differentiating human endometrium.

Additional analysis revealed no association between *TLR4* transcript levels and uNK cell density, age or BMI of the patients. Similarly, no correlation was found between these demographic details and expression of either *F2RL1* or *SCNN1A* transcripts (Figure 4.2.5.3).

The expression and activity of TLR4 is tightly regulated by several post-translational mechanisms, including ubiquitylation and proteosomal degradation (Liew et al., 2005). Hence, TLR4 protein levels were determined in a second cohort of snap-frozen biopsies by Western blot analysis. The median [range] day of biopsy was LH+9 [+5 - +12] and LH+8 [+5 - +10] in the RIF and RM groups, respectively. The demographic details of this cohort are tabulated in Appendix 6. Expression was normalized to β-actin levels and quantified by densitometry using Syngene GeneTools analysis software. By contrast to the mRNA analysis, TLR4 protein levels were significantly reduced in RM compared to RIF biopsies ($P < 0.01$; Figure 4.2.5.4). Interestingly, TLR4 protein levels did correlate to BMI ($r = 0.41$, $P = 0.04$), and uNK cell density ($r = 0.44$, $P = 0.02$), but not to the age of the patient ($r = 0.29$, $P = 0.12$) (Figure 4.2.5.5).

I speculated that increased endometrial *PRSS8* expression in RM subjects could account for the discrepancy between TLR4 mRNA and protein levels. Although *PRSS8* transcript levels were indeed raised in RM subjects when compared to RIF patients ($P < 0.05$), Western blot analysis showed no difference between the two clinical groups ($P > 0.05$; Figure 4.2.5.6), indicating that endogenous cleavage is unlikely to account for the lower TLR4 levels in RM patients.

Taken together, the data show that endometrial TLR4 expression differs between RIF and RM patients. Additional IHC studies are needed to examine the tissue distribution of TLR4 in these patient groups. Furthermore, it would be interesting to test if endometrial TLR4 expression is predictive of subsequent pregnancy outcome in

women suffering from persistent reproductive failure.

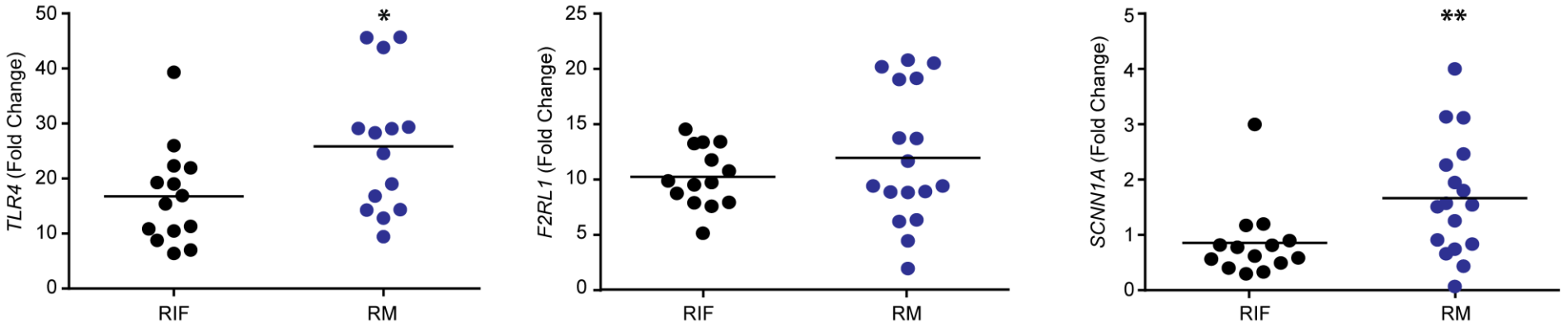

Figure 4.2.5.1 *TLR4, F2RL1 and SCNN1A* transcript expression levels in patients with RIF or RM. RNA was extracted from 28 mid-luteal endometrial biopsies (RIF, n = 14; RM, n = 14) and transcript expression analysed via qRT-PCR. Selected patients were all aged between 25 and 37 years with a healthy BMI (demographic details are tabulated in Appendix 5). All values were normalised to *L19*. Data are presented as mean values. TLR4, *P* = 0.0395; F2RL1, *P* = 0.5112; SCNN1A, *P* = 0.0021. The Mann Whitney test was used for statistical analysis. **P*<0.05; ***P*<0.01; ****P*<0.001.

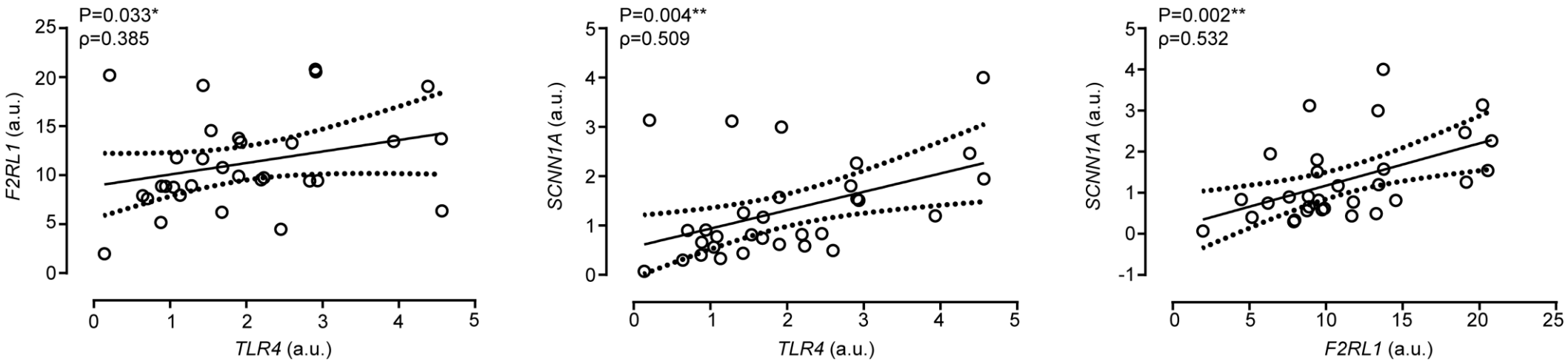

Figure 4.2.5.2 Regression analysis of *TLR4, F2RL1 and SCNN1A* transcript levels in a cohort of reproductive failure patients. RNA was extracted from 28 mid-luteal endometrial biopsies taken (RIF, n = 14; RM, n = 14) and transcript expression analysed via qRT-PCR. All values were normalised to *L19*. Patient demographic details are tabulated in Appendix 5. Dotted lines represent 95% confidence intervals. Spearman's ρ value and probability (P) shown. **P*<0.05; ***P*<0.01; ****P*<0.001.

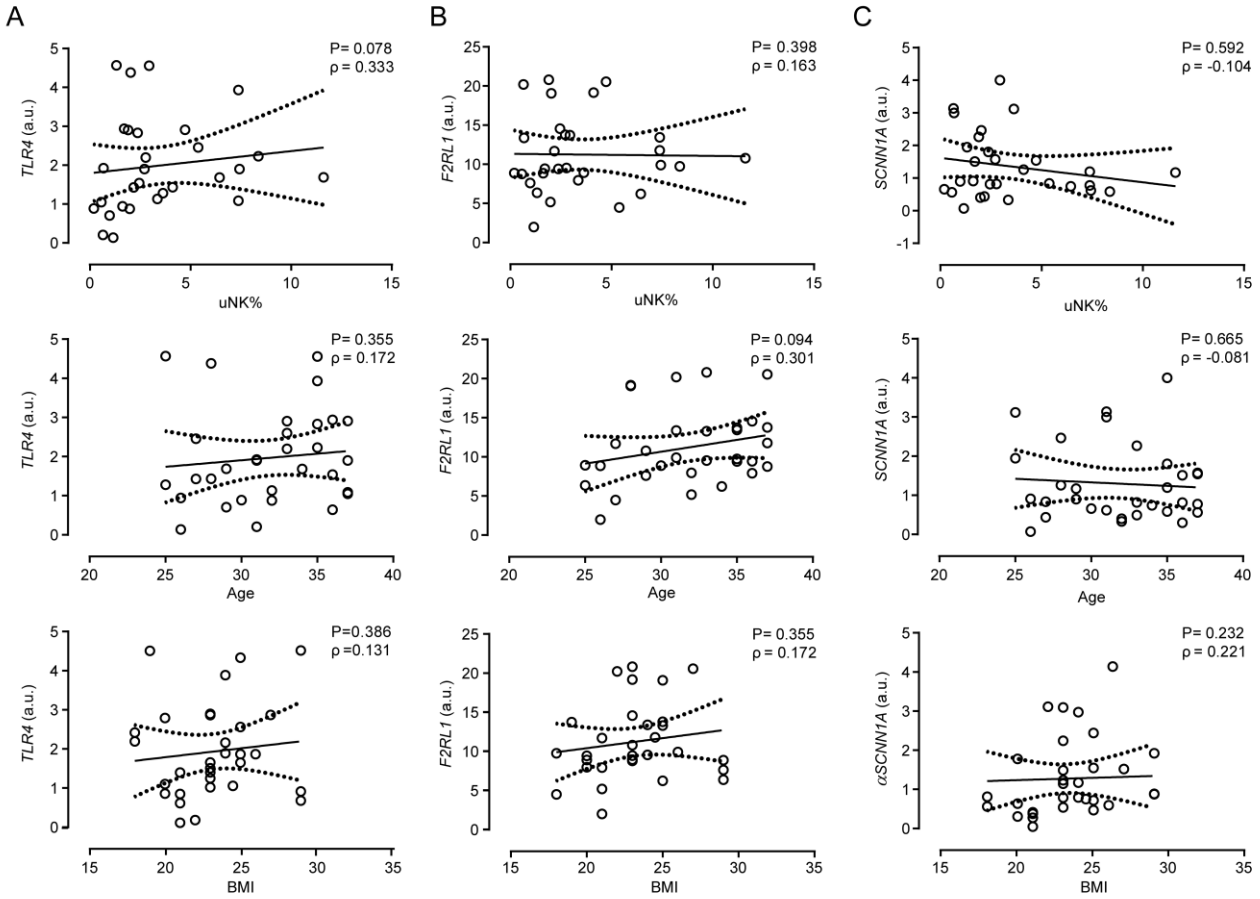

Figure 4.2.5.3 Regression analysis of *TLR4, F2RL1 and SCNN1A* transcript levels and demographic details in a cohort of reproductive failure patients. Correlation between uNK cell density (%), age (years), BMI and (a) *TLR4*, (b) *F2RL1*, (c) *SCNN1A* transcript expression. RNA was extracted from 28 mid-luteal endometrial biopsies (RIF, n = 14; RM, n = 14) and transcript expression analysed via qRT-PCR. All values were normalised to *L19*. Patient demographic details are tabulated in Appendix 5. Dotted lines represent 95% confidence intervals. Spearman's ρ value and probability (P) shown. **P*<0.05; ***P*<0.01; ****P*<0.001.

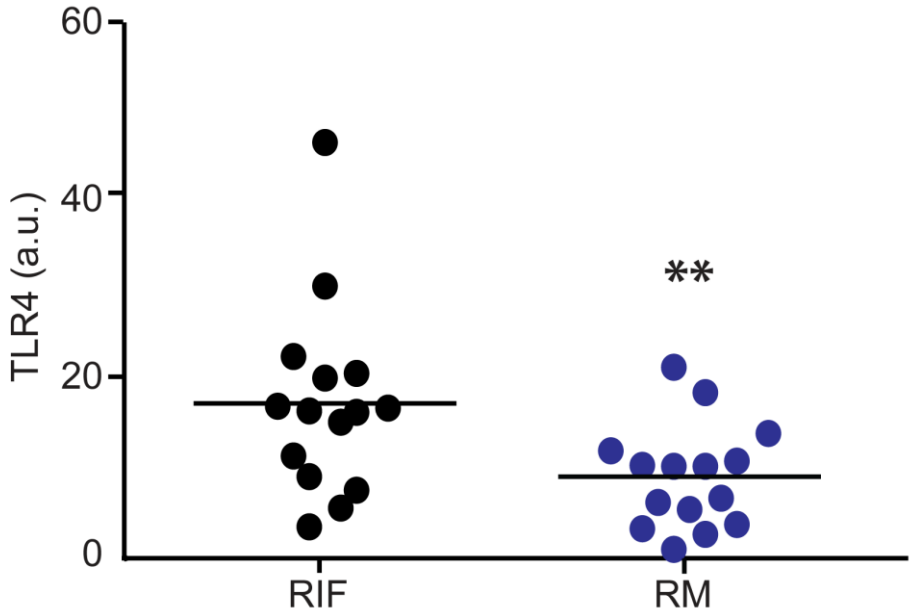

Figure 4.2.5.4 TLR4 protein levels in patients with RIF or RM. Protein was extracted from 30 endometrial biopsies (RIF, n = 15; RM, n = 15) and analysed via Western blot. Patient demographic details are tabulated in Appendix 6. β-actin was used as a loading control. Western blots are included in Appendix 7. Densitometry was performed using Syngene GeneTools analysis software and the results are shown as % change from UCM. Data are presented as mean values. The Mann Whitney test was used for statistical analysis. **P*<0.05; ***P*<0.01; ****P*<0.001.

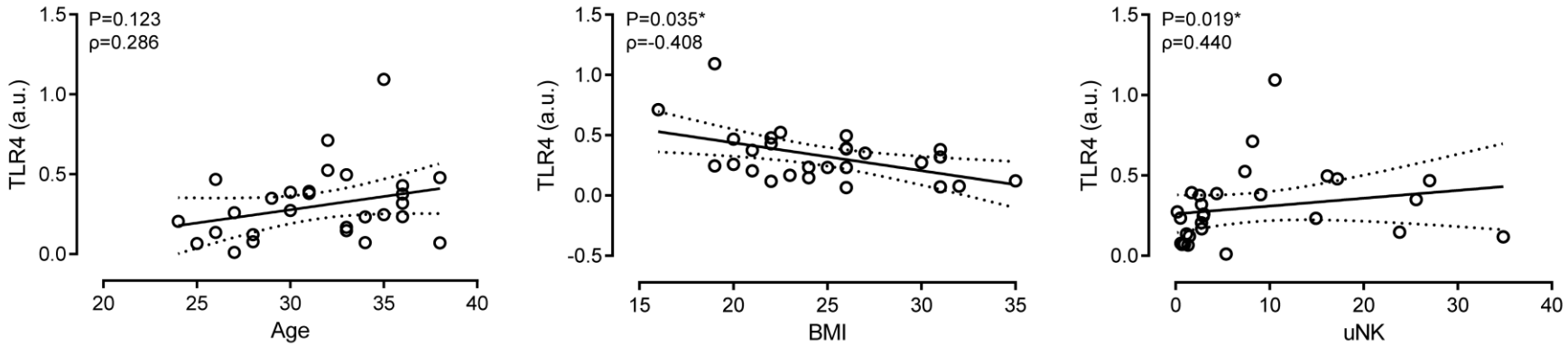

Figure 4.2.5.5 Regression analysis of TLR4 protein levels and demographic details in a cohort of reproductive failure patients. Correlation between uNK cell density (%), age (years), BMI and TLR4 protein expression. Protein was extracted from 30 endometrial biopsies (RIF, n = 15; RM, n = 15) and analysed via Western blot. Patient demographic details are tabulated in Appendix 6. β-actin was used as a loading control. Dotted lines represent 95% confidence intervals. Spearman's ρ value and probability (P) shown. **P*<0.05; ***P*<0.01; ****P*<0.001.

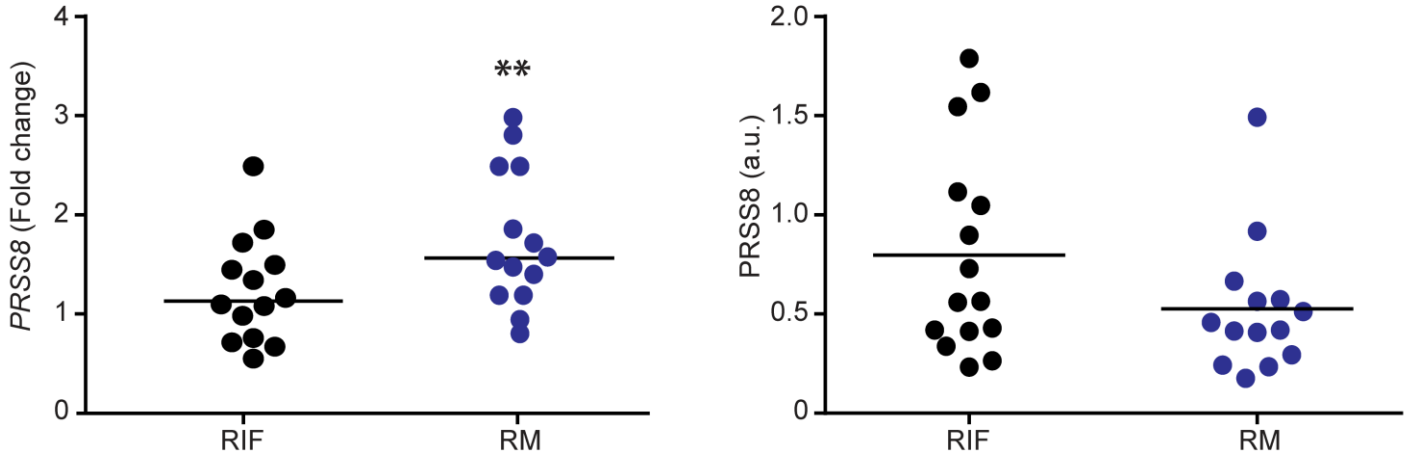

Figure 4.2.5.6 *PRSS8* transcript and protein expression in patients with RIF or RM. RNA was extracted from 28 endometrial biopsies (RIF, n = 14; RM, n = 14) and transcript expression analysed via qRT-PCR. Patient demographic details are tabulated in Appendix 5. All values were normalised to *L19*. Protein was extracted from 30 endometrial biopsies (RIF, n = 15; RM, n = 15) and analysed via Western blot. Patient demographic details are tabulated in Appendix 6. β-actin was used as a loading control. Western blots are included in Appendix 7. Densitometry was performed using Syngene GeneTools analysis software and the results are shown as % change from UCM. Data are presented as mean values. The Mann-Whitney test was used for statistical analysis. *P<0.05; **P<0.01; ***P<0.001.

4.3 Discussion

In chapter 3, we showed that embryo-derived trypsin-like proteases can regulate cell signalling events in the human endometrium. Despite evidence for ENaC cleavage inducing similar signalling in the mouse, I show that additional maternal receptors may be responsible for interpreting the conserved embryo-derived signals in humans.

By measuring transcript and protein levels in endometrial cells I demonstrate that PAR2, TLR4 and ENaC (receptors regulated by trypsin, PRSS8 and TMPRSS2) are present in the endometrium and up-regulated at the time of implantation. Furthermore, by showing increased receptor expression in HESCs compared to HEECs via ICC and Western blot, I highlight a role for ENaC and TLR4 beyond initial breaching of the epithelium by the embryo. The peak of protease-regulated receptor expression on day 4 in DESCs and co-ordinated transcriptional regulation of *TLR4*, *SCNN1A* and *F2RL1* in endometrial biopsies indicates priming of the stromal compartment ready for synchronised proteolytic processing by embryo-derived signals.

In order to identify the specific interactions between embryo-derived proteases and maternal receptors, day 4 DESCs were co-cultured with ECM. Although preliminary, the data show that the presence of embryo-derived signals, specifically from successfully implanting embryos, directly affects the structure of TLR4 and down-regulates TLR4 activity. The result is a markedly diminished immune response to LPS, which mimicked the addition of a TLR4-specific inhibitor and could be crucial in permitting the implantation of a semi-allogenic embryo into the maternal decidua.

The homogenous localisation of TLR4 across the luminal epithelia, detected via IHC

analysis of fixed endometrial sections, indicates a pre-implantation role of this receptor in addition to a post-implantation function. This is consistent with previously identified TLR4 protein expression in both the epithelial and stromal compartments of the human endometrium (Hirata et al., 2005). Yet, in contrast to the TLR4 localisation observed in patients suffering from RM (Figure 4.2.4.1), IHC analysis of biopsies from hysterectomy patients indicates weak TLR4 staining in the apical epithelium and intense TLR4 staining in the endometrial glands (Fazeli et al., 2005). This discrepancy in TLR4 localisation may be explained by inter-patient variability and highlights the need for comprehensive IHC studies on phase-matched biopsies from larger cohorts of patients, encompassing differing aetiologies.

To further test whether TLR4 is crucial at implantation, we assessed whether TLR4 becomes de-regulated in cases of reproductive failure. In agreement with evidence that TLR4 is under strict post-translational control (Liew et al., 2005) but in contrast to the transcript expression, TLR4 protein levels were decreased in RM, compared to RIF, samples. Further, reduced TLR4 protein levels showed a correlation with increased BMI and uNK cell density. It is important to highlight that these findings are limited due to a lack of samples from fertile controls, which are difficult to obtain in our clinical setting.

It is foreseeable that a reduced level of active TLR4 receptors in the endometrium of RM patients is responsible for less stringent embryo selection at the time of implantation. The resulting dampened immune response would predispose to pregnancy loss by permitting the implantation of developmentally incompetent embryos, which would require subsequent disposal at a later selection checkpoint.

Chapter 5

Discussion

5.1 A changing implantation paradigm

ART is based on a ‘double binary’ view of the drivers of reproductive success; i.e. implantation of a ‘normal’ but not an ‘abnormal’ embryo in a ‘receptive’ but not a ‘non-receptive’ endometrium results in a successful pregnancy. Should these four variables occur randomly and combine by chance, the likelihood of successful pregnancy per implantation event would be 25%. This predicted incidence is remarkably similar to the average fecundity rate in humans. Further, the fact that many IVF units, including ours, now achieve ~ 50% pregnancy rates in women under the age of 35 years could be viewed as indirectly validating the ‘double binary’ paradigm. In other words, by constantly upgrading the methods and strategies for selection of ‘normal’ embryos and ‘receptive’ endometrium, pregnancy rates are set to rise further, miscarriage rates will gradually fall and, ultimately, IVF success will become guaranteed.

However, the ‘double binary’ view of implantation is based upon a number of unsubstantiated assumptions and misleading observations. For example, the concept of ‘normal’ and ‘abnormal’ embryos stems from the belief that embryonic aneuploidies are caused solely, or at least predominately, by meiotic errors. Consequently, genetic analysis of one or more blastomeres from a cleavage-stage embryo should enable incontrovertible selection of normal embryos, thus eliminating one of the two obstacles that prevent total reproductive success. Despite the initial enthusiasm and widespread adoption of preimplantation genetic screening (PGS), randomized controlled trials showed that PGS not only failed to improve but actually diminished on-going IVF pregnancy and live birth rates (Mastenbroek et al., 2007, Mastenbroek et al., 2011, Staessen et al., 2004). Undaunted by the initial failure of PGS, an upgraded screening procedure, designated PGS#2, is now heavily marketed to improve live-birth rates in IVF. PGS#2 in comparison to PGS#1 is

characterized by: (i) trophectoderm biopsy on day 5 or 6 embryos in place of day 3 embryo biopsy; and (ii) fluorescence in-situ hybridization (FISH) of limited chromosome numbers is replaced by techniques that enable screening of all 24 chromosome pairs (Gleicher et al., 2014). A few clinical trials have been published to date in support of PGS#2 (Rubio et al., 2013) but these studies have been heavily criticised for methodological flaws and misrepresentation of data (Gleicher et al., 2014).

At the heart of the PGS controversy lies the assumption that aneuploidy is always detrimental. This conjecture is of course highly intuitive because of the link between aneuploidy and disease. Aneuploidy is the leading cause of mental retardation and sporadic miscarriage and a key characteristic of cancer, as >90% of all solid human tumours harbour aneuploid genomes (Weaver and Cleveland, 2006). However, a wealth of data has emerged in recent years demonstrating that genomic instability is not pathological per se but intrinsic to the early stages of human embryo development.

A systematic review of the chromosomal constitution of human embryos found, on average, 73% of pre-implantation embryos to be mosaic (van Echten-Arends et al., 2011). This high rate of mosaicism has been confirmed by subsequent analysis of all blastomeres in normally developing cleavage stage embryos via aCGH (71.4%) (Mertzanidou et al., 2013) and firmly undermines the reliability of PGS. Despite extensive reports of mosaicism amongst blastocysts (Evsikov and Verlinsky, 1998, Magli et al., 2000, Sandalinas et al., 2001, Santos et al., 2010), the prevalence of these chromosomal abnormalities appears to be reduced when compared to cleavage stage embryos, suggesting a degree of 'self-correction' during embryo development (Fragouli et al., 2013, Vanneste et al., 2009). The nature of such a mechanism remains to be identified but the shuttling of abnormal cells away from the ICM and towards the trophectoderm lineage has been disproved (Evsikov and

Verlinsky, 1998, Magli et al., 2000, Sandalinas et al., 2001, Santos et al., 2010). Contrary to the assumption underpinning PGS that only euploid embryos should be considered ‘normal’, new evidence has confirmed that mosaic embryos can result in the birth of healthy babies (Greco et al., 2015).

While mosaicism may be a hallmark of human embryos, the purpose of chromosomally abnormal blastomeres in human embryos is a pertinent but largely ignored question in reproductive biology. Based on observations in yeast, aneuploidy has been shown to facilitate rapid phenotypic evolution and acquisition of adaptive traits under stress (Chen et al., 2012). When placed in an evolutionary context, transient aneuploidy in early development confers plasticity and adaptability to ecological changes. Another hypothesis is that aneuploid blastomeres, through mechanisms as yet not understood, contribute to the invasiveness of the embryo. More refined, this hypothesis purports that, depending on the degree of aneuploidy and the nature of chromosomal errors, mosaic embryos may either arrest, implant normally, or even have an implantation advantage.

Chromosomes 15, 16, 21 and 22 are those most commonly associated with aneuploidy in human embryos (Gutiérrez-Mateo et al., 2011, Fragouli et al., 2011), with chromosomes 16 and 22 being the most frequently trisomic (Rubio et al., 2003, Bettio et al., 2008). Interestingly, the aneuploidies observed amongst human embryos involve trisomies and monosomies in equal proportion (Fragouli et al., 2013). Yet, aneuploidies are differentially tolerated during pregnancy according to the affected chromosome and trisomies are more compatible with human life than monosomies. Trisomy 16, thought to affect 1% of all conceptions, is the aneuploidy most strongly correlated with first trimester miscarriage (Benn, 1998). Thus, despite leading to non-viable pregnancies, these trisomic embryos commonly evade the selection checkpoints during the implantation process. It becomes pertinent that the gene encoding PRSS8, a protease more highly expressed by successfully implanting

embryos, is located on chromosome 16. The increased gene dosage in trisomic embryos could result in an over-production of embryo-derived proteases involved at implantation, promoting invasion of the chromosomally 'abnormal' embryo (Quenby et al., 2002). Measuring the levels of embryo-derived proteases in PGS embryos, to determine whether they correlate with gene dosage, would be an important follow-up study.

5.2 Embryo selection at implantation

Embryo 'biosensoring' by the endometrium was first demonstrated in cattle (Sandra and Renard, 2011). Emerging evidence indicates that abnormal decidualization in humans causes loss of the embryo selectivity checkpoint, which renders the endometrium excessively permissive to implantation but unable to sustain the conceptus (Weimar et al., 2012a, Salker et al., 2010). This hypothesis is supported by *in vitro* studies demonstrating that RM is associated with aberrant responsiveness of HESCs to decidualizing signals (Weimar et al., 2012b), although the underlying mechanisms are unknown. This process of embryo selection is either positive or negative; in other words, a decidualizing endometrium responds to embryonic signals in a manner that either supports further development or leads to rapid demise through menstruation-like shedding; thus increasing the likelihood of future reproductive success by safeguarding resources and expediting recovery.

87% of miscarriages prior to 10 weeks gestation are karyotypically abnormal (Burgoyne 1991). Therefore, these losses represent negative selection via a maternal response to abnormal embryos rather than a maternal aetiological cause. Various selection hurdles are imposed, predominantly within the first trimester of pregnancy, in order to obstruct non-viable pregnancies in a timely manner, which restrict the level of detriment to the mother and enable maximal reproductive success. The importance of these quality control mechanisms are highlighted by

the high rates of early pregnancy loss observed in humans (Teklenburg et al., 2010a).

Firstly, a prolonged gestational interval following implantation relies upon corpus luteal rescue by the embryo in order to maintain progesterone levels for the maintenance of pregnancy (Baird et al., 2003). Secondly, the onset of maternal arterial circulation, notably between 9 and 10 weeks gestation, poses a transient phase of placental oxidative stress, representing an additional selective challenge (Jaffe et al., 1997). Prior to this, plugging of distal portions of spiral arteries by cytotrophoblast aggregates restricts arterial circulation to intracellular spaces, resulting in low oxygen tension within the placenta (Jauniaux et al., 2000). If the level of oxidative stress rises too sharply or becomes too great during this phase the cellular defenses become overwhelmed and normal cellular function becomes impaired (Watson et al., 1998) resulting in trophoblastic degeneration, and pregnancy failure (Jauniaux et al., 1994).

5.3 The molecular harbingers of embryonic developmental competence

SGK1 plays an important role in embryo implantation by protecting the feto-maternal interface from oxidative cell death. Further, SGK1 is up- and down- regulated in mid-secretory endometrial biopsies taken from women with unexplained infertility and RM, respectively (Salker et al., 2011). The effects of SGK1 are mediated both by direct activation of ENaC and the ability to enhance *ENaC* expression via NEDD4-2 inhibition. ENaC not only regulates PGE_2 release during mouse implantation but uterine expression levels of ENaC have also been associated with pregnancy outcome in humans (Ruan et al., 2012). As ENaC is regulated via proteolytic processing we focused on identifying embryo-derived proteases that may function at implantation.

For the first time, we provide evidence that human embryos generate trypsin and tryptic activity, with enhanced expression at the blastocyst stage. Furthermore, we identify a conserved up-regulation of two serine proteases, TMPRSS2 and PRSS8, in mice and human blastocysts. PRSS8 is produced by human placental trophoblasts and has been implicated in early pregnancy establishment (Ma et al., 2009). *Prss8* knockout mice display lethality due to placental insufficiency (Hummler et al., 2013) and a PRSS8 polymorphism has been related to severe pre-eclampsia and shallow trophoblast invasion (Luo et al., 2014). Although *Tmprss2* double knockout mice develop normally, TMPRSS2 is thought to play important roles in embryo development, cell growth, proliferation, differentiation, migration, angiogenesis and inflammation via regulation of target genes (Kim et al., 2006). *TMPRSS2* drives ETS-related gene (*ERG*) over-expression through gene fusion, resulting in more aggressive prostate tumour phenotypes and poorer prognoses (Demichelis et al., 2007, Tomlins et al., 2005). PRSS8 and TMPRSS2 are membrane-bound proteases that become cleaved upon activation (Jack et al., 1995), display trypsin-like activity and are able to regulate membrane bound receptors, such as ENaC (Donaldson et al., 2002). PRSS8 and TMPRSS2 are both encoded by genes located on chromosomes commonly associated with aneuploidy in human embryos, 16 and 21, respectively.

We provide evidence that the levels of these embryo-derived proteases relate to implantation outcome upon embryo transfer, with PRSS8 and TMPRSS2 being more highly expressed in successful and unsuccessful implantation events, respectively. Yet the complexity of the embryonic protease signal must not be disregarded and further investigations must be done in order to more closely characterise embryo-secreted products at implantation. It is important to highlight that measurements of ECM are not straightforward, require optimization and include confounding factors, such as the components of embryo culture medium itself.

5.4 Protease-sensitive receptors in the human endometrium

Following a systematic literature search of putative targets of TMPRSS2 and PRSS8, we focused on the *in vivo* and *in vitro* expression of three transmembrane receptors able to regulate cell signalling within the endometrium (ENAC, PAR2 and TLR4). We included both α and γ subunits of ENaC in our experiments as these contain the receptor's key sites of proteolytic processing. Increasing *ENaC*, *TLR4* and *PAR2* transcript levels were identified within the endometrium during the mid-secretory phase, with heightened expression of ENaC and TLR4 in HESCs compared to HEECs. Crucially, decidualization revealed a dynamic phenotype of receptor expression, with a distinctive peak at day 4, in line with the transient pro-inflammatory response in HESCs, which regulates the expression of receptivity genes.

Co-culture of ECM and day 4 DESCs failed to demonstrate cleavage and activation of ENaC or PAR2. This may be explained by the high dilution factor (1:100) required to permit the analysis of individual embryos on DESC monolayers and could possibly be overcome by direct co-cultures of embryos and DESCs.

We did identify TLR4 cleavage upon co-culture with ECM, particularly from successfully implanting embryos, suggesting an increased sensitivity of this receptor to embryo-derived proteases in comparison to ENaC and PAR2. Further, we demonstrated that this inactivation by ECM renders the receptor unable to induce an inflammatory response upon activation by its cognate ligand, LPS. PRSS8 is the most likely embryo-derived protease involved in TLR4 cleavage, as it can directly cleave and inactivate the receptor (Uchimura et al., 2014), is detectable in ECM and increased PRSS8 levels were associated with successful implantation. Strategies to formally test this PRSS8-TLR4 interaction at implantation could involve the application of recombinant PRSS8, PRSS8 blocking antibodies or inhibitors and

endogenous PRSS8 knockdown.

5.5 Summary

In view of the incidence of genetic instability in human embryos, it is remarkable that little if anything is known about the fate of developmentally incompetent embryos at implantation. The reason for this lack of insight is obvious. On the one hand, our understanding of the implantation process is largely based on animal models, such as mouse, with a low incidence of chromosomally aberrant embryos. On the other, the prevailing belief is that most aberrant embryos cannot breach the luminal epithelium and disintegrate in the uterine cavity. Obvious exceptions on this rule are embryos with numeric aneuplodies, such as trisomies, which cause clinical miscarriages.

My observations challenge this view and suggest that embryos generate complex soluble signals that either lead to active maternal rejection or induce an immune-privileged and supportive environment. My studies uncovered the importance of the PRSS8-TLR4 pathway in maternal selection of implanting embryos. Silencing of TLR4 directly couples implantation to an innate immune response in the endometrium. Importantly, I showed that embryos that fail to secrete sufficient PRSS8 are less likely to implant, which may relate to partial or incomplete TLR4 inactivation. Conversely, lack of endometrial TLR4 expression may impair the selectivity checkpoint at implantation, thus predisposing for recurrent miscarriage and superfertility. The complexity of embryonic protease signals, combined with the expression of multiple responsive receptors in the endometrium, renders implantation exceptionally dynamic. Nevertheless, an in-depth understanding of the mechanisms that control selection is poised to lead to effective strategies for the detection and prevention of persistent reproductive failure.

Appendices

Appendix 1: qRT-PCR primers

Gene	Forward Primer	Reverse Primer
F2RL1	5'-ATCCTGCTAGCAGCCTCTC-3'	5'-GTGGGATGTGCCATCAACCTT -3'
IL8	5'-CCAAGGAAAACTGGGTGCAGA-3'	5'-TTCACTGATTCTTGGATACCACAG-3'
L19	5'-GCGGAAGGGTACAGCCAA-3'	5'-GCAGCCGGGCGCAAA-3'
PRSS8	5'-CCTGACTTGAGCCACTCCTT-3'	5'-AAAGCACACCCAGAAGAATGG-3'
PTGS2	5'-CCAGCACTTCACGCATCAGT-3'	5'-GGGTGGACTTAAATCATATTTACGGT-3'
SCNN1A	5'-CATCCCTGGAGGAGGACA-3'	5'-TGGTGGAAGTGAGAGTAATTCG-3'
TLR4	5'-AGCCATGGCCTTCCTCTC-3'	5'-ACTTCAGCTCCATGCATTGATAA-3'

Appendix 2: Up-regulated human genes: Fold Change ≥2.0

Dev. Stage	Gene	Classification	Fold change	*P* value
1 cell	*ECE2*	Metalloproteases	136.67	0.17
	ANPEP	Metalloproteases	111.03	0.17
	USP13	Cysteine Proteases	102.47	0.01
	USP2	Cysteine Proteases	93.82	0.01
	PSEN2	Aspartic Proteases	93.18	0.01
	ENPEP	Metalloproteases	86.64	0.03
	USP35	Cysteine Proteases	60.86	0.05
	BRCC3 (C6.1A)	Metalloproteases	53.72	0.02
	TMPRSS2	Serine Proteases	47.39	0.02
	CAPN13	Cysteine Proteases	37.84	0.01
	RISC/SCPEP1	Serine Proteases	34.46	0.06
	PA2G4	Metalloproteases	33.15	0.01
	TFRC	Metalloproteases	31.52	0.00
	PRSS8	Serine Proteases	30.56	0.10
	SENP8	Cysteine Proteases	20.95	0.01
	CAPN7	Cysteine Proteases	20.31	0.13
	PRSS23	Serine Proteases	19.49	0.00
	CYLD1 (CYLD)	Cysteine Proteases	18.44	0.00
	ADAM22	Metalloproteases	17.93	0.17
	BEM46L1/ABHD13	Serine Proteases	17.10	0.19
	PRSS15/LONP1	Serine Proteases	17.07	0.16
	UCHL1	Cysteine Proteases	16.72	0.00
	PMPCB	Metalloproteases	16.54	0.00
	UQCRC1	Metalloproteases	15.36	0.08
	BACE2	Aspartic Proteases	15.08	0.06
	ADAMTS1	Metalloproteases	14.82	0.49
	NRD1	Metalloproteases	14.60	0.00
	CPVL	Serine Proteases	13.29	0.00
	USP44	Cysteine Proteases	11.63	0.12
	PGA4	Aspartic Proteases	11.62	0.16
	CAPN3	Cysteine Proteases	10.67	0.00
	USP45	Cysteine Proteases	10.25	0.02
	SENP6	Cysteine Proteases	10.20	0.16
	PSEN1	Aspartic Proteases	10.19	0.05
	GGTL4 (GGTLC2)	Threonine Proteases	9.69	0.25
	USP34	Cysteine Proteases	9.57	0.01
	USP10	Cysteine Proteases	8.77	0.00
	KLKB1	Serine Proteases	8.71	0.29
	DPP4	Serine Proteases	8.34	0.13
	ADAM9	Metalloproteases	8.13	0.12
	PCOLN3 (CHMP1A)	Metalloproteases	7.84	0.00
	APEH	Serine Proteases	7.58	0.03
	TRA1/TRRAP	Serine Proteases	7.41	0.01
	USP20	Cysteine Proteases	7.36	0.04

	THOP1	Metalloproteases	7.27	0.00
	PIM2	Serine Proteases	6.81	0.05
	USP15	Cysteine Proteases	6.67	0.02
	PPGB/CATHEPSIN A	Serine Proteases	6.47	0.26
	PRCP	Serine Proteases	6.21	0.13
	CASP9	Cysteine Proteases	6.06	0.00
	LGMN	Cysteine Proteases	5.99	0.03
	METAP1	Metalloproteases	5.78	0.21
	USP21	Cysteine Proteases	5.59	0.05
	ABHD4	Serine Proteases	5.53	0.00
	PGPEP1	Cysteine Proteases	5.40	0.03
	PEPD	Metalloproteases	5.31	0.00
	AQPEP	Metalloproteases	5.18	0.00
	C1S	Serine Proteases	5.16	0.29
	CLN2/TPP1	Serine Proteases	5.00	0.06
	YME1L1	Metalloproteases	4.89	0.02
	AUTL1 (ATG4C)	Cysteine Proteases	4.87	0.20
	DPP7	Serine Proteases	4.85	0.01
	PSH1 (SPPL3)	Aspartic Proteases	4.80	0.08
	CAPN14	Cysteine Proteases	4.68	0.25
	CLPP	Serine Proteases	4.67	0.27
	PLG	Serine Proteases	4.67	0.06
	CEZANNE (OTUD7B)	Cysteine Proteases	4.59	0.01
	PSMB9	Threonine Proteases	4.30	0.01
	ABHD12/BEM46L3	Serine Proteases	4.25	0.00
	USP9X	Cysteine Proteases	4.18	0.05
	ADAMTS16	Metalloproteases	4.15	0.23
	ASPA	Metalloproteases	4.09	0.09
	SUP16H	Metalloproteases	3.95	0.02
	ADAM1A	Metalloproteases	3.84	0.16
	GFPT1	Cysteine Proteases	3.80	0.00
	TMPRSS4	Serine Proteases	3.75	0.56
	MEP1A	Metalloproteases	3.63	0.85
	XPNPEPL (XPNPEP1)	Metalloproteases	3.53	0.00
	USP4	Cysteine Proteases	3.45	0.01
	CG1 58/ABHD5	Serine Proteases	3.31	0.13
	KLK8	Serine Proteases	3.29	0.38
	MMP20	Metalloproteases	3.18	0.23
	COPS6	Metalloproteases	3.17	0.00
	GZMM	Serine Proteases	3.16	0.93
	OSGEP	Metalloproteases	3.13	0.17
	PROC	Serine Proteases	3.12	0.82
	PROCL	Serine Proteases	3.12	0.82
	USP30	Cysteine Proteases	3.12	0.03
	CAPN10	Cysteine Proteases	3.09	0.22
	ESPL1	Cysteine Proteases	3.03	0.09
	CFD/ADIPSIN	Serine Proteases	3.01	0.13

	USP47	Cysteine Proteases	2.93	0.16
	CTRL	Serine Proteases	2.91	0.34
	SPC18/SEC11A	Serine Proteases	2.88	0.56
	USP25	Cysteine Proteases	2.84	0.02
	SPC21/SEC11C	Serine Proteases	2.80	0.27
	AUTL2 (ATG4A)	Cysteine Proteases	2.79	0.01
	EPHXRP/EPHX4	Serine Proteases	2.79	0.44
	RHBDL4/RHBDL3	Serine Proteases	2.78	0.01
	ADAM32	Metalloproteases	2.69	0.05
	LAP3	Metalloproteases	2.67	0.10
	USP52 (PAN2)	Cysteine Proteases	2.66	0.03
	PSMA5	Threonine Proteases	2.61	0.02
	AFG3L2	Metalloproteases	2.59	0.03
	USP5	Cysteine Proteases	2.57	0.18
	TFR2	Metalloproteases	2.57	0.00
	HGF/SOS1	Serine Proteases	2.56	0.09
	RNPEP	Metalloproteases	2.52	0.01
	PRSS7	Serine Proteases	2.51	0.06
	MMP24	Metalloproteases	2.51	0.05
	ADAM7	Metalloproteases	2.45	0.04
	MMP13	Metalloproteases	2.44	0.08
	HTRA2	Serine Proteases	2.42	0.00
	ADAMDEC1	Metalloproteases	2.38	0.15
	PIP	Aspartic Proteases	2.38	0.01
	KLK14	Serine Proteases	2.37	0.15
	PRPF8	Metalloproteases	2.33	0.02
	ADAM18	Metalloproteases	2.33	0.57
	USP1	Cysteine Proteases	2.33	0.28
	PSMD7	Metalloproteases	2.32	0.16
	GGH	Cysteine Proteases	2.29	0.05
	HPN	Serine Proteases	2.28	0.48
	EGFR-RS/RHBDF1	Serine Proteases	2.27	0.07
	PRSS27/MARAPSIN	Serine Proteases	2.25	0.89
	LPA	Serine Proteases	2.25	0.43
	TRAP1	Serine Proteases	2.23	0.04
	GGT5 (GGTLA1)	Threonine Proteases	2.21	0.42
	ADAMTS19	Metalloproteases	2.19	0.42
	ADAMTS18	Metalloproteases	2.18	0.03
	USP16	Cysteine Proteases	2.17	0.02
	DNPEP	Metalloproteases	2.16	0.23
	LTF	Serine Proteases	2.14	0.61
	USP37	Cysteine Proteases	2.12	0.07
	PSMA2	Threonine Proteases	2.12	0.00
	ADAM30	Metalloproteases	2.12	0.64
	ELA1	Serine Proteases	2.08	0.41
	USP31	Cysteine Proteases	2.04	0.04
	USP48	Cysteine Proteases	2.04	0.04

	USP18	Cysteine Proteases	2.03	0.15
2 Cell	*ANPEP*	Metalloproteases	115.04	0.17
	USP13	Cysteine Proteases	103.60	0.06
	USP2	Cysteine Proteases	88.60	0.01
	ENPEP	Metalloproteases	75.41	0.03
	PSEN2	Aspartic Proteases	66.44	0.01
	BRCC3 (C6.1A)	Metalloproteases	65.10	0.02
	PRSS8	Serine Proteases	48.27	0.10
	USP35	Cysteine Proteases	43.37	0.03
	TFRC	Metalloproteases	40.01	0.00
	ADAM22	Metalloproteases	38.77	0.16
	PRSS23	Serine Proteases	34.89	0.01
	CAPN13	Cysteine Proteases	33.29	0.10
	PA2G4	Metalloproteases	28.84	0.01
	TMPRSS2	Serine Proteases	26.24	0.02
	RISC/SCPEP1	Serine Proteases	26.22	0.07
	ECE2	Metalloproteases	25.48	0.18
	BACE2	Aspartic Proteases	20.69	0.03
	CYLD1 (CYLD)	Cysteine Proteases	19.50	0.00
	PMPCB	Metalloproteases	19.13	0.01
	PRSS15/LONP1	Serine Proteases	18.58	0.16
	SENP8	Cysteine Proteases	16.09	0.09
	NRD1	Metalloproteases	14.96	0.00
	CPVL	Serine Proteases	14.91	0.00
	ADAMTS1	Metalloproteases	14.20	0.49
	UQCRC1	Metalloproteases	14.14	0.08
	UCHL1	Cysteine Proteases	14.03	0.00
	CAPN7	Cysteine Proteases	12.94	0.31
	CAPN3	Cysteine Proteases	12.15	0.01
	PGA4	Aspartic Proteases	11.76	0.04
	DPP4	Serine Proteases	10.30	0.13
	USP44	Cysteine Proteases	10.12	0.23
	PIM2	Serine Proteases	9.78	0.06
	ADAM9	Metalloproteases	8.78	0.11
	SENP6	Cysteine Proteases	8.67	0.38
	USP20	Cysteine Proteases	8.66	0.10
	PSEN1	Aspartic Proteases	8.02	0.10
	PCOLN3 (CHMP1A)	Metalloproteases	7.72	0.00
	APEH	Serine Proteases	7.68	0.02
	USP45	Cysteine Proteases	7.54	0.08
	USP10	Cysteine Proteases	7.42	0.01
	PEPD	Metalloproteases	7.39	0.00
	USP34	Cysteine Proteases	7.35	0.27
	THOP1	Metalloproteases	7.29	0.01
	BEM46L1/ABHD13	Serine Proteases	7.04	0.22

	HPN	Serine Proteases	6.98	0.19
	YME1L1	Metalloproteases	6.97	0.01
	PPGB/CATHEPSIN A	Serine Proteases	6.94	0.26
	USP15	Cysteine Proteases	6.46	0.12
	USP21	Cysteine Proteases	6.08	0.08
	PRCP	Serine Proteases	6.02	0.13
	CAPN14	Cysteine Proteases	5.98	0.46
	METAP1	Metalloproteases	5.57	0.21
	GGTL4 (GGTLC2)	Threonine Proteases	5.52	0.51
	PLG	Serine Proteases	5.41	0.03
	TRA1/TRRAP	Serine Proteases	5.22	0.01
	KLKB1	Serine Proteases	5.22	0.33
	USP4	Cysteine Proteases	5.14	0.06
	CLN2/TPP1	Serine Proteases	4.93	0.06
	CASP9	Cysteine Proteases	4.79	0.07
	PSMD7	Metalloproteases	4.62	0.07
	PSMB9	Threonine Proteases	4.42	0.01
	DPP7	Serine Proteases	4.38	0.00
	PGPEP1	Cysteine Proteases	4.36	0.06
	XPNPEPL (XPNPEP1)	Metalloproteases	4.33	0.00
	AFG3L2	Metalloproteases	4.29	0.00
	SUP16H	Metalloproteases	4.20	0.03
	PSH1 (SPPL3)	Aspartic Proteases	4.06	0.01
	USP9X	Cysteine Proteases	3.81	0.14
	USP11	Cysteine Proteases	3.80	0.40
	ABHD4	Serine Proteases	3.78	0.01
	SPC18/SEC11A	Serine Proteases	3.74	0.51
	MEP1A	Metalloproteases	3.67	0.85
	KLK8	Serine Proteases	3.61	0.36
	COPS6	Metalloproteases	3.61	0.01
	CLPP	Serine Proteases	3.58	0.31
	AQPEP	Metalloproteases	3.56	0.00
	TMPRSS4	Serine Proteases	3.56	0.58
	CEZANNE (OTUD7B)	Cysteine Proteases	3.42	0.09
	RHBDL4/RHBDL3	Serine Proteases	3.42	0.12
	USP37	Cysteine Proteases	3.40	0.09
	USP47	Cysteine Proteases	3.32	0.30
	SPC21/SEC11C	Serine Proteases	3.28	0.24
	LAP3	Metalloproteases	3.28	0.06
	GZMM	Serine Proteases	3.26	0.92
	GFPT1	Cysteine Proteases	3.17	0.22
	AUTL1 (ATG4C)	Cysteine Proteases	3.11	0.49
	USP25	Cysteine Proteases	3.11	0.00
	USP52 (PAN2)	Cysteine Proteases	3.11	0.08
	LGMN	Cysteine Proteases	3.08	0.32
	USP30	Cysteine Proteases	3.05	0.04
	GGT5 (GGTLA1)	Threonine Proteases	3.05	0.27

	ASPA	Metalloproteases	3.02	0.09
	TRHDE	Metalloproteases	3.02	0.91
	CTRL	Serine Proteases	2.91	0.34
	C1S	Serine Proteases	2.82	0.40
	TRAP1	Serine Proteases	2.78	0.01
	USP5	Cysteine Proteases	2.72	0.14
	ESPL1	Cysteine Proteases	2.71	0.08
	ADAM1A	Metalloproteases	2.68	0.21
	CG1 58/ABHD5	Serine Proteases	2.68	0.16
	PRPF8	Metalloproteases	2.61	0.02
	CFD/ADIPSIN	Serine Proteases	2.60	0.12
	ELA1	Serine Proteases	2.60	0.31
	CAPN10	Cysteine Proteases	2.52	0.04
	CAPN12	Cysteine Proteases	2.50	0.08
	OSGEP	Metalloproteases	2.48	0.20
	HGF/SOS1	Serine Proteases	2.47	0.17
	ADAM3B	Metalloproteases	2.43	0.25
	POH1 (PSMD14)	Metalloproteases	2.43	0.01
	DNPEP	Metalloproteases	2.41	0.20
	KLK6	Serine Proteases	2.41	0.56
	RELN	Serine Proteases	2.39	0.30
	PIP	Aspartic Proteases	2.39	0.00
	ADAM7	Metalloproteases	2.35	0.03
	PRTN3	Serine Proteases	2.35	0.90
	ADAM18	Metalloproteases	2.34	0.61
	RNPEP	Metalloproteases	2.33	0.01
	MMP24	Metalloproteases	2.30	0.06
	PCSK2	Serine Proteases	2.28	0.63
	PSMA5	Threonine Proteases	2.27	0.14
	ADAMTS18	Metalloproteases	2.22	0.03
	CPGL (CNDP2)	Metalloproteases	2.20	0.20
	HTRA2	Serine Proteases	2.19	0.01
	CASP2	Cysteine Proteases	2.17	0.51
	PCSK6	Serine Proteases	2.16	0.31
	TFR2	Metalloproteases	2.16	0.02
	CPA5	Metalloproteases	2.11	0.02
	FACE1 (ZMPSTE24)	Metalloproteases	2.08	0.01
	OTUB2	Cysteine Proteases	2.07	0.57
	EPHXRP/EPHX4	Serine Proteases	2.06	0.57
	PRSS7	Serine Proteases	2.03	0.09
	AUTL2 (ATG4A)	Cysteine Proteases	2.01	0.23
	ADAMTS5	Metalloproteases	2.00	0.60
4 Cell	*ENPEP*	Metalloproteases	144.46	0.03
	ANPEP	Metalloproteases	141.93	0.17
	USP2	Cysteine Proteases	92.92	0.01
	USP13	Cysteine Proteases	88.81	0.06

PSEN2	Aspartic Proteases	54.98	0.03
CAPN13	Cysteine Proteases	34.92	0.01
USP35	Cysteine Proteases	32.39	0.08
ECE2	Metalloproteases	27.54	0.18
TMPRSS2	Serine Proteases	27.09	0.02
PRSS8	Serine Proteases	26.16	0.10
BRCC3 (C6.1A)	Metalloproteases	24.87	0.02
PA2G4	Metalloproteases	22.49	0.00
CPVL	Serine Proteases	19.54	0.00
CAPN7	Cysteine Proteases	16.61	0.02
CYLD1 (CYLD)	Cysteine Proteases	14.63	0.01
CAPN3	Cysteine Proteases	14.37	0.12
SENP8	Cysteine Proteases	14.12	0.09
UCHL1	Cysteine Proteases	14.06	0.00
RISC/SCPEP1	Serine Proteases	11.46	0.06
ADAM22	Metalloproteases	11.39	0.18
BACE2	Aspartic Proteases	11.35	0.03
PGA4	Aspartic Proteases	10.97	0.02
USP10	Cysteine Proteases	10.57	0.04
KLKB1	Serine Proteases	9.03	0.29
USP34	Cysteine Proteases	8.82	0.00
PRSS23	Serine Proteases	8.70	0.00
USP20	Cysteine Proteases	8.59	0.03
TRA1/TRRAP	Serine Proteases	8.49	0.00
THOP1	Metalloproteases	8.48	0.00
USP45	Cysteine Proteases	8.07	0.06
PIM2	Serine Proteases	7.95	0.05
UQCRC1	Metalloproteases	7.90	0.08
USP44	Cysteine Proteases	7.83	0.07
PSEN1	Aspartic Proteases	7.80	0.04
BEM46L1/ABHD13	Serine Proteases	7.68	0.21
ASPA	Metalloproteases	7.43	0.06
GGTL4 (GGTLC2)	Threonine Proteases	6.65	0.33
PMPCB	Metalloproteases	6.51	0.01
SENP6	Cysteine Proteases	6.34	0.19
USP21	Cysteine Proteases	6.26	0.04
USP15	Cysteine Proteases	6.16	0.00
ADAM9	Metalloproteases	6.11	0.12
NRD1	Metalloproteases	6.07	0.01
METAP1	Metalloproteases	6.01	0.20
DPP4	Serine Proteases	5.91	0.12
PCOLN3 (CHMP1A)	Metalloproteases	5.76	0.01
USP4	Cysteine Proteases	5.50	0.16
USP29	Cysteine Proteases	5.07	0.21
TFRC	Metalloproteases	4.83	0.06
PSMB9	Threonine Proteases	4.73	0.08
USP9X	Cysteine Proteases	4.71	0.03

AQPEP	Metalloproteases	4.68	0.02
PEPD	Metalloproteases	4.65	0.00
MEP1A	Metalloproteases	4.64	0.81
GZMM	Serine Proteases	4.38	0.89
ABHD12/BEM46L3	Serine Proteases	4.35	0.02
HPN	Serine Proteases	4.00	0.23
APEH	Serine Proteases	3.99	0.02
TMPRSS4	Serine Proteases	3.88	0.56
USP11	Cysteine Proteases	3.83	0.16
AFG3L2	Metalloproteases	3.77	0.01
USP37	Cysteine Proteases	3.75	0.06
RHBDL4/RHBDL3	Serine Proteases	3.72	0.02
MMP20	Metalloproteases	3.69	0.20
CEZANNE (OTUD7B)	Cysteine Proteases	3.67	0.04
DPP7	Serine Proteases	3.63	0.03
CASP9	Cysteine Proteases	3.59	0.01
CAPN14	Cysteine Proteases	3.57	0.19
YME1L1	Metalloproteases	3.56	0.01
PRCP	Serine Proteases	3.56	0.15
XPNPEPL (XPNPEP1)	Metalloproteases	3.46	0.00
CLPP	Serine Proteases	3.39	0.32
ADAM30	Metalloproteases	3.31	0.44
KLK8	Serine Proteases	3.28	0.38
PSMD7	Metalloproteases	3.27	0.12
LGMN	Cysteine Proteases	3.18	0.03
PLG	Serine Proteases	3.12	0.07
USP47	Cysteine Proteases	3.04	0.05
GFPT1	Cysteine Proteases	3.03	0.01
PSH1 (SPPL3)	Aspartic Proteases	3.01	0.04
ELA1	Serine Proteases	3.01	0.28
OSGEP	Metalloproteases	2.97	0.16
PPGB/CATHEPSIN A	Serine Proteases	2.97	0.38
HGF/SOS1	Serine Proteases	2.95	0.01
USP5	Cysteine Proteases	2.95	0.00
PRSS15/LONP1	Serine Proteases	2.92	0.41
USP52 (PAN2)	Cysteine Proteases	2.84	0.06
RNPEP	Metalloproteases	2.78	0.01
PROC	Serine Proteases	2.76	0.84
PROCL	Serine Proteases	2.76	0.84
GGT5 (GGTLA1)	Threonine Proteases	2.65	0.05
MMP13	Metalloproteases	2.63	0.07
USP25	Cysteine Proteases	2.60	0.07
CG1 58/ABHD5	Serine Proteases	2.57	0.15
CFD/ADIPSIN	Serine Proteases	2.56	0.16
USP30	Cysteine Proteases	2.55	0.10
CPA5	Metalloproteases	2.55	0.01
SUP16H	Metalloproteases	2.53	0.05

	ADAM1A	Metalloproteases	2.46	0.23
	CAPN10	Cysteine Proteases	2.45	0.01
	PRSS7	Serine Proteases	2.44	0.04
	ADAMTS16	Metalloproteases	2.42	0.43
	ABHD4	Serine Proteases	2.37	0.05
	ADAM7	Metalloproteases	2.35	0.00
	EPHXRP/EPHX4	Serine Proteases	2.34	0.51
	FACE1 (ZMPSTE24)	Metalloproteases	2.32	0.01
	AUTL1 (ATG4C)	Cysteine Proteases	2.31	0.28
	PGPEP1	Cysteine Proteases	2.31	0.10
	MMP21	Metalloproteases	2.31	0.78
	CAPN12	Cysteine Proteases	2.30	0.07
	PIP	Aspartic Proteases	2.27	0.00
	SPC18/SEC11A	Serine Proteases	2.27	0.66
	TMPRSS6	Serine Proteases	2.26	0.40
	ESPL1	Cysteine Proteases	2.25	0.12
	AOPEP (C9ORF3)	Metalloproteases	2.25	0.12
	AUTL2 (ATG4A)	Cysteine Proteases	2.18	0.06
	SPC21/SEC11C	Serine Proteases	2.17	0.37
	C1S	Serine Proteases	2.16	0.53
	CPGL (CNDP2)	Metalloproteases	2.13	0.15
	PRPF8	Metalloproteases	2.05	0.10
	PSMA5	Threonine Proteases	2.05	0.04
	GGT7 (GGTL3)	Threonine Proteases	2.04	0.14
	LPA	Serine Proteases	2.01	0.34
	ADAMDEC1	Metalloproteases	2.01	0.21
8 Cell	*ENPEP*	Metalloproteases	59.43	0.03
	PRSS8	Serine Proteases	46.68	0.10
	ANPEP	Metalloproteases	42.61	0.17
	CPVL	Serine Proteases	23.14	0.00
	BRCC3 (C6.1A)	Metalloproteases	20.68	0.01
	CAPN13	Cysteine Proteases	19.44	0.02
	PSEN2	Aspartic Proteases	15.19	0.21
	USP13	Cysteine Proteases	13.59	0.27
	USP2	Cysteine Proteases	11.60	0.13
	RISC/SCPEP1	Serine Proteases	11.52	0.06
	MMP20	Metalloproteases	9.12	0.16
	UCHL1	Cysteine Proteases	8.65	0.00
	BACE2	Aspartic Proteases	8.29	0.15
	BEM46L1/ABHD13	Serine Proteases	7.90	0.22
	PSMD7	Metalloproteases	7.81	0.05
	PSMB9	Threonine Proteases	7.02	0.51
	ADAM9	Metalloproteases	6.87	0.09
	USP35	Cysteine Proteases	6.87	0.14
	TMPRSS2	Serine Proteases	6.70	0.00
	PSMB8	Threonine Proteases	6.51	0.73

AFG3L2	Metalloproteases	6.17	0.01
METAP1	Metalloproteases	6.10	0.20
ACE2	Metalloproteases	6.02	0.13
UQCRC1	Metalloproteases	5.93	0.07
ECE2	Metalloproteases	5.81	0.23
PEPD	Metalloproteases	5.44	0.02
SUP16H	Metalloproteases	5.26	0.02
XPNPEPL (XPNPEP1)	Metalloproteases	5.12	0.03
CAPN3	Cysteine Proteases	5.06	0.01
THOP1	Metalloproteases	4.95	0.05
PIM2	Serine Proteases	4.78	0.06
SENP5	Cysteine Proteases	4.57	0.28
PMPCB	Metalloproteases	4.53	0.03
NRD1	Metalloproteases	4.47	0.03
DESC1/TMPRSS11E	Serine Proteases	4.35	0.29
HGF/SOS1	Serine Proteases	4.35	0.01
CYLD1 (CYLD)	Cysteine Proteases	4.32	0.03
TFRC	Metalloproteases	4.19	0.06
CPGL (CNDP2)	Metalloproteases	3.98	0.71
USP29	Cysteine Proteases	3.92	0.40
PLG	Serine Proteases	3.74	0.07
KLK8	Serine Proteases	3.72	0.36
ABHD12/BEM46L3	Serine Proteases	3.66	0.01
ADAM10	Metalloproteases	3.59	0.21
FACE1 (ZMPSTE24)	Metalloproteases	3.45	0.04
PA2G4	Metalloproteases	3.45	0.00
RNPEP	Metalloproteases	3.33	0.01
TAF2	Metalloproteases	3.33	0.15
CAD	Metalloproteases	3.30	0.06
PRSS23	Serine Proteases	3.21	0.23
TRAP1	Serine Proteases	3.15	0.06
LGMN	Cysteine Proteases	3.15	0.58
AOPEP (C9ORF3)	Metalloproteases	3.13	0.05
PGA4	Aspartic Proteases	3.10	0.02
APEH	Serine Proteases	3.09	0.12
ASPA	Metalloproteases	2.93	0.08
CTRL	Serine Proteases	2.93	0.35
USP20	Cysteine Proteases	2.76	0.13
HPN	Serine Proteases	2.72	0.31
AFG3L1 (AFG3L1P)	Metalloproteases	2.65	0.13
POH1 (PSMD14)	Metalloproteases	2.62	0.07
MBTPS2	Metalloproteases	2.61	0.29
USP10	Cysteine Proteases	2.55	0.31
CAPN14	Cysteine Proteases	2.52	0.33
AQPEP	Metalloproteases	2.48	0.25
HSPCA/HSP90AA1	Serine Proteases	2.41	0.18
MIPEP	Metalloproteases	2.40	0.13

	ADAM33	Metalloproteases	2.38	0.43
	HTRA2	Serine Proteases	2.37	0.01
	SPC21/SEC11C	Serine Proteases	2.35	0.43
	IMP1L	Serine Proteases	2.35	0.48
	CAPN12	Cysteine Proteases	2.34	0.04
	GZMM	Serine Proteases	2.33	0.96
	ADAMTS2	Metalloproteases	2.30	0.25
	SPC18/SEC11A	Serine Proteases	2.19	0.75
	PCSK1	Serine Proteases	2.19	0.90
	CAPN11	Cysteine Proteases	2.19	0.30
	GGT1	Threonine Proteases	2.19	0.34
	EGFR-RS/RHBDF1	Serine Proteases	2.13	0.21
	USP34	Cysteine Proteases	2.08	0.56
	PRSS16	Serine Proteases	2.07	0.19
	ADAM1A	Metalloproteases	2.07	0.39
	TPSB1	Serine Proteases	2.04	0.72
	DPP4	Serine Proteases	2.00	0.35
Morula	*ENPEP*	Metalloproteases	28.97	0.03
	PRSS8	Serine Proteases	22.58	0.10
	TMPRSS2	Serine Proteases	15.44	0.00
	CPVL	Serine Proteases	13.48	0.00
	ACE2	Metalloproteases	12.10	0.13
	LTA4H	Metalloproteases	9.64	0.00
	ADAM9	Metalloproteases	8.15	0.12
	PIM2	Serine Proteases	8.11	0.06
	ADAMTS1	Metalloproteases	7.50	0.53
	LACTB	Serine Proteases	7.49	0.12
	MBTPS2	Metalloproteases	6.15	0.15
	XPNPEPL (XPNPEP1)	Metalloproteases	6.09	0.01
	GZMM	Serine Proteases	5.49	0.87
	CPGL (CNDP2)	Metalloproteases	5.47	0.85
	LGMN	Cysteine Proteases	5.47	0.21
	MBTPS1	Serine Proteases	5.34	0.14
	ANPEP	Metalloproteases	5.02	0.22
	PSMB9	Threonine Proteases	5.02	0.14
	CLN2/TPP1	Serine Proteases	4.51	0.07
	BRCC3 (C6.1A)	Metalloproteases	4.21	0.02
	SENP5	Cysteine Proteases	4.14	0.24
	BEM46L1/ABHD13	Serine Proteases	4.02	0.28
	ABHD4	Serine Proteases	3.83	0.01
	PRCP	Serine Proteases	3.71	0.16
	HSPCA/HSP90AA1	Serine Proteases	3.71	0.11
	TMPRSS4	Serine Proteases	3.67	0.56
	IMMP2L	Serine Proteases	3.54	0.02
	PSMD7	Metalloproteases	3.46	0.10
	KLK14	Serine Proteases	3.28	0.08

	CG1 58/ABHD5	Serine Proteases	3.13	0.14
	CAPN13	Cysteine Proteases	3.09	0.02
	USP13	Cysteine Proteases	3.05	0.26
	TRAP1	Serine Proteases	2.95	0.02
	INPP5E	Metalloproteases	2.85	0.01
	AQPEP	Metalloproteases	2.80	0.00
	TPP2	Serine Proteases	2.78	0.03
	ABHD12/BEM46L3	Serine Proteases	2.74	0.01
	AOPEP (C9ORF3)	Metalloproteases	2.64	0.09
	ADAM10	Metalloproteases	2.58	0.28
	RNPEP	Metalloproteases	2.53	0.01
	CAPN14	Cysteine Proteases	2.52	0.66
	AFG3L2	Metalloproteases	2.41	0.02
	UQCRC1	Metalloproteases	2.38	0.19
	METAP1	Metalloproteases	2.36	0.37
	SPC21/SEC11C	Serine Proteases	2.31	0.33
	RISC/SCPEP1	Serine Proteases	2.28	0.16
	TRHDE	Metalloproteases	2.27	0.95
	USP7	Cysteine Proteases	2.27	0.00
	ADAM6	Metalloproteases	2.26	0.81
	PEPD	Metalloproteases	2.23	0.06
	POH1 (PSMD14)	Metalloproteases	2.22	0.02
	TAF2	Metalloproteases	2.20	0.24
	CTSF	Cysteine Proteases	2.19	0.22
	ECEL1	Metalloproteases	2.16	0.87
	TPSG1	Serine Proteases	2.16	0.47
	THOP1	Metalloproteases	2.13	0.01
	MIPEP	Metalloproteases	2.12	0.18
	TPSB1	Serine Proteases	2.11	0.70
	DPP3	Metalloproteases	2.10	0.56
	PCSK1	Serine Proteases	2.06	0.92
	HGF/SOS1	Serine Proteases	2.05	0.01
	KLK6	Serine Proteases	2.01	0.66
	BACE2	Aspartic Proteases	2.00	0.39

Appendix 3: Up-regulated mouse genes: Fold Change ≥2.0

Dev. Stage	Gene	Classification	Fold change	*P* value
Oocyte	*Enpep*	Metalloproteases	117.18	0.00
	Uchl1	Cysteine Proteases	60.96	0.01
	Cathepsin A	Serine Proteases	32.15	0.00
	Ctsh	Cysteine Proteases	30.39	0.00
	CpnCpn1	Metalloproteases	29.04	0.02
	Usp2	Cysteine Proteases	24.58	0.01
	Lap3	Metalloproteases	20.38	0.01
	Xpnpep1	Metalloproteases	17.68	0.00
	Bace2	Aspartic Proteases	16.30	0.01
	Otub2	Cysteine Proteases	16.16	0.00
	Prss8	Serine Proteases	14.71	0.00
	Osgep	Metalloproteases	14.04	0.00
	Uqcrc1	Metalloproteases	13.69	0.01
	Dpp4	Serine Proteases	12.26	0.01
	Yme1L1	Metalloproteases	11.35	0.03
	Sva	Aspartic Proteases	11.26	0.05
	Pepd	Metalloproteases	9.77	0.04
	St14	Serine Proteases	9.74	0.01
	Psen2	Aspartic Proteases	9.37	0.00
	Clpp	Serine Proteases	9.01	0.00
	Spg7	Metalloproteases	8.90	0.18
	Casp8	Cysteine Proteases	8.88	0.02
	Lta4H	Metalloproteases	8.47	0.01
	NpeppsPsa	Metalloproteases	7.46	0.05
	Tmprss2	Serine Proteases	7.00	0.09
	Hsp841	Serine Proteases	6.70	0.01
	Usp21	Cysteine Proteases	6.70	0.06
	Metap1	Metalloproteases	6.43	0.06
	Klk7	Serine Proteases	6.35	0.04
	C2	Serine Proteases	6.28	0.07
	Dpp7	Serine Proteases	5.89	0.02
	Cad	Metalloproteases	5.69	0.01
	Usp3	Cysteine Proteases	5.61	0.00
	Usp9X	Cysteine Proteases	5.51	0.02
	Afg3L1	Metalloproteases	5.47	0.00
	Pga5 (Pepf)	Aspartic Proteases	5.35	0.00
	Usp19	Cysteine Proteases	5.13	0.00
	Cela3B Ii	Serine Proteases	5.10	0.24
	Prtn3	Serine Proteases	4.81	0.08
	TrfrTrfrc	Metalloproteases	4.68	0.03
	Senp6	Cysteine Proteases	4.57	0.01
	Dnpep	Metalloproteases	4.52	0.00
	Capn9	Cysteine Proteases	4.45	0.20
	Dpp3	Metalloproteases	4.36	0.00

Eif3S5Eif3F	Metalloproteases	4.23	0.00
Pgpi (Pgpep1)	Cysteine Proteases	4.20	0.02
Ctsf	Cysteine Proteases	4.12	0.16
Adam19	Metalloproteases	3.98	0.00
Acy1	Metalloproteases	3.79	0.26
Rhbdd2	Serine Proteases	3.69	0.16
Tpp1	Serine Proteases	3.53	0.00
Pcsk4	Serine Proteases	3.49	0.22
Senp1	Cysteine Proteases	3.46	0.01
Pcsk1	Serine Proteases	3.34	0.30
Rnpep	Metalloproteases	3.33	0.01
Tranb1 (Trabid)	Cysteine Proteases	3.25	0.01
Mst1	Serine Proteases	3.24	0.20
Cpxm1Cpx1	Metalloproteases	3.18	0.00
Pan2 (Usp52)	Cysteine Proteases	3.13	0.01
Psmd7	Metalloproteases	3.05	0.03
Psmd14Poh1	Metalloproteases	3.01	0.01
Usp4	Cysteine Proteases	3.01	0.05
Anpep	Metalloproteases	2.97	0.69
Usp15	Cysteine Proteases	2.95	0.08
Aspa	Metalloproteases	2.95	0.05
Usp20	Cysteine Proteases	2.86	0.01
Pa2G4	Metalloproteases	2.83	0.11
Capn7	Cysteine Proteases	2.82	0.00
Mep1B	Metalloproteases	2.77	0.01
Prss28	Serine Proteases	2.74	0.25
Ctrb1	Serine Proteases	2.65	0.39
Pmpcb	Metalloproteases	2.65	0.01
Cflar	Cysteine Proteases	2.61	0.20
Usp16	Cysteine Proteases	2.57	0.01
Shh	Cysteine Proteases	2.56	0.67
Lgmn	Cysteine Proteases	2.53	0.00
Pcsk6	Serine Proteases	2.52	0.01
Ide	Metalloproteases	2.48	0.02
Cts6	Cysteine Proteases	2.41	0.69
Atg4B (Autl1)	Cysteine Proteases	2.34	0.01
Mbtps1	Serine Proteases	2.33	0.00
Rhbdl3	Serine Proteases	2.31	0.19
Usp11	Cysteine Proteases	2.31	0.02
Adam34	Metalloproteases	2.31	0.44
Usp-Ps (Dub2)	Cysteine Proteases	2.30	0.60
Face1	Metalloproteases	2.29	0.08
Usp18	Cysteine Proteases	2.22	0.41
Psen1	Aspartic Proteases	2.17	0.01
Ggh	Cysteine Proteases	2.16	0.27
Eif3S3	Metalloproteases	2.08	0.08
Capn12	Cysteine Proteases	2.05	0.01

1 Cell	*Enpep*	Metalloproteases	92.45	0.00
	Uchl1	Cysteine Proteases	65.01	0.04
	Clpp	Serine Proteases	61.46	0.00
	Osgep	Metalloproteases	53.35	0.00
	Cathepsin A	Serine Proteases	52.12	0.01
	Usp2	Cysteine Proteases	46.19	0.00
	CpnCpn1	Metalloproteases	45.20	0.02
	Mep1B	Metalloproteases	36.36	0.01
	Psen2	Aspartic Proteases	28.95	0.00
	Lap3	Metalloproteases	27.79	0.01
	Eif3S5Eif3F	Metalloproteases	25.25	0.00
	Psmd14Poh1	Metalloproteases	20.59	0.01
	Ctsh	Cysteine Proteases	18.65	0.02
	Usp21	Cysteine Proteases	17.86	0.00
	Xpnpep1	Metalloproteases	15.77	0.00
	Cad	Metalloproteases	13.89	0.01
	Dnpep	Metalloproteases	13.87	0.00
	Casp8	Cysteine Proteases	13.54	0.02
	Uqcrc1	Metalloproteases	12.96	0.01
	Yme1L1	Metalloproteases	11.78	0.03
	Tmprss2	Serine Proteases	9.68	0.08
	Pmpcb	Metalloproteases	9.32	0.01
	Klk7	Serine Proteases	9.14	0.05
	Bace2	Aspartic Proteases	9.08	0.25
	St14	Serine Proteases	8.74	0.00
	Senp6	Cysteine Proteases	8.69	0.03
	Senp1	Cysteine Proteases	8.64	0.02
	Otub2	Cysteine Proteases	8.22	0.01
	Lta4H	Metalloproteases	8.15	0.01
	Capn9	Cysteine Proteases	7.98	0.07
	Dpp7	Serine Proteases	7.75	0.01
	Usp15	Cysteine Proteases	7.63	0.01
	Usp19	Cysteine Proteases	7.49	0.00
	Dpp4	Serine Proteases	7.47	0.01
	Cts6	Cysteine Proteases	7.43	0.26
	Prss8	Serine Proteases	7.41	0.00
	Pepd	Metalloproteases	7.18	0.04
	Pitrm1	Metalloproteases	7.06	0.01
	Usp9X	Cysteine Proteases	6.68	0.00
	Eif3S3	Metalloproteases	6.65	0.02
	Cops6	Metalloproteases	6.17	0.01
	NpeppsPsa	Metalloproteases	6.00	0.05
	Prtn3	Serine Proteases	5.46	0.07
	Mmp23	Metalloproteases	5.29	0.20
	Pan2 (Usp52)	Cysteine Proteases	5.03	0.00

Cops5	Metalloproteases	4.91	0.00
Afg3L1	Metalloproteases	4.83	0.00
Rhbdd2	Serine Proteases	4.83	0.13
Capn7	Cysteine Proteases	4.76	0.02
Shh	Cysteine Proteases	4.73	0.47
Dpp3	Metalloproteases	4.44	0.01
Hsp841	Serine Proteases	4.27	0.02
TrfrTrfrc	Metalloproteases	4.21	0.03
Cflar	Cysteine Proteases	4.19	0.03
Usp-Ps (Dub2)	Cysteine Proteases	3.92	0.31
Metap1	Metalloproteases	3.88	0.09
Usp3	Cysteine Proteases	3.84	0.07
Usp38	Cysteine Proteases	3.55	0.00
Acy1	Metalloproteases	3.51	0.27
Sva	Aspartic Proteases	3.49	0.81
Prss28	Serine Proteases	3.49	0.19
Cela3B Ii	Serine Proteases	3.47	0.32
Cpxm1Cpx1	Metalloproteases	3.46	0.00
Ctsf	Cysteine Proteases	3.41	0.74
Mst1	Serine Proteases	3.40	0.19
Aspa	Metalloproteases	3.27	0.03
Spg7	Metalloproteases	3.26	0.30
Usp18	Cysteine Proteases	3.11	0.14
Adam21	Metalloproteases	3.04	0.10
Adam19	Metalloproteases	2.97	0.01
Usp20	Cysteine Proteases	2.88	0.02
Ide	Metalloproteases	2.80	0.01
C2	Serine Proteases	2.79	0.14
Usp27X	Cysteine Proteases	2.74	0.00
Psmd7	Metalloproteases	2.68	0.03
Usp47	Cysteine Proteases	2.63	0.00
Tpp1	Serine Proteases	2.53	0.01
Capn12	Cysteine Proteases	2.52	0.01
Face1	Metalloproteases	2.49	0.06
Nrd1	Metalloproteases	2.48	0.01
Ctsr	Cysteine Proteases	2.47	0.53
Pgpi (Pgpep1)	Cysteine Proteases	2.45	0.32
Casp14	Cysteine Proteases	2.43	0.17
Prss30	Serine Proteases	2.42	0.76
Tmprss8	Serine Proteases	2.42	0.76
Dpep3	Metalloproteases	2.41	0.51
Pcsk6	Serine Proteases	2.38	0.01
Klk11	Serine Proteases	2.37	0.76
Usp7	Cysteine Proteases	2.36	0.00
Rnpep	Metalloproteases	2.35	0.00
Sval2	Aspartic Proteases	2.29	0.29
Adam7	Metalloproteases	2.24	0.08

	Trap1	Serine Proteases	2.16	0.01
	Pga5 (Pepf)	Aspartic Proteases	2.16	0.02
	Ctse	Aspartic Proteases	2.14	0.26
	Trrap	Serine Proteases	2.14	0.00
	Pcsk1	Serine Proteases	2.11	0.50
	Usp11	Cysteine Proteases	2.08	0.04
	Rhbdl3	Serine Proteases	2.04	0.26
	Usp45	Cysteine Proteases	2.03	0.18
	Prpf8	Metalloproteases	2.02	0.01
2 Cell	*Enpep*	Metalloproteases	112.68	0.00
	Sva	Aspartic Proteases	47.66	0.04
	Uchl1	Cysteine Proteases	19.90	0.02
	Lta4H	Metalloproteases	12.21	0.01
	Gfpt1	Cysteine Proteases	11.70	0.01
	Usp-Ps (Dub2)	Cysteine Proteases	11.45	0.00
	Ctsh	Cysteine Proteases	10.81	0.00
	Usp2	Cysteine Proteases	10.03	0.04
	Klk7	Serine Proteases	9.72	0.04
	Ctss	Cysteine Proteases	9.71	0.02
	Usp21	Cysteine Proteases	8.73	0.04
	Lap3	Metalloproteases	7.82	0.01
	Usp12 (Ubh1)	Cysteine Proteases	7.79	0.00
	Senp6	Cysteine Proteases	7.52	0.00
	Prep	Serine Proteases	7.50	0.11
	Dpp4	Serine Proteases	7.22	0.02
	Afg3L1	Metalloproteases	7.21	0.00
	St14	Serine Proteases	7.18	0.01
	Dpp7	Serine Proteases	7.17	0.02
	Usp15	Cysteine Proteases	6.92	0.01
	Uqcrc1	Metalloproteases	6.77	0.01
	Usp16	Cysteine Proteases	6.49	0.01
	Shh	Cysteine Proteases	6.44	0.45
	Htra2	Serine Proteases	6.34	0.00
	Prss8	Serine Proteases	5.74	0.00
	Pepd	Metalloproteases	5.63	0.05
	Tpp1	Serine Proteases	5.63	0.00
	Rhbdd2	Serine Proteases	5.61	0.12
	Hsp841	Serine Proteases	5.59	0.02
	Tmprss2	Serine Proteases	5.47	0.10
	Pmpcb	Metalloproteases	5.46	0.01
	Uqcrc2	Metalloproteases	5.41	0.02
	Usp38	Cysteine Proteases	5.31	0.01
	Cflar	Cysteine Proteases	5.29	0.03
	Capn9	Cysteine Proteases	4.83	0.14
	Brcc3C61A	Metalloproteases	4.83	0.00
	Ide	Metalloproteases	4.71	0.01

Pitrm1	Metalloproteases	4.68	0.01
Cops5	Metalloproteases	4.15	0.00
Casp3	Cysteine Proteases	4.08	0.00
Otub2	Cysteine Proteases	3.96	0.02
Usp33	Cysteine Proteases	3.82	0.01
Osgep	Metalloproteases	3.73	0.00
Spg7	Metalloproteases	3.67	0.27
Tranb1 (Trabid)	Cysteine Proteases	3.65	0.02
Mep1B	Metalloproteases	3.62	0.01
Usp18	Cysteine Proteases	3.60	0.03
Ctsb	Cysteine Proteases	3.52	0.07
Dpp3	Metalloproteases	3.26	0.01
Apeh	Serine Proteases	3.16	0.00
Usp1	Cysteine Proteases	3.14	0.02
Metap1	Metalloproteases	3.07	0.11
Usp9X	Cysteine Proteases	3.05	0.01
Cpxm1Cpx1	Metalloproteases	3.01	0.00
Prss28	Serine Proteases	2.99	0.23
Scaf11 (Casp11)	Cysteine Proteases	2.96	0.02
Prtn3	Serine Proteases	2.92	0.13
Acy1	Metalloproteases	2.90	0.32
Aspa	Metalloproteases	2.83	0.04
Cts6	Cysteine Proteases	2.81	0.77
Psmd14Poh1	Metalloproteases	2.81	0.01
Pcsk6	Serine Proteases	2.78	0.01
Psen2	Aspartic Proteases	2.75	0.04
Spc21	Serine Proteases	2.75	0.01
Prss30	Serine Proteases	2.74	0.71
Tmprss8	Serine Proteases	2.74	0.71
Senp1	Cysteine Proteases	2.55	0.01
Eif3S5Eif3F	Metalloproteases	2.51	0.00
Dnpep	Metalloproteases	2.42	0.00
Adam19	Metalloproteases	2.41	0.01
Hspca	Serine Proteases	2.41	0.00
Usp47	Cysteine Proteases	2.36	0.00
Mmp11	Metalloproteases	2.32	0.49
Casp8	Cysteine Proteases	2.32	0.20
Rnpepl1	Metalloproteases	2.31	0.05
Pcsk1	Serine Proteases	2.30	0.46
Cts3	Cysteine Proteases	2.29	0.43
Adam9	Metalloproteases	2.28	0.00
Usp20	Cysteine Proteases	2.28	0.09
Capn8	Cysteine Proteases	2.23	0.01
CpnCpn1	Metalloproteases	2.23	0.12
Ctsf	Cysteine Proteases	2.21	0.39
Ggh	Cysteine Proteases	2.18	0.10
Mmp23	Metalloproteases	2.15	0.45

	Prpf8	Metalloproteases	2.14	0.01
	Anpep	Metalloproteases	2.13	0.82
	Trap1	Serine Proteases	2.13	0.02
	Ctsq	Cysteine Proteases	2.03	0.87
	Folh1	Metalloproteases	2.02	0.61
	Clpp	Serine Proteases	2.00	0.04
8 cell	*Htra1*	Serine Proteases	73.41	0.03
	Enpep	Metalloproteases	29.96	0.00
	Prss8	Serine Proteases	13.37	0.00
	Tpp1	Serine Proteases	12.76	0.00
	CpnCpn1	Metalloproteases	11.33	0.02
	Cts6	Cysteine Proteases	10.02	0.14
	Gfpt1	Cysteine Proteases	7.91	0.06
	Klk7	Serine Proteases	7.52	0.05
	Ctsz	Cysteine Proteases	7.38	0.05
	Apeh	Serine Proteases	6.71	0.00
	Capn9	Cysteine Proteases	6.63	0.09
	Tmprss2	Serine Proteases	5.47	0.11
	Lta4H	Metalloproteases	5.44	0.01
	Ctsh	Cysteine Proteases	5.44	0.05
	Spg7	Metalloproteases	4.45	0.23
	Psmb8	Threonine Proteases	4.41	0.79
	Usp33	Cysteine Proteases	4.37	0.13
	Lap3	Metalloproteases	4.32	0.01
	Ctsb	Cysteine Proteases	3.88	0.07
	Pitrm1	Metalloproteases	3.80	0.01
	St14	Serine Proteases	3.79	0.02
	Abhd5	Serine Proteases	3.46	0.02
	Prep	Serine Proteases	3.45	0.17
	Usp16	Cysteine Proteases	3.25	0.00
	Usp1	Cysteine Proteases	3.23	0.00
	Ggh	Cysteine Proteases	3.07	0.02
	Adam19	Metalloproteases	3.00	0.02
	Usp10	Cysteine Proteases	2.92	0.03
	Parl	Serine Proteases	2.90	0.08
	Usp12 (Ubh1)	Cysteine Proteases	2.87	0.10
	Tmprss5	Serine Proteases	2.85	0.32
	Bace2	Aspartic Proteases	2.76	0.47
	Ctsk	Cysteine Proteases	2.64	0.24
	Ide	Metalloproteases	2.58	0.01
	Htra2	Serine Proteases	2.58	0.01
	Usp38	Cysteine Proteases	2.55	0.06
	Ctsc	Cysteine Proteases	2.53	0.01
	Usp20	Cysteine Proteases	2.52	0.07
	Pcsk6	Serine Proteases	2.48	0.01
	Pepd	Metalloproteases	2.46	0.12

	Cpxm1Cpx1	Metalloproteases	2.40	0.02
	Ctsl	Cysteine Proteases	2.40	0.00
	Psh1 (Sppl3)	Aspartic Proteases	2.39	0.13
	Ctsg	Serine Proteases	2.39	0.64
	Sva	Aspartic Proteases	2.35	0.28
	Rnpepl1	Metalloproteases	2.33	0.17
	Afg3L2	Metalloproteases	2.33	0.01
	Acy3	Metalloproteases	2.31	0.03
	Casp3	Cysteine Proteases	2.31	0.02
	Xpnpep1	Metalloproteases	2.29	0.00
	Uqcrc1	Metalloproteases	2.27	0.03
	Pcsk4	Serine Proteases	2.27	0.38
	NpeppsPsa	Metalloproteases	2.23	0.14
	Afg3L1	Metalloproteases	2.21	0.00
	Mmp12	Metalloproteases	2.20	0.65
	Ctss	Cysteine Proteases	2.18	0.94
	Proc	Serine Proteases	2.15	0.20
	Procl	Serine Proteases	2.15	0.20
	Usp18	Cysteine Proteases	2.12	0.66
	Psmb10	Threonine Proteases	2.10	0.17
	Ppat	Cysteine Proteases	2.09	0.00
	Dpp3	Metalloproteases	2.09	0.01
	Dnpep	Metalloproteases	2.05	0.00
	Usp14	Cysteine Proteases	2.04	0.00
	Pga5 (Pepf)	Aspartic Proteases	2.03	0.15

Appendix 4: Total number of embryos used for ICC

	Mouse	**Human**
ENTK	8	21
AMBP	8	24
PRSS8	9	19
TMPRSS2	9	11
Total	34	75

Appendix 5: Patient characteristics (Figures 4.2.5.1, 4.2.5.2, 4.2.5.3, 4.2.5.6)

(median [range])	RIF **n=14**	RM **n=14**
Age (years):	30 [25-37]	33 [29-37]
Body Mass Index (BMI):	23 [18-30]	23.5 [18-29]
uNK Density (%):	2.17%	3.35%

Appendix 6: Patient characteristics (Figures 4.2.5.4, 4.2.5.5, 4.2.5.6)

(median [range])	RIF **n=15**	RM **n=15**
Age (years):	31 [24-38]	33 [25-38]
Body Mass Index (BMI):	22.5 [16-35]	22.5 [19-32]
uNK Density (%):	4.37%	2.76%

Appendix 7: Western blots (Figures 4.2.5.4 and 4.2.5.6)

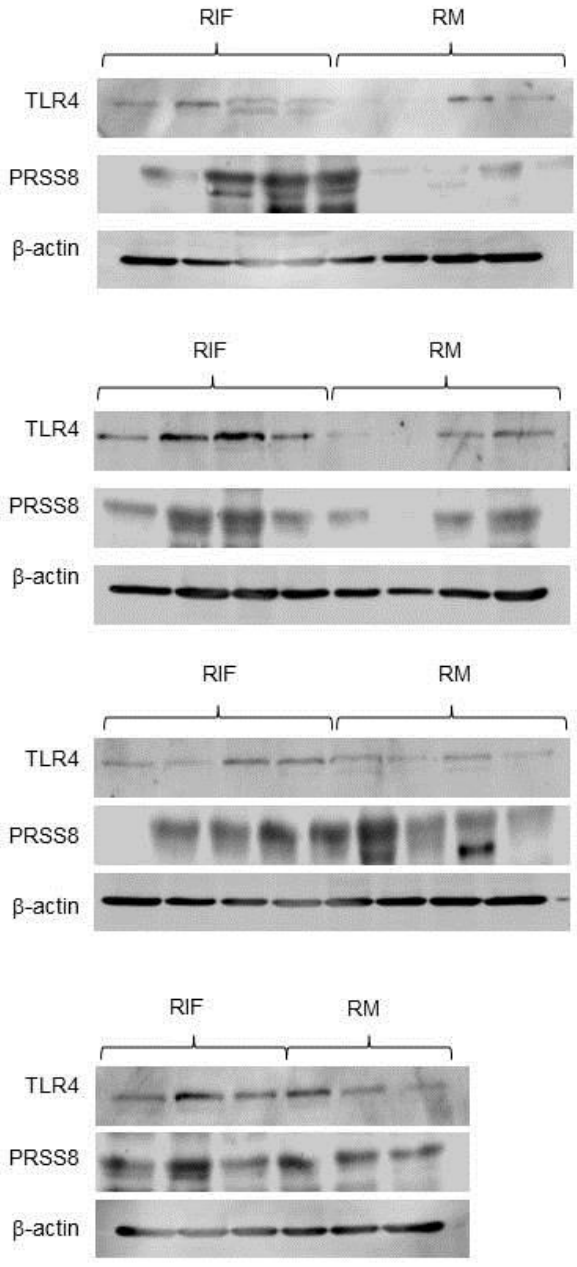

Appendix 8: Western blots (Figure 4.2.2.3)

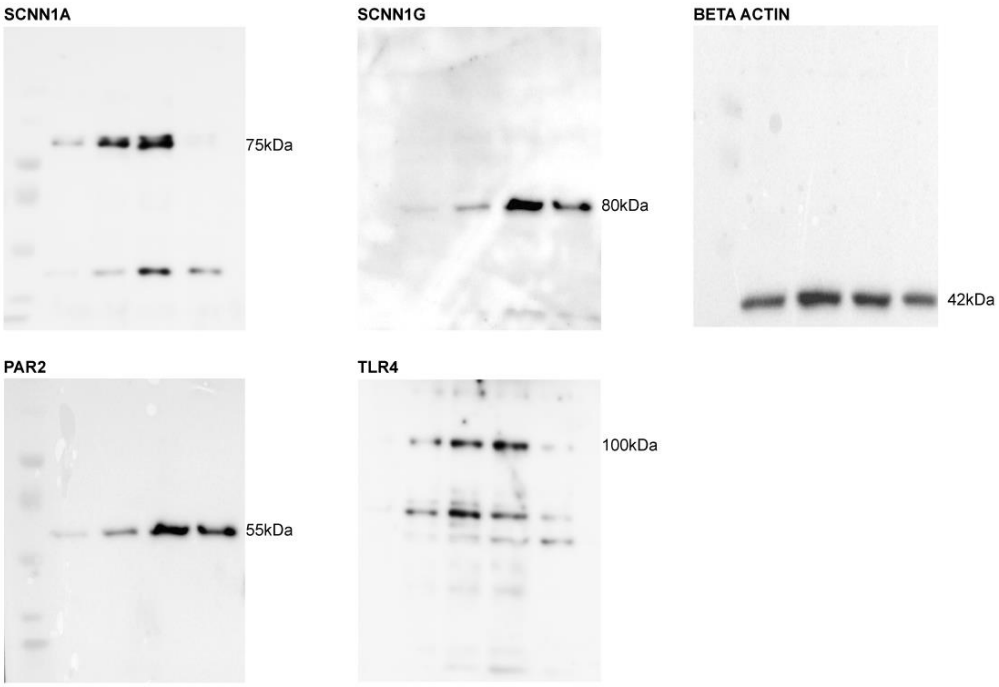

Protein extracted from decidualizing HESCs.
Bands from left to right; day 0, day 2, day 4, day 8 of treatment.

Appendix 9: Western blots (Figure 4.2.3.1a)

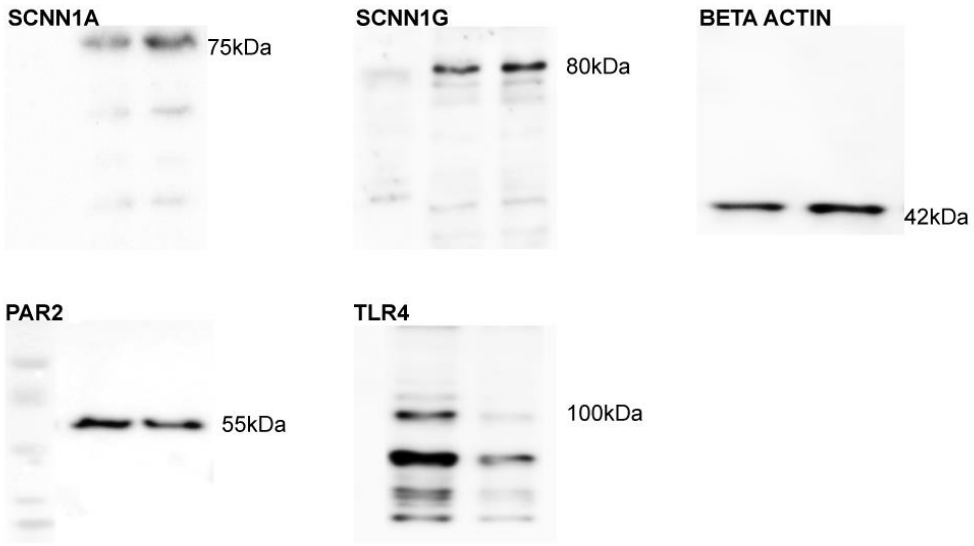

Protein extracted from day 4 DESCs treated with UCM (left band) or ECM (right band).

References

Achache, H. and Revel, A. (2006) 'Endometrial receptivity markers, the journey to successful embryo implantation', *Human reproduction update,* 12(6), pp. 731-746.

Aplin, J., Hey, N. and Li, T. (1996) 'MUC1 as a cell surface and secretory component of endometrial epithelium: reduced levels in recurrent miscarriage', *American Journal of Reproductive Immunology,* 35(3), pp. 261-266.

Aplin, J. D. (1997) 'Adhesion molecules in implantation', *Reviews of Reproduction,* 2(2), pp. 84-93.

Arici, A., Engin, O., Attar, E. and Olive, D. L. (1995) 'Modulation of leukemia inhibitory factor gene expression and protein biosynthesis in human endometrium', *The Journal of Clinical Endocrinology & Metabolism,* 80(6), pp. 1908-1915.

Baird, D. D., Weinberg, C. R., McConnaughey, D. R. and Wilcox, A. J. (2003) 'Rescue of the corpus luteum in human pregnancy', *Biology of reproduction,* 68(2), pp. 448-456.

Baranao, R., Piazza, A., Rumi, L. and Fried, E. (1997) 'Determination of IL-1 and IL-6 Levels in Human Embryo Culture-Conditioned Media', *American journal of reproductive immunology,* 37(2), pp. 191-194.

Beaujean, N., Taylor, J., Gardner, J., Wilmut, I., Meehan, R. and Young, L. (2004) 'Effect of limited DNA methylation reprogramming in the normal sheep embryo on somatic cell nuclear transfer', *Biology of reproduction,* 71(1), pp. 185-193.

Bell, C. E., Calder, M. D. and Watson, A. J. (2008) 'Genomic RNA profiling and the programme controlling preimplantation mammalian development', *Molecular human reproduction,* 14(12), pp. 691-701.

Benn, P. (1998) 'Trisomy 16 and trisomy 16 mosaicism: a review', *American journal of medical genetics,* 79(2), pp. 121-133.

Bentin-Ley, U. (2000) 'Relevance of endometrial pinopodes for human blastocyst implantation', *Human reproduction (Oxford, England),* 15, pp. 67.

Bettio, D., Venci, A. and Setti, P. L. (2008) 'Chromosomal abnormalities in miscarriages after different assisted reproduction procedures', *Placenta,* 29, pp. 126-128.

Bhatt, H., Brunet, L. J. and Stewart, C. L. (1991) 'Uterine expression of leukemia inhibitory factor coincides with the onset of blastocyst implantation', *Proceedings of the National Academy of Sciences,* 88(24), pp. 11408-11412.

Bird, G. S., DeHaven, W. I., Smyth, J. T. and Putney, J. W. (2008) 'Methods for studying store-operated calcium entry', *Methods,* 46(3), pp. 204-212.

Blaszkowska, J. (2005) 'Effect of Ascaris trypsin inhibitor on fetal development of mice', *Wiadomości Parazytologiczne,* 51(2).

Boomsma, C., Kavelaars, A., Eijkemans, M., Lentjes, E., Fauser, B., Heijnen, C. and

Macklon, N. (2009) 'Endometrial secretion analysis identifies a cytokine profile predictive of pregnancy in IVF', *Human Reproduction,* 24(6), pp. 1427-1435.

Bowman, P. and McLaren, A. (1970) 'The reaction of the mouse blastocyst and its zona pellucida to enzymes in vitro', *Journal of Embryology and Experimental Morphology,* 24(2), pp. 331-334.

Braude, P., Bolton, V. and Moore, S. (1988) 'Human gene expression first occurs between the four-and eight-cell stages of preimplantation development', *Nature,* 332(6163), pp. 459-461.

Braude, P., Pelham, H., Flach, G. and Lobatto, R. (1979) 'Post-transcriptional control in the early mouse embryo'.

Brosens, J. J., Parker, M. G., McIndoe, A., Pijnenborg, R. and Brosens, I. A. (2009) 'A role for menstruation in preconditioning the uterus for successful pregnancy', *American journal of obstetrics and gynecology,* 200(6), pp. 615. e1-615. e6.

Brosens, J. J., Pijnenborg, R. and Brosens, I. A. (2002) 'The myometrial junctional zone spiral arteries in normal and abnormal pregnancies: a review of the literature', *American journal of obstetrics and gynecology,* 187(5), pp. 1416-1423.

Brosens, J. J., Salker, M. S., Teklenburg, G., Nautiyal, J., Salter, S., Lucas, E. S., Steel, J. H., Christian, M., Chan, Y.-W. and Boomsma, C. M. (2014) 'Uterine selection of human embryos at implantation', *Scientific reports,* 4.

Brubaker, S. W., Bonham, K. S., Zanoni, I. and Kagan, J. C. (2015) 'Innate immune pattern recognition: a cell biological perspective', *Annual review of immunology,* 33, pp. 257-290.

Bruns, J. B., Carattino, M. D., Sheng, S., Maarouf, A. B., Weisz, O. A., Pilewski, J. M., Hughey, R. P. and Kleyman, T. R. (2007) 'Epithelial Na+ channels are fully activated by furin-and prostasin-dependent release of an inhibitory peptide from the γ-subunit', *Journal of Biological Chemistry,* 282(9), pp. 6153-6160.

Burton, G. J., Jauniaux, E. and Watson, A. L. (1999) 'Maternal arterial connections to the placental intervillous space during the first trimester of human pregnancy: the Boyd collection revisited', *American journal of obstetrics and gynecology,* 181(3), pp. 718-724.

Burton, G. J., Watson, A. L., Hempstock, J., Skepper, J. N. and Jauniaux, E. (2002) 'Uterine glands provide histiotrophic nutrition for the human fetus during the first trimester of pregnancy', *The Journal of Clinical Endocrinology & Metabolism,* 87(6), pp. 2954-2959.

Caldwell, R. A., Boucher, R. C. and Stutts, M. J. (2004) 'Serine protease activation of near-silent epithelial Na+ channels', *American Journal of Physiology-Cell Physiology,* 286(1), pp. C190-C194.

Cha, J., Sun, X. and Dey, S. K. (2012) 'Mechanisms of implantation: strategies for successful pregnancy', *Nature medicine,* 18(12), pp. 1754-1767.

Chan, R. W., Schwab, K. E. and Gargett, C. E. (2004) 'Clonogenicity of human endometrial epithelial and stromal cells', *Biology of reproduction,* 70(6), pp. 1738-1750.

Chard, T. (1991) 'Frequency of implantation and early pregnancy loss in natural cycles', *Baillieres Clin Obstet Gynaecol,* 5(1), pp. 179-89.

Charnock-Jones, D., Sharkey, A., Fenwick, P. and Smith, S. (1994) 'Leukaemia inhibitory factor mRNA concentration peaks in human endometrium at the time of implantation and the blastocyst contains mRNA for the receptor at this time', *Journal of Reproduction and Fertility,* 101(2), pp. 421-426.

Chen, G., Bradford, W. D., Seidel, C. W. and Li, R. (2012) 'Hsp90 stress potentiates rapid cellular adaptation through induction of aneuploidy', *Nature,* 482(7384), pp. 246-250.

Chraïbi, A., Vallet, V., Firsov, D., Hess, S. K. and Horisberger, J.-D. (1998) 'Protease modulation of the activity of the epithelial sodium channel expressed in Xenopus oocytes', *The Journal of general physiology,* 111(1), pp. 127-138.

Christian, M., Mak, I., White, J. O. and Brosens, J. J. (2002) 'Mechanisms of decidualization', *Reproductive BioMedicine Online,* 4, pp. 24-30.

Clarke, G. N. (2006) 'ART and history, 1678–1978', *Human Reproduction,* 21(7), pp. 1645-1650.

Corcoran, D., Fair, T., Park, S., Rizos, D., Patel, O., Smith, G., Coussens, P., Ireland, J., Boland, M. and Evans, A. (2006) 'Suppressed expression of genes involved in transcription and translation in in vitro compared with in vivo cultured bovine embryos', *Reproduction,* 131(4), pp. 651-660.

Cork, B., Tuckerman, E., Warren, M., Li, T. and Laird, S. 'Expression of LIF and IL-6 in endometrial epithelial cells of normal fertile women and women who suffer unexplained recurrent miscarriage'. *Human Reproduction*: OXFORD UNIV PRESS GREAT CLARENDON ST, OXFORD OX2 6DP, ENGLAND, 228-228.

COWELL, T. P. (1969) 'Implantation and development of mouse eggs transferred to the uteri of non-progestational mice', *Journal of reproduction and fertility,* 19(2), pp. 239-245.

Crosby, I., Gandolfi, F. and Moor, R. (1988) 'Control of protein synthesis during early cleavage of sheep embryos', *Journal of reproduction and fertility,* 82(2), pp. 769-775.

De Neubourg, D., Gerris, J., Mangelschots, K., Van Royen, E., Vercruyssen, M. and Elseviers, M. (2004) 'Single top quality embryo transfer as a model for prediction of early pregnancy outcome', *Human Reproduction,* 19(6), pp. 1476-1479.

Demichelis, F., Fall, K., Perner, S., Andrén, O., Schmidt, F., Setlur, S., Hoshida, Y., Mosquera, J., Pawitan, Y. and Lee, C. (2007) 'TMPRSS2: ERG gene fusion associated with lethal prostate cancer in a watchful waiting cohort', *Oncogene,*

26(31), pp. 4596-4599.

Dobson, A. T., Raja, R., Abeyta, M. J., Taylor, T., Shen, S., Haqq, C. and Pera, R. A. R. (2004) 'The unique transcriptome through day 3 of human preimplantation development', *Human Molecular Genetics,* 13(14), pp. 1461-1470.

Dominguez, F., Yanez-Mo, M., Sanchez-Madrid, F. and Simon, C. (2005) 'Embryonic implantation and leukocyte transendothelial migration: different processes with similar players?', *The FASEB journal,* 19(9), pp. 1056-1060.

Donaldson, S. H., Hirsh, A., Li, D. C., Holloway, G., Chao, J., Boucher, R. C. and Gabriel, S. E. (2002) 'Regulation of the epithelial sodium channel by serine proteases in human airways', *Journal of Biological Chemistry,* 277(10), pp. 8338-8345.

Dunglison, G., Barlow, D. and Sargent, I. (1996) 'Leukaemia inhibitory factor significantly enhances the blastocyst formation rates of human embryos cultured in serum-free medium', *Human Reproduction,* 11(1), pp. 191-196.

Déry, O., Corvera, C. U., Steinhoff, M. and Bunnett, N. W. (1998) 'Proteinase-activated receptors: novel mechanisms of signaling by serine proteases', *American Journal of Physiology-Cell Physiology,* 274(6), pp. C1429-C1452.

Edgar, R., Domrachev, M. and Lash, A. E. (2002) 'Gene Expression Omnibus: NCBI gene expression and hybridization array data repository', *Nucleic acids research,* 30(1), pp. 207-210.

Edwards, R., Steptoe, P. and Purdy, J. (1970) 'Fertilization and cleavage in vitro of preovulator human oocytes', *Nature,* 227(5265), pp. 1307-1309.

Edwards, R., Steptoe, P. and Purdy, J. (1980) 'ESTABLISHING FULL-TERM HUMAN PREGNANCIES USING CLEAVING EMBRYOS GROWN IN VITRO*', *BJOG: An International Journal of Obstetrics & Gynaecology,* 87(9), pp. 737-756.

Edwards, R. G., Bavister, B. D. and Steptoe, P. C. (1969) 'Early stages of fertilization in vitro of human oocytes matured in vitro', *Nature,* 221, pp. 632-35.

Emera, D., Romero, R. and Wagner, G. (2012) 'The evolution of menstruation: A new model for genetic assimilation', *Bioessays,* 34(1), pp. 26-35.

Evsikov, S. and Verlinsky, Y. (1998) 'Mosaicism in the inner cell mass of human blastocysts', *Human Reproduction,* 13(11), pp. 3151-3155.

Ferretti, C., Bruni, L., Dangles-Marie, V., Pecking, A. and Bellet, D. (2007) 'Molecular circuits shared by placental and cancer cells, and their implications in the proliferative, invasive and migratory capacities of trophoblasts', *Human reproduction update,* 13(2), pp. 121-141.

Finn, C. (1966) 'Endocrine control of endometrial sensitivity during the induction of the decidual cell reaction in the mouse', *Journal of Endocrinology,* 36(3), pp. 239-248.

Flach, G., Johnson, M., Braude, P., Taylor, R. and Bolton, V. (1982) 'The transition from

maternal to embryonic control in the 2-cell mouse embryo', *The EMBO journal,* 1(6), pp. 681.

Foote, R. H. and Carney, E. W. (1988) 'Factors limiting reproductive efficiency in selected laboratory animals', *Ann N Y Acad Sci,* 541, pp. 683-96.

Fragouli, E., Alfarawati, S., Daphnis, D. D., Goodall, N.-n., Mania, A., Griffiths, T., Gordon, A. and Wells, D. (2011) 'Cytogenetic analysis of human blastocysts with the use of FISH, CGH and aCGH: scientific data and technical evaluation', *Human Reproduction,* 26(2), pp. 480-490.

Fragouli, E., Alfarawati, S., Spath, K., Jaroudi, S., Sarasa, J., Enciso, M. and Wells, D. (2013) 'The origin and impact of embryonic aneuploidy', *Human genetics,* 132(9), pp. 1001-1013.

Frank (1994) 'Prostaglandin E2 enhances human endometrial stromal cell differentiation', *Endocrinology,* 134(1), pp. 258-263.

Fronius, M. and Clauss, W. G. (2008) 'Mechano-sensitivity of ENaC: may the (shear) force be with you', *Pflügers Archiv-European Journal of Physiology,* 455(5), pp. 775-785.

Fulka, H., Mrazek, M., Tepla, O. and Fulka, J. (2004) 'DNA methylation pattern in human zygotes and developing embryos', *Reproduction,* 128(6), pp. 703-708.

Gardner, D. K., Lane, M., Stevens, J., Schlenker, T. and Schoolcraft, W. B. (2000) 'Blastocyst score affects implantation and pregnancy outcome: towards a single blastocyst transfer', *Fertility and sterility,* 73(6), pp. 1155-1158.

Gargett, C. E. and Masuda, H. (2010) 'Adult stem cells in the endometrium', *Molecular human reproduction,* 16(11), pp. 818-834.

Gargett, C. E., Schwab, K. E. and Deane, J. A. (2015) 'Endometrial stem/progenitor cells: the first 10 years', *Human reproduction update*, pp. dmv051.

Garty, H. and Palmer, L. G. (1997) 'Epithelial sodium channels: function, structure, and regulation', *Physiological reviews,* 77(2), pp. 359-396.

Gee, K. R., Brown, K., Chen, W. U., Bishop-Stewart, J., Gray, D. and Johnson, I. (2000) 'Chemical and physiological characterization of fluo-4 Ca 2+-indicator dyes', *Cell calcium,* 27(2), pp. 97-106.

Gellersen, B., Brosens, I. A. and Brosens, J. J. (2007) 'Decidualization of the human endometrium: mechanisms, functions, and clinical perspectives', *Seminars In Reproductive Medicine,* 25(6), pp. 445-453.

Gellersen, B. and Brosens, J. (2003) 'Cyclic AMP and progesterone receptor cross-talk in human endometrium: a decidualizing affair', *Journal of Endocrinology,* 178(3), pp. 357-372.

Gellersen, B. and Brosens, J. J. (2014) 'Cyclic decidualization of the human endometrium in reproductive health and failure', *Endocrine reviews,* 35(6), pp. 851-905.

Genbacev, O. D., Prakobphol, A., Foulk, R. A., Krtolica, A. R., Ilic, D., Singer, M. S., Yang, Z.-Q., Kiessling, L. L., Rosen, S. D. and Fisher, S. J. (2003) 'Trophoblast L-selectin-mediated adhesion at the maternal-fetal interface', *Science Signaling,* 299(5605), pp. 405.

Gleicher, N., Kushnir, V. A. and Barad, D. H. (2014) 'Preimplantation genetic screening (PGS) still in search of a clinical application: a systematic review', *Reprod Biol Endocrinol,* 12(1), pp. 22.

Gray, C. A., Bartol, F. F., Tarleton, B. J., Wiley, A. A., Johnson, G. A., Bazer, F. W. and Spencer, T. E. (2001) 'Developmental biology of uterine glands', *Biology of reproduction,* 65(5), pp. 1311-1323.

Greco, E., Minasi, M. G. and Fiorentino, F. (2015) 'Healthy Babies after Intrauterine Transfer of Mosaic Aneuploid Blastocysts', *New England Journal of Medicine,* 373(21), pp. 2089-2090.

Grewal, S., Carver, J. G., Ridley, A. J. and Mardon, H. J. (2008) 'Implantation of the human embryo requires Rac1-dependent endometrial stromal cell migration', *Proceedings of the National Academy of Sciences,* 105(42), pp. 16189-16194.

Groothuis, P. G., Dassen, H. H. N. M., Romano, A. and Punyadeera, C. (2007) 'Estrogen and the endometrium: lessons learned from gene expression profiling in rodents and human', *Human Reproduction Update,* 13(4), pp. 405-417.

Gutiérrez-Mateo, C., Colls, P., Sánchez-García, J., Escudero, T., Prates, R., Ketterson, K., Wells, D. and Munné, S. (2011) 'Validation of microarray comparative genomic hybridization for comprehensive chromosome analysis of embryos', *Fertility and sterility,* 95(3), pp. 953-958.

Hanna, J., Goldman-Wohl, D., Hamani, Y., Avraham, I., Greenfield, C., Natanson-Yaron, S., Prus, D., Cohen-Daniel, L., Arnon, T. I. and Manaster, I. (2006) 'Decidual NK cells regulate key developmental processes at the human fetal-maternal interface', *Nature medicine,* 12(9), pp. 1065-1074.

Hassold, T. and Hunt, P. (2001) 'To err (meiotically) is human: the genesis of human aneuploidy', *Nature Reviews Genetics,* 2(4), pp. 280-291.

Henriet, P., Chevronnay, H. P. G. and Marbaix, E. (2012) 'The endocrine and paracrine control of menstruation', *Molecular and cellular endocrinology,* 358(2), pp. 197-207.

Hertig, A. T., Rock, J. and Adams, E. C. (1956) 'A description of 34 human ova within the first 17 days of development', *American Journal of Anatomy,* 98(3), pp. 435-493.

Hertig, A. T., Rock, J., Adams, E. C. and Mulligan, W. J. (1954) 'ON THE PREIMPLANTATION STAGES OF THE HUMAN OVUM-A DESCRIPTION OF 4 NORMAL AND 4 ABNORMAL SPECIMENS RANGING FROM THE 2ND TO THE 5TH DAY OF DEVELOPMENT', *Contributions to Embryology,* 35(240), pp.

201-&.

Hirata, T., Osuga, Y., Hamasaki, K., Hirota, Y., Nose, E., Morimoto, C., Harada, M., Takemura, Y., Koga, K. and Yoshino, O. (2007) 'Expression of toll-like receptors 2, 3, 4, and 9 genes in the human endometrium during the menstrual cycle', *Journal of reproductive immunology,* 74(1), pp. 53-60.

Hirata, T., Osuga, Y., Hirota, Y., Koga, K., Yoshino, O., Harada, M., Morimoto, C., Yano, T., Nishii, O. and Tsutsumi, O. (2005) 'Evidence for the presence of toll-like receptor 4 system in the human endometrium', *The Journal of Clinical Endocrinology & Metabolism,* 90(1), pp. 548-556.

Hirota, Y., Osuga, Y., Hirata, T., Koga, K., Yoshino, O., Harada, M., Morimoto, C., Nose, E., Yano, T. and Tsutsumi, O. (2005) 'Evidence for the presence of protease-activated receptor 2 and its possible implication in remodeling of human endometrium', *The Journal of Clinical Endocrinology & Metabolism,* 90(3), pp. 1662-1669.

Holm, P., Booth, P. and Callesen, H. (2002) 'Kinetics of early in vitro development of bovine in vivo-and in vitro-derived zygotes produced and/or cultured in chemically defined or serum-containing media', *Reproduction,* 123(4), pp. 553-565.

Holmes, P. and Gordashko, B. (1980) 'Evidence of prostaglandin involvement in blastocyst implantation', *Journal of embryology and experimental morphology,* 55(1), pp. 109-122.

Holmes, P., Sjögren, A. and Hamberger, L. (1990) 'Prostaglandin-E2 released by pre-implantation human conceptuses', *Journal of reproductive immunology,* 17(1), pp. 79-86.

Huang, J.-C., Wun, W.-S. A., Goldsby, J. S., Matijevic-Aleksic, N. and Wu, K. K. (2004) 'Cyclooxygenase-2-derived endogenous prostacyclin enhances mouse embryo hatching', *Human Reproduction,* 19(12), pp. 2900-2906.

Hummler, E., Dousse, A., Rieder, A., Stehle, J.-C., Rubera, I., Osterheld, M.-C., Beermann, F., Frateschi, S. and Charles, R.-P. (2013) 'The channel-activating protease CAP1/Prss8 is required for placental labyrinth maturation', *PloS one,* 8(2).

Hustin, J. and Schaaps, J.-P. (1987) 'Echocardiograhic and anatomic studies of the maternotrophoblastic border during the first trimester of pregnancy', *American journal of obstetrics and gynecology,* 157(1), pp. 162-168.

Ichikawa, S., Shibata, T., Takehara, Y., Tamada, H., Oda, K. and Murao, S. (1985) 'Effects of proteinase inhibitors on preimplantation embryos in the rat', *Journal of reproduction and fertility,* 73(2), pp. 385-390.

Ir, S. T. A., Toskess, P. P., Liddle, R. and McGrath, K. (1996) 'Hereditary pancreatitis is caused by a mutation in the cationic trypsinogen gene', *Nature genetics,* 14.

Itoh, H., Tomita, M., Kobayashi, T., Uchino, H., Maruyama, H. and Nawa, Y. (1996) 'Expression of inter-α-trypsin inhibitor light chain (bikunin) in human pancreas', *Journal of biochemistry,* 120(2), pp. 271-275.

Jack, X. Y., Chao, L. and Chao, J. (1995) 'Molecular cloning, tissue-specific expression, and cellular localization of human prostasin mRNA', *Journal of Biological Chemistry,* 270(22), pp. 13483-13489.

Jaffe, R., Jauniaux, E. and Hustin, J. (1997) 'Maternal circulation in the first-trimester human placenta—myth or reality?', *American journal of obstetrics and gynecology,* 176(3), pp. 695-705.

Jauniaux, E., Farquharson, R. G., Christiansen, O. B. and Exalto, N. (2006) 'Evidence-based guidelines for the investigation and medical treatment of recurrent miscarriage', *Human reproduction,* 21(9), pp. 2216-2222.

Jauniaux, E., Watson, A. L., Hempstock, J., Bao, Y.-P., Skepper, J. N. and Burton, G. J. (2000) 'Onset of maternal arterial blood flow and placental oxidative stress: a possible factor in human early pregnancy failure', *The American journal of pathology,* 157(6), pp. 2111-2122.

Jauniaux, E., Zaidi, J., Jurkovic, D., Campbell, S. and Hustin, J. (1994) 'Pregnancy: Comparison of colour Doppler features and pathological findings in complicated early pregnancy', *Human reproduction,* 9(12), pp. 2432-2437.

Jiang, Y.-h., Shi, Y., He, Y.-p., Du, J., Li, R.-s., Shi, H.-j., Sun, Z.-g. and Wang, J. (2011) 'Serine protease inhibitor 4-(2-aminoethyl) benzenesulfonyl fluoride hydrochloride (AEBSF) inhibits the rat embryo implantation in vivo and interferes with cell adhesion in vitro', *Contraception,* 84(6), pp. 642-648.

Jones, H. W. (2003) 'IVF: past and future', *Reproductive biomedicine online,* 6(3), pp. 375-381.

Jurisicova, A., Antenos, M., Kapasi, K., Meriano, J. and Casper, R. F. (1999) 'Variability in the expression of trophectodermal markers β-human chorionic gonadotrophin, human leukocyte antigen-G and pregnancy specific β-1 glycoprotein by the human blastocyst', *Human Reproduction,* 14(7), pp. 1852-1858.

Kane, M. (1986) 'A survey of the effects of proteases and glycosidases on culture of rabbit morulae to blastocysts', *Journal of reproduction and fertility,* 78(1), pp. 225-230.

Kauma, S. W. and Matt, D. W. (1995) 'Coculture cells that express leukemia inhibitory factor (LIF) enhance mouse blastocyst developmentin vitro', *Journal of assisted reproduction and genetics,* 12(2), pp. 153-156.

Kellenberger, S. and Schild, L. (2002) 'Epithelial sodium channel/degenerin family of ion channels: a variety of functions for a shared structure', *Physiological reviews,* 82(3), pp. 735-767.

Kim, T. S., Heinlein, C., Hackman, R. C. and Nelson, P. S. (2006) 'Phenotypic analysis

of mice lacking the Tmprss2-encoded protease', *Molecular and cellular biology,* 26(3), pp. 965-975.

Klentzeris, L., Bulmer, J., Trejdosiewicz, L., Morrison, L. and Cooke, I. (1993) 'Infertility: Beta-1 integrin cell adhesion molecules in the endometrium of fertile and infertile women', *Human Reproduction,* 8(8), pp. 1223-1230.

Kleyman, T. R., Carattino, M. D. and Hughey, R. P. (2009) 'ENaC at the cutting edge: regulation of epithelial sodium channels by proteases', *Journal of Biological Chemistry,* 284(31), pp. 20447-20451.

Knijn, H. M., Wrenzycki, C., Hendriksen, P. J., Vos, P. L., Zeinstra, E. C., van der Weijden, G. C., Niemann, H. and Dieleman, S. J. (2006) 'In vitro and in vivo culture effects on mRNA expression of genes involved in metabolism and apoptosis in bovine embryos', *Reproduction, Fertility and Development,* 17(8), pp. 775-784.

Knobil, E. (2013) 'The neuroendocrine control of the menstrual cycle', *Recent progress in hormone research,* 36, pp. 53-88.

Kojima, K., Kanzaki, H., Iwai, M., Hatayama, H., Fujimoto, M., Inoue, T., Horie, K., Nakayama, H., Fujita, J. and Mori, T. (1994) 'Expression of leukemia inhibitory factor in human endometrium and placenta', *Biology of Reproduction,* 50(4), pp. 882-887.

Komatsu, H., Shimose, A., Shimizu, T., Mukai, Y., Kobayashi, J., Ohama, T. and Sato, K. (2012) 'Trypsin inhibits lipopolysaccharide signaling in macrophages via toll-like receptor 4 accessory molecules', *Life sciences,* 91(3), pp. 143-150.

Koot, Y., Boomsma, C., Eijkemans, M., Lentjes, E. and Macklon, N. 'Is pre-clinical pregnancy loss a ëcauseí of unexplained infertility?'. *HUMAN REPRODUCTION*: OXFORD UNIV PRESS GREAT CLARENDON ST, OXFORD OX2 6DP, ENGLAND, I29-I30.

Koot, Y. E., van Hooff, S. R., Boomsma, C. M., van Leenen, D., Koerkamp, M. J. G., Goddijn, M., Eijkemans, M. J., Fauser, B. C., Holstege, F. C. and Macklon, N. S. (2016) 'An endometrial gene expression signature accurately predicts recurrent implantation failure after IVF', *Scientific Reports,* 6, pp. 19411.

Koot, Y. E. M., Teklenburg, G., Salker, M. S., Brosens, J. J. and Macklon, N. S. (2012) 'Molecular aspects of implantation failure', *Biochimica et biophysica acta,* 1822(12).

Kubo, H., Spindle, A. and Pedersen, R. A. (1981) 'Inhibition of mouse blastocyst attachment and outgrowth by protease inhibitors', *Journal of Experimental Zoology,* 216(3), pp. 445-451.

Kunitz, M. (1939) 'Formation of trypsin from crystalline trypsinogen by means of enterokinase', *The Journal of general physiology,* 22(4), pp. 429-446.

Kuokkanen, S., Chen, B., Ojalvo, L., Benard, L., Santoro, N. and Pollard, J. W. (2010)

'Genomic profiling of microRNAs and messenger RNAs reveals hormonal regulation in microRNA expression in human endometrium', *Biology of reproduction,* 82(4), pp. 791-801.

Laird, S., Tuckerman, E., Cork, B., Linjawi, S., Blakemore, A. and Li, T. (2003) 'A review of immune cells and molecules in women with recurrent miscarriage', *Human reproduction update,* 9(2), pp. 163-174.

Laird, S., Tuckerman, E., Dalton, C., Dunphy, B., Li, T. and Zhang, X. (1997) 'The production of leukaemia inhibitory factor by human endometrium: presence in uterine flushings and production by cells in culture', *Human Reproduction,* 12(3), pp. 569-574.

Laird, S., Tuckerman, E., Li, T. and Bolton, A. (1994) 'Implantation: Stimulation of human endometrial epithelial cell interleukin 6 production by interleukin 1 and placental protein 14', *Human Reproduction,* 9(7), pp. 1339-1343.

Lalitkumar, S., Boggavarapu, N. R., Menezes, J., Dimitriadis, E., Zhang, J.-G., Nicola, N. A., Gemzell-Danielsson, K. and Lalitkumar, L. P. (2013) 'Polyethylene glycated leukemia inhibitory factor antagonist inhibits human blastocyst implantation and triggers apoptosis by down-regulating embryonic AKT', *Fertility and sterility,* 100(4), pp. 1160-1169. e2.

Leitao, B., Jones, M. C., Fusi, L., Higham, J., Lee, Y., Takano, M., Goto, T., Christian, M., Lam, E. W.-F. and Brosens, J. J. (2010) 'Silencing of the JNK pathway maintains progesterone receptor activity in decidualizing human endometrial stromal cells exposed to oxidative stress signals', *The FASEB Journal,* 24(5), pp. 1541-1551.

Lejeune, B., Lecocq, R., Lamy, F. and Leroy, F. (1982) 'Changes in the pattern of endometrial protein synthesis during decidualization in the rat', *Journal of reproduction and fertility,* 66(2), pp. 519-523.

Lejeune, B., Van Hoeck, J. and Leroy, F. (1981) 'Transmitter role of the luminal uterine epithelium in the induction of decidualization in rats', *Journal of reproduction and fertility,* 61(1), pp. 235-240.

Lessey, B., Castelbaum, A., Sawin, S. and Sun, J. (1995) 'Integrins as markers of uterine receptivity in women with primary unexplained infertility', *Fertility and sterility,* 63(3), pp. 535-542.

Li, Q., Wang, J., Armant, D. R., Bagchi, M. K. and Bagchi, I. C. (2002) 'Calcitonin down-regulates E-cadherin expression in rodent uterine epithelium during implantation', *Journal of Biological Chemistry,* 277(48), pp. 46447-46455.

Liew, F. Y., Xu, D., Brint, E. K. and O'Neill, L. A. (2005) 'Negative regulation of toll-like receptor-mediated immune responses', *Nature Reviews Immunology,* 5(6), pp. 446-458.

Lim, H. and Dey, S. (1997) 'Prostaglandin E2 Receptor Subtype EP2 Gene Expression

in the Mouse Uterus Coincides with Differentiation of the Luminal Epithelium for Implantation 1', *Endocrinology,* 138(11), pp. 4599-4606.

Lim, H., Gupta, R. A., Ma, W.-g., Paria, B. C., Moller, D. E., Morrow, J. D., DuBois, R. N., Trzaskos, J. M. and Dey, S. K. (1999) 'Cyclo-oxygenase-2-derived prostacyclin mediates embryo implantation in the mouse via PPARδ', *Genes & development,* 13(12), pp. 1561-1574.

Lim, K. J., Odukoya, O. A., Ajjan, R. A., Li, T.-C., Weetman, A. P. and Cooke, I. D. (2000) 'The role of T-helper cytokines in human reproduction', *Fertility and sterility,* 73(1), pp. 136-142.

Lin, H. Y., Zhang, H., Yang, Q., Wang, H. X., Wang, H. M., Chai, K. X., Chen, L. M. and Zhu, C. (2006) 'Expression of prostasin and protease nexin-1 in rhesus monkey (Macaca mulatta) endometrium and placenta during early pregnancy', *J Histochem Cytochem,* 54(10), pp. 1139-47.

Lindsay, L. L. and Hedrick, J. L. (1998) 'Treatment of Xenopus laevis coelomic eggs with trypsin mimics pars recta oviductal transit by selectively hydrolyzing envelope glycoprotein gp43, increasing sperm binding to the envelope, and rendering eggs fertilizable', *Journal of Experimental Zoology,* 281(2), pp. 132-138.

Liu, Y., Yin, H., Zhao, M. and Lu, Q. (2014) 'TLR2 and TLR4 in autoimmune diseases: a comprehensive review', *Clinical reviews in allergy & immunology,* 47(2), pp. 136-147.

Lonergan, P. and Fair, T. (2008) 'In vitro-produced bovine embryos—Dealing with the warts', *Theriogenology,* 69(1), pp. 17-22.

Lopes, A., Madsen, S., Ramsing, N., Løvendahl, P., Greve, T. and Callesen, H. (2007) 'Investigation of respiration of individual bovine embryos produced in vivo and in vitro and correlation with viability following transfer', *Human Reproduction,* 22(2), pp. 558-566.

Lopes, F. L., Desmarais, J. A. and Murphy, B. D. (2004) 'Embryonic diapause and its regulation', *Reproduction,* 128(6), pp. 669-678.

Lu, Y.-C., Yeh, W.-C. and Ohashi, P. S. (2008) 'LPS/TLR4 signal transduction pathway', *Cytokine,* 42(2), pp. 145-151.

Lucas, E. S., Dyer, N. P., Murakami, K., Hou Lee, Y., Chan, Y. W., Grimaldi, G., Muter, J., Brighton, P. J., Moore, J. D. and Patel, G. (2015) 'Loss of Endometrial Plasticity in Recurrent Pregnancy Loss', *STEM CELLS*.

Lucas, E. S., Salker, M. S. and Brosens, J. J. (2013) 'Uterine plasticity and reproductive fitness', *Reproductive biomedicine online,* 27(5), pp. 506-514.

Luo, D., Zhang, Y., Bai, Y., Liu, X., Gong, Y., Zhou, B., Zhang, L., Luo, L. and Zhou, R. (2014) 'Prostasin gene polymorphism at rs12597511 is associated with severe preeclampsia in Chinese Han women', *Chin Med J (Engl),* 127(11), pp. 2048-52.

Ma, X. J., Fu, Y. Y., Li, Y. X., Chen, L. M., Chai, K. and Wang, Y. L. (2009) 'Prostasin

inhibits cell invasion in human choriocarcinomal JEG-3 cells', *Histochem Cell Biol,* 132(6), pp. 639-46.

Macklon, N. S. and Brosens, J. J. (2014) 'The human endometrium as a sensor of embryo quality', *Biology of reproduction,* 91(4), pp. 98.

Macklon, N. S., Geraedts, J. P. and Fauser, B. C. (2002) 'Conception to ongoing pregnancy: the 'black box'of early pregnancy loss', *Human Reproduction Update,* 8(4), pp. 333-343.

Magli, M., Jones, G., Gras, L., Gianaroli, L., Korman, I. and Trounson, A. (2000) 'Chromosome mosaicism in day 3 aneuploid embryos that develop to morphologically normal blastocysts in vitro', *Human Reproduction,* 15(8), pp. 1781-1786.

Markee, J. (1978) 'Menstruation in intraocular endometrial transplants in the Rhesus monkey', *American journal of obstetrics and gynecology,* 131(5), pp. 558-559.

Mastenbroek, S., Twisk, M., van der Veen, F. and Repping, S. (2011) 'Preimplantation genetic screening: a systematic review and meta-analysis of RCTs', *Human reproduction update,* 17(4), pp. 454-466.

Mastenbroek, S., Twisk, M., van Echten-Arends, J., Sikkema-Raddatz, B., Korevaar, J. C., Verhoeve, H. R., Vogel, N. E., Arts, E. G., De Vries, J. W. and Bossuyt, P. M. (2007) 'In vitro fertilization with preimplantation genetic screening', *New England Journal of Medicine,* 357(1), pp. 9-17.

Masuda, H., Matsuzaki, Y., Hiratsu, E., Ono, M., Nagashima, T., Kajitani, T., Arase, T., Oda, H., Uchida, H. and Asada, H. (2010) 'Stem cell-like properties of the endometrial side population: implication in endometrial regeneration', *PloS one,* 5(4), pp. e10387.

Matsumoto, H., Ma, W.-g., Smalley, W., Trzaskos, J., Breyer, R. M. and Dey, S. K. (2001) 'Diversification of Cyclooxygenase-2-Derived Prostaglandins in Ovulation and Implantation', *Biology of Reproduction,* 64(5), pp. 1557-1565.

McHughes, C., Springer, G., Spate, L., Li, R., Woods, R., Green, M., Korte, S., Murphy, C., Green, J. and Prather, R. (2009) 'Identification and quantification of differentially represented transcripts in in vitro and in vivo derived preimplantation bovine embryos', *Molecular reproduction and development,* 76(1), pp. 48-60.

Mertzanidou, A., Wilton, L., Cheng, J., Spits, C., Vanneste, E., Moreau, Y., Vermeesch, J. and Sermon, K. (2013) 'Microarray analysis reveals abnormal chromosomal complements in over 70% of 14 normally developing human embryos', *Human Reproduction,* 28(1), pp. 256-264.

Meseguer, M., Aplin, J. D., Caballero-Campo, P., O'Connor, J. E., Martín, J. C., Remohí, J., Pellicer, A. and Simón, C. (2001) 'Human endometrial mucin MUC1 is up-regulated by progesterone and down-regulated in vitro by the human blastocyst', *Biology of reproduction,* 64(2), pp. 590-601.

Mishra, A. and Seshagiri, P. (2000) 'Evidence for the involvement of a species-specific embryonic protease in zona escape of hamster blastocysts', *Molecular human reproduction,* 6(11), pp. 1005-1012.

Miyazaki, K., Maruyama, T., Masuda, H., Yamasaki, A., Uchida, S., Oda, H., Uchida, H. and Yoshimura, Y. (2012) 'Stem cell-like differentiation potentials of endometrial side population cells as revealed by a newly developed in vivo endometrial stem cell assay'.

Moffett, A. and Loke, C. (2006) 'Immunology of placentation in eutherian mammals', *Nature Reviews Immunology,* 6(8), pp. 584-594.

Moor, R. and Cragle, R. (1971) 'The sheep egg: enzymatic removal of the zona pellucida and culture of eggs in vitro', *Journal of reproduction and fertility,* 27(3), pp. 401-409.

Mor, G., Cardenas, I., Abrahams, V. and Guller, S. (2011) 'Inflammation and pregnancy: the role of the immune system at the implantation site', *Annals of the New York Academy of Sciences,* 1221(1), pp. 80-87.

Muter, J. 2015. Uncoupling of circadian and other maternal cues in decidualizing endometrial cells. PhD thesis, University of Warwick.

Muter, J., Lucas, E. S., Chan, Y.-W., Brighton, P. J., Moore, J. D., Lacey, L., Quenby, S., Lam, E. W.-F. and Brosens, J. J. (2015) 'The clock protein period 2 synchronizes mitotic expansion and decidual transformation of human endometrial stromal cells', *The FASEB Journal,* 29(4), pp. 1603-1614.

Nachtigall, M. J., Kliman, H. J., Feinberg, R. F., Olive, D. L., Engin, O. and Arici, A. (1996) 'The effect of leukemia inhibitory factor (LIF) on trophoblast differentiation: a potential role in human implantation', *The Journal of Clinical Endocrinology & Metabolism,* 81(2), pp. 801-806.

Niakan, K. K., Han, J., Pedersen, R. A., Simon, C. and Pera, R. A. R. (2012) 'Human pre-implantation embryo development', *Development,* 139(5), pp. 829-841.

Nikas, G., Drakakis, P., Loutradis, D., Mara-Skoufari, C., Koumantakis, E., Michalas, S. and Psychoyos, A. (1995) 'Implantation: Uterine pinopodes as markers of the ‘nidation window’in cycling women receiving exogenous oestradiol and progesterone', *Human Reproduction,* 10(5), pp. 1208-1213.

Nikas, G. and Psychoyos, A. (1997) 'Uterine Pinopodes in Peri-implantation Human Endometrium Clinical Relevance', *Annals of the New York Academy of Sciences,* 816(1), pp. 129-142.

Norwitz, E. R., Schust, D. J. and Fisher, S. J. (2001) 'Implantation and the survival of early pregnancy', *New England Journal of Medicine,* 345(19), pp. 1400-1408.

Noyes, R., Hertig, A. and Rock, J. (1950) 'Dating the endometrial biopsy', *Obstetrical & Gynecological Survey,* 5(4), pp. 561-564.

Nystedt, S., Emilsson, K., Larsson, A. K., Strömbeck, B. and Sundelin, J. (1995)

'Molecular Cloning and Functional Expression of the Gene Encoding the Human Proteinase-Activated Receptor 2', *European Journal of Biochemistry,* 232(1), pp. 84-89.

O'Sullivan, C. M., Rancourt, S. L., Liu, S. Y. and Rancourt, D. E. (2001) 'A novel murine tryptase involved in blastocyst hatching and outgrowth', *Reproduction,* 122(1), pp. 61-71.

Panter, G. and Jerala, R. (2011) 'The ectodomain of the Toll-like receptor 4 prevents constitutive receptor activation', *Journal of Biological Chemistry,* 286(26), pp. 23334-23344.

Patel, A. N., Park, E., Kuzman, M., Benetti, F., Silva, F. J. and Allickson, J. G. (2008) 'Multipotent menstrual blood stromal stem cells: isolation, characterization, and differentiation', *Cell transplantation,* 17(3), pp. 303-311.

Patrizio, P. and Sakkas, D. (2009) 'From oocyte to baby: a clinical evaluation of the biological efficiency of in vitro fertilization', *Fertility and sterility,* 91(4), pp. 1061-1066.

Peng, Q., Yang, H., Xue, S., Shi, L., Yu, Q. and Kuang, Y. (2012) 'Secretome profile of mouse oocytes after activation using mass spectrum', *Journal of assisted reproduction and genetics,* 29(8), pp. 765-771.

Perona, R. M. and Wassarman, P. M. (1986) 'Mouse blastocysts hatch< i> in vitro</i> by using a trypsin-like proteinase associated with cells of mural trophectoderm', *Developmental biology,* 114(1), pp. 42-52.

Puente, X. S., Sánchez, L. M., Overall, C. M. and López-Otín, C. (2003) 'Human and mouse proteases: a comparative genomic approach', *Nature Reviews Genetics,* 4(7), pp. 544-558.

Quenby, S., Anim-Somuah, M., Kalumbi, C., Farquharson, R. and Aplin, J. D. (2007) 'Different types of recurrent miscarriage are associated with varying patterns of adhesion molecule expression in endometrium', *Reproductive biomedicine online,* 14(2), pp. 224-234.

Quenby, S., Vince, G., Farquharson, R. and Aplin, J. (2002) 'Recurrent miscarriage: a defect in nature's quality control?', *Human reproduction,* 17(8), pp. 1959-1963.

Quinn, C., Ryan, E., Claessens, E. A., Greenblatt, E., Hawrylyshyn, P., Cruickshank, B., Hannam, T., Dunk, C. and Casper, R. F. (2007) 'The presence of pinopodes in the human endometrium does not delineate the implantation window', *Fertility and sterility,* 87(5), pp. 1015-1021.

Rai, R. and Regan, L. (2006) 'Recurrent miscarriage', *The Lancet,* 368(9535), pp. 601-611.

Revel, A., Achache, H., Stevens, J., Smith, Y. and Reich, R. (2011) 'MicroRNAs are associated with human embryo implantation defects', *Human reproduction,* 26(10), pp. 2830-2840.

Robertson, S. A., Chin, P. Y., Glynn, D. J. and Thompson, J. G. (2011) 'Peri-Conceptual Cytokines–Setting the Trajectory for Embryo Implantation, Pregnancy and Beyond', *American Journal of Reproductive Immunology,* 66(s1), pp. 2-10.

Rogers, P. A. (1996) 'Structure and function of endometrial blood vessels', *Human reproduction update,* 2(1), pp. 57-62.

Ruan, Y. C., Guo, J. H., Liu, X., Zhang, R., Tsang, L. L., Da Dong, J., Chen, H., Yu, M. K., Jiang, X. and Zhang, X. H. (2012) 'Activation of the epithelial Na+ channel triggers prostaglandin E2 release and production required for embryo implantation', *Nature medicine,* 18(7), pp. 1112-1117.

Ruan, Y. C., Wang, Z., Du, J. Y., Zuo, W. L., Guo, J. H., Zhang, J., Wu, Z. L., Wong, H. Y., Chung, Y. W. and Chan, H. C. (2008) 'Regulation of smooth muscle contractility by the epithelium in rat vas deferens: role of ATP-induced release of PGE2', *The Journal of physiology,* 586(20), pp. 4843-4857.

Ruan, Y. C., Zhou, W. and Chan, H. C. (2011) 'Regulation of smooth muscle contraction by the epithelium: role of prostaglandins', *Physiology,* 26(3), pp. 156-170.

Rubio, C., Bellver, J., Rodrigo, L., Bosch, E., Mercader, A., Vidal, C., De los Santos, M. J., Giles, J., Labarta, E. and Domingo, J. (2013) 'Preimplantation genetic screening using fluorescence in situ hybridization in patients with repetitive implantation failure and advanced maternal age: two randomized trials', *Fertility and sterility,* 99(5), pp. 1400-1407.

Rubio, C., Simon, C., Vidal, F., Rodrigo, L., Pehlivan, T., Remohi, J. and Pellicer, A. (2003) 'Chromosomal abnormalities and embryo development in recurrent miscarriage couples', *Human Reproduction,* 18(1), pp. 182-188.

Saboia-Vahia, L., Borges-Veloso, A., Mesquita-Rodrigues, C., Cuervo, P., Dias-Lopes, G., Britto, C., de Barros Silva, A. P. and De Jesus, J. B. (2013) 'Trypsin-like serine peptidase profiles in the egg, larval, and pupal stages of Aedes albopictus', *Parasites & vectors,* 6(1), pp. 1-11.

Sakoff, J. and Murdoch, R. (1996) 'The role of calcium in the artificially induced decidual cell reaction in pseudopregnant mice', *Biochemical and molecular medicine,* 57(2), pp. 81-90.

Salamonsen, L. A. and Nie, G. (2002) 'Proteases at the endometrial–trophoblast interface: their role in implantation', *Reviews in Endocrine and Metabolic Disorders,* 3(2), pp. 133-143.

Salamonsen, L. A., Zhang, J. and Brasted, M. (2002) 'Leukocyte networks and human endometrial remodelling', *Journal of reproductive immunology,* 57(1), pp. 95-108.

Salker, M., Teklenburg, G., Molokhia, M., Lavery, S., Trew, G., Aojanepong, T., Mardon, H. J., Lokugamage, A. U., Rai, R. and Landles, C. (2010) 'Natural selection of human embryos: impaired decidualization of endometrium disables embryo-maternal interactions and causes recurrent pregnancy loss', *PloS one,* 5(4), pp.

e10287.

Salker, M. S., Christian, M., Steel, J. H., Nautiyal, J., Lavery, S., Trew, G., Webster, Z., Al-Sabbagh, M., Puchchakayala, G. and Föller, M. (2011) 'Deregulation of the serum-and glucocorticoid-inducible kinase SGK1 in the endometrium causes reproductive failure', *Nature medicine,* 17(11), pp. 1509-1513.

Salker, M. S., Nautiyal, J., Steel, J. H., Webster, Z., Šućurović, S., Nicou, M., Singh, Y., Lucas, E. S., Murakami, K. and Chan, Y.-W. (2012) 'Disordered IL-33/ST2 activation in decidualizing stromal cells prolongs uterine receptivity in women with recurrent pregnancy loss', *PLoS One,* 7(12), pp. e52252.

Sandalinas, M., Sadowy, S., Alikani, M., Calderon, G., Cohen, J. and Munné, S. (2001) 'Developmental ability of chromosomally abnormal human embryos to develop to the blastocyst stage', *Human Reproduction,* 16(9), pp. 1954-1958.

Sandra, O. and Renard, J.-P. (2011) 'The endometrium is an early biosensor of the embryo capacity to develop to term'.

Santos, M. A., Teklenburg, G., Macklon, N. S., Van Opstal, D., Schuring-Blom, G. H., Krijtenburg, P.-J., de Vreeden-Elbertse, J., Fauser, B. C. and Baart, E. B. (2010) 'The fate of the mosaic embryo: chromosomal constitution and development of Day 4, 5 and 8 human embryos', *Human Reproduction,* 25(8), pp. 1916-1926.

Sawada, H., Yamazaki, K. and Hoshi, M. (1990) 'Trypsin-like hatching protease from mouse embryos: evidence for the presence in culture medium and its enzymatic properties', *Journal of Experimental Zoology,* 254(1), pp. 83-87.

Shimazu, R., Akashi, S., Ogata, H., Nagai, Y., Fukudome, K., Miyake, K. and Kimoto, M. (1999) 'MD-2, a molecule that confers lipopolysaccharide responsiveness on Toll-like receptor 4', *The Journal of experimental medicine,* 189(11), pp. 1777-1782.

Simmons, D. G., Fortier, A. L. and Cross, J. C. (2007) 'Diverse subtypes and developmental origins of trophoblast giant cells in the mouse placenta', *Developmental biology,* 304(2), pp. 567-578.

Simon, C., Frances, A., Piquette, G., El Danasouri, I., Zurawski, G., Dang, W. and Polan, M. (1994) 'Embryonic implantation in mice is blocked by interleukin-1 receptor antagonist', *Endocrinology,* 134(2), pp. 521-528.

Simón, C., Gimeno, M. J., Mercader, A., O'Connor, J. E., RemohÍ, J., Polan, M. L. and Pellicer, A. (1997) 'Embryonic Regulation of Integrins β3, α 4, and α1 in Human Endometrial Epithelial Cells in Vitro 1', *The Journal of Clinical Endocrinology & Metabolism,* 82(8), pp. 2607-2616.

Singh, M., Chaudhry, P. and Asselin, E. (2011) 'Bridging endometrial receptivity and implantation: network of hormones, cytokines, and growth factors', *Journal of Endocrinology,* 210(1), pp. 5-14.

Skern-Mauritzen, R., Frost, P., Dalvin, S., Kvamme, B. O., Sommerset, I. and Nilsen, F.

(2009) 'A trypsin-like protease with apparent dual function in early Lepeophtheirus salmonis (Krøyer) development', *BMC Molecular Biology,* 10(1), pp. 1-11.

Song, B.-S., Kim, J.-S., Kim, C.-H., Han, Y.-M., Lee, D.-S., Lee, K.-K. and Koo, D.-B. (2009) 'Prostacyclin stimulates embryonic development via regulation of the cAMP response element-binding protein–cyclo-oxygenase-2 signalling pathway in cattle', *Reproduction, Fertility and Development,* 21(3), pp. 400-407.

Spallanzani, L. (1785) 'Esperimenti che servono nella storio della genera-zione di animali e piante', *Publicatio: Barthelmi Ciro, Genova*.

Staessen, C., Platteau, P., Van Assche, E., Michiels, A., Tournaye, H., Camus, M., Devroey, P., Liebaers, I. and Van Steirteghem, A. (2004) 'Comparison of blastocyst transfer with or without preimplantation genetic diagnosis for aneuploidy screening in couples with advanced maternal age: a prospective randomized controlled trial', *Human Reproduction,* 19(12), pp. 2849-2858.

Steptoe, P. C. and Edwards, R. G. (1978) 'Birth after the reimplantation of a human embryo', *The Lancet,* 312(8085), pp. 366.

Stevens, V. C. (1997) 'Some reproductive studies in the baboon', *Hum Reprod Update,* 3(6), pp. 533-40.

Stewart, C. L., Kaspar, P., Brunet, L. J., Bhatt, H., Gadi, I., Köntgen, F. and Abbondanzo, S. J. (1992) 'Blastocyst implantation depends on maternal expression of leukaemia inhibitory factor', *Nature,* 359(6390), pp. 76-79.

Strassmann, B. I. (1996) 'The evolution of endometrial cycles and menstruation', *Quarterly Review of Biology*, pp. 181-220.

Sun, Z.-g., Shi, H.-j., Gu, Z., Wang, J. and Shen, Q.-x. (2007) 'A single intrauterine injection of the serine protease inhibitor 4-(2-aminoethyl) benzenesulfonyl fluoride hydrochloride reversibly inhibits embryo implantation in mice', *Contraception,* 76(3), pp. 250-255.

Tabibzadeh, S. (1998) 'Molecular control of the implantation window', *Human Reproduction Update,* 4(5), pp. 465-471.

Tabibzadeh, S. and Sun, X. (1992) 'Cytokine expression in human endometrium throughout the menstrual cycle', *Human Reproduction,* 7(9), pp. 1214-1221.

Takano, M., Lu, Z., Goto, T., Fusi, L., Higham, J., Francis, J., Withey, A., Hardt, J., Cloke, B. and Stavropoulou, A. V. (2007) 'Transcriptional cross talk between the forkhead transcription factor forkhead box O1A and the progesterone receptor coordinates cell cycle regulation and differentiation in human endometrial stromal cells', *Molecular endocrinology,* 21(10), pp. 2334-2349.

Talbi, S., Hamilton, A., Vo, K., Tulac, S., Overgaard, M. T., Dosiou, C., Le Shay, N., Nezhat, C., Kempson, R. and Lessey, B. (2006) 'Molecular phenotyping of human endometrium distinguishes menstrual cycle phases and underlying

biological processes in normo-ovulatory women', *Endocrinology,* 147(3), pp. 1097-1121.

Teklenburg, G., Salker, M., Heijnen, C., Macklon, N. S. and Brosens, J. J. (2010a) 'The molecular basis of recurrent pregnancy loss: impaired natural embryo selection', *Molecular human reproduction,* 16(12), pp. 886-895.

Teklenburg, G., Salker, M., Molokhia, M., Lavery, S., Trew, G., Aojanepong, T., Mardon, H. J., Lokugamage, A. U., Rai, R. and Landles, C. (2010b) 'Natural selection of human embryos: decidualizing endometrial stromal cells serve as sensors of embryo quality upon implantation', *PLoS One,* 5(4), pp. e10258.

Tomlins, S. A., Rhodes, D. R., Perner, S., Dhanasekaran, S. M., Mehra, R., Sun, X.-W., Varambally, S., Cao, X., Tchinda, J. and Kuefer, R. (2005) 'Recurrent fusion of TMPRSS2 and ETS transcription factor genes in prostate cancer', *Science,* 310(5748), pp. 644-648.

Tsai, H.-D., Chang, C.-C., Hsieh, Y.-Y., Lo, H.-Y., Hsu, L.-W. and Chang, S.-C. (1999) 'Recombinant human leukemia inhibitory factor enhances the development of preimplantation mouse embryo in vitro', *Fertility and sterility,* 71(4), pp. 722-725.

Uchimura, K., Hayata, M., Mizumoto, T., Miyasato, Y., Kakizoe, Y., Morinaga, J., Onoue, T., Yamazoe, R., Ueda, M. and Adachi, M. (2014) 'The serine protease prostasin regulates hepatic insulin sensitivity by modulating TLR4 signalling', *Nature communications,* 5.

Vallet, V., Chraibi, A., Gaeggeler, H.-P., Horisberger, J.-D. and Rossier, B. C. (1997) 'An epithelial serine protease activates the amiloride-sensitive sodium channel', *Nature,* 389(6651), pp. 607-610.

van Echten-Arends, J., Mastenbroek, S., Sikkema-Raddatz, B., Korevaar, J. C., Heineman, M. J., van der Veen, F. and Repping, S. (2011) 'Chromosomal mosaicism in human preimplantation embryos: a systematic review', *Human reproduction update,* 17(5), pp. 620-627.

van Mourik, M. S., Macklon, N. S. and Heijnen, C. J. (2009) 'Embryonic implantation: cytokines, adhesion molecules, and immune cells in establishing an implantation environment', *Journal of leukocyte biology,* 85(1), pp. 4-19.

Vanneste, E., Melotte, C., Voet, T., Robberecht, C., Debrock, S., Pexsters, A., Staessen, C., Tomassetti, C., Legius, E. and D'Hooghe, T. (2011) 'PGD for a complex chromosomal rearrangement by array comparative genomic hybridization', *Human reproduction,* 26(4), pp. 941-949.

Vanneste, E., Voet, T., Le Caignec, C., Ampe, M., Konings, P., Melotte, C., Debrock, S., Amyere, M., Vikkula, M. and Schuit, F. (2009) 'Chromosome instability is common in human cleavage-stage embryos', *Nature medicine,* 15(5), pp. 577-583.

Vilella, F., Ramirez, L., Berlanga, O., Martinez, S., Alama, P., Meseguer, M., Pellicer, A.

and Simon, C. (2013) 'PGE2 and PGF2α concentrations in human endometrial fluid as biomarkers for embryonic implantation', *The Journal of Clinical Endocrinology & Metabolism,* 98(10), pp. 4123-4132.

Von Wolff, M., Thaler, C., Strowitzki, T., Broome, J., Stolz, W. and Tabibzadeh, S. (2000) 'Regulated expression of cytokines in human endometrium throughout the menstrual cycle: dysregulation in habitual abortion', *Molecular human reproduction,* 6(7), pp. 627-634.

Voullaire, L., Slater, H., Williamson, R. and Wilton, L. (2000) 'Chromosome analysis of blastomeres from human embryos by using comparative genomic hybridization', *Human genetics,* 106(2), pp. 210-217.

Wang, H. and Dey, S. K. (2006) 'Roadmap to embryo implantation: clues from mouse models', *Nature Reviews Genetics,* 7(3), pp. 185-199.

Wang, Q. T., Piotrowska, K., Ciemerych, M. A., Milenkovic, L., Scott, M. P., Davis, R. W. and Zernicka-Goetz, M. (2004) 'A genome-wide study of gene activity reveals developmental signaling pathways in the preimplantation mouse embryo', *Developmental cell,* 6(1), pp. 133-144.

Watson, A. L., Skepper, J. N., Jauniaux, E. and Burton, G. J. (1998) 'Susceptibility of Human Placental Syncytiotrophoblastic Mitochondria to Oxygen-Mediated Damage in Relation to Gestational Age 1', *The Journal of Clinical Endocrinology & Metabolism,* 83(5), pp. 1697-1705.

Weaver, B. A. and Cleveland, D. W. (2006) 'Does aneuploidy cause cancer?', *Current opinion in cell biology,* 18(6), pp. 658-667.

Weimar, C., Kavelaars, A., Brosens, J. J., Gellersen, B., de Vreeden-Elbertse, J., Heijnen, C. J. and Macklon, N. S. (2012a) 'Endometrial stromal cells of women with recurrent miscarriage fail to discriminate between high-and low-quality human embryos', *PLoS One,* 7(7), pp. e41424.

Weimar, C. H., Kavelaars, A., Brosens, J. J., Gellersen, B., de Vreeden-Elbertse, J. M., Heijnen, C. J. and Macklon, N. S. (2012b) 'Endometrial stromal cells of women with recurrent miscarriage fail to discriminate between high-and low-quality human embryos', *PLoS One,* 7(7), pp. e41424.

Wells, D. and Delhanty, J. D. (2000) 'Comprehensive chromosomal analysis of human preimplantation embryos using whole genome amplification and single cell comparative genomic hybridization', *Molecular Human Reproduction,* 6(11), pp. 1055-1062.

Wikimedia 2015. http://upload.wikimedia.org/wikipedia/commons/thumb/b/ba/ENaC_membrane_side_eng.svg/500px-ENaC_membrane_side_eng.svg.png.

Wilcox, A. J., Weinberg, C. R., O'CONNOR, J. F., Baird, D. D., Schlatterer, J. P., Canfield, R. E., Armstrong, E. G. and Nisula, B. C. (1989) 'Incidence of early loss

of pregnancy', *Obstetrical & Gynecological Survey,* 44(2), pp. 147-148.

Wiley 2015. http://higheredbcs.wiley.com/legacy/college/tortora/0470565101/hearthis_ill/pap13e_ch28_illustr_audio_mp3_am/simulations/figures/female.jpg.

Wilson, S., Greer, B., Hooper, J., Zijlstra, A., Walker, B., Quigley, J. and Hawthorne, S. (2005) 'The membrane-anchored serine protease, TMPRSS2, activates PAR-2 in prostate cancer cells', *Biochemical Journal,* 388(3), pp. 967-972.

Wolff, E. F., Wolff, A. B., Du, H. and Taylor, H. S. (2007) 'Demonstration of multipotent stem cells in the adult human endometrium by in vitro chondrogenesis', *Reproductive sciences,* 14(6), pp. 524-533.

Xu, X., Liu, X. and Tao, J. (2013) 'Changes in Biochemical Composition and Digestive Enzyme Activity During the Embryonic Development of the Marine Crab, Charybdis japonica (Crustadea: Decapoda)', *Zoological science,* 30(3), pp. 160-166.

Yamada, K., Takabatake, T. and Takeshima, K. (2000) 'Isolation and characterization of three novel serine protease genes from Xenopus laevis', *Gene,* 252(1), pp. 209-216.

Zeng, F. and Schultz, R. M. (2005) 'RNA transcript profiling during zygotic gene activation in the preimplantation mouse embryo', *Developmental biology,* 283(1), pp. 40-57.

SCIENTIFIC REPORTS

OPEN

SUBJECT AREAS:
REPRODUCTIVE BIOLOGY
EMBRYOLOGY

Received
2 October 2013

Accepted
8 January 2014

Published
6 February 2014

Correspondence and requests for materials should be addressed to J.J.B. (J.J.Brosens@warwick.ac.uk)

Uterine Selection of Human Embryos at Implantation

Jan J. Brosens[1], Madhuri S. Salker[1,2], Gijs Teklenburg[3], Jaya Nautiyal[2], Scarlett Salter[1], Emma S. Lucas[1], Jennifer H. Steel[2], Mark Christian[1], Yi-Wah Chan[4], Carolien M. Boomsma[3], Jonathan D. Moore[4], Geraldine M. Hartshorne[1], Sandra Šućurović[5], Biserka Mulac-Jericevic[5], Cobi J. Heijnen[3], Siobhan Quenby[1], Marian J. Groot Koerkamp[6], Frank C. P. Holstege[6], Anatoly Shmygol[1] & Nick S. Macklon[3,7]

[1]Division of Reproductive Health, Warwick Medical School, Clinical Sciences Research Laboratories, University Hospital, Coventry CV2 2DX, UK, [2]Institute of Reproductive and Developmental Biology, Imperial College London, Hammersmith Hospital, London W12 ONN, UK, [3]Department for Reproductive Medicine and Gynecology, University Medical Center Utrecht, PO Box 85500, 3508 GA, Utrecht, The Netherlands, [4]Warwick Systems Biology Centre, University of Warwick, Coventry CV4 7AL, UK, [5]Department of Physiology and Immunology, Medical School, University of Rijeka, Braće Branchetta 20, 51000 Rijeka, Croatia, [6]Molecular Cancer Research, University Medical Center Utrecht, PO Box 85500, 3508 GA, Utrecht, The Netherlands, [7]Division of Developmental Origins of Adult Diseases (DOHaD), University of Southampton, Coxford Road, Southampton SO16 5YA, UK.

Human embryos frequently harbor large-scale complex chromosomal errors that impede normal development. Affected embryos may fail to implant although many first breach the endometrial epithelium and embed in the decidualizing stroma before being rejected via mechanisms that are poorly understood. Here we show that developmentally impaired human embryos elicit an endoplasmic stress response in human decidual cells. A stress response was also evident upon *in vivo* exposure of mouse uteri to culture medium conditioned by low-quality human embryos. By contrast, signals emanating from developmentally competent embryos activated a focused gene network enriched in metabolic enzymes and implantation factors. We further show that trypsin, a serine protease released by pre-implantation embryos, elicits Ca^{2+} signaling in endometrial epithelial cells. Competent human embryos triggered short-lived oscillatory Ca^{2+} fluxes whereas low-quality embryos caused a heightened and prolonged Ca^{2+} response. Thus, distinct positive and negative mechanisms contribute to active selection of human embryos at implantation.

Reproduction in humans is marred by early pregnancy failure. Approximately 15% of clinically recognized pregnancies miscarry. When combined with pre-clinical losses, the true incidence is closer to 50%, rendering miscarriage by far the most common complication of pregnancy[1,2]. This exceptional attrition rate is attributed to the intrinsic invasiveness of human embryos and the high prevalence of chromosomal errors. Based on genome-wide screening of individual blastomeres, in excess of 70% of high-quality cleavage-stage IVF embryos reportedly harbor cells with complex large-scale structural chromosomal imbalances, some caused by meiotic aneuploidies but most by mitotic non-disjunction[3–5]. The incidence of aneuploidy in human embryos is estimated to be an order of magnitude higher than in other mammalian species. Further, a vast array of chromosomal errors has been detected in human embryos throughout all stages of pre-implantation development. Many of the chromosomal abnormalities observed in blastocysts have never been recorded in clinical miscarriage samples[3], suggesting that these embryos either fail to implant or are rejected soon after breaching the endometrial luminal epithelium[2,6–8].

Evidence from several mammalian species indicates that the endometrium is intrinsically capable of mounting an implantation response that is tailored to individual embryos. For example, microarray analysis of bovine endometrium has identified gene signatures that are dependent on the origins (e.g. somatic cell nuclear transfer, IVF, or artificial insemination) and developmental potential of the attaching embryo[9]. Using a co-culture system, we reported previously that human endometrial stromal cells (HESCs) become sensitive to embryonic signals upon differentiation into decidual cells and respond selectively to low-quality human embryos by inhibiting the secretion of key implantation factors, including interleukin-1 beta, heparin-binding EGF-like growth factor, and leukemia inhibitory factor[10]. Furthermore, aberrant decidualization of HESCs and lack of embryo sensoring are strongly associated with recurrent pregnancy loss[11–14]. These observations led to the hypothesis that active embryo selection

at implantation is essential for reproductive success[11–14], although the underlying mechanisms remain as yet poorly characterized.

A major obstacle is that human implantation events cannot be studied directly. In culture, the developmental potential of human embryos can only be assessed indirectly, foremost on morphological criteria, and over a legally restricted period. To overcome these hurdles, we prospectively collected conditioned medium of individually cultured human pre-implantation embryos and then characterized the maternal response, *in vitro* as well as in a heterologous *in vivo* model, to soluble factors produced by low-quality human embryos and embryos of proven developmental competence. We report that human embryos presage their developmental competence even prior to implantation. The spectrum of endometrial responses to cues from different embryos ranges widely, from enhanced expression of key implantation factors to overt endoplasmic reticulum (ER) stress. We also provide evidence that embryo-derived serine proteases are involved in eliciting a maternal response tailored to the developmental potential of the conceptus.

Results

Developmentally impaired human embryos induce ER stress response in decidualizing HESCs. We systematically collected the conditioned medium of day 4 human IVF embryos, which had been cultured individually for 72 h in microdroplets overlaid with mineral oil. Next, we incubated primary decidualizing HESCs with pooled culture supernatants from developmentally impaired embryos (DIEs), which were deemed unsuitable for transfer[15], and from embryos that resulted in ongoing pregnancies after single embryo transfer (developmentally competent embryos, DCEs; Table S1). Control cultures consisted of decidualizing HESCs incubated with unconditioned embryo culture medium (ECM). Incubation of primary cultures was repeated three times with separate pools of conditioned media from DCEs and DIEs. RNA was isolated from decidualizing HESCs after 12 h of incubation and analyzed by genome-wide expression profiling using DNA microarrays. Surprisingly, only 15 decidual genes were found to respond significantly ($P < 0.01$) to signals emanating from DCEs. In contrast, 449 maternal genes were perturbed in response to medium conditioned by DIEs (Fig. 1*A*; Table S1). Gene ontology annotation categorized half of these maternal genes into three broad biological processes: transport (20%), translation (17%), and cell cycle (13%) (Fig. 1*B*).

To investigate further the response of decidual cells to compromised embryos, we focused on *HSPA8*, the most downregulated gene in the array analysis (Table S2). This gene encodes HSC70, a ubiquitously and constitutively expressed member of the heat shock protein 70 family of molecular chaperones involved in the assembly of multiprotein complexes, transport of nascent polypeptides and regulation of protein folding[16,17]. HSC70 levels increased in primary HESCs decidualized for 4 or more days (Fig. 1*C*). Small interfering (si)RNA-mediated knockdown of this molecular chaperone reduced the secretion of prolactin (PRL) and insulin-like growth factor-binding protein 1 (IGFBP1) (Fig. 1*D* and *E*), two highly sensitive differentiation markers[18]. Cell viability was not affected significantly (Fig. 1*F*).

Because of its role in protein homeostasis[19,20], we postulated that loss of HSC70 causes ER stress in decidual cells. In fact, decidualizing HESCs mount a physiological unfolded protein response (UPR) associated with ER expansion and acquisition of a secretory phenotype[21]. This UPR was characterized by synchronous induction of various chaperones, including protein disulfide isomerase (PDI), BIP (GRP78), endoplasmic oxidoreductin-1α (ERO1α), and calnexin (Fig. 2*A*). In addition, differentiating HESCs upregulate the expression of the three key ER signaling proteins, the serine/threonine kinase inositol-requiring enzyme 1α (IRE1α), PKR-like ER-localized eIF2α kinase (PERK), and the protease-activated transcription factor ATF6, which collectively determine the cellular response to ER stress signals[21]. Interestingly, HSC70 knockdown had little or no effect on the expression of other ER chaperones or ATF6

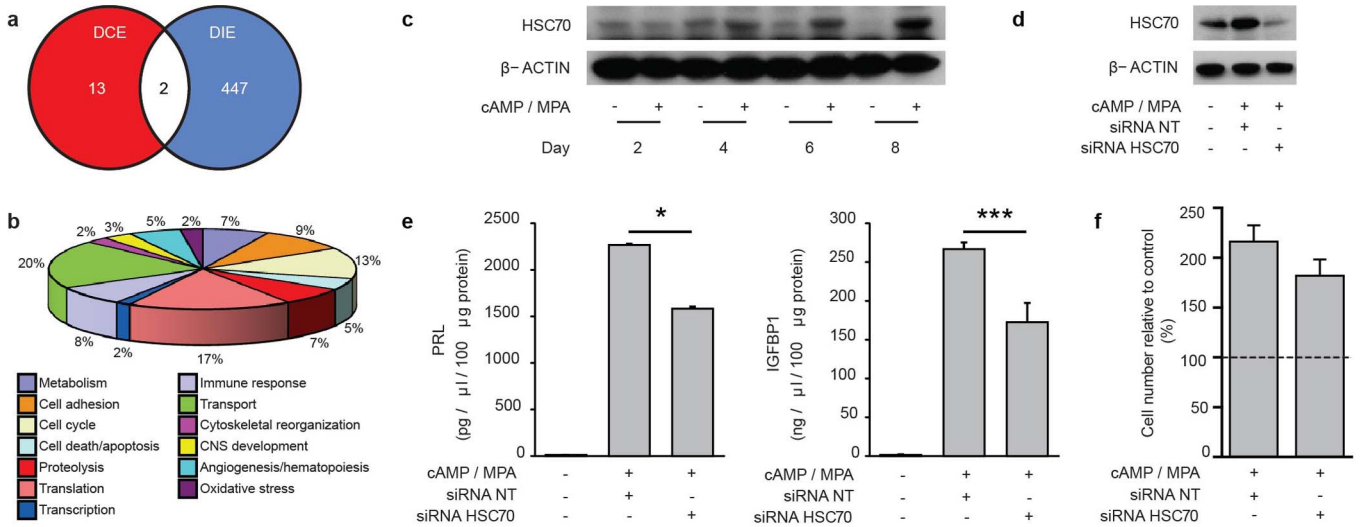

Figure 1 | Decidualizing endometrial cells are biosensors of embryo quality. (a) Venn diagram presenting the number of transcripts regulated in decidualizing HESCs significantly ($P < 0.01$) regulated in response to signals from developmentally competent embryos (DCE) and developmentally impaired embryos (DIE). (b) Gene Ontology classification of decidual genes regulated in response to soluble factors secreted by DIE. (c) Western blot analysis demonstrating the kinetics of HSC70 induction in primary HESC cultures decidualized with cAMP and MPA in a time-course lasting 8 d. β-ACTIN served as a loading control. A representative result from three different primary cultures is shown. Full length images are presented as Supplementary Information. (d) Primary HESCs were transfected with non-targeting (NT) siRNA or siRNA targeting HSC70, decidualized for 5 d, and then immunoblotted for HSC70. β-ACTIN served as a loading control. Full length images are presented as Supplementary Information. (e) HSC70 knockdown inhibits the secretion of decidual markers, PRL and IGFBP1, in primary HESC cultures differentiated *in vitro* for 5 d. The data represent mean (±SD) of triplicate experiments. * indicates $P < 0.05$, and *** $P < 0.001$. (f) The percentage of viable HESCs, transfected first with non-targeting (NT) siRNA or HSC70 targeting siRNA and then decidualized for 5 d, is presented relative to the number of viable cells in mock-transfected, undifferentiated cells (dotted line). The data represent the mean (±SD) of three biological repeat experiments.

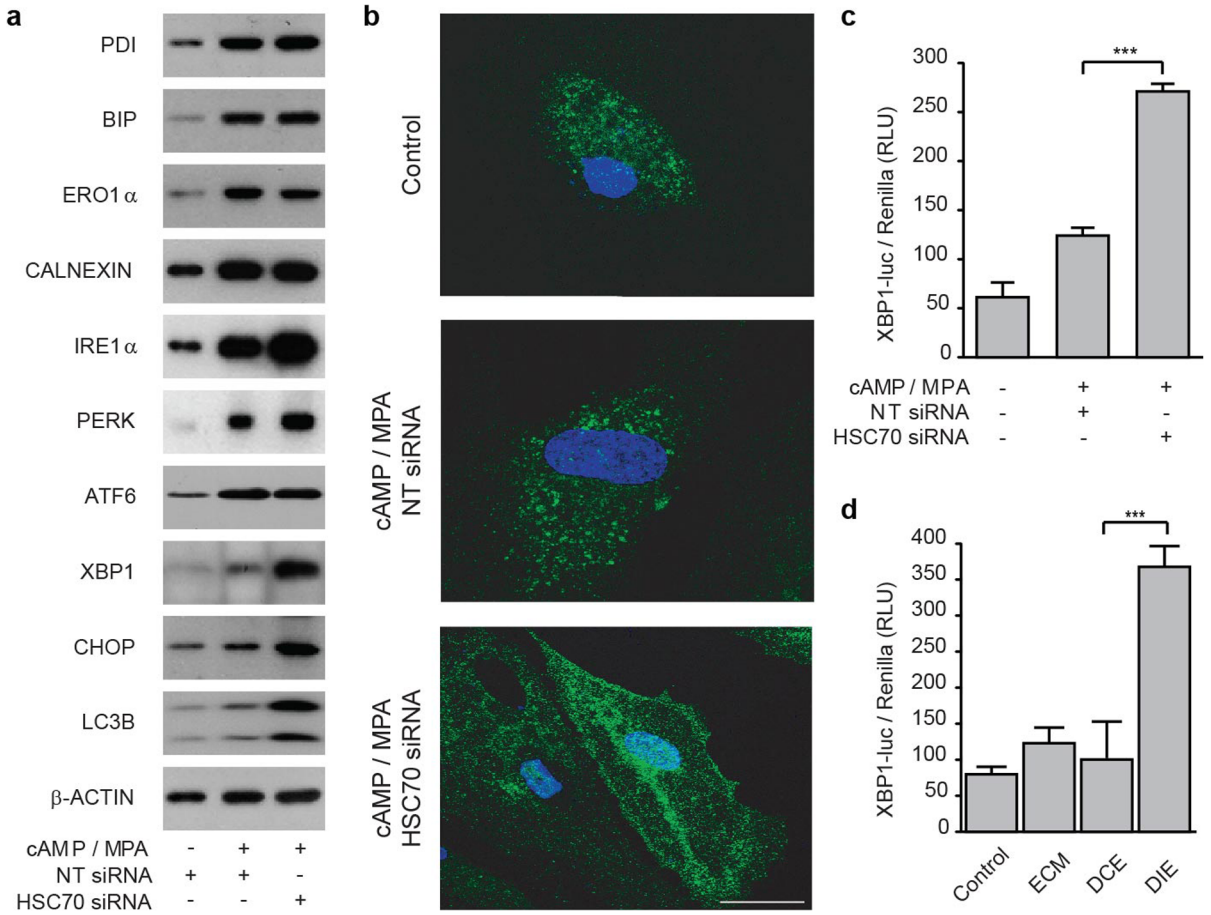

Figure 2 | HSC70 knockdown induces ER stress in decidualizing stromal cells. (a) Total cell lysates from primary HESC cultures, transfected first with non-targeting (NT) siRNA or siRNA targeting HSC70 and then decidualized with cAMP and MPA for 5 d, were immunoprobed for various proteins involved in UPR, ER stress, and autophagy as indicated. β-ACTIN served as a loading control. Full length images are presented as Supplementary Information. (b) HSC70 knockdown in HESCs promotes autophagosome formation. Primary cells cultured on chamber slides were transfected with either non-targeting (NT) or HSC70 targeting siRNA, decidualized for 5 d, stained for LC3B expression (green) and subjected to confocal microscopy. The nuclei were visualized with DAPI (blue). (c) Primary cultures were co-transfected with pcDNA3/XBP1-luc, pRL-sv40 and either siRNA targeting HSC70 or NT siRNA. The cells were left untreated or differentiated for 5 d before measuring luciferase activity. The results show the normalized mean firefly luciferase activity (±SD), expressed in relative light units (RLU), of four biological repeat experiments. *** indicates $P < 0.001$. (d) Confluent cultures were transfected as described in (c), left untreated (control) or decidualized for 5 d, and then exposed to 30 μl of unconditioned embryo culture medium (ECM) or media conditioned by DCEs or DIEs for 12 h. The results show normalized mean luciferase activity (±SD), expressed in relative light units (RLU), of three biological repeat experiments. *** indicates $P < 0.001$.

but further enhanced the induction of IRE1α and PERK. In addition, silencing of this molecular chaperone protein in decidualizing cells markedly upregulated the levels of X-box binding protein 1 (XBP1) and C/EBP-homologous protein (CHOP), downstream transcription factors that couple ER stress to translational inhibition, induction of ER chaperones, cell cycle arrest and death[21]. We speculated that lack of overt cell death upon HSC70 knockdown could be accounted for by augmented autophagy[21]. In keeping with this notion, the abundance of the microtubule-associated protein light chain 3B (LC3B), a marker of autophagic activity[22], increased markedly upon HSC70 knockdown in decidualizing cells (Fig. 2*A*). Confocal microscopy showed that the pattern of LC3B staining changed from being punctate and finely granular in undifferentiated and decidualizing cells to immunoreactive aggregates upon HSC70 silencing (Fig. 2*B*).

To test further the assertion that decidualizing HESCs mount an ER stress response upon HSC70 knockdown, we transfected primary cultures with pcDNA3/XBP1-luc, a plasmid in which human XBP1 cDNA is fused upstream of luciferase cDNA[23]. Under non-ER stress conditions, the presence of an in-frame stop codon prevents the expression of the downstream luciferase gene. Under ER stress conditions, however, activated IRE1α splices the XBP1-luc transcript, allowing translation of the luciferase cDNA. As shown in Fig. 2*C*, decidualization of HESCs transfected with pcDNA3/XBP1-luc only marginally enhanced luciferase levels whereas simultaneous HSC70 knockdown elicited a 5-fold induction. We then reasoned that decidualizing HESCs transfected with pcDNA3/XBP1-luc could serve as a bioassay to monitor ER stress responses induced by limited amounts of ECM. Primary cells seeded in 96-well plates were first transfected with the reporter construct, decidualized for 5 d, and then exposed for 12 h to either unconditioned ECM or pooled spent medium from DCEs or DIEs. In keeping with the array findings, soluble factors derived from DIEs strongly induced luciferase expression whereas this response was entirely absent upon incubation with unconditioned ECM or medium conditioned by DCEs (Fig. 2*D*).

Developmentally competent human embryos signal to promote implantation. We next explored if the developmental potential of human embryos impacts on the expression of uterine implantation genes *in vivo*. Female C57BL/6 mice were hormonally stimulated to

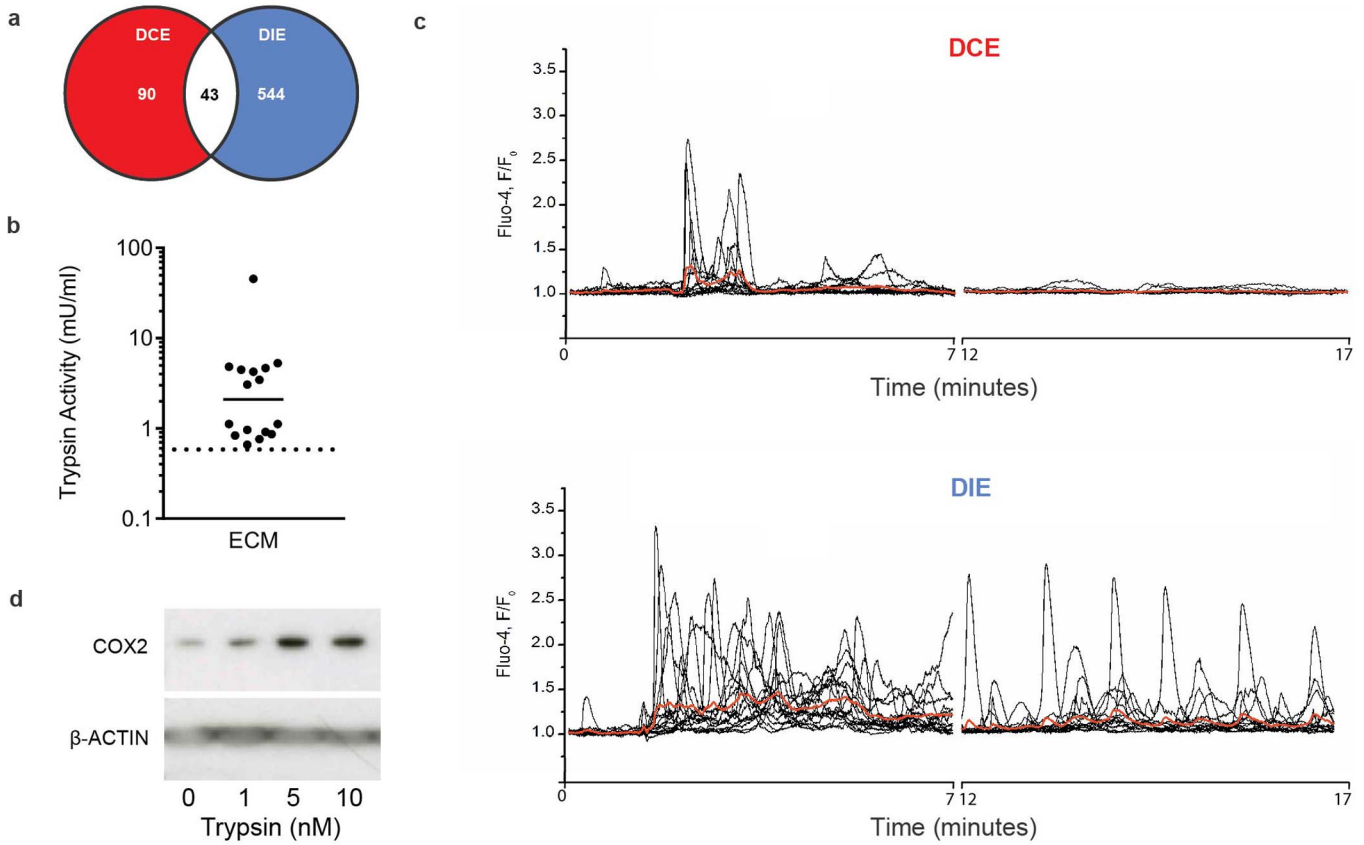

Figure 3 | Competent pre-implantation human embryos actively induce a supportive uterine environment. (a) Venn diagram presenting the number of maternal genes significantly ($P < 0.01$) altered 24 h after exposure of mouse uterus to unconditioned embryo culture medium or medium conditioned by either developmentally competent or impaired human embryos (DCE and DIE, respectively). (b) Tryptic activity was measured in 16 cultures containing a total of 163 human embryos between day 4 to 6 of development. Activity in unconditioned medium was below dotted line. (c) Application of embryo-conditioned medium induces $[Ca^{2+}]_i$ oscillations in Ishikawa cells. Black traces show $[Ca^{2+}]_i$ recordings from individual cells in response to application of 1 : 20 diluted culture medium obtained from DCE (top panel) or DIE (bottom panel). Red traces represent average of all individual traces in each panel. (d) Total protein lysates obtained from Ishikawa cells 24 h after treatment with trypsin (10 nM) for 5 min were subjected to western blot analysis and immunoprobed for COX2. β-ACTIN served as a loading control. Full length images are presented as Supplementary Information.

induce uterine receptivity and the lumen flushed with 50 µl of unconditioned ECM or pooled conditioned culture medium from human DCEs or DIEs. The animals were sacrificed 24 h later and the uterine transcriptome sequenced. As in the experiments with primary HESCs, many more genes (~6×) were altered in response to exposure of the uterine lumen to DIE versus DCE conditioned medium (Fig. 3*A*). However, the extent and amplitude of the transcriptional response to DCE was much more pronounced *in vivo* when compared to decidualizing primary HESC cultures. Strikingly, 27 of 90 (30%) uterine genes solely responsive to DCE signals code factors that have already been implicated in the implantation process (Table S3), including COX-2 (*Ptgs2*), Cytochrome P450 26a1 (*Cyp26a1*), and osteopontin (*Spp1*)[24–26]. In addition, exposure to DCE signals strongly upregulated a group of metabolic genes, which included *Fabp4*, *Plin1*, *Cidec*, *Adipoq*, *Retn*, and *Car3* (Fig. S1). Fatty acid binding protein 4 (*Fabp4*) is a widely used marker of differentiating adipocytes[27]. Cell death-inducing DFF45-like effector c (*Cidec*) promotes lipid droplet expansion whereas perilipin 1 (*Plin1*) prevents lipase-dependent breakdown of lipid droplets under basal conditions[28]. Further, adiponectin (*Adipoq*) and resistin (*Retn*) are key adipokines involved in regulating energy intake and expenditure as well as insulin sensitivity[29]. Taken together, the data point towards the existence of an evolutionarily conserved network of maternal genes that is responsive to embryonic signals and contributes to post-implantation development. By contrast, the response to DIE signals had the hallmarks of a stress response (Fig. S2). This was confirmed by Western blot analysis demonstrating strong uterine expression of Xbp1, Chop and Lc3b in response to DIE signals (Fig. S3). Notably, a modest stress-like response was also apparent upon flushing of the uterine lumen with medium conditioned by DCEs, which may point towards the induction of a decidual response and associated UPR.

The role of embryo-derived trypsin in maternal embryo recognition. A surprising observation was the induction of *Prss28* (68-fold) and *Prss29* (6-fold) mRNAs in the mouse uterus in response to DCE signals (Table S3). Prss28 and Prss29 are implantation-specific serine proteases that exhibit trypsin-like substrate specificity[30,31]. Embryonic tryptases activate Ca^{2+} signaling and upregulate COX-2 levels in murine endometrial epithelial cells (EECs), leading to prostaglandin production required for implantation[26]. *Prss28* and *Prss29* have no functional homologs in humans[32], suggesting a compensatory role for other serine proteases or, perhaps, that tryptic activity is no longer involved in embryo-EEC signaling. Comparative analysis of gene expression data showed that (Fig. S4 & S5), unlike their murine counterparts, developing human embryos up- and down-regulate the expression of *TMPRSS15* and *AMBP* coding for the trypsinogen activator (enterokinase) and trypsin inhibitor (trypstatin/bikunin precursor), respectively (Fig. S5). Trypsin activity was detectable in culture medium conditioned by human embryos (Fig. 3*B*). Furthermore, exposure of Ishikawa cells (a cell line model for human EECs) to spent embryo medium induced

oscillatory increases in intracellular Ca^{2+} ($[Ca^{2+}]_i$). Interestingly, $[Ca^{2+}]_i$ oscillations were discrete, lasting approximately 5 min, in response to DCE medium (Fig. 3*C*, upper panel). This contrasted to more pronounced and much longer oscillations when cells were exposed to DIE signals (Fig. 3*C*, lower panel). The $[Ca^{2+}]_i$ fluxes induced by embryonic cues bore a striking similarity to $[Ca^{2+}]_i$ oscillations induced upon application of trypsin (Fig. S6*A* and *D*). Soybean trypsin inhibitor dramatically decreased $[Ca^{2+}]_i$ signals induced by spent embryo medium (Fig. S6*B* and *D*). Conversely, embryo-induced $[Ca^{2+}]_i$ oscillations greatly attenuated the subsequent $[Ca^{2+}]_i$ responses to trypsin (Fig. S6*C* and *D*). Finally, short exposure to trypsin (5 min) was sufficient to upregulate COX-2 expression in Ishikawa cells (Fig. 3*D*). These data indicate that EECs serve to amplify discrete embryonic protease signals that induce a supportive maternal environment.

Discussion

Conflict between parent and offspring is thought to drive reproductive evolution and innovation[33]. This hypothesis predicts that the embryonic genome evolves to extract as much as possible from the mother to ensure its propagation whereas maternal genes will adapt to safeguard the success of current as well as future offspring. Thus, reproductive success in different species depends on balancing evolving embryonic and maternal traits[34–36]. A singular feature of the reproductive cycle in humans, shared with very few other mammalian species, is menstruation, a process triggered by 'spontaneous' decidualization of the endometrium in an embryo-independent manner[36,37]. When placed in the context of fetal-maternal conflict[33,38], our findings indicate that cyclic decidualization coupled to menstruation emerged as a strategy for early detection and active rejection of developmentally abnormal embryos that have breached the luminal epithelium. We show that decidual cells mount an extraordinarily polarized transcriptional response to embryonic signals, ranging from being exceptionally discrete in case of a competent embryo to extensive and complex in the presence of a low-quality embryo. We further demonstrate that *HSPA8* is particularly sensitive to signals from DIEs. Down-regulation of this molecular chaperone in decidual cells converts the differentiation-associated UPR into an overt ER stress response, which in turn compromises secretion of decidual factors, including PRL and IGFBP1, essential for placental formation and fetal development.

Conversely, this study shows that competent pre-implantation human embryos have retained the ability to actively enhance the uterine environment for implantation. This response to DCE signals is characterized by the induction of 29 known implantation factors, including COX-2, as well as various metabolic enzymes involved in lipid accumulation, glucose uptake, and energy expenditure (Table S3). Interestingly, several of these metabolic genes (e.g. *Cidec*, *Plin1*, *Adipoq*, *Retn* and *Fabp4*) are transcriptionally regulated by peroxisome proliferator-activated receptor gamma (PPARγ) in adipocytes[39–41], suggesting that embryonic signals activate this nuclear receptor in the endometrium, perhaps indirectly via induction of COX-2-dependent prostaglandin production[42]. In mice, initiation of implantation requires release of embryonic serine proteases, which in turn activate epithelial Na^+ channel (ENaC) in EECs, triggering Ca^{2+} influx and induction of COX-2[26]. Several lines of evidence indicate that this implantation pathway is not only conserved in humans but also important for embryo sensoring. We found that tryptic activity is detectable in medium conditioned by human embryos even before hatching. Incubation of EECs with ECM elicited $[Ca^{2+}]_i$ oscillations, a response markedly blunted by soybean trypsin inhibitor and recapitulated upon treatment of cells with low concentrations of trypsin. Further, brief exposure of EECs to trypsin was sufficient to induce COX-2 expression. *In silico* analysis showed that progression to the blastocyst stage is associated with gene changes predictive of increased expression and activation of various proteases implicated in ENaC activation, although the pattern of expression of individual genes during pre-implantation development frequently differs between mouse and human embryos (Fig. S4 & S5 and data not shown). Remarkably, cues from competent human embryos strongly induced two non-conserved implantation-specific serine proteinases, Prss28 (also known as implantation serine protease 1 or ISP1) and Prss29 (ISP2), in the mouse uterus. These proteases are also co-expressed in pre-implantation murine embryos[30,31]. ISP1 and 2 heterodimerize and form an enzymatic complex essential for blastocyst hatching, outgrowth and implantation in mice. Taken together, these observations suggest that endometrial protease production accelerates as the embryo approaches the surface epithelium, perhaps aligning hatching of the blastocyst with implantation. By contrast, low-quality human embryos triggered prolonged and disorganized $[Ca^{2+}]_i$ oscillations in EECs and an uterine stress response *in vivo*. The mechanism that couples these events warrants further investigations, although it is likely to involve illicit, excessive or unopposed activation of embryonic proteases, leading to proteotoxic stress in both the conceptus and surrounding maternal cells. This conjecture is supported by the observation that DCE but not DIE signals strongly enhance uterine expression of *Spink3*, which codes for the secreted serine protease inhibitor Kazal type 3 (SPINK3). The human homolog SPINK1 critically protects the pancreas from autodigestion by preventing premature protease activation[43,44].

In summary, reproductive success in humans depends on sustained maternal investment in one - occasionally two - implanting embryos. Genomic instability, giving rise to a vast array of chromosomal errors of variable complexity[3], is prevalent in human embryos throughout all stages of pre-implantation development. This engrained diversity in embryo quality poses an obvious maternal challenge. Our observations show that both positive and negative selection mechanisms govern implantation (Fig. 4), rendering this process intrinsically dynamic and adaptable to individual embryos.

Methods

Experimental ethics policy. This study was approved by the Medical Review Ethics Committee of the University Medical Center Utrecht, the Central Committee for Research on Human Subjects in The Netherlands (NL 12481.000.06), and the Hammersmith and Queen Charlotte's & Chelsea Research Ethics Committee (1997/5065). Written informed consent was obtained from all participating subjects.

Primary cultures. Endometrial samples were obtained during the secretory phase at the time of hysterectomy for benign indications or as an outpatient procedure using using a Wallach EndocellTM sampler (Wallach, USA) under ultrasound guidance. HESC cultures were established, passaged once and decidualized with 0.5 mM 8-Bromo-cAMP (Sigma, UK) and 10^{-6} M medroxyprogesterone acetate (MPA; Sigma, UK) as previously described[45].

Embryo conditioned media. All patients underwent ovarian stimulation with recombinant FSH and final oocyte maturation was triggered with hCG. Human embryos were cultured in microdroplets (30 µl) of Human Tubal Fluid medium, supplemented with 5% GPO (40 g/l pasteurized plasma protein, containing 95% albumin) under mineral oil from the second day after oocyte retrieval until day 4 (morula stage). The supernatants were collected from individually cultured embryo that resulted in pregnancy after transfer of a single fresh embryo (n = 40) and from embryos deemed of poor quality (n = 49), and unsuitable for embryo transfer based on standard morphological criteria[15]. In parallel, microdroplets not containing embryos were collected for control experiments.

Microarray analysis of primary HESC cultures and gene ontology. Primary HESCs were plated in 48-well tissue culture-grade plates, decidualized with 8-Bromo-cAMP and MPA for 5 d, and then incubated for 12 h with 100 µl of separately pooled supernatants, each derived from 10 individually cultured embryos. Three pools of conditioned media used were from DCEs and three from DIEs. Total RNA from HESCs in individual wells was subjected to microarray analysis. Human 70-mer oligos (Operon, Human V2 AROS) spotted onto Codelink Activated slides (Surmodics USA) were used for genome-wide expression profiling. RNA amplifications, labeling and hybridizations were performed as described[46]. Briefly, 500 ng of each amplified cRNA was coupled to Cy3 or Cy5 fluorophores (Amersham, UK) and subsequently hybridized on a Tecan HS4800PRO and scanned on an Agilent G2565BA microarray scanner. After data extraction using Imagene 8.0 (BioDiscovery), print-tip Loess normalization was performed on mean spot-intensities without background subtraction 30. Data were analyzed using ANOVA (R version 2.2.1/MAANOVA version 0.98-7) (http://www.r-project.org/). Genes with a

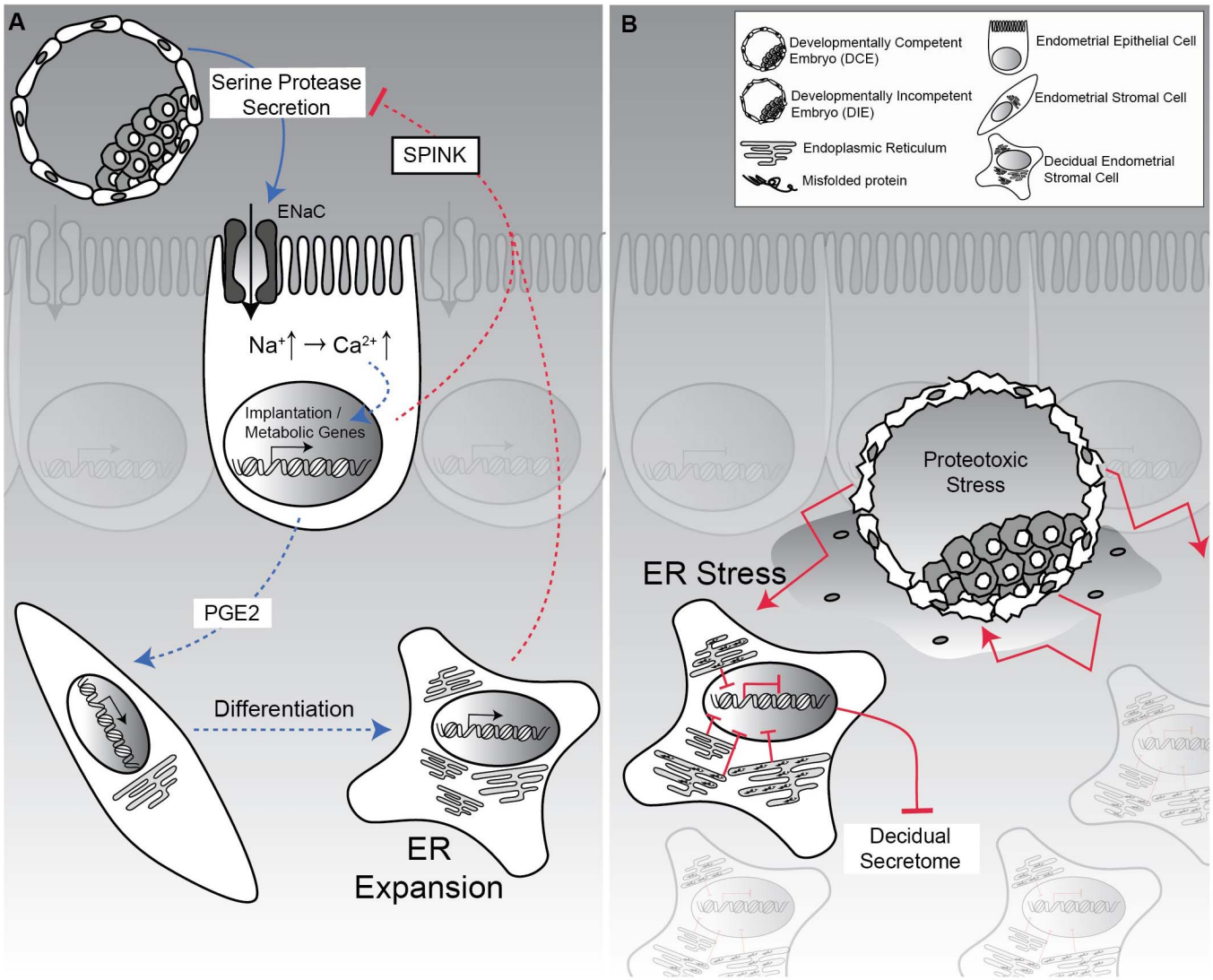

Figure 4 | Positive and negative mechanisms contribute to active selection of human embryos at implantation. (A) Developmentally competent human embryos secrete evolutionary conserved serine proteases that activate epithelial Na^+ channel (ENaC) expressed on luminal epithelial cells[26], triggering Ca^{2+} signalling and, ultimately, induction of genes involved in implantation and post-implantation embryo development. In concert, the decidualizing endometrium secretes serine protease inhibitors, such as murine SPINK3 and the human homolog SPINK1, to limit embryo-derived proteolytic activity. Note that acquisition of a secretory phenotype upon decidualization depends on massive expansion of the ER in HESCs. (B) By contrast, excessive protease activity emanating from developmentally compromised embryos that have breached the luminal epithelium down-regulates the expression of molecular chaperones in surrounding decidual cells, leading to accumulation of misfolded proteins and ER stress. This in turn compromises decidual cell functions and triggers tissue breakdown and early maternal rejection.

$P < 0.01$ after false discovery rate correction were considered significant. In addition, a 1.2 fold-change cutoff was applied and the resulting gene lists used for gene ontology (GO) analysis. Regulated genes were mapped to GO-slim categories according to the Gene Ontology Consortium: (http://www.geneontology.org/GO_slims/goslim_generic.obo). Microarray data have been submitted to ArrayExpress under accession number E-TABM-1064.

Animal experiments. C57BL/6 mice were purchased from Charles River Ltd (Margate, UK) and all experiments were carried out in accordance with the UK Home Office Project Licence (PPL70/6867). Immature female (3-week old) mice received a single dose of 1 mg progesterone and 10 μg/kg/day β-estradiol (Sigma) for a total of 3 d to prime the uterus for embryo transfer. The uterine horns of control and study mice were injected with an equal volume (50 μl) of either unconditioned embryo culture medium (ECM), serving as controls, or pooled conditioned media from DCE (n = 9) or DIE embryos (n = 18). The cervix was not clamped. Then, the incision was closed to allow recovery of the mice. The control and treatment groups each consisted of three animals. The mice were sacrificed 24 h later and uteri either fixed in formalin or snap-frozen and stored at −80°C for RNAseq and protein analyses. Both uterine horns of each animal were analyzed individually.

RNAseq analysis of mouse uteri. Uterine mRNA profiles of 25-day old wild-type (WT) mice were generated by deep sequencing, in triplicate, using Illumina HiSeq 2000 platform. The sequence reads that passed quality filters were analyzed with the following methods: Bowtie Alignment followed by TopHat (splice junctions mapper) and Cufflinks (transcript abundance). Sequence data have been submitted to GEO (GSE47019).

Transfections of primary endometrial cells. Primary HESCs at 80% confluency were transfected with DNA vectors or small interfering RNA (siRNA) oligonucleotides by the calcium phosphate co-precipitation method using the ProFection mammalian transfection kit (Promega, Madison, WI) according to the manufacturer's instructions. Reporter assays were done in 96-well plates. The X-box binding protein 1 (pcDNA3/XBP1-luc) reporter construct was a kind gift from Dr. Etsu Tashiro (Keio University, Tokyo, Japan). A constitutively active renilla expression vector (pRL-sv40) served as an internal transfection control. The plates were washed twice in phosphate-buffered saline (PBS) and firefly and Renilla activities were measured using the Luclite luciferase reporter assay system (Luclite, PerkinElmer, Boston, MA) and the luminescence was measured on a Victor II plate reader (PerkinElmer). For gene-silencing studies, HESCs were cultured in 6-well plates until 80% confluency and transiently transfected with 100 nM of the following siRNA reagents (Dharmacon, Lafayette, CO): siCONTROL non-targeting (NT) siRNA pool and HSPA8 siGENOME SMARTpool. All experiments were performed on three or more primary cultures from different endometrial biopsies.

Western blot analysis. Protein extracts were prepared by lysing cells in RIPA buffer. Protein yield was quantified using the Bio-Rad DC protein assay kit (Bio-Rad, USA). Equal amounts of protein were separated by 10% SDS-Polyacrylamide Gel Electrophoresis (SDS-PAGE) before wet-transfer onto PVDF membrane (Amersham Biosciences, UK). Nonspecific binding sites were blocked by overnight incubation with 5% nonfat dry milk in Tris-buffered saline with 1% Tween (TBS-T; 130 mmol/L NaCl, 20 mmol/L Tris, pH7.6 and 1% Tween). Primary antibodies used were anti-HSC70 (Abcam, UK), anti-BiP, anti-Calnexin, anti-ERo1α, anti-CHOP, anti-PERK, anti-PDI, anti-LC3B, anti-COX2 (Cell Signaling, USA) and β-ACTIN (Abcam, UK) which was used as a loading control. All primary antibodies were diluted 1 : 1000; except for the anti-β-ACTIN, which was diluted 1 : 100,000. Full length scans are presented as supplementary information. Note that some images were reflected for consistency in the sequence of presentation.

PRL, IGFBP1, and trypsin activity measurements. PRL and IGFBP-1 levels in the HESC culture media were determined using an amplified two-step sandwich-type immunoassay (R&D Systems, UK) according to the manufacturer's protocol. The Trypsin Activity Assay Kit (ABCAM) was used according to the manufacturer's instructions to measure trypsin activity in undiluted ECM and unconditioned culture medium (control). Trypsin activity in ECM was measured between day 4–6 of embryo development in 16 cultures (containing a total of 163 embryos). The ECM and unconditioned control medium were stored at −80°c until analysis.

Cell viability assays. Cultured HESCs were seeded in 96-well black plates with clear bases and maintained in 10% DCC/DMEM until they become confluent. Cells were transfected with or without siRNA targeting *HSPA8* and then subsequently decidualized or left untreated for a total of 6 d. Cell viability was evaluated using the ApoTox-Glo™ Triplex Assay (Promega, USA) according to the manufacturer's instructions.

Confocal microscopy and immunohistochemistry. Primary HESCs cultured on chamber slides were transfected with either siRNA targeting *HSPA8* or non-targeting siRNA and then either remained untreated or were decidualized with 8-Bromo-cAMP and MPA for 5 d. ER stress in control cultures was induced by treating cells with thapsigargin for 12 h (Sigma, UK). Cells were then fixed in 4% para-formaldehyde and permeabilized in 0.5% Triton. Primary antibodies, incubated overnight at 4°C in a humidified chamber (anti-LC3B 1 : 400). The secondary antibody used was labeled with Alexa Fluor® 488 (1 : 200; Invitrogen). Slides were mounted with proGOLD (Invitrogen) and stained with 4′,6-diamidino-2-phenylindole (DAPI) to visualize nuclei. Images were captured using a Leica SP5 II confocal microscope.

Confocal imaging of intracellular calcium ($[Ca^{2+}]_i$). Experiments were performed on Ishikawa cells cultured in glass bottomed 35 mm Petri dishes as described. For imaging of $[Ca^{2+}]_i$, cells were incubated for 40 min at room temperature in physiological saline solution (PSS) containing 5 μM Fluo-4/AM (Invitrogen, UK). Non-ionic detergent Pluronic F127 (0.025%, w/v) was included to aid the dye loading. After incubation with Fluo-4/AM, the cells were washed with PSS and the dish was mounted in a temperature-controlled environmental chamber on the stage of a confocal microscope (LSM 510 META, Carl Zeiss, UK). The cells were superfused with pre-warmed (35°C) Krebs solution for 20–30 min to ensure complete de-esterification of Fluo-4/AM. For image acquisition, perfusion was stopped and solution volume in the Petri dish adjusted to 200 μl. Fluo-4 fluorescence was excited using 488 nm line of argon ion laser. Images were recorded at 1 frame per second through the C-Apochromat 63×/1.20 W objective lens. Two time series were acquired from each Petri dish. During the first time series, baseline activity was recorded for 2 min, then 10 μl of conditioned embryo culture medium was added to the Petri dish and the recording continued for another 5 min. The second time series was acquired from the same viewing field after 10 min break. In control experiments, 10 μl of unconditioned instead of conditioned ECM was added. Experiments with trypsin and trypsin inhibitor were conducted in a similar manner. Trypsin (TRLS, Cat# LS003734) and soybean trypsin inhibitor (SI, Cat# LS003570) were purchased from Worthington Biochemical Corp., Lakewood, NJ, USA). Off-line image analysis was performed using ImageJ (NIH, http://imagej.nih.gov/ij/). Regions of interest (ROI) were drawn around each cell within the field of view. The Multi Measure function in the ImageJ ROI Manager was used to extract intensity profiles over time for each ROI. Intensity profiles were imported into Origin 8.5 (OriginLab Corporation, USA) for further processing, graphing and statistical analysis. Each trace was normalized to its corresponding baseline to yield a self-ratio trace (F/F0). The $[Ca^{2+}]_i$ signals induced by embryo-conditioned media were quantified as area under the curve (AUC) calculated above the base line (ΔF/F0) for the first and the last 5 min time periods of the conditioned medium treatment.

Statistical analysis. Statistical analysis was performed by ANOVA with Bonferroni correction, Student *t*-test or Mann Whitney U test, as appropriate.

1. Macklon, N. S., Geraedts, J. P. & Fauser, B. C. Conception to ongoing pregnancy: the 'black box' of early pregnancy loss. *Hum Reprod Update* **8**, 333–343 (2002).
2. Rai, R. & Regan, L. Recurrent miscarriage. *Lancet* **368**, 601–611 (2006).
3. Fragouli, E. *et al.* The origin and impact of embryonic aneuploidy. *Hum Genet*, doi:10.1007/s00439-013-1309-0 (2013).
4. Mertzanidou, A. *et al.* Microarray analysis reveals abnormal chromosomal complements in over 70% of 14 normally developing human embryos. *Hum Reprod* **28**, 256–264, doi:10.1093/humrep/des362 (2013).
5. Vanneste, E. *et al.* Chromosome instability is common in human cleavage-stage embryos. *Nat Med* **15**, 577–583 (2009).
6. Quenby, S., Vince, G., Farquharson, R. & Aplin, J. Recurrent miscarriage: a defect in nature's quality control? *Hum Reprod* **17**, 1959–1963 (2002).
7. Rajcan-Separovic, E. *et al.* Identification of copy number variants in miscarriages from couples with idiopathic recurrent pregnancy loss. *Hum Reprod* **25**, 2913–2922, doi:10.1093/humrep/deq202 (2010).
8. Stephenson, M. D., Awartani, K. A. & Robinson, W. P. Cytogenetic analysis of miscarriages from couples with recurrent miscarriage: a case-control study. *Hum Reprod* **17**, 446–451 (2002).
9. Mansouri-Attia, N. *et al.* Endometrium as an early sensor of in vitro embryo manipulation technologies. *Proc Natl Acad Sci U S A* **106**, 5687–5692 (2009).
10. Teklenburg, G. *et al.* Natural selection of human embryos: decidualizing endometrial stromal cells serve as sensors of embryo quality upon implantation. *PLoS One* **5**, e10258 (2010).
11. Salker, M. *et al.* Natural selection of human embryos: impaired decidualization of the endometrium disables embryo-maternal interactieons and causes recurrent pregnant loss. *PLoS One* **5**, e10287, doi: 10.1371/journal.pone.0010287 (2010).
12. Salker, M. S. *et al.* Deregulation of the serum- and glucocorticoid-inducible kinase SGK1 in the endometrium causes reproductive failure. *Nat Med* **17**, 1509–1513, doi:10.1038/nm.2498 (2011).
13. Salker, M. S. *et al.* Disordered IL-33/ST2 activation in decidualizing stromal cells prolongs uterine receptivity in women with recurrent pregnancy loss. *PLoS One* **7**, e52252, doi:10.1371/journal.pone.0052252 (2012).
14. Weimar, C. H. *et al.* Endometrial stromal cells of women with recurrent miscarriage fail to discriminate between high- and low-quality human embryos. *PLoS One* **7**, e41424, doi:10.1371/journal.pone.0041424 (2012).
15. Heijnen, E. M. *et al.* A mild treatment strategy for in-vitro fertilisation: a randomised non-inferiority trial. *Lancet* **369**, 743–749, doi:10.1016/S0140-6736(07)60360-2 (2007).
16. Hartl, F. U. & Hayer-Hartl, M. Converging concepts of protein folding in vitro and in vivo. *Nat Struct Mol Biol* **16**, 574–581, doi:10.1038/nsmb.1591 (2009).
17. Kampinga, H. H. & Craig, E. A. The HSP70 chaperone machinery: J proteins as drivers of functional specificity. *Nat Rev Mol Cell Biol* **11**, 579–592, doi:10.1038/nrm2941 (2010).
18. Cloke, B. *et al.* The androgen and progesterone receptors regulate distinct gene networks and cellular functions in decidualizing endometrium. *Endocrinology* **149**, 4462–4474 (2008).
19. Benbrook, D. M. & Long, A. Integration of autophagy, proteasomal degradation, unfolded protein response and apoptosis. *Exp Oncol* **34**, 286–297 (2012).
20. Kaushik, S. & Cuervo, A. M. Chaperone-mediated autophagy: a unique way to enter the lysosome world. *Trends Cell Biol* **22**, 407–417, doi:10.1016/j.tcb.2012.05.006 (2012).
21. Walter, P. & Ron, D. The unfolded protein response: from stress pathway to homeostatic regulation. *Science* **334**, 1081–1086, doi:10.1126/science.1209038 (2011).
22. Kabeya, Y. *et al.* LC3, GABARAP and GATE16 localize to autophagosomal membrane depending on form-II formation. *J Cell Sci* **117**, 2805–2812, doi:10.1242/jcs.01131 (2004).
23. Iwawaki, T., Akai, R., Kohno, K. & Miura, M. A transgenic mouse model for monitoring endoplasmic reticulum stress. *Nat Med* **10**, 98–102, doi:10.1038/nm970 (2004).
24. Altmae, S. *et al.* Research resource: interactome of human embryo implantation: identification of gene expression pathways, regulation, and integrated regulatory networks. *Mol Endocrinol* **26**, 203–217, doi:10.1210/me.2011-1196 (2012).
25. Han, B. C., Xia, H. F., Sun, J., Yang, Y. & Peng, J. P. Retinoic acid-metabolizing enzyme cytochrome P450 26a1 (cyp26a1) is essential for implantation: functional study of its role in early pregnancy. *J Cell Physiol* **223**, 471–479, doi:10.1002/jcp.22056 (2010).
26. Ruan, Y. C. *et al.* Activation of the epithelial Na+ channel triggers prostaglandin E(2) release and production required for embryo implantation. *Nat Med* **18**, 1112–1117, doi:10.1038/nm.2771 (2012).
27. Furuhashi, M. & Hotamisligil, G. S. Fatty acid-binding proteins: role in metabolic diseases and potential as drug targets. *Nat Rev Drug Discov* **7**, 489–503, doi:10.1038/nrd2589 (2008).
28. Yang, H., Galea, A., Sytnyk, V. & Crossley, M. Controlling the size of lipid droplets: lipid and protein factors. *Current Opin Cell Biol* **24**, 509–516, doi:10.1016/j.ceb.2012.05.012 (2012).
29. Kadowaki, T. *et al.* Adiponectin and adiponectin receptors in insulin resistance, diabetes, and the metabolic syndrome. *J Clin Invest* **116**, 1784–1792, doi:10.1172/JCI29126 (2006).
30. Sharma, N. *et al.* Implantation serine proteinase 1 exhibits mixed substrate specificity that silences signaling via proteinase-activated receptors. *PLoS One* **6**, e27888, doi:10.1371/journal.pone.0027888 (2011).
31. Sharma, N. *et al.* Implantation Serine Proteinases heterodimerize and are critical in hatching and implantation. *BMC Dev Biol* **6**, 61, doi:10.1186/1471-213X-6-61 (2006).
32. Wong, G. W., Yasuda, S., Morokawa, N., Li, L. & Stevens, R. L. Mouse chromosome 17A3.3 contains 13 genes that encode functional tryptic-like serine

proteases with distinct tissue and cell expression patterns. *J Biol Chem* **279**, 2438–2452, doi:10.1074/jbc.M308209200 (2004).
33. Haig, D. Genetic conflicts in human pregnancy. *Q Rev Biol* **68**, 495–532 (1993).
34. Chuong, E. B., Rumi, M. A., Soares, M. J. & Baker, J. C. Endogenous retroviruses function as species-specific enhancer elements in the placenta. *Nat Genet* **45**, 325–329, doi:10.1038/ng.2553 (2013).
35. Crespi, B. & Semeniuk, C. Parent-offspring conflict in the evolution of vertebrate reproductive mode. *Am Nat* **163**, 635–653, doi:10.1086/382734 (2004).
36. Emera, D., Romero, R. & Wagner, G. The evolution of menstruation: a new model for genetic assimilation: explaining molecular origins of maternal responses to fetal invasiveness. *BioEssays* **34**, 26–35, doi:10.1002/bies.201100099 (2012).
37. Brosens, J. J., Parker, M. G., McIndoe, A., Pijnenborg, R. & Brosens, I. A. A role for menstruation in preconditioning the uterus for successful pregnancy. *Am J Obstet Gynecol* **200**, 615 e611–616 (2009).
38. Emera, D. *et al.* Convergent evolution of endometrial prolactin expression in primates, mice, and elephants through the independent recruitment of transposable elements. *Mol Biol Evol* **29**, 239–247, doi:10.1093/molbev/msr189 (2012).
39. Kim, Y. J. *et al.* Transcriptional activation of Cidec by PPARgamma2 in adipocyte. *Biochem Biophys Res Commun* **377**, 297–302, doi:10.1016/j.bbrc.2008.09.129 (2008).
40. Arimura, N., Horiba, T., Imagawa, M., Shimizu, M. & Sato, R. The peroxisome proliferator-activated receptor gamma regulates expression of the perilipin gene in adipocytes. *J Biol Chem* **279**, 10070–10076, doi:10.1074/jbc.M308522200 (2004).
41. Iwaki, M. *et al.* Induction of adiponectin, a fat-derived antidiabetic and antiatherogenic factor, by nuclear receptors. *Diabetes* **52**, 1655–1663 (2003).
42. Forman, B. M. *et al.* 15-Deoxy-delta 12, 14-prostaglandin J2 is a ligand for the adipocyte determination factor PPAR gamma. *Cell* **83**, 803–812 (1995).
43. Ohmuraya, M. *et al.* Autophagic cell death of pancreatic acinar cells in serine protease inhibitor Kazal type 3-deficient mice. *Gastroenterology* **129**, 696–705, doi:10.1016/j.gastro.2005.05.057 (2005).
44. Kazal, L. A., Spicer, D. S. & Brahinsky, R. A. Isolation of a crystalline trypsin inhibitor-anticoagulant protein from pancreas. *J Am Chem Soc* **70**, 3034–3040 (1948).
45. Brosens, J. J., Hayashi, N. & White, J. O. Progesterone receptor regulates decidual prolactin expression in differentiating human endometrial stromal cells. *Endocrinology* **140**, 4809–4820 (1999).
46. Yang, Y. H. *et al.* Normalization for cDNA microarray data: a robust composite method addressing single and multiple slide systematic variation. *Nucleic Acids Res* **30**, e15 (2002).

Acknowledgments

We are grateful to all couples who participated in this study. We are also indebted to Dr. Etsu Tashiro (Keio University, Japan) for the pcDNA3/XBP1-luc construct. This study was supported by a grant from the Netherlands Organization for Scientific Research (NWO), the Biomedical Research Unit in Reproductive Health at University Hospital Coventry and Warwickshire, and a studentship from the Genesis Research Trust (M.S.S.).

Author contributions

J.J.B., M.S.S. and N.S.M. designed the experiments. M.S.S., G.T., S.S., E.S.L. and A.S. performed the *in vitro* experiments. J.N., J.H.S. and M.C. performed the *in vivo* studies and were assisted in the tissue analysis by S.Š. and B.M.-J. Embryo culture media and clinical data collection were performed by G.T., C.M.B., C.J.H. and N.S.M. Microarray analysis was performed and the data interpreted by M.J.G.K. and F.C.P.H. RNA sequencing data were analyzed by Y.-W.C., E.S.L., S.S. and J.D.M. Confocal imaging of calcium was performed by A.S., who also analyzed the data. S.Q. and G.M.H. provided clinical resources and contributed to data interpretation. E.S.L. and J.J.B. prepared Figure 4. J.J.B. wrote the paper and M.S.S., J.N., S.S., E.S.L., M.C., Y.-W.C., G.M.H., S.Š., B.M.-J., S.Q., M.J.G.K., F.C.P.H., N.S.M. and A.S. edited the manuscript.

Additional information

Supplementary information accompanies this paper at http://www.nature.com/scientificreports

Competing financial interests: The authors declare no competing financial interests.

How to cite this article: Brosens, J.J. *et al.* Uterine Selection of Human Embryos at Implantation. *Sci. Rep.* **4**, 3894; DOI:10.1038/srep03894 (2014).